

Excess Molar Enthalpies of Binary and Ternary Systems Involving Hydrocarbons and Ethers

A Thesis Submitted to the College of
Graduate Studies and Research
in Partial Fulfillment of the Requirements for the Degree of
Master of Science
in the Department of Chemical and Biological Engineering
University of Saskatchewan
Saskatoon

By

S. M. Nazmul Hasan

PERMISSION TO USE

In presenting this thesis in partial fulfilment of the requirements for a Postgraduate degree from the University of Saskatchewan, I agree that the Libraries of this University may make it freely available for inspection. I further agree that permission for copying of this thesis in any manner, in whole or in part, for scholarly purposes may be granted by the professor or professors who supervised my thesis work or, in their absence, by the Head of the Department or the Dean of the College in which my thesis work was done. It is understood that any copying or publication or use of this thesis or parts thereof for financial gain shall not be allowed without my written permission. It is also understood that due recognition shall be given to me and to the University of Saskatchewan in any scholarly use which may be made of any material in my thesis.

Requests for permission to copy or to make other use of material in this thesis in whole or part should be addressed to:

Head
Department of Chemical and Biological Engineering
University of Saskatchewan
57 Campus Drive
Saskatoon, SK S7N 5A9
Canada

ABSTRACT

In modern separation design, an important part of many phase-equilibrium calculations is the mathematical representation of pure-component and mixture enthalpies. Mixture enthalpy data are important not only for determination of heat loads, but also for the design of distillation units. Further, mixture enthalpy data, when available, are useful for extending vapor-liquid equilibria to higher (or lower) temperatures, through the use of the Gibbs-Helmholtz equation.

In this connection excess molar enthalpies for several binary and ternary mixtures involving ethers and hydrocarbons have been measured at the temperature 298.15 K and atmospheric pressure, over the whole mole fraction range. Values of the excess molar enthalpies were measured by means of a modified flow microcalorimeter (LKB 10700-1) and the systems show endothermic behavior.

The Redlich-Kister equation has been used to correlate experimental excess molar enthalpy data of binary mixtures. Smooth representations of the excess molar enthalpy values of ternary mixtures are accomplished by means of the Tsao-Smith equation with an added ternary contribution term and are used to construct excess enthalpy contours on Roozeboom diagrams. The values of the standard deviations indicate good agreement between experimental results and those calculated from the smoothing equations.

The experimental excess enthalpy data are also correlated and predicted by means of solution theories (Flory theory and Liebermann-Fried model) for binary and ternary mixtures, respectively. These solution theories correlate the binary heats of mixing data with reasonable accuracy. The prediction of ternary excess molar enthalpy by means of the solution theories are

also presented on Roozeboom diagrams. The predictions of ternary excess enthalpy data by means of these theories are reasonably reliable.

ACKNOWLEDGEMENTS

I am heartily grateful to my supervisor, Dr. Ding-Yu Peng, whose encouragement, constant guidance, and support from the initial to the final level enabled me to develop an understanding of the subject.

I would like to express sincere gratitude to my advisory committee members: Dr. Aaron Phoenix and Dr. Jafar Solatan for their invaluable suggestions during the course of my research.

I would like to thank Rlee Prokopishyn, Dragan Cekic, Richard Blondin, and Robert Wilson (Bob) for providing technical assistance in various stages of this work. My sincere thank goes to Rlee Prokopishyn for building the controllers for the pumps and to Bob for fixing the gears of the pump systems.

I would also like to thanks my friends Kawsar, Nazmul, Tariq, Siraj, and colleagues in the department, who helped to make my time in Saskatoon and in the department as pleasant as it could be.

Last but not the least, I deeply appreciate the encouragements and support from my parents, and other family members.

DEDICATION

To My Parents

TABLE OF CONTENTS

| | |
|---|----------|
| PERMISSION TO USE | I |
| ABSTRACT | II |
| ACKNOWLEDGEMENTS | IV |
| DEDICATION | V |
| TABLE OF CONTENTS | VI |
| LIST OF TABLES | IX |
| LIST OF FIGURES | XII |
| LIST OF ABBREVIATIONS | XVII |
| NOMENCLATURE | XVIII |
| 1. INTRODUCTION | 1 |
| 1.1 Purpose | 1 |
| 1.2 Excess Molar Enthalpy | 2 |
| 1.3 Objectives and Scope | 3 |
| 1.4 Thesis Outline | 4 |
| 2. LITERATURE REVIEW | 6 |
| 2.1 Methods for Obtaining Heats of Mixing | 6 |
| 2.1.1 Flow Calorimeter | 7 |
| 2.1.2 Isothermal Titration Calorimeter | 8 |
| 2.1.3 Differential Scanning Calorimeter | 9 |
| 2.2 System Studied | 10 |
| 2.3 Correlation of Excess Molar Enthalpy | 13 |
| 2.3.1 Empirical Expression | 13 |

| | |
|---|-----------|
| 2.3.2 Solution Theories | 15 |
| 3. MATERIALS AND METHODS | 20 |
| 3.1 Materials | 20 |
| 3.1.1 Degassing of Liquids | 21 |
| 3.2 Experimental Setup | 23 |
| 3.2.1 Calibration of the Calorimeter | 25 |
| 3.3 Operational Procedure | 27 |
| 3.3.1 Binary System | 27 |
| 3.3.2 Ternary System | 28 |
| 3.4 Verification of the Calorimeter | 31 |
| 4. RESULTS AND DISCUSSION | 34 |
| 4.1 Excess Molar Enthalpy of the Binary Systems | 34 |
| 4.1.1 Experimental Data Correlation: Binary Mixtures | 37 |
| 4.2 Excess Molar Enthalpy of Ternary Systems | 53 |
| 4.2.1 Predictions by means of the Flory Theory | 75 |
| 4.2.2 Prediction by means of the Liebermann-Fried Model | 79 |
| 5. CONCLUSIONS AND RECOMMENDATIONS | 84 |
| 5.1 Conclusions | 84 |
| 5.2 Recommendations | 85 |
| 6. REFERENCES | 86 |
| APPENDICES | |
| APPENDIX A | 91 |
| A1. Modification of Syringe Pump Motor Controller | 92 |

| | |
|---|-----|
| A2. Determination of Pump Constant | 94 |
| APPENDIX B | 99 |
| B1. Heats of Mixing of Binary Mixture | 100 |
| B2. Correcting of Weights for the Buoyancy of Air | 112 |
| B3. Heats of Mixing of Pseudo-Binary Mixture | 115 |
| APPENDIX C | 122 |
| C1.1 Statistics of Data Correlation | 123 |
| C2. Solution Theory Representation of Binary Systems | 125 |
| C3. Solution Theory Representation of Ternary Systems | 133 |

LIST OF TABLES

| | | |
|--------------------|---|----|
| Table 2.1. | Matrix of binary mixtures of interest in the current study | 11 |
| Table 2.2. | Six (6) ternary systems studied in this project | 12 |
| Table 3.1. | Source, purity and densities of component liquids at 298.15 K | 20 |
| Table 4.1. | Binary mixtures of current interest | 34 |
| Table 4.2a. | Experimental excess molar enthalpies, $H_{m,ij}^E$, at 298.15 K, for the binary systems | 35 |
| Table 4.2b. | Experimental excess molar enthalpies, $H_{m,ij}^E$, at 298.15 K, for the binary systems | 36 |
| Table 4.3. | Coefficients h_k and standard deviations s for the representations of the excess molar enthalpies $H_{m,ij}^E$ of the constituent binary mixtures at 298.15 K by means of equation (4.1) | 38 |
| Table 4.4. | Parameters used in Flory theory correlation | 46 |
| Table 4.5. | Interchange energy parameter, χ_{ij} , site fraction ratio, s_i/s_j , and standard deviations s for the representations of the excess molar enthalpies $H_{m,ij}^E$ of the constituent binary mixtures at 298.15 K by equation (4.3) | 47 |
| Table 4.6. | Parameter used in the Liebermann-Fried model correlation | 50 |
| Table 4.7. | Liebermann-Fried model parameters A_{ij} and A_{ji} , and standard deviations s for the representations of the excess molar enthalpies $H_{m,ij}^E$ of the constituent binary mixtures at 298.15 K by means of the equation (4.17) | 51 |
| Table 4.8. | Ternary mixtures studied | 53 |
| Table 4.9. | Experimental excess molar enthalpies $H_{m,1+23}^E$ and the calculated values of $H_{m,123}^E$ for the $x_1\text{DNPE} + x_2\text{DNBE} + (1 - x_1 - x_2)\text{1HX}$ ternary system at 298.15 K | 55 |
| Table 4.10. | Values of the coefficients in equation (4.19) and standard deviation of the fit for the ternary mixtures of current interest | 56 |
| Table 4.11. | Experimental excess molar enthalpies $H_{m,1+23}^E$ and the calculated values of $H_{m,123}^E$ for the $x_1\text{DNPE} + x_2\text{DNBE} + (1 - x_1 - x_2)\text{THF}$ ternary system at 298.15 K | 60 |

| | | |
|---------------------|--|-----|
| Table 4.12. | Experimental excess molar enthalpies $H_{m,1+23}^E$ and the calculated values of $H_{m,123}^E$ for the x_1 DNPE + x_2 22DMB + $(1 - x_1 - x_2)$ 23DMB ternary system at 298.15 K | 63 |
| Table 4.13. | Experimental excess molar enthalpies $H_{m,1+23}^E$ and the calculated values of $H_{m,123}^E$ for the x_1 DNBE + x_2 22DMB + $(1 - x_1 - x_2)$ 23DMB ternary system at 298.15 K | 66 |
| Table 4.14. | Experimental excess molar enthalpies $H_{m,1+23}^E$ and the calculated values of $H_{m,123}^E$ for the x_1 1HX + x_2 THF + $(1 - x_1 - x_2)$ 22DMB ternary system at 298.15 K | 69 |
| Table 4.15. | Experimental excess molar enthalpies $H_{m,1+23}^E$ and the calculated values of $H_{m,123}^E$ for the x_1 1HX + x_2 THF + $(1 - x_1 - x_2)$ 23DMB ternary system at 298.15 K | 72 |
| Table 4.16. | Interchange energy parameter χ_{ij} and the standard deviation s of the prediction of ternary system excess enthalpies by means of the Flory theory | 75 |
| Table 4.17. | Liebermann-Fried model parameter (A_{ij} and A_{ji}) matrix for binary systems | 79 |
| Table 4.18. | Standard deviation s of the prediction of ternary systems by means of the Liebermann-Fried model | 80 |
| Table A2.1. | Calibration Results for Pump A | 95 |
| Table A2. 2. | Calibration Results for Pump B | 97 |
| Table B-1.1. | Pure component properties | 100 |
| Table B1.2. | Calibration results of THF with pump A | 100 |
| Table B1.3. | Calibration results of 22DMB with pump B | 102 |
| Table B1.4. | Primary experimental data for THF (1) + 22DMB (2) binary mixture | 104 |
| Table B1.5. | Calculated excess molar enthalpy for THF (1) + 22DMB (2) binary system over the whole mole fraction range | 111 |
| Table B2.1. | Sample calculation: Binary mixture of {THF (1) + 22DMB (2)} | 113 |
| Table B2.2. | Summary of weighing | 113 |
| Table B3.1. | Pseudo pure mixture of {THF (1) + 22DMB (2)} | 115 |
| Table B3.2. | Calibration results of 1-hexene with pump A | 116 |

| | | |
|--------------------|--|-----|
| Table B3.3. | Calibration results of mixture # 2 {THF (1) + 22DMB (2)} with pump B | 118 |
| Table B3.4. | Primary experimental data for 1-hexene (1) + {THF (1) + 22DMB (2)} (2) binary mixture | 120 |
| Table B3.5. | Calculated excess molar enthalpy for [1-hexene (1) + {THF (1) + 22DMB (2)} (2)] pseudo binary mixture over the whole mole fraction range | 121 |
| Table C1.1. | <i>F</i> -statistical test summary | 125 |

LIST OF FIGURES

| | | |
|-----------------------|---|----|
| Figure 3.1. | Schematic diagram of vacuum degassing process | 22 |
| Figure 3.2. | Schematic diagram of experimental setup for heats of mixing measurement | 23 |
| Figure 3.3. | Schematics of the calorimeter unit | 24 |
| Figure 3.4. | Calibration circuit diagram | 26 |
| Figure 3.5. | Deviations $\delta H^E = \{H_m^E - H_{m,ij}^E \text{ (eq 3.11)}\}$ of the excess molar enthalpy at temperature 298.15K for the x_1 ethanol (1) + $(1 - x_1)$ <i>n</i> - hexane (2) system plotted against mole fraction x_1 . | 32 |
| Figure 4.1(a). | Excess molar enthalpies, $H_{m,ij}^E$, for the binary systems presented in Table 4.2a and 4.2b at the temperature 298.15 K. | 39 |
| Figure 4.1(b). | Excess molar enthalpies, $H_{m,ij}^E$, for the binary systems presented in Table 4.2a and 4.2b at the temperature 298.15 K. | 40 |
| Figure 4.1(c). | Excess molar enthalpies, $H_{m,ij}^E$, for the binary systems presented in Table 4.2a and 4.2b at the temperature 298.15 K. | 41 |
| Figure 4.1(d). | Excess molar enthalpies, $H_{m,ij}^E$, for the binary systems presented in Table 4.2b at the temperature 298.15 K. | 42 |
| Figure 4.2. | Excess molar enthalpies, $H_{m,ij}^E$, representation by means of the Flory theory for the binary systems presented in Table 4.2a and 4.2b at the temperature 298.15 K. | 48 |
| Figure 4.3. | Excess molar enthalpies, $H_{m,ij}^E$, representation by means of the Liebermann-Fried model for the binary systems presented in Table 4.2a and 4.2b at the temperature 298.15 K. | 52 |
| Figure 4.4. | Excess molar enthalpies, $H_{m,1+23}^E$, for the x_1 DNPE + x_2 DNBE + $(1 - x_1 - x_2)$ 1HX mixture at the temperature 298.15 K. | 58 |
| Figure 4.5. | Contours for constant values of $H_{m,123}^E / (\text{J} \cdot \text{mol}^{-1})$ for the x_1 DNPE + x_2 DNBE + $(1 - x_1 - x_2)$ 1HX system at 298.15 K. | 59 |
| Figure 4.6. | Excess molar enthalpies, $H_{m,1+23}^E$, for the x_1 DNPE + x_2 DNBE + $(1 - x_1 - x_2)$ THF mixture at the temperature 298.15 K. | 61 |
| Figure 4.7. | Contours for constant values of $H_{m,123}^E / (\text{J} \cdot \text{mol}^{-1})$ for the x_1 DNPE + x_2 DNBE + $(1 - x_1 - x_2)$ THF system at 298.15 K. | 62 |

| | | |
|---------------------|--|-----|
| Figure 4.8. | Excess molar enthalpies, $H_{m,1+23}^E$, for the x_1 DNPE + x_2 22DMB + $(1 - x_1 - x_2)$ 23DMB mixture at the temperature 298.15 K. | 64 |
| Figure 4.9. | Contours for constant values of $H_{m,123}^E/(J \cdot mol^{-1})$ for the x_1 DNPE + x_2 22DMB + $(1 - x_1 - x_2)$ 23DMB system at 298.15 K. | 65 |
| Figure 4.10. | Excess molar enthalpies, $H_{m,1+23}^E$, for the x_1 DNBE + x_2 22DMB + $(1 - x_1 - x_2)$ 23DMB mixture at the temperature 298.15 K. | 67 |
| Figure 4.11. | Contours for constant values of $H_{m,123}^E/(J \cdot mol^{-1})$ for the x_1 DNBE + x_2 22DMB + $(1 - x_1 - x_2)$ 23DMB system at 298.15 K. | 68 |
| Figure 4.12. | Excess molar enthalpies, $H_{m,1+23}^E$, for the x_1 1HX + x_2 THF + $(1 - x_1 - x_2)$ 22DMB mixture at the temperature 298.15 K. | 70 |
| Figure 4.13. | Contours for constant values of $H_{m,123}^E/(J \cdot mol^{-1})$ for the x_1 1HX + x_2 THF + $(1 - x_1 - x_2)$ 22DMB system at 298.15 K. | 71 |
| Figure 4.14. | Excess molar enthalpies, $H_{m,1+23}^E$, for the x_1 1HX + x_2 THF + $(1 - x_1 - x_2)$ 23DMB mixture at the temperature 298.15 K. | 73 |
| Figure 4.15. | Contours for constant values of $H_{m,123}^E/(J \cdot mol^{-1})$ for the x_1 1HX + x_2 THF + $(1 - x_1 - x_2)$ 23DMB system at 298.15 K. | 74 |
| Figure 4.16. | Excess molar enthalpies, $H_{m,1+23}^E$, for the x_1 DNPE + x_2 DNBE + $(1 - x_1 - x_2)$ 1HX mixture at the temperature 298.15 K (Flory theory representation). | 76 |
| Figure 4.17. | Contours for constant values of $H_{m,123}^E/(J \cdot mol^{-1})$ for the x_1 DNPE + x_2 DNBE + $(1 - x_1 - x_2)$ 1HX system at 298.15 K (Flory theory representation). | 77 |
| Figure 4.18. | Excess molar enthalpies, $H_{m,1+23}^E$, for the x_1 DNPE + x_2 DNBE + $(1 - x_1 - x_2)$ 1HX mixture at the temperature 298.15 K (Liebermann-Fried model representation). | 81 |
| Figure 4.19. | Contours for constant values of $H_{m,123}^E/(J \cdot mol^{-1})$ for the x_1 DNPE + x_2 DNBE + $(1 - x_1 - x_2)$ 1HX system at 298.15 K (Liebermann-Fried model representation). | 82 |
| Figure A1.1. | Schematic diagram of syringe pump controller. | 92 |
| Figure A2.1. | Calibration Curve for Pump A. | 96 |
| Figure A2.2. | Calibration Curve for Pump B. | 98 |
| Figure B1.1. | Calibration curve for THF in Pump A | 101 |
| Figure B1.2. | Calibration curve for 22DMB in Pump B | 103 |

| | |
|---|-----|
| Figure B3.1. Calibration curve for 1-hexene in Pump A | 117 |
| Figure B3.2. Mixture Calibration curve: {THF (1) + 22DMB (2)} in Pump B | 119 |
| Figure C2.1(a). Excess molar enthalpies $H_{m,ij}^E$ for the binary systems presented in Table 4.2a and 4.2b at the temperature 298.15 K (Flory theory representation). | 126 |
| Figure C2.1(b). Excess molar enthalpies $H_{m,ij}^E$ for the binary systems presented in Table 4.2a and 4.2b at the temperature 298.15 K (Flory theory representation). | 127 |
| Figure C2.1(c). Excess molar enthalpies $H_{m,ij}^E$ for the binary systems presented in Table 4.2a and 4.2b at the temperature 298.15 K (Flory theory representation). | 128 |
| Figure C2.1(d). Excess molar enthalpies $H_{m,ij}^E$ for the binary systems presented in Table 4.2b at the temperature 298.15 K (Flory theory representation). | 129 |
| Figure C2.2(a). Excess molar enthalpies $H_{m,ij}^E$ for binary the systems presented in Table 4.2a and 4.2b at the temperature 298.15 K (Liebermann-Fried model representation). | 130 |
| Figure C2.2(b). Excess molar enthalpies $H_{m,ij}^E$ for the binary systems presented in Table 4.2a and 4.2b at the temperature 298.15 K (Liebermann-Fried model representation). | 131 |
| Figure C2.2(c). Excess molar enthalpies $H_{m,ij}^E$ for the binary systems presented in Table 4.2a and 4.2b at the temperature 298.15 K (Liebermann-Fried model representation). | 132 |
| Figure C2.2(d). Excess molar enthalpies $H_{m,ij}^E$ for the binary systems presented in Table 4.2b at the temperature 298.15 K (Liebermann-Fried model representation). | 133 |
| Figure C3.1. Excess molar enthalpies, $H_{m,1+23}^E$, for the x_1 DNPE + x_2 DNBE + $(1 - x_1 - x_2)$ THF mixture at the temperature 298.15 K (Flory theory representation). | 134 |
| Figure C3.2. Contours for constant values of $H_{m,123}^E/(J \cdot \text{mol}^{-1})$ for the x_1 DNPE + x_2 DNBE + $(1 - x_1 - x_2)$ THF system at 298.15 K (Flory theory representation). | 135 |

- Figure C3.3.** Excess molar enthalpies, $H_{m,1+23}^E$, for the x_1 DNPE + x_2 22DMB + $(1 - x_1 - x_2)$ 23DMB mixture at the temperature 298.15 K (Flory theory representation). 136
- Figure C3.4.** Contours for constant values of $H_{m,123}^E/(J \cdot \text{mol}^{-1})$ for the x_1 DNPE + x_2 22DMB + $(1 - x_1 - x_2)$ 23DMB system at 298.15 K (Flory theory representation). 137
- Figure C3.5.** Excess molar enthalpies, $H_{m,1+23}^E$, for the x_1 DNBE + x_2 22DMB + $(1 - x_1 - x_2)$ 23DMB mixture at the temperature 298.15 K (Flory theory representation). 138
- Figure C3.6.** Contours for constant values of $H_{m,123}^E/(J \cdot \text{mol}^{-1})$ for the x_1 DNBE + x_2 22DMB + $(1 - x_1 - x_2)$ 23DMB system at 298.15 K (Flory theory representation). 139
- Figure C3.7.** Excess molar enthalpies, $H_{m,1+23}^E$, for the x_1 1HX + x_2 THF + $(1 - x_1 - x_2)$ 22DMB mixture at the temperature 298.15 K (Flory theory representation). 140
- Figure C3.8.** Contours for constant values of $H_{m,123}^E/(J \cdot \text{mol}^{-1})$ for the x_1 1HX + x_2 THF + $(1 - x_1 - x_2)$ 22DMB system at 298.15 K (Flory theory representation). 141
- Figure C3.9.** Excess molar enthalpies, $H_{m,1+23}^E$, for the x_1 1HX + x_2 THF + $(1 - x_1 - x_2)$ 23DMB mixture at the temperature 298.15 K (Flory theory representation). 142
- Figure C3.10.** Contours for constant values of $H_{m,123}^E/(J \cdot \text{mol}^{-1})$ for $\{x_1$ 1HX + x_2 THF + $(1 - x_1 - x_2)$ 23DMB $\}$ at 298.15 K (Flory theory representation). 143
- Figure C3.11.** Excess molar enthalpies, $H_{m,1+23}^E$, for the x_1 DNPE + x_2 DNBE + $(1 - x_1 - x_2)$ THF mixture at the temperature 298.15 K (Liebermann-Fried model representation). 144
- Figure C3.12.** Contours for constant values of $H_{m,123}^E/(J \cdot \text{mol}^{-1})$ for the x_1 DNPE + x_2 DNBE + $(1 - x_1 - x_2)$ THF system at 298.15 K (Liebermann-Fried model representation). 145
- Figure C3.13.** Excess molar enthalpies, $H_{m,1+23}^E$, for the x_1 DNPE + x_2 22DMB + $(1 - x_1 - x_2)$ 23DMB mixture at the temperature 298.15 K (Liebermann-Fried model representation). 146
- Figure C3.14.** Contours for constant values of $H_{m,123}^E/(J \cdot \text{mol}^{-1})$ for the x_1 DNPE + x_2 22DMB + $(1 - x_1 - x_2)$ 23DMB system at 298.15 K (Liebermann-Fried model representation). 147

- Figure C3.15.** Excess molar enthalpies, $H_{m,1+23}^E$, for the x_1 DNBE + x_2 22DMB + $(1 - x_1 - x_2)$ 23DMB mixture at the temperature 298.15 K (Liebermann-Fried model representation). 148
- Figure C3.16.** Contours for constant values of $H_{m,123}^E / (\text{J} \cdot \text{mol}^{-1})$ for the x_1 DNBE + x_2 22DMB + $(1 - x_1 - x_2)$ 23DMB system at 298.15 K (Liebermann-Fried model representation). 149
- Figure C3.17.** Excess molar enthalpies, $H_{m,1+23}^E$, for the x_1 1HX + x_2 THF + $(1 - x_1 - x_2)$ 22DMB mixture at the temperature 298.15 K (Liebermann-Fried model representation). 150
- Figure C3.18.** Contours for constant values of $H_{m,123}^E / (\text{J} \cdot \text{mol}^{-1})$ for the x_1 1HX + x_2 THF + $(1 - x_1 - x_2)$ 22DMB system at 298.15 K (Liebermann-Fried model representation). 151
- Figure C3.19.** Excess molar enthalpies, $H_{m,1+23}^E$, for the x_1 1HX + x_2 THF + $(1 - x_1 - x_2)$ 23DMB mixture at the temperature 298.15 K (Liebermann-Fried model representation). 152
- Figure C3.20.** Contours for constant values of $H_{m,123}^E / (\text{J} \cdot \text{mol}^{-1})$ for the x_1 1HX + x_2 THF + $(1 - x_1 - x_2)$ 23DMB system at 298.15 K (Liebermann-Fried model representation). 153

LIST OF ABBREVIATIONS

| | |
|-------|-----------------------------------|
| 1HX | 1-hexene |
| 22DMB | 2,2-dimethylbutane |
| 23DMB | 2,3-dimethylbutane |
| DC | Direct Current |
| DNBE | Di- <i>n</i> -butyl ether |
| DNPE | Di- <i>n</i> -propyl ether |
| DSC | Differential Scanning Calorimeter |
| DTA | Differential Thermal Analysis |
| HP | Hewlett-Packard |
| NRCC | National Research Council Canada |
| PFG | Precision Frequency Generator |
| THF | Tetrahydrofuran |

NOMENCLATURE

ENGLISH LETTERS

| | | |
|-----------------|---|--|
| <i>A</i> | Liebermann-Fried model interaction parameter | |
| <i>c</i> | Ternary parameter | |
| <i>E</i> | Voltage reading | volts (v) |
| <i>F</i> | A quantity used in eq C1.2 | |
| <i>f</i> | Molar flow rate | $\text{mol} \cdot \text{s}^{-1}$ |
| <i>G</i> | Gibbs free energy | $\text{J} \cdot \text{mol}^{-1}$ |
| \mathbb{G} | Gear Ratio | |
| <i>H</i> | Excess molar enthalpy | $\text{J} \cdot \text{mol}^{-1}$ |
| <i>h</i> | Redlich-Kister polynomial coefficient | |
| <i>I</i> | Current | ampere (A) |
| K_p | Pump calibration constant | $\text{cm}^3 \cdot \text{count}^{-1}$ |
| <i>k</i> | Coefficient in eq 3.2 | |
| <i>M</i> | Molecular weight | $\text{g} \cdot \text{gmol}^{-1}$ |
| <i>m</i> | Mass of substance | g |
| <i>N</i> | Number of components | |
| <i>n</i> | Number of experimental points | |
| <i>P</i> | Pressure | kPa |
| <i>p</i> | Parameter number | |
| <i>Q</i> | Volumetric flow rate | $\text{cm}^3 \cdot \text{s}^{-1}$ |
| <i>R</i> | Universal gas constant | $\text{J} \cdot \text{K}^{-1} \cdot \text{mol}^{-1}$ |
| <i>r</i> | Electrical resistance | ohm (Ω) |
| <i>S</i> | Entropy | $\text{J} \cdot \text{K}^{-1} \cdot \text{mol}^{-1}$ |
| <i>s</i> | Number of segments in a molecule (Flory theory) | |
| <i>T</i> | Temperature | K |
| <i>t</i> | Temperature | $^{\circ}\text{C}$ |
| <i>V</i> | Volume | cm^3 |
| <i>x</i> | Apparent mole fraction of component | |
| <i>Z</i> | Excess Property | |

GREEK LETTERS

| | | |
|---------------|---|-------------------------------|
| Λ | Wilson equation parameter (eq 2.2) | |
| α | Isobaric thermal expansivity | K^{-1} |
| γ | Activity coefficient | |
| Δ | Property change | |
| κ | Isothermal compressibility | atm^{-1} |
| ϵ | Calibration constant | $J \cdot v^{-1} \cdot s^{-1}$ |
| ϕ | Volume fraction | |
| χ | Interchange energy parameter (Flory theory) | |
| Ψ | A quantity used in eq 4.3 | |
| Φ | Segment fraction | |
| θ | Site fraction | |
| ρ | Density | $g \cdot cm^{-3}$ |
| \mathcal{R} | Counter reading | $counts \cdot s^{-1}$ |
| σ | Standard error | |
| ν, ι | Degrees of freedom | |

SUPERSCRIPTS

| | |
|---|---------------------------------|
| 0 | Ideal/Baseline |
| E | Excess function |
| * | Hardcore property |
| ~ | Reduced property (Flory theory) |

SUBSCRIPTS

| | |
|-----------------|---|
| 1, 2 | Pump indices |
| i, j, k, p, q | Component indices |
| A, B | Pumps notation |
| I | Interaction effect (Liebermann-Fried model) |

| | |
|------------|--------------------------------------|
| <i>cal</i> | Calculated values |
| <i>exp</i> | Experimental data |
| <i>H</i> | Humidity |
| <i>k</i> | Parameter indices |
| <i>M</i> | Mixture |
| <i>m</i> | Molar property |
| <i>P</i> | Isobaric properties |
| <i>p</i> | Pump |
| <i>r</i> | Reduced properties |
| <i>T</i> | Isothermal properties |
| <i>V</i> | Size effect (Liebermann-Fried model) |

1 INTRODUCTION

1.1 Purpose

The addition of oxygenated compounds to gasoline as additives instead of lead reduces the emissions of hazardous compounds mainly carbon monoxide. Ethers have been suggested as gasoline additives (Marsh et al. 1999). In this context the use of ethers as gasoline blending agents, requires the thermodynamic properties of mixtures involving hydrocarbons and ethers. Experimental data of the thermodynamic properties of these mixtures are required for process design calculation as well as to provide essential knowledge (i.e., types of molecular interaction) from the theoretical point of view.

Excess thermodynamic properties (excess molar enthalpy, excess molar volume, etc.) are of considerable practical importance to the development of chemical and petrochemical processes. The effects resulting from the mixing of two or more pure streams at constant temperature and pressure is of direct relevance to the design of process equipment. In particular the heat effect is directly related to the design of heat exchangers. For example the heat duty is directly proportional to excess molar enthalpy; which is one of the important thermodynamic properties of mixtures. Excess molar enthalpies can be either measured experimentally or estimated on the basis of solution theories.

The main purpose of the present study is to measure the experimental excess molar enthalpy (or heat of mixing) for several binary and ternary mixtures. Experimental data are used to test the applicability of existing solution theory/models (Flory theory and Liebermann-Fried model). Excess molar enthalpies of multicomponent mixtures are presented by this solution theory, using the parameters of constituent binary systems and properties of pure components.

1.2 Excess Molar Enthalpy

Thermophysical properties of real solutions are best described by the excess properties.

An excess molar property, Z_m^E , is defined by the following relation

$$Z_m^E = \Delta Z_m - \Delta Z_m^0 \quad (1.1)$$

where ΔZ_m is the molar property change of mixing of the real fluids, and ΔZ_m^0 is the molar property change of mixing of the same system when it behaves like an ideal solution. The molar property change of mixing for a real solution is given by the following equation

$$\Delta Z_m = Z_m - \sum_i x_i Z_{m,i} \quad (1.2)$$

where Z_m is the molar property of the real solution and $Z_{m,i}$ is the molar property of the pure component i , and x_i is its mole fraction in the mixture. Equations (1.1) and (1.2) give

$$Z_m^E = (Z_m - \sum_i x_i Z_{m,i}) - \Delta Z_m^0 \quad (1.3)$$

There are several excess properties that describe the behavior of a real solution mixture. They are the excess molar Gibbs free energy (G_m^E), excess molar entropy (S_m^E), excess molar volume (V_m^E), and excess molar enthalpy (H_m^E). In an ideal solution, the changes of these four molar properties due to mixing are

$$\Delta G_m^0 = RT \sum_i x_i \ln x_i \quad (1.4)$$

$$\Delta S_m^0 = -R \sum_i x_i \ln x_i \quad (1.5)$$

$$\Delta V_m^0 = 0 \quad (1.6)$$

$$\Delta H_m^0 = 0 \quad (1.7)$$

While the molar volume and molar enthalpy changes on mixing are zero at all (x, P, T) conditions for ideal solutions, the molar Gibbs free energy and molar entropy changes on mixing are non-zero for ideal solutions.

Thus the excess molar enthalpy, which is the main object of interest in the current study, is defined as

$$H_m^E = \Delta H_m \quad (1.8)$$

The excess molar enthalpy is identical with the molar enthalpy change on mixing and therefore is often termed as the heat of mixing. In experimental thermodynamics, this excess molar enthalpy is very important due to certain characteristics. First of all, it provides information about the energy content of the mixture, and secondly, it reflects the types of interaction involved between the molecules in the particular mixture (Smith et al. 2007). The information contained in the excess molar enthalpy (H_m^E) or excess molar Gibbs free energy (G_m^E) is the same as that contained in the activity coefficients (γ_i), according to the equation

$$H_m^E = -RT^2 \left[\frac{\partial(G_m^E)}{\partial T} \right]_{P,x} = -RT^2 \sum_i x_i \left[\frac{\partial(\ln \gamma_i)}{\partial T} \right]_{P,x} \quad (1.9)$$

The activity coefficients are one of the fundamental properties used for the design of chemical processes involving phase equilibria. In this connection, the excess molar enthalpy is very important not only for theoretical purposes but also for practical process design.

1.3 Objectives and Scope

This study is a part of a research program initiated in our laboratory to measure and describe the hydrocarbons and ethers mixtures thermodynamic properties such as excess enthalpies. The main experimental technique used in this work is flow calorimetry.

Flow calorimeters, similar to the one used in this work, are flexible and universal research tools. This excess enthalpy data can be used to obtain the vapor-liquid equilibria data.

Besides this the mixture prepared for measuring the ternary excess enthalpy can be used to determine the excess volumes.

The objectives of this work were the following:

1. Measure excess molar enthalpy for selected hydrocarbons and ethers systems over the whole mole fraction range at atmospheric pressure and temperature condition.
2. Correlate and predict the excess enthalpy data by means of the solution theories.

This study focuses on the calorimetric measurement of the excess enthalpy of a significant number of hydrocarbons-ethers systems (i.e., 10 binary and six ternary). The correlation of binary excess enthalpy data for the systems of interest is considered by means of the two solution theory (Flory theory, and Liebermann-Fried model). The parameters obtained in the correlation process of binary systems will be of considerable importance in predicting the multicomponent excess enthalpy of the systems containing the species considered in this study. This experimental investigation will enrich the thermophysical properties required for process design, especially system containing hydrocarbons and ethers.

1.4 Thesis Outline

This thesis is divided into five chapters. Chapter 1 provides a general overview of the importance of the excess molar enthalpy of hydrocarbons and ethers. The definition of the excess molar enthalpy is also presented in this chapter and the objectives and scope are stated.

Chapter 2 presents the review of the literature related to different types of calorimeters currently available for measuring the heats of mixing as well as different methods of representing excess molar enthalpy data.

Chapter 3 describes the material properties along with a detail description of the equipment and procedures used in this project. Validation of experimental set up and procedures are also presented in this chapter.

Chapter 4 presents and discusses the results obtained in this study. The representations of the experimental data are also stated in this chapter.

Finally, several conclusions and recommendation for future work have been summarized in chapter 5.

2 LITERATURE REVIEW

This chapter covers the review of literature related to different types of calorimeters for measuring heats of mixing, a search of literature for heat of mixing values, and the advantages and shortcomings for correlation and prediction of excess molar enthalpy data.

2.1 Methods for Obtaining Heats of Mixing

Excess molar enthalpy measurement is carried out by means of a calorimeter. Although, heat of mixing can, in principle, be calculated directly from excess molar Gibbs free energy measurements at multiple temperatures using the Gibbs-Helmholtz relation below.

$$H_m^E = -T^2 \left[\frac{\partial(G_m^E/T)}{\partial T} \right]_{P,x} \quad (2.1)$$

In practice, the results from this procedure are rarely of comparable accuracy to the heats of mixing values measured directly in a calorimeter and often do not even agree in sign. To obtain accurate values of excess molar enthalpy (heat of mixing) it is necessary to use a calorimeter.

A calorimeter is a device for measuring the heat effect that arises from the physical or chemical processes upon mixing of two or more components. Various types of calorimeters have been developed based on different modes of operation for measuring heats of mixing during the last several decades. There are three types of commercial calorimeters that are currently employed for measuring heats of mixing: flow microcalorimeters, isothermal titration calorimeters, and differential scanning calorimeters. This review is limited to those calorimeters that are operated under normal temperatures and pressures.

2.1.1 Flow Calorimeter

In a flow calorimeter, two component liquids are added to the mixing cell at steady flow rates and the change of enthalpy resulting from mixing process is measured under constant temperature and pressure. Monk and Wadso (1968) described a prototype of a flow reaction microcalorimeter (LKB 10700-1) for determining the heat of dilution of aqueous electrolyte. Later Tanaka et al. (1975) depicted the potential application of the flow microcalorimeter (LKB 10700-1) to non-electrolyte solutions. In the same paper they presented a modification of the flow microcalorimeter (LKB 10700-1) to measure the heat of mixing of hydrocarbons. In their modification, they improved the accuracy of heat of mixing measurement by modifying several auxiliary components of the calorimeter. The operating techniques of the flow microcalorimeter (LKB 10700-1) were further modified by Kimura et al. (1983). They reported 0.5% better precision than the previous measurement with the same type of calorimeter. The flow calorimeter became extremely popular among the investigators because these calorimeters can be used to generate high quality data. Their introduction also gave new momentum to the study of heats of mixing (Marsh and O'Hare, 1994). The research group of Dr. Benson at the University of Ottawa reported a substantial number of reliable excess molar enthalpy data of non-electrolyte systems with this calorimeter. The flow microcalorimeters have a variety of applications ranging from heats of mixing to kinetics of chemical reaction, and bio-molecular interaction (Leskiv et al. 2009).

One of the main advantages of the flow calorimeter is that with a variable flow setting a complete excess molar enthalpy composition curve can be produced very efficiently.

2.1.2 Isothermal Titration Calorimeter

Isothermal titration calorimeters are built on the similar heat conduction principle as the flow calorimeters. In a titration calorimeter, a fixed amount of liquid A is placed inside a vessel. While liquid A is continuously stirred by a magnetic stirrer, a second liquid B is injected by a syringe pump. The heat evolved during the interaction of liquid A with liquid B is monitored by the calorimeter. Liquid B can be introduced either continuously or periodically in fixed volumes. A prototype of an isothermal titration calorimeter was first described and developed by Christensen et al. (1968) and Wadso (1968). Initially the calorimeter was developed for measuring the heat of reaction of aqueous solutions. Holt and Smith (1974) modified the calorimeter for measuring the heats of mixing of hydrocarbons. The reported accuracy in excess molar enthalpy measurement by Holt and Smith (1974) is higher than that of the previous results. For measuring the heats of mixing with greater accuracy, the isothermal titration calorimeters are further developed by Rodriguez de Rivera et al. (2009). Previously this type of calorimeter was mostly used for measuring the thermodynamic properties of bio-molecular interaction. Most recently, Liao et al. (2010) reported an improved accuracy in excess enthalpy measurements for hydrocarbon containing systems with a commercial isothermal titration calorimeter. The advantage of using an isothermal titration calorimeter for measuring excess molar enthalpy is that it requires a smaller amount of component liquid and the measurement requires less time when compared with other types of calorimeters. But the use of isothermal titration calorimeters in excess molar enthalpy measurement is still in its preliminary stage.

2.1.3 Differential Scanning Calorimeter

Another versatile calorimeter is the differential scanning calorimeters (DSC). DSCs are used to measure a wide range of thermophysical properties of pure components as well as mixtures. The technique used with this type of calorimeter is known as differential thermal analysis (DTA). In differential thermal analysis “the difference in energy inputs into a substance (and/or its reaction product(s)) and a reference material is measured as a function of temperature whilst the substance and reference material are subjected to a controlled temperature programme” (Mackenzie, 1985). The first differential scanning calorimeter was developed by Watson et al. (1964). Differential scanning calorimeters are mainly used for glass transition temperature, crystallization, fusion, oxidation, heats of reaction, and heat capacity measurement. Application of differential scanning calorimeters to excess enthalpy measurement is very limited. Jablonski et al. (2003) applied the differential isothermal scanning technique which is one of the modes of operation of DSC that is suitable for measuring the heats of mixing. The reported accuracy of the measured excess molar enthalpy for the ethylene glycol + water system by means of the DSC was higher than that measured by the flow calorimeter. Though the accuracy of measurement is low in comparison with the flow calorimeter, it has several advantages over the others. For example, this type of calorimeter requires a very small amount of calorimetric fluid and measurement is relatively faster.

On the basis of the above discussion, a flow type calorimeter is selected for this study. However, the selection of calorimeter is dependent on the research requirements. As for the nature of the calorimetric experiments, a differential scanning calorimeter and an isothermal titration calorimeter is usually suitable for processes such as chemical reaction, phase change,

and bio-processes, whereas a flow calorimeter is much more efficient and reliable for measuring heat of mixing of liquid systems.

2.2 System Studied

Marsh et al. (1999) reviewed several thermophysical properties (excess enthalpy, excess volume, and vapor-liquid equilibria) of binary and ternary mixtures containing oxygenates (gasoline additives) and hydrocarbons. This review presents that there are still significant number of systems for which thermodynamic property measurement are insufficient. Based on that review, six (6) species (hydrocarbons and ethers) were selected in this study.


1. 1-hexene (1HX)
2. 2,2-dimethylbutane (22DMB)
3. 2,3-dimethylbutane (23DMB)
4. Di-*n*-butyl ether (DNBE)
5. Di-*n*-propyl ether (DNPE)
6. Tetrahydrofuran (THF)

Automotive fuels usually contain six main classes of organic compounds: paraffins, isoparaffins, olefins, naphthenes, aromatics (including polyaromatic compounds), and oxygenates. In this study the three hydrocarbon's (1HX, 22DMB, and 23DMB) are selected as they are the usual component of gasoline. The three ethers; DNBE, DNPE, and THF, are selected as the oxygen containing compound of gasoline. These ethers are currently being used or have potential to be used as a gasoline additive. Marsh et al. (1999) found that there is very little excess molar enthalpy measurement on systems containing branched alkanes and ethers. In the case of the

ethers, a large amount excess enthalpy data is available for systems containing DNBE but little excess enthalpy data is available for systems containing either of the other two ethers (DNPE, and THF). This six (6) species forms 15 binary systems. This is shown in a matrix as given by Table 2.1.

Table 2.1. Matrix of binary mixtures of interest in the current study

| Species | 1HX | DNBE | DNPE | THF | 22DMB | 23DMB |
|---------|-----|---------------------|------|-------------------|---------------------|-------------------------|
| 1HX | | Wang et al. (2004b) | | Lan et al. (2006) | Wang et al. (2004a) | Wang et al. (2004a) |
| DNBE | | | | | | |
| DNPE | | | | | | |
| THF | | | | | | |
| 22DMB | | | | | | Hamam and Benson (1986) |
| 23DMB | | | | | | |

 Mixtures studied in this project

Heats of mixing for the binary systems 1HX + 22DMB and 1HX + 23DMB were reported by Wang et al. (2004a). Since the structures of 22DMB and 23DMB are similar, the difference in magnitude of the heat of mixing for these systems is small. For the systems of 1-hexene with di-*n*-butyl ether and tetrahydrofuran, the excess molar enthalpy values have been reported by Wang et al. (2004b) and Lan et al. (2006), respectively. For the 1-hexene + di-*n*-butyl ether system, the heat of mixing values are exothermic and their magnitude is low, whereas

in the case of 1-hexene + tetrahydrofuran the heat of mixing values are endothermic with magnitude that are much higher than the other binary system. This is because during the mixing process the bond breaking of cyclic ether (tetrahydrofuran) requires more energy than the normal ether. Hamam and Benson (1986) reported excess enthalpy values for the 22DMB and 23DMB binary system. Since the components are similar in structure, they form a nearly ideal mixture, which is evident from the magnitude of excess enthalpy values. For the other ten binary mixtures involved in this work, there are no experimental results reported in the literature.

Twenty ternary systems can be formed by the six (6) species. There are no experimental results reported for these 20 ternary systems. However, as shown in Table 2.2, only six (6) among this 20 ternary systems have been chosen for this study due to the time constrain and a vast amount of experimental work.

Table 2.2. Six (6) ternary systems studied in this project

| Substance 1 | Substance 2 | Substance 3 |
|----------------------------|---------------------------|--------------------|
| Di- <i>n</i> -butyl ether | 2,2-dimethylbutane | 2,3-dimethylbutane |
| 1-hexene | Tetrahydrofuran | 2,2-dimethylbutane |
| | Tetrahydrofuran | 2,3-dimethylbutane |
| Di- <i>n</i> -propyl ether | 2,2-dimethylbutane | 2,3-dimethylbutane |
| | Di- <i>n</i> -butyl ether | Tetrahydrofuran |
| | Di- <i>n</i> -butyl ether | 1-hexene |

The literature search was performed using DECHEMA and DDBST GmbH online databank.

2.3 Correlation of Excess Molar Enthalpy

In thermodynamics, immense effort has been dedicated to finding ways of reliably correlating the thermodynamic properties of mixtures, particularly of two or more liquids. Data correlation approaches are very important in experimental work, because correlations reduce the difficulties involved in experimental procedures. There are several approaches available for correlating thermodynamic data of mixtures, some of them are empirical and some of them are theoretical. In the present study both of these two correlation approaches have been used for experimental data correlation. These two data correlation approaches for binary and ternary systems are described in the following section.

2.3.1 Empirical Expression

In scientific practice, a mathematical model can often be used to describe a property quantitatively. Empirical expressions are mathematical models that describe the general behavior of a property. In the representation of a thermodynamic property, empirical expressions are very useful and convenient but empirical expressions have limitations. The parameters of these expressions are fitted to the experimental data and the number of parameters can be determined according to the correlation accuracy required.

Binary Systems

There are several empirical expressions available in the literature for presenting excess thermodynamic properties of binary liquid mixtures. A universally used one is the simple algebraic relation of Redlich and Kister (1948), who assumed a particular form of H^E as a

function of mole fraction (x) with one or more adjustable parameters. The parameters are chosen by the method of least square to minimize the error in H^E . This equation obeys the general characteristic of H^E i.e., for both pure components, the H^E become zero. By choosing a sufficient number of parameters this equation can be fit to any set of experimental data. The expression of the Redlich-Kister polynomial is presented in section 4.1.1 of chapter 4.

Ternary Systems

As the number of components in the mixture increases, the determination of thermodynamic properties becomes more painstaking. Therefore, the applicability of predictive methods is of great interest for estimating ternary properties from the constituent binary experimental data. The main advantage of using empirical expressions is that they use the binary excess enthalpy data to calculate the ternary excess enthalpy data. There are several correlations that have been proposed for predicting ternary heats of mixing from constituent binary mixtures. Some of the models proposed are; Redlich and Kister (1948), Scatchard et al. (1952), Tsao and Smith (1953), and Kohler (1960). All of these models can be used satisfactorily to predict ternary heats of mixing from corresponding binaries. Among these, the Tsao and Smith (1953) correlation method with an added ternary contribution term by Morris et al. (1975) is popularly used due to its prediction accuracy. Benson and coworkers (1992-2006) found that the Tsao and Smith (1953) correlation method with a Morris et al. (1975) type ternary contribution term provides the best fit of excess molar enthalpy for ternary mixtures over the other correlation approach. These equations are presented in section 4.2 of chapter 4.

2.3.2 Solution Theories

Another approach for H^E correlation and prediction is based upon solution theory. The main purpose of the solution theories is to describe the behavior of the liquid mixture in terms of intermolecular interaction and structure of the molecules. There are several solution theories available in the literature and most of these solution theories are based on two concepts of liquid mixtures; the regular solution theory and the local composition theory. Although many solution theories have been developed to date, due to a limited understanding of intermolecular forces, they are still in an empirical or semi-empirical level. Usually, some of the parameters of these models have to be determined by regressing experimental data.

The very first solution theory that was developed for excess molar enthalpy was the van Laar model in the year 1906, which is based on the assumption that $V^E = S^E = 0$. Later this assumption of van Laar termed as the regular solution theory (Sandler, 1999). The regular solutions obey the relations $G^E = U^E = H^E$, $V^E = S^E = 0$, i.e. the same assumption as van Laar used.

The regular solution models are based on random mixing of molecules. However, due to intermolecular forces, the mixing of molecules is never entirely random; Wilson (1964) found a way to account for the non-randomness which led him to the famous Gibbs free energy equation based on the local composition concept.

$$G^E/RT = -\sum_i x_i \ln(1 - \sum_j x_j \Lambda_{ji}) \quad (2.2)$$

There are several models, which employ the local composition concept. As the local composition models account for the non-randomness of molecules, they can describe the mixture behavior more rationally than the regular solution models. Although there are many successful local composition models, it could be reasonably argued that the most well known and widely

used ones are the Wilson (Wilson, 1964), NRTL (Renon and Prausnitz, 1968), and UNIQUAC (Abrams and Prausnitz, 1975) equations. These local composition models are reported in the literature, and they all rely on different expression for excess Gibbs free energy. These models are originally developed for phase equilibria calculation and are also called activity coefficient models. These activity coefficient models can be used to represent the excess molar enthalpy of binary and multicomponent systems by means of the Gibbs-Helmholtz relation (eq 2.1)

Benson and coworkers (1993-2006) studied the heats of mixing for large number of binary and ternary mixtures involving hydrocarbons and oxygenates (alcohols & ethers). During the course of their study, they found that the Flory theory (Flory, 1965; Abe and Flory, 1965) and the Liebermann-Fried Gibbs free energy model (Liebermann and Fried, 1972a,b) have great potential to correlate and predict the excess molar enthalpy of non-polar binary and ternary systems, especially system containing hydrocarbons and ethers. Hence, these two solution models are adopted in this study to investigate the present binary and ternary mixtures. A short review of these two solution models is presented in the following section.

Flory Theory

The Flory theory (Flory, 1965; Abe and Flory, 1965) was originally proposed for liquid mixture of chain molecules. Based on the simple partition function, an equation of state was derived which is related to the excess function of mixtures (Flory, 1965). Benson and Pflug (1970) used the Flory equation for correlating the excess molar enthalpies of binary mixtures. In their approach they used the pure component properties, such as molar volume (V_m) isobaric thermal expansivity (α_p), and the isothermal compressibility (κ_T), and a single binary parameter, the interchange energy parameter (χ_{ij}), which is usually determined from the

regression of experimental data. Realizing the potential application of Flory theory in predicting a multicomponent mixture excess molar enthalpy using only the interaction parameters obtained from the constituent binary mixture and pure component properties, Wang et al. (1993), successfully applied the Flory theory to multicomponent mixture using the equation outlined by Brostow and Sochanski (1975). Later, Benson and coworkers (1993-2001) applied the Flory theory to a significant number of multicomponent systems. Peng et al. (1999) correlated the interchange energy parameter (χ_{ij}) of the Flory theory for 94 binary system in terms of acentric factor. The Flory equation for excess molar enthalpy for multicomponent system is presented in section 4.1.1 of chapter 4.

Liebermann-Fried Model

Many solution theories cannot be used to predict Gibbs free energy (G^E) from the experimental excess molar enthalpy (H^E) data with the aid of Gibbs-Helmholtz equation (eq 2.1) or *vice versa*. Realizing this fact, Liebermann and Fried (Liebermann and Fried, 1972a,b) proposed a Gibbs free energy (G^E) model, which is based on the sum of two separate terms.

$$G^E = G_I^E - RTf(G_V^E) \quad (2.3)$$

For binary system these two terms have the following expression

$$G_I^E = - \frac{x_1 x_2 \ln(A_{12} A_{21})}{(x_1 + x_2 A_{12})(x_2 + x_1 A_{21})} \quad (2.4)$$

and

$$RTf(G_V^E) = RT[x_1 \ln(x_1 + x_2 V_{m2}/V_{m1}) + x_2 \ln(x_2 + x_1 V_{m1}/V_{m2})] \quad (2.5)$$

The first term is responsible for the non-ideal behavior of liquid mixture due to intermolecular interaction. The second term accounts for the presence of different sized molecules in the mixture. This proposed model of Liebermann and Fried has two empirical parameters, which were determined by regressing either experimental G^E or H^E data. Another shortcoming of many solution theories is the temperature independency of the empirical parameter. This was also overcome by Liebermann and Fried (1972b) who introduced a correlation to account for the temperature dependency of the interaction parameter. The expression of the correlation presented by Liebermann and Fried (1972b) is

$$k = \frac{A''_{ij}}{A'_{ij}} \quad (2.6)$$

where, A'_{ij} is the interaction parameter at a reference temperature T' obtained by regressing the experimental data. A''_{ij} is the interaction parameter at a different temperature T'' . And the constant k is obtained from the following relation

$$2 \ln k - k \left(\frac{T'}{T''} \right)^2 \ln(A'_{ij}A'_{ji}) + \ln(A'_{ij}A'_{ji}) = 0 \quad (2.7)$$

Wang and Lu (2000) used the Lieberman-Fried model to correlate the experimental excess molar enthalpy and successfully predicted the binary vapor-liquid equilibria (VLE) for a methyl *tert*-butyl ether + alkanes mixture using the parameters determined earlier at a different temperature. Peng et al. (2001a, b) predicted the multicomponent VLE from the Liebermann-Fried model using only the binary interaction parameters determined from the excess molar enthalpy values of the constituent binary mixtures. They also showed that the parameter determined from the excess molar enthalpy data at one temperature can be used to predict VLE of the same system at another temperature. Wang et al. (2001) also showed that the Lieberman-Fried model can be employed for the prediction of ternary excess molar enthalpy using only the

constituent binary interaction parameters. The equation for representing the excess molar enthalpy from the Liebermann-Fried model is presented in section 4.1.1 of chapter 4.

3 MATERIALS AND METHODS

3.1 Materials

The properties along with the source and purities of the chemicals used in this study are listed in Table 3.1. Apart from storing the ethanol over Type 4A molecular sieve beds, all the chemical were used without further purification. All the chemicals were degassed prior to use by means of the vacuum technique.

Table 3.1. Source, purity and densities of component liquids at 298.15 K

| Materials | Source | Purity (%) | Density/ ($\text{g} \cdot \text{cm}^{-3}$) | |
|----------------------------|---------------|------------|--|------------------------|
| | | | Measured | Literature |
| Ethanol | Alcohol Inc. | >99.9 | 0.78520 | 0.78560 ^(a) |
| <i>n</i> -hexane | Alfa Aesar | >99 | 0.65516 | 0.65512 ^(a) |
| 1-hexene | Alfa Aesar | >99 | 0.66876 | 0.66873 ^(b) |
| 2, 2-dimethylbutane | Alfa Aesar | >99 | 0.64459 | 0.64492 ^(b) |
| 2, 3-dimethylbutane | Sigma-Aldrich | >99 | 0.65702 | 0.66236 ^(b) |
| Di- <i>n</i> -propyl ether | Alfa Aesar | >99 | 0.74198 | 0.74259 ^(c) |
| Di- <i>n</i> -butyl ether | Sigma-Aldrich | >99 | 0.76399 | 0.76394 ^(d) |
| Tetrahydrofuran | Sigma-Aldrich | >99 | 0.88208 | 0.88209 ^(e) |

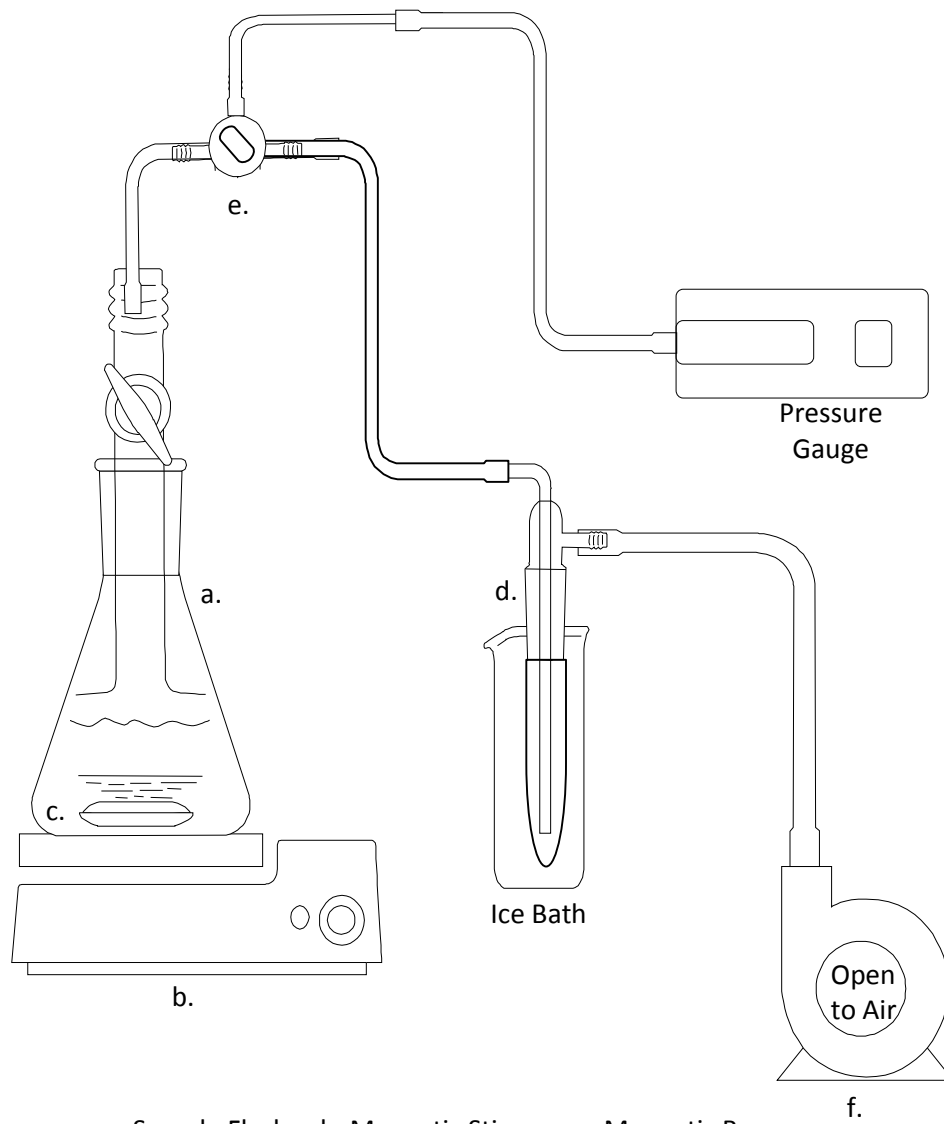
^(a)Wang et al. (1992); ^(b)Wang et al. (2004a); ^(c)Liao et al. (1997)^(d); Peng et al. (2002); ^(e)Lan et al. (2006).

The densities of these materials were determined by means of an Anton Paar digital density meter (DMA-5000M). The uncertainty of density and temperature measurement were $\pm 0.000005 \text{ g} \cdot \text{cm}^{-3}$ and $\pm 0.001 \text{ }^\circ\text{C}$, respectively as provided by the manufacturer. In Table 3.1 the measured density (at $t = 24.999 \text{ }^\circ\text{C}$) in the current study were given along with literature values.

3.1.1 Degassing of Liquid

Dissolved gases in pure component liquid have erroneous effect on the thermodynamic property measurement (excess molar enthalpy, vapor-liquid equilibria and density). Most of the gases (air, nitrogen, oxygen, hydrogen and carbon dioxide etc) that are dissolved in hydrocarbons decrease the density except carbon dioxide, which increases the density (Ashcroft and Isa, 1997). In flow microcalorimetric excess molar enthalpy measurement, dissolved gas increases the possibility of bubble formation in the mixing cell. This bubble formation leads to erroneous results of excess molar enthalpy (Tanaka et al. 1975). To avoid these shortcomings, all the component liquids were degassed by means of the vacuum (pressure reduction) method (Figure 3.1).

The flask (a) with a pure component liquid was placed on a magnetic stirrer (b), which drove the magnetic bar (c) inside the flask to agitate the liquid. The outlet of the flask was connected to a vacuum trap (d) through a 3-way valve (e). The other end of the vacuum trap was connected to the vacuum pump (f). When the vacuum pump was turned on a negative pressure was created in the system, which reduced the solubility of the dissolved gas in the component liquid. Stirring under reduced pressure helps to increase the efficiency of degassing. The degassing process is relatively faster and easier than other method of degassing (Heating, Substitution by inert gas). The vacuum trap was placed in an ice batch, which prevents the release of the component liquid as vapor, the component vapor condensing with the trap. This degassing process continues until the gas bubbles in the pure liquid have disappeared. This process requires about five to ten minutes.



a. Sample Flask; b. Magnetic Stirrer; c. Magnetic Bar;
 d. Vacuum Trap; e. 3-way Valve ; f. Vacuum Pump

Figure 3.1. Schematic diagram of vacuum degassing process

3.2 Experimental Setup

Excess molar enthalpies have been measured by means of a modified flow microcalorimeter (LKB 10700-1). The auxiliary equipment and the operating procedure of the microcalorimeter were modified by Tanaka et al. (1975) to improve the precision of heats of mixing measurement. The modification made in particular to the original air bath temperature controlling system. The output of the thermopile circuit was digitized by acquiring the data in a microcomputer through amplification. The original calibration circuit was modified to provide a digital measure of the current supplied. Also the original flow system of the calorimeter was modified.

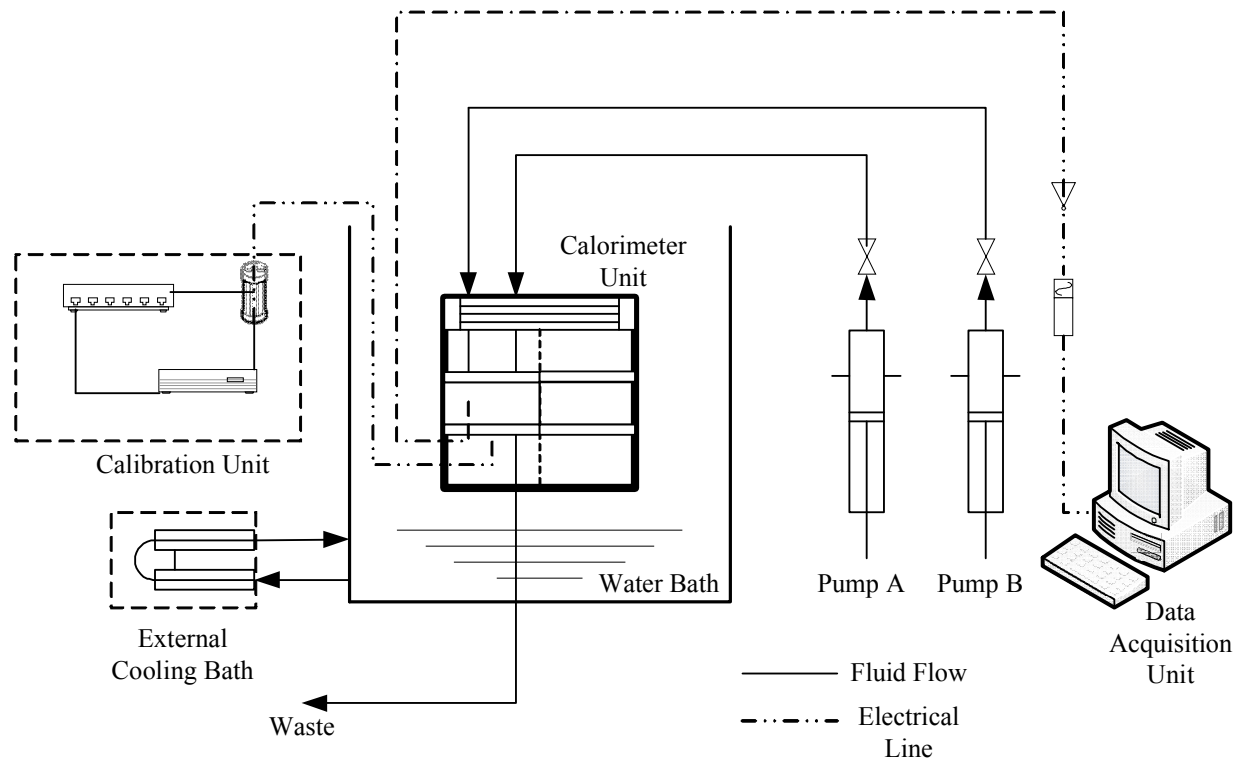


Figure 3.2. Schematic diagram of experimental setup for heats of mixing measurement

Figure 3.2 shows the schematic diagram of experimental setup, which consist of a calorimeter, a calibration unit, an external thermostatic bath, flow system, and data acquisition unit. The calorimeter unit is placed in the water bath whose temperature is controlled by the external thermostatic bath at a desired temperature. The temperature of the water bath is monitored by means of thermometer (HP, Model-2804A). The temperature of the water bath is maintained at 0.005 °C variation under the experimental condition. Two precision positive displacement syringe pumps with four adjustable gear ratios, built in the national research council Canada (NRCC) is used to delivered the calorimetric fluid through the teflon tubing at a constant flow rate in the calorimeter mixing cell. The previous analog flow measuring unit (Tanaka et al. 1975) is replaced by a microprocessor equipped flow measuring unit. The details of the modification are presented in Appendix A1. The details of the calibration unit and calibration process are described in section 3.2.1. The data acquisition unit consists of a signal amplifier (NUDAM, ND-6011), a digital signal converter (NUDAM, ND-6520) and a microcomputer.

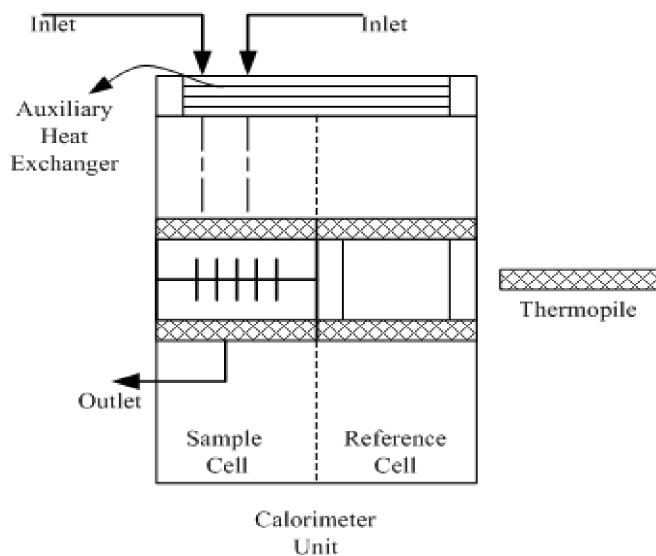


Figure 3.3. Schematics of the calorimeter unit

The microcalorimeter unit (Figure 3.3) consists of an auxiliary heat exchanger, two calorimetric cells and a series of thermocouples (thermopile). Originally, of the two calorimetric cells, one was functioning as the main mixing cell and the other as a reference cell. Tanaka et al. (1975) found that the baseline voltage of the calorimeter can be reduced if the reference cell was kept empty and they connected the inlet and outlet of the reference cell together. The mixing cell was sandwiched between two thermopiles (series of thermocouples). Any changes in temperature in the mixing cell are detected by these thermopiles and the thermopile differential voltage is collected in the computer through the data acquisition system.

3.2.1 Calibration of the Calorimeter

Calibration plays a very important role in the heat of mixing measurement. It establishes the relation between the heat effect and thermoelectric output when there is no mixing of fluids. This relation is established for each pure fluid at constant temperature, and for each syringe pump at different flow rates. For establishing this relation there are two different approaches available in calorimetric practice: electrical and chemical. Only the electrical calibration procedure is discussed here. In this procedure, one pure component liquid was pumped at a constant motor speed (i.e., 450, 690, 830, 1070, 1310 and 1650 counts \cdot s⁻¹) through the mixing cell. The baseline voltage due to flow (E_Q^0) was recorded. The calibration heater was then turned on, to simulate the mixing process. At this point the baseline voltage shifts, after a certain period of time the voltage became steady, and then the voltage (E_Q) was recorded.

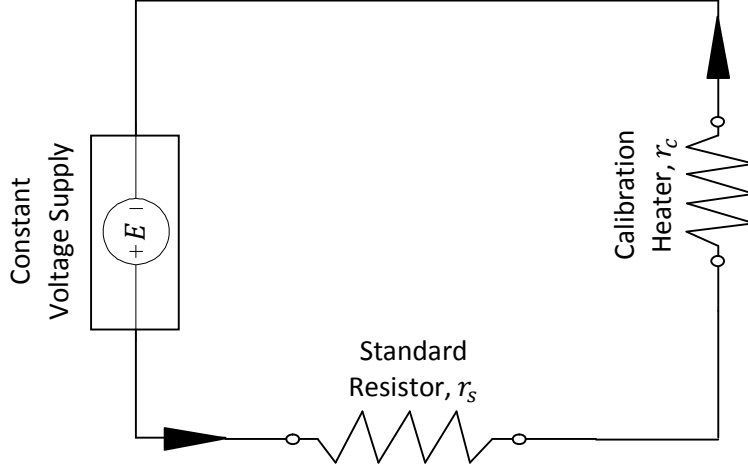


Figure 3.4. Calibration circuit diagram

For this purpose a constant DC voltage from a power supply (Trygon PLS 50-1) was applied to the calorimeter heater through a standard resistance r_s in series, while the fluid flow through the calorimeter at a selected flow rate. The potential across the resistance and the current passes through the heater were recorded using a digital multimeter (Keithly Model 171). The current ($I = E/r_s$) passing through the calorimeter heater having a resistance r_c , supplies a power of $I^2 r_c$ to the calorimetric cell. This power causes the baseline voltage to shift to E_Q . The calibration constant is thus, calculated by the following equation.

$$\mathcal{E}/(J \cdot s^{-1} \cdot v^{-1}) = \frac{I^2 r_c}{E_Q^0 - E_Q} = \frac{(E/r_s)^2 r_c}{E_Q^0 - E_Q} \quad (3.1)$$

where the units of I, E (E & E_Q), and r (r_s & r_c) are ampere(A), volts(v), and ohm(Ω) respectively. The value of the standard resistance, r_s , was 10.00Ω , and the calibration resistance, r_c , was 49.52Ω .

This procedure was repeated for different flow rates. A calibration curve showing \mathcal{E} vs. counter reading(\mathcal{R}) was then obtained for each calorimetric fluid.

Tanaka et al. (1975) found that the calibration constant is a function of volumetric flow rate and the volumetric heat capacity. Later Kimura et al. (1983) used a water bath instead of the

air bath originally used by Tanaka et al. (1975) and found that the effect of volumetric heat capacity is negligible for normal operation. Replacement of the air bath by the water bath also improves the stability of the baseline voltages. A similar relation between calibration constant, \mathcal{E} , and flow rate, \mathcal{R} , has been found in the present:

$$\mathcal{E} = k_0 + k_1\mathcal{R} \quad (3.2)$$

where k_0 and k_1 are constant for a given liquid, and the flow rate \mathcal{R} has units of $\text{counts} \cdot \text{s}^{-1}$.

3.3 Operational Procedure

3.3.1 Binary System

The heat of mixing measurement was started when the external water bath had been kept running for several hour to get a steady temperature of 25.000 ± 0.005 °C. For a binary system, the component liquids after degassing were charged to the syringe pump. Then both the component liquids were pumped at specified constant flow rates that would lead to the combined flow rate of the two pumps equal to $0.005 \text{ cm}^{-3} \cdot \text{s}^{-1}$. By doing this, it was possible to set the motor speed and gear ratio to produce any mole fraction within an estimated error of ± 0.0005 (Tanaka et al. 1975).

To check the repeatability of the measurement, the measurement was started at a mole fraction near $x_1 = 0.5$ and ended with a pure component 1 (i.e., $x_1 = 1.0$) changing the mole fraction in increments of 0.05. This finished one half of the run. The measurement was started again near $x_1 = 0.5$ and ended with pure component 2 (i.e., $x_1 = 0.0$).

The voltage readings at $x_1 = 0.0$ and $x_1 = 1.0$ were taken as baseline voltages $E_2^0(Q_2)$ and $E_1^0(Q_1)$, respectively, for the pure component liquids. The baseline voltage for a mixture $E_M^0(Q)$, the same as that presented by Tanaka et al. (1975).

$$E_M^0(q) = \phi_1 E_1^0(Q) + \phi_2 E_2^0(Q) \quad (3.3)$$

where ϕ_i is the volume fraction of component i , which is defined as $\phi_i = Q_i / \sum_j Q_j$.

The voltage reading for every experimental point was registered on a computer through an instrument coupler (ICS Electronics Corporation, Model: 4880). An average of 200 data points was taken as the final voltage reading of the mixture.

The values of excess molar enthalpies of the mixture are calculated from the relation given by Tanaka et al. (1975):

$$H_m^E = \frac{\mathcal{E}_M [E_M(Q) - E_M^0(Q)]}{(Q_1/V_{m_1} + Q_2/V_{m_2}) \times (Q_1 + Q_2)} \quad (3.4)$$

where V_{m_i} is the molar volume of component i . The mixture calibration constant, \mathcal{E}_M , for the mixture was obtained from the pure component calibration constant, \mathcal{E}_i and the flow rates of the constituent pure substances by the following equation.

$$\mathcal{E}_M / (\text{J} \cdot \text{v}^{-1} \cdot \text{cm}^3) = Q_1 \mathcal{E}_1 + Q_2 \mathcal{E}_2 \quad (3.5)$$

Details of the calculation procedure for binary system are presented in Appendix B1.

3.3.2 Ternary System

Measurement of ternary heats of mixing involved several steps. First of all, the excess molar enthalpy for the binary mixtures of component 2 and component 3 were measured over the whole mole fraction range. Then the experimental data was fitted with a smoothing equation (Redlich-Kister) to get excess molar enthalpy at any desired mole fraction. In the second step, three binary mixture of component 2 and component 3 at a fixed mole fraction ratio ($x_2/x_3 = 0.25, 0.50, 0.75$) were prepared. The prepared binary mixtures were taken to be a pseudo-pure component to measure the excess molar enthalpy $H_{m,1+23}^E$ for the ternary mixture consisting of

component 1 and the binary mixture of component 2 and component 3. Since the mixtures of components 1+23 used in this step are not true binary mixtures, they are referred to as pseudo-binary mixture. Finally, the ternary excess molar enthalpy $H_{m,123}^E$ was determined by means of the following equation.

$$H_{m,123}^E = H_{m,1+23}^E + (1 - x_1)H_{m,23}^E \quad (3.6)$$

where $H_{m,23}^E$ is the excess molar enthalpy of particular binary mixture and x_1 is the mole fraction of component 1.

Preparation of the Pseudo-Binary Mixture

A Mettler H315 precision balance (Fisher Scientific Company) with a readability of 0.1 mg and a range of 1000 g was used for preparing all the binary mixtures in this study. An appropriate amount of degassed component 2 was weighed and poured in to a flask. Then component 3 was weighed and poured into the same flask. Prepared binary mixture were stored in a glass flask with a magnetic stirring bar and place on a magnetic stirrer for proper mixing. Before the measurement the room temperature, barometric pressure and relative humidity were recorded to correct the measurement to give the weight in vacuum.

The preparation of a specified composition binary mixture involves two steps: pre-estimation of weights and the correction of the measurements to give the weights in vacuum.

Pre-estimation of Weights

Before the preparation of a specific binary mixture, the amounts of each component required were estimated. The weight estimation process is described in the following example: For a specific binary mixture, the mole fractions were calculated by the following formula:

$$x_1 = \frac{\frac{m_1}{M_1}}{\frac{m_1}{M_1} + \frac{m_2}{M_2}} \quad \text{and} \quad x_2 = \frac{\frac{m_2}{M_2}}{\frac{m_1}{M_1} + \frac{m_2}{M_2}} \quad (3.7)$$

where, M_i and m_i are the molecular weight and expected mass of component i , respectively.

For a binary mixture of $x_1 = x_2 = 0.50$ the weight ratio is as follows

$$\frac{m_1}{M_1} = \frac{m_2}{M_2} \quad \text{or} \quad m_2 = M_2 \frac{m_1}{M_1} \quad (3.8)$$

The m_1 and m_2 can be expressed in terms of the volume by the following equation

$$m_i = \rho_i V_i \quad (3.9)$$

where, ρ_i and V_i are density and volume of component i , respectively.

With equations (3.8) and (3.9), the volume ratio of the two components was then determined as

$$V_2 = \frac{m_2}{\rho_2} = \frac{m_1 M_2}{M_1 \rho_2} \quad (3.10)$$

Equations (3.7) to (3.10) provide a guideline for preparing binary mixture at a selected mole fraction.

Weight Correction

According to Archimedes principle, when an object is weighed while immersed in a fluid environment that object is subject to a buoyancy effect from the surrounding fluid. In this connection, when a sample is weighed upon any analytical balance, the sample experiences the effect of buoyancy of the surrounded air (Bauer, 1959). In the present study, the pure component liquid being weighed also experiences this buoyant effect of air. So, before calculating the mole fraction and molecular weight of the prepared binary mixture, the weight of pure component liquid must be corrected to account for the buoyancy of air by means of the formula given by Bauer (1959). A sample calculation of the weight correction in vacuum is presented in Appendix B2.

Measurement of $H_{m,1+23}^E$ Pseudo Binary mixtures

Pure component 1 was pumped into the calorimeter by pump A, while a prepared binary mixture consisting of component 2 and component 3 was pumped as a pseudo-pure component to the mixing cell by pump B. Excess molar enthalpy calculation procedure for the pseudo binary mixture is identical to that for a binary mixture.

All the prepared ‘fixed composition’ binary mixtures were calibrated using pump B. The calibration procedure for the mixture is the same as that outlined for the pure substance in section 3.2.1. A complete sample calculation of heat of mixing for a pseudo binary mixture is presented in Appendix B3.

3.4 Verification of the Calorimeter

It was necessary to check the reliability of the experimental setup in order to ensure the accuracy of the experimental results. In this respect, the ethanol (1) + *n*-hexane (2) binary system was used to check the reliability of the calorimeter. O’Shea and Stokes (1986) measured the heat of mixing of this system by means of an isothermal dilution calorimeter.

The works of O’Shea and Stokes (1986) presents the most complete set of data and is taken as the main reference system. However, current data is also compared with the data from Wang et al. (1992), who used a flow microcalorimeter (LKB 10700-1), and from Mato et al. (2006) whose data were measured by a Calvet microcalorimeter. The result of the present study along with the results of the above mentioned three different investigations of the same binary system have been correlated using the smoothing function given by O’Shea and Stokes (1986).

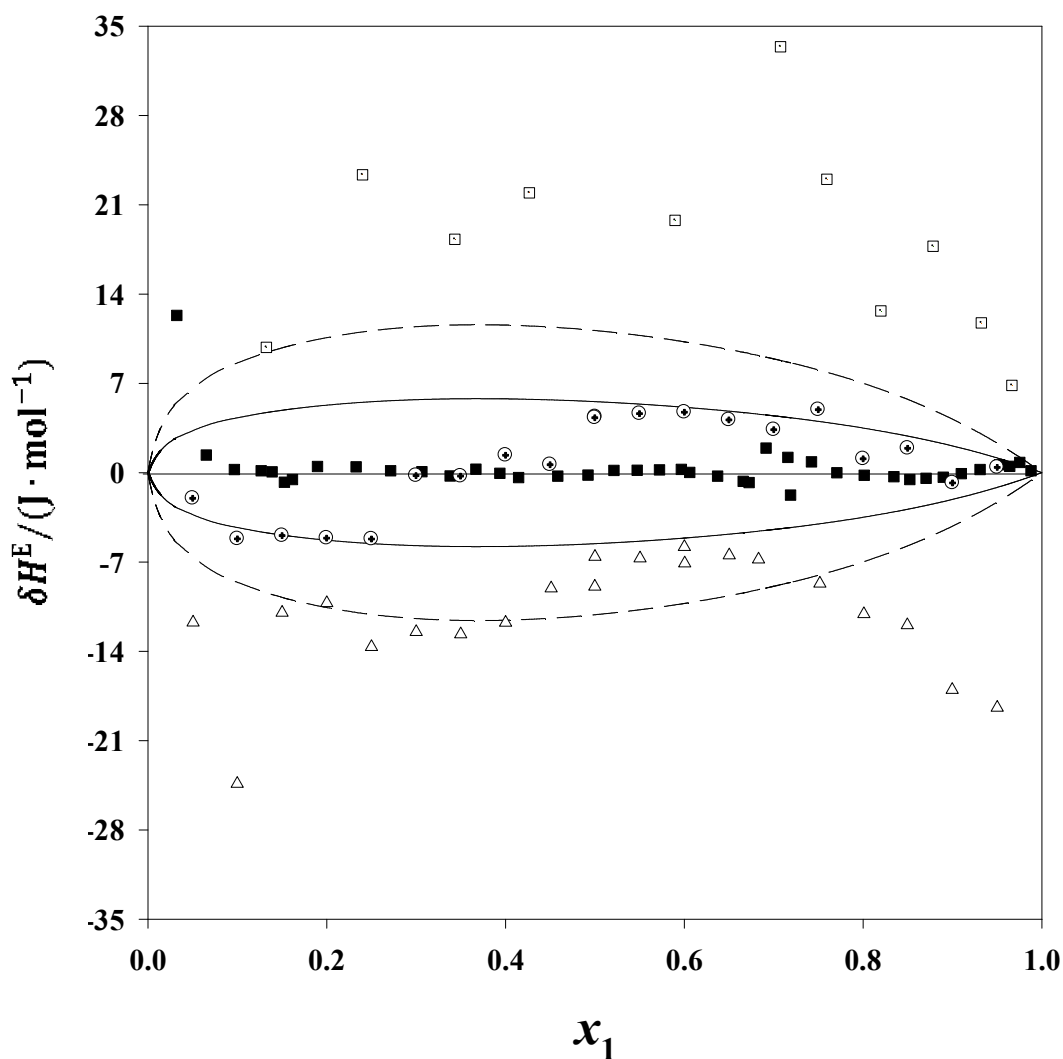


Figure 3.5. Deviations $\delta H^E = \{H_m^E - H_{m,ij}^E \text{ (eq 3.11)}\}$ of the excess molar enthalpy at temperature 298.15K for x_1 ethanol(1) + x_2 *n*-hexane(2) plotted against mole fraction x_1 . Experimental Results: \oplus , Present work; \blacksquare , O'Shea and Stokes (1986); Δ , Wang et al. (1992); \square , Mato et al. (2006); Curves: — , $\pm 1\%$, and --- , $\pm 2\%$ deviation from equation (3.11).

$$H_m^E / (\text{J} \cdot \text{mol}^{-1}) = x_1(1 - x_1) \{1 + 0.96(2x_1 - 1)\}^{-1} \{2227.55(2x_1 - 1) + 1472.22(2x_1 - 1)^2 + 470.59(2x_1 - 1)^3 + 641.92(2x_1 - 1)^4 + 212.41(2x_1 - 1)^5\} \quad (3.11)$$

The deviations of experimental results from the smoothed results of O'Shea and Stokes are plotted and compared with other sets of data from the literature in Figure 3.5. The figure serves to show that the average discrepancy of the present data is less than $\pm 1\%$ of the calculated enthalpy from the O'Shea and Stokes correlation for each mole fraction in the central range of composition.

4 RESULTS AND DISCUSSION

The heats of mixing for the ten binary and six ternary systems of interest are presented and discussed in this chapter. The experimental results for the binary mixtures along with the Redlich-Kister correlation are presented first. The experimental results are also correlated using the Flory theory (1965) and the Liebermann-Fried model (1972). The excess molar enthalpy for six ternary mixtures and the correlation of the experimental data by means of the Tsao and Smith (1953) equation are then presented and discussed. The excess enthalpy predictions of the ternary systems by means of the solution theories are also presented.

4.1 Excess Molar Enthalpy of the Binary Systems

The ten (10) binary systems studied in this project are listed in Table 4.1. The experimental excess molar enthalpy data for these mixtures were determined at 298.15 K and are summarized in Tables 4.2a and 4.2b.

Table 4.1. Binary mixtures of current interest

| System | Component 1 | Component 2 |
|--------|-------------|-------------|
| 1 | THF | 22DMB |
| 2 | THF | 23DMB |
| 3 | DNBE | 22DMB |
| 4 | DNBE | 23DMB |
| 5 | DNBE | THF |
| 6 | DNPE | THF |
| 7 | DNPE | 1HX |
| 8 | DNPE | DNBE |
| 9 | DNPE | 22DMB |
| 10 | DNPE | 23DMB |

Table 4.2a. Experimental mole fractions x_i and excess molar enthalpies, $H_{m,ij}^E$, at 298.15 K, for the binary systems

| x_i | $\frac{H_{m,ij}^E}{(\text{J} \cdot \text{mol}^{-1})}$ | x_i | $\frac{H_{m,ij}^E}{(\text{J} \cdot \text{mol}^{-1})}$ | x_i | $\frac{H_{m,ij}^E}{(\text{J} \cdot \text{mol}^{-1})}$ | x_i | $\frac{H_{m,ij}^E}{(\text{J} \cdot \text{mol}^{-1})}$ |
|-----------------------------|---|--------|---|--------|---|--------|---|
| THF (i) + 22DMB (j) | | | | | | | |
| 0.0500 | 128.4 | 0.2999 | 568.4 | 0.5001 | 685.0 | 0.7500 | 525.0 |
| 0.1000 | 240.4 | 0.3498 | 619.4 | 0.5500 | 679.5 | 0.8002 | 448.4 |
| 0.1500 | 344.3 | 0.4000 | 655.8 | 0.6003 | 660.2 | 0.8501 | 359.9 |
| 0.2000 | 431.5 | 0.4500 | 675.4 | 0.6499 | 628.1 | 0.9000 | 255.3 |
| 0.2505 | 507.7 | 0.5002 | 684.7 | 0.7001 | 584.2 | 0.9500 | 136.4 |
| THF (i) + 23DMB (j) | | | | | | | |
| 0.0500 | 126.7 | 0.3000 | 566.7 | 0.5002 | 678.0 | 0.7500 | 516.6 |
| 0.0999 | 241.7 | 0.3500 | 614.7 | 0.5502 | 671.2 | 0.7999 | 445.0 |
| 0.1500 | 343.3 | 0.4000 | 648.1 | 0.6000 | 652.1 | 0.8500 | 356.9 |
| 0.2000 | 431.6 | 0.4499 | 669.5 | 0.6502 | 619.0 | 0.9000 | 255.7 |
| 0.2500 | 507.1 | 0.5002 | 677.9 | 0.6999 | 576.3 | 0.9500 | 137.1 |
| DNBE (i) + 22DMB (j) | | | | | | | |
| 0.0500 | 27.2 | 0.2996 | 93.7 | 0.5004 | 102.5 | 0.7501 | 72.3 |
| 0.1000 | 46.7 | 0.3501 | 99.1 | 0.5499 | 99.8 | 0.8000 | 62.2 |
| 0.1499 | 62.7 | 0.3998 | 102.9 | 0.6002 | 95.3 | 0.8500 | 49.7 |
| 0.2001 | 75.2 | 0.4497 | 104.2 | 0.6498 | 89.3 | 0.9000 | 36.8 |
| 0.2502 | 85.7 | 0.5003 | 102.9 | 0.6999 | 82.6 | 0.9500 | 22.1 |
| DNBE (i) + 23DMB (j) | | | | | | | |
| 0.0500 | 25.4 | 0.3000 | 90.0 | 0.5002 | 101.2 | 0.7500 | 75.8 |
| 0.1000 | 43.6 | 0.3499 | 95.6 | 0.5493 | 100.0 | 0.8001 | 66.7 |
| 0.1501 | 58.9 | 0.3998 | 99.5 | 0.5999 | 95.9 | 0.8500 | 55.5 |
| 0.2000 | 72.0 | 0.4501 | 101.8 | 0.6501 | 90.6 | 0.9001 | 42.4 |
| 0.2502 | 82.0 | 0.5000 | 101.7 | 0.7000 | 83.5 | 0.9500 | 28.1 |
| DNBE (i) + THF (j) | | | | | | | |
| 0.0500 | 78.8 | 0.3000 | 305.6 | 0.4998 | 339.3 | 0.7501 | 240.4 |
| 0.0998 | 143.6 | 0.3499 | 324.9 | 0.5498 | 331.9 | 0.8000 | 204.1 |
| 0.1502 | 198.4 | 0.4000 | 336.8 | 0.6002 | 318.2 | 0.8500 | 162.2 |
| 0.2000 | 243.4 | 0.4502 | 341.5 | 0.6499 | 297.9 | 0.9000 | 112.1 |
| 0.2500 | 278.7 | 0.4998 | 339.0 | 0.7000 | 272.7 | 0.9500 | 59.5 |

Table 4.2b. Experimental mole fractions x_i and excess molar enthalpies, $H_{m,ij}^E$, at 298.15 K, for the binary systems

| x_i | $\frac{H_{m,ij}^E}{(\text{J} \cdot \text{mol}^{-1})}$ | x_i | $\frac{H_{m,ij}^E}{(\text{J} \cdot \text{mol}^{-1})}$ | x_i | $\frac{H_{m,ij}^E}{(\text{J} \cdot \text{mol}^{-1})}$ | x_i | $\frac{H_{m,ij}^E}{(\text{J} \cdot \text{mol}^{-1})}$ |
|-----------------------------|---|--------|---|--------|---|--------|---|
| DNPE (i) + THF(j) | | | | | | | |
| 0.0500 | 52.3 | 0.2998 | 216.9 | 0.4998 | 248.6 | 0.7499 | 184.5 |
| 0.1000 | 96.9 | 0.3503 | 232.8 | 0.5499 | 244.6 | 0.7999 | 159.4 |
| 0.1501 | 136.1 | 0.3998 | 242.6 | 0.5999 | 236.3 | 0.8500 | 127.7 |
| 0.2000 | 168.2 | 0.4500 | 247.3 | 0.6502 | 223.7 | 0.9000 | 90.5 |
| 0.2498 | 195.9 | 0.4998 | 248.3 | 0.7003 | 206.2 | 0.9500 | 48.1 |
| DNPE (i) + 1HX(j) | | | | | | | |
| 0.0529 | 6.6 | 0.3002 | 24.9 | 0.5001 | 28.0 | 0.7500 | 21.5 |
| 0.1001 | 12.1 | 0.3499 | 26.5 | 0.5500 | 27.7 | 0.8003 | 18.8 |
| 0.1500 | 16.5 | 0.4001 | 27.4 | 0.5998 | 26.8 | 0.8500 | 15.4 |
| 0.2001 | 20.1 | 0.4501 | 28.1 | 0.6499 | 25.5 | 0.9000 | 11.3 |
| 0.2500 | 22.8 | 0.5001 | 28.0 | 0.6996 | 23.9 | 0.9500 | 6.1 |
| DNPE (i) + DNBE(j) | | | | | | | |
| 0.0500 | 2.2 | 0.3000 | 9.6 | 0.5004 | 11.9 | 0.7500 | 9.9 |
| 0.1000 | 4.3 | 0.3500 | 10.3 | 0.5500 | 11.9 | 0.8000 | 8.2 |
| 0.1500 | 5.9 | 0.3998 | 10.9 | 0.6001 | 11.9 | 0.8503 | 6.7 |
| 0.2001 | 7.3 | 0.4497 | 11.5 | 0.6500 | 11.3 | 0.9000 | 4.6 |
| 0.2500 | 8.6 | 0.4998 | 11.9 | 0.6999 | 10.9 | 0.9500 | 2.6 |
| DNPE (i) + 22DMB (j) | | | | | | | |
| 0.0500 | 37.9 | 0.2998 | 137.1 | 0.5497 | 151.1 | 0.8001 | 94.5 |
| 0.1000 | 68.1 | 0.3499 | 145.9 | 0.6001 | 145.1 | 0.8500 | 74.8 |
| 0.1500 | 89.7 | 0.3998 | 150.8 | 0.6500 | 135.8 | 0.9000 | 53.2 |
| 0.2000 | 109.4 | 0.4501 | 154.7 | 0.7001 | 124.8 | 0.9500 | 28.3 |
| 0.2499 | 124.6 | 0.4995 | 154.7 | 0.7503 | 111.0 | | |
| DNPE (i) + 23DMB (j) | | | | | | | |
| 0.0500 | 35.4 | 0.3001 | 134.2 | 0.4998 | 157.6 | 0.7502 | 117.0 |
| 0.1000 | 63.6 | 0.3499 | 144.6 | 0.5500 | 155.5 | 0.8000 | 101.4 |
| 0.1500 | 86.0 | 0.4000 | 152.5 | 0.5999 | 150.3 | 0.8500 | 80.9 |
| 0.2001 | 105.4 | 0.4498 | 156.4 | 0.6501 | 142.4 | 0.9000 | 57.9 |
| 0.2500 | 120.5 | 0.4998 | 157.3 | 0.7000 | 131.5 | 0.9500 | 31.4 |

4.1.1 Experimental Data Correlation: Binary Mixtures

The experimental excess molar enthalpies of the binary systems are correlated by means of an empirical expression (Redlich-Kister polynomial) and two theories of solution; the Flory theory and the Liebermann-Fried model.

Representation by means of the Redlich-Kister Polynomial

The equation presented by Redlich and Kister (1948) for correlating excess thermodynamic properties is widely used for the representation of excess molar enthalpy. The Redlich-Kister polynomial used in correlating the experimental data has the following form:

$$H_m^E / (\text{J} \cdot \text{mol}^{-1}) = x_i(1 - x_i) \sum_{k=1}^p h_k (1 - 2x_i)^{k-1} \quad (4.1)$$

For fitting the Redlich-Kister polynomial to the binary excess molar enthalpy values, the unweighted least square method was used. The values of the coefficients h_k were determined based on the minimization of the standard error of the estimates. The standard error is defined as

$$\sigma = \sqrt{\frac{\sum_{r=1}^n (H_{exp,r}^E - H_{cal,r}^E)^2}{(n-p)}} \quad (4.2)$$

In equations (4.1) and (4.2) H_{exp}^E and H_{cal}^E stand for the experimental and calculated excess molar enthalpy values, respectively; n denotes the number of experimental observations and p refers to the number of parameter used in the polynomial. The number of parameters is determined by applying an F -test. Details of the statistical test are given in Appendix C1. Results of the data correlation for the binary systems by means of equation (4.1) are summarized in Table 4.3, along with the standard deviations of the representations. Plots of the experimental data along with the representation from equation (4.1) are shown in Figures 4.1(a) to 4.1(d). In

general, excess molar enthalpy for the ten binary systems tested show endothermic behavior ($H_m^E > 0$) over the whole mole fraction range. The maximum value of the excess molar enthalpy occurs at $x_1 \approx 0.45$ to 0.50 . Over most of the composition range, the errors of excess molar enthalpies and those of the mole fractions of the measurement are estimated to be less than $0.005 \cdot |H_m^E|$ and less than $5 \cdot 10^{-4}$, respectively.

Table 4.3. Coefficients h_k and standard deviations σ for the representations of the excess molar enthalpies $H_{m,ij}^E$ of the constituent binary mixtures at 298.15 K by means of equation (4.1)

| Component | | h_1 | h_2 | h_3 | h_4 | h_5 | $\frac{\sigma}{(\text{J} \cdot \text{mol}^{-1})}$ |
|-----------|-------|---------|--------|--------|--------|--------|---|
| i | j | | | | | | |
| THF | 22DMB | 2738.75 | -74.77 | 40.42 | -39.65 | - | 1.05 |
| THF | 23DMB | 2707.62 | -31.43 | 82.59 | 100.42 | - | 0.66 |
| DNBE | 22DMB | 412.27 | 72.41 | 3.32 | -7.41 | 130.29 | 0.60 |
| DNBE | 23DMB | 406.56 | 44.46 | 15.30 | -51.56 | 155.96 | 0.34 |
| DNBE | THF | 1358.44 | 193.12 | 111.25 | 30.86 | - | 0.49 |
| DNPE | THF | 993.78 | 66.65 | 91.65 | -36.23 | -23.01 | 0.43 |
| DNPE | 1HX | 111.98 | 7.48 | 26.22 | -3.83 | - | 0.10 |
| DNPE | DNBE | 47.28 | -7.34 | 3.61 | 6.59 | - | 0.06 |
| DNPE | 22DMB | 617.19 | 63.00 | 20.45 | 47.60 | 88.93 | 0.45 |
| DNPE | 23DMB | 630.19 | 10.77 | -5.69 | 38.46 | 117.65 | 0.39 |
| 1HX | DNBE | -96.38 | -4.17 | -8.76 | - | - | 0.20 ⁽¹⁾ |
| 1HX | THF | 1461.17 | -50.90 | 68.34 | -34.75 | - | 0.94 ⁽²⁾ |
| 1HX | 22DMB | 250.01 | 9.09 | 12.29 | - | - | 0.62 ⁽³⁾ |
| 1HX | 23DMB | 317.88 | 25.12 | -11.17 | -18.03 | - | 0.29 ⁽³⁾ |
| 22DMB | 23DMB | 5.27 | - | - | - | - | 0.03 ⁽⁴⁾ |

⁽¹⁾Wang et al. (2004b); ⁽²⁾Lan et al. (2006); ⁽³⁾Wang et al. (2004a); ⁽⁴⁾Hamam and Benson (1986)

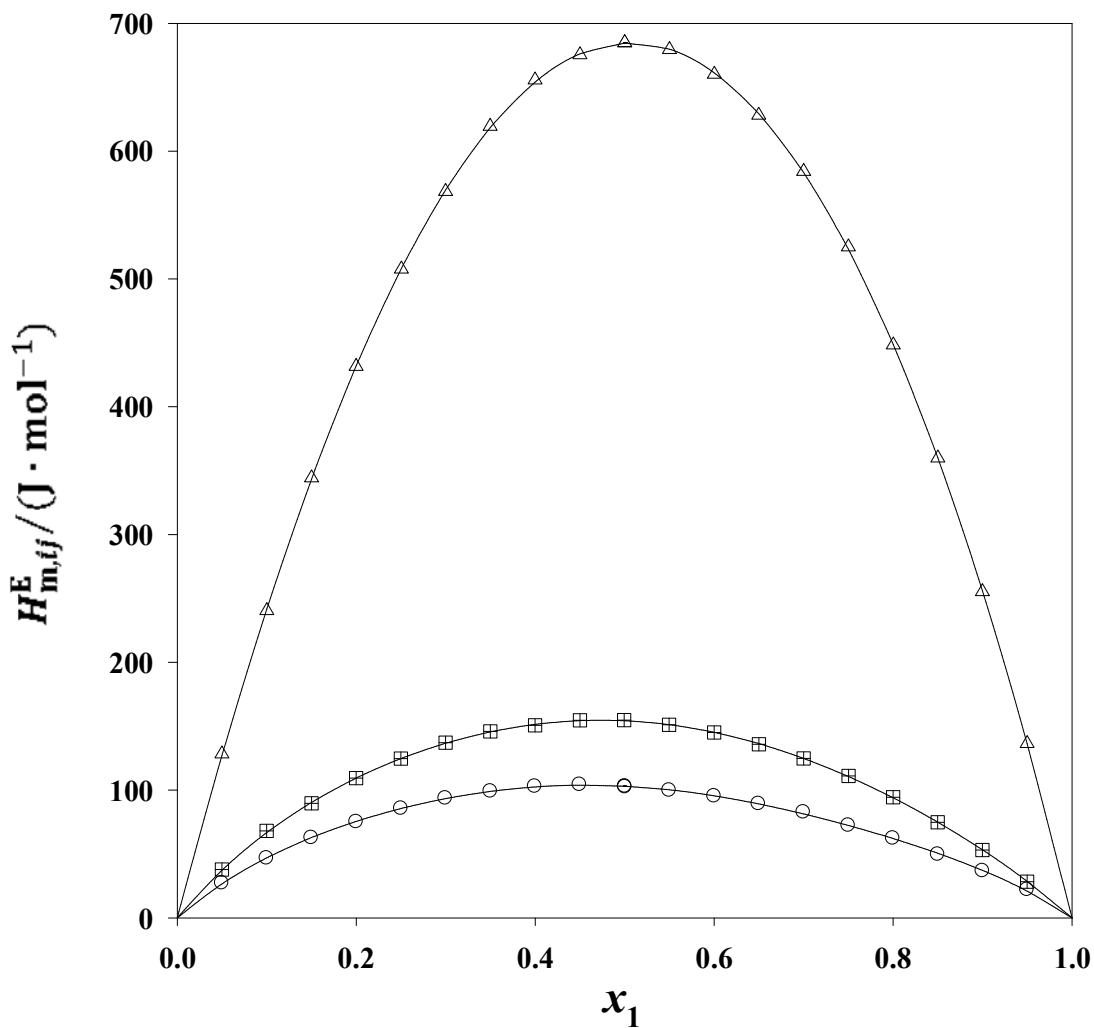


Figure 4.1(a). Excess molar enthalpies, $H_{m,ij}^E$, for the binary systems presented in Tables 4.2a and 4.2b at the temperature 298.15 K. Experimental results: Δ , x_1 THF + $(1 - x_1)$ 22DMB; \boxplus , x_1 DNPE + $(1 - x_1)$ 22DMB; \oplus , x_1 DNBE + $(1 - x_1)$ 22DMB. Curves: —, calculated from the representations of the results by equation (4.1) with values of the coefficients given in Table 4.3.

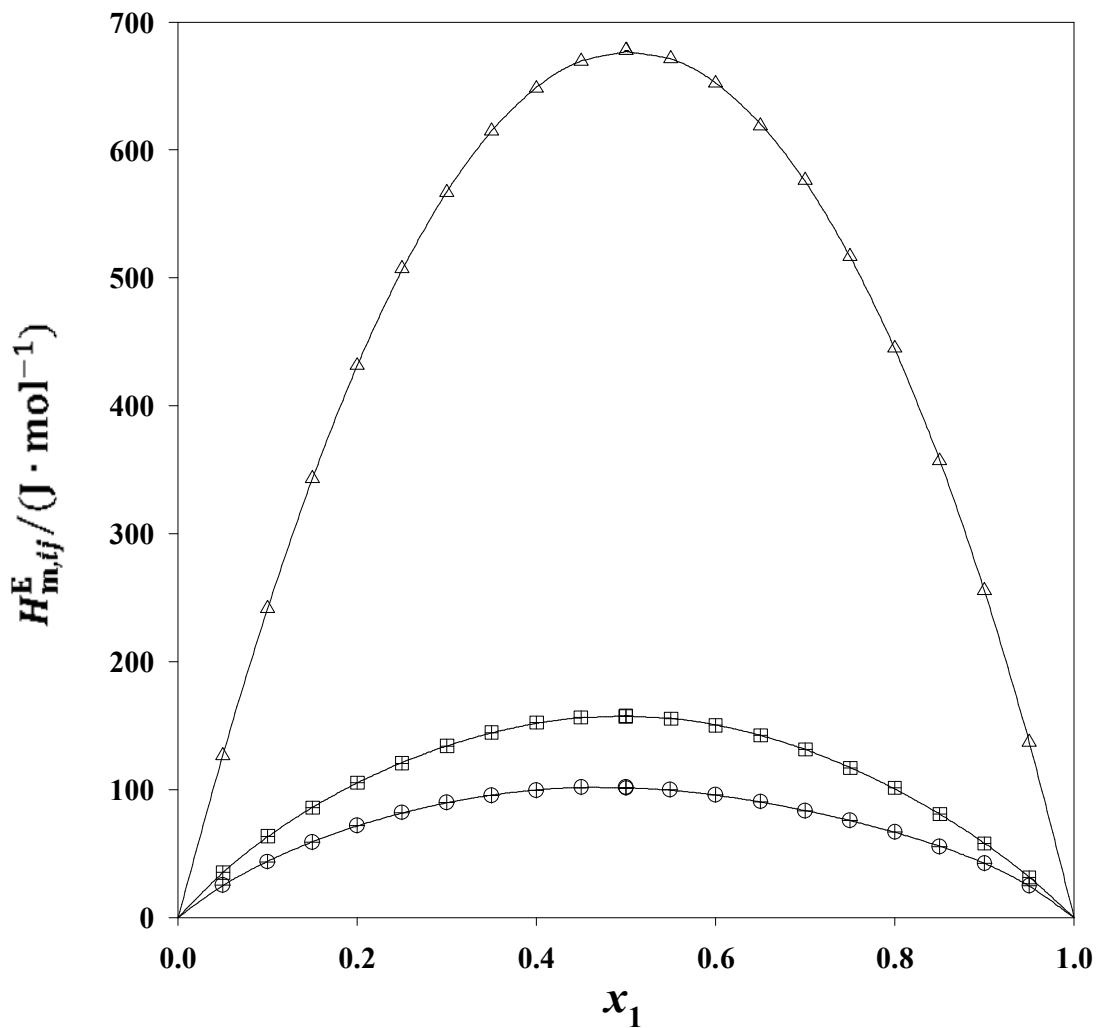


Figure 4.1(b). Excess molar enthalpies, $H_{m,ij}^E$, for the binary systems presented in Tables 4.2a and 4.2b at the temperature 298.15 K. Experimental results: Δ , x_1 THF + $(1 - x_1)$ 23DMB; \boxplus , x_1 DNPE + $(1 - x_1)$ 23DMB; \oplus , x_1 DNBE + $(1 - x_1)$ 23DMB. Curves: —, calculated from the representations of the results by equation (4.1) with values of the coefficients given in Table 4.3.

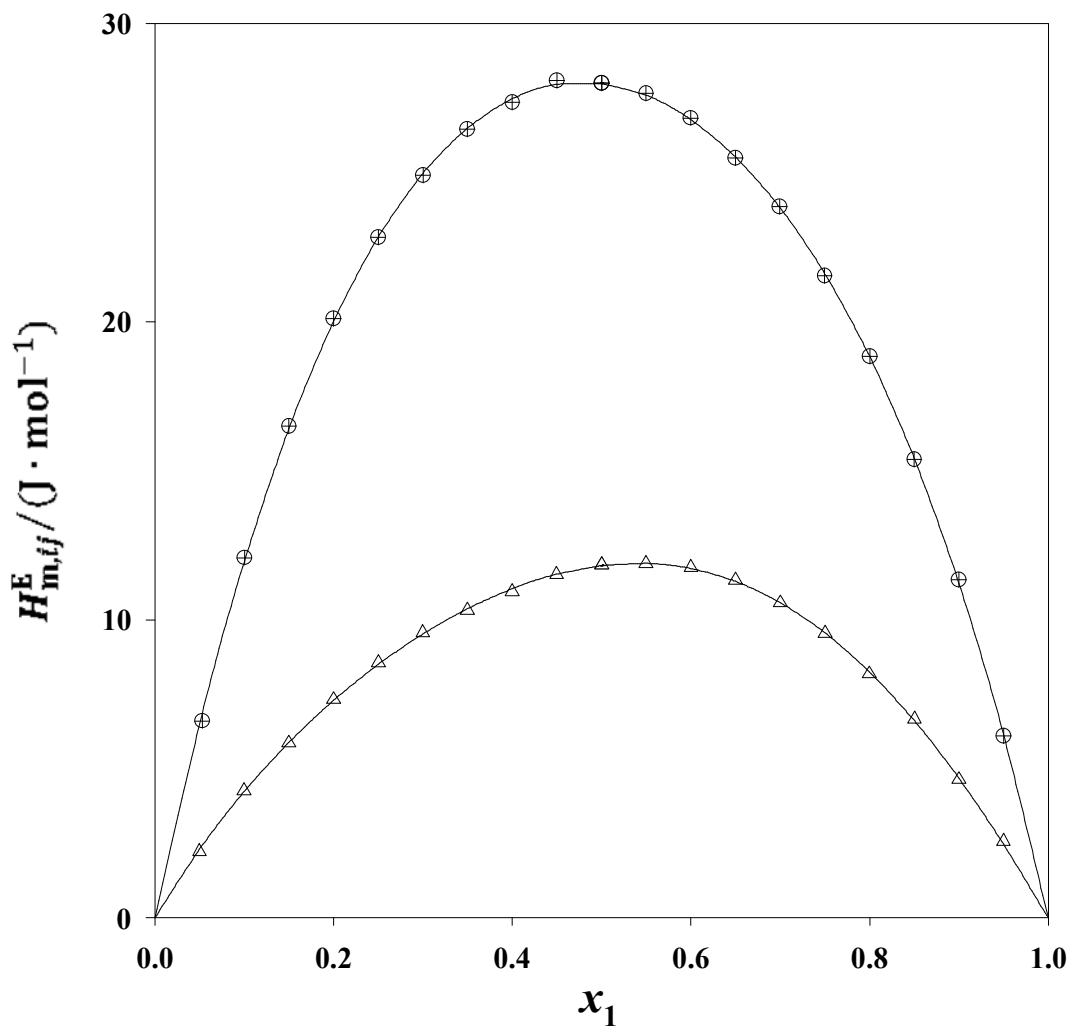


Figure 4.1(c). Excess molar enthalpies, $H_{m,ij}^E$, for the binary systems presented in Tables 4.2a and 4.2b at the temperature 298.15 K. Experimental results: Δ , x_1 DNPE + $(1 - x_1)$ THF; \oplus , x_1 DNBE + $(1 - x_1)$ THF. Curves: —, calculated from the representations of the results by equation (4.1) with values of the coefficients given in Table 4.3.

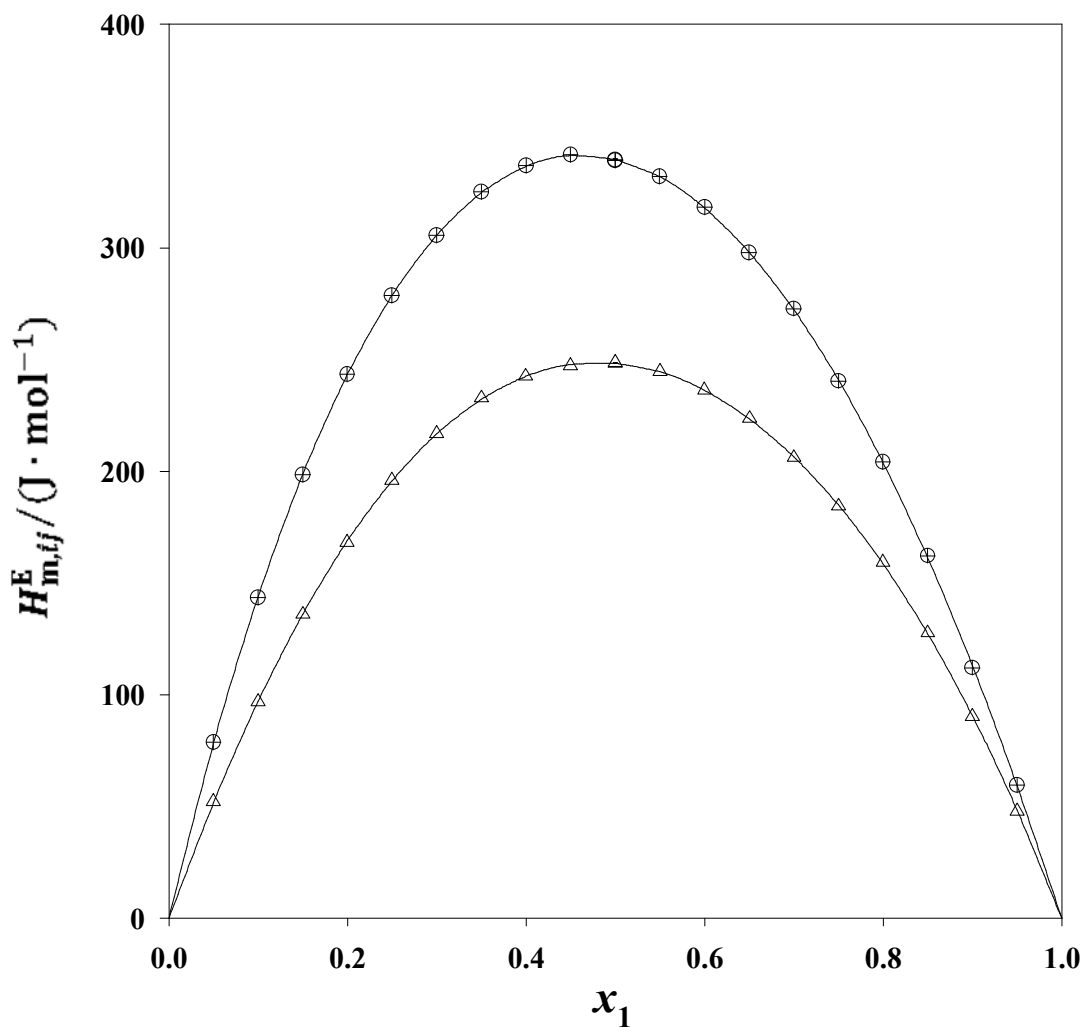


Figure 4.1(d). Excess molar enthalpies, $H_{m,ij}^E$, for the binary systems presented in Tables 4.2b at the temperature 298.15 K. Experimental results: Δ , x_1 DNPE + $(1 - x_1)$ DNBE; \oplus , x_1 DNPE + $(1 - x_1)$ 1HX Curves: —, calculated from the representations of the results by equation (4.1) with values of the coefficients given in Table 4.3.

Figures 4.1(a) and 4.1(b) show that the excess molar enthalpy values for systems containing branched alkanes (22DMB or 23DMB) and ethers (THF, DNBE, DNPE) increases with the decrease of the carbon number in the ether molecule. As the structures of the branched alkanes are similar the heats of mixing of mixtures containing these two branched alkanes are of the same order of magnitude.

The maximum excess enthalpy value for the THF (1) + 22DMB (2), or THF (1) + 23DMB (2) system is highest among the three ethers and the difference in magnitude with normal ethers is fairly significant. During the mixing process for breaking the bond between the molecules of cyclic-ether usually requires more energy than the normal chain ethers (Castro et al. 1994). It can be noticed from Figures 4.1(a) and 4.1(b) that for the THF containing systems, denoted by the symbol(Δ), the maximum value occurs at $x_1 \approx 0.5000$, and the magnitudes are $H_m^E/(\text{J} \cdot \text{mol}^{-1}) = 685.0$ and 678.0 for 22DMB and 23DMB, respectively.

For the DNBE (1) + 22 DMB (2), and DNBE (1) + 23DMB (2) systems, the magnitude of excess molar enthalpy at the mole fraction $x_1 \approx 0.5000$ is the lowest among the three ethers. In Figures 4.1 (a) and 4.1 (b), the symbol(\oplus), represent these systems, which are slightly skewed toward pure DNBE. The maximum values occur at $x_1 \approx 0.4500$, and the magnitudes are $H_m^E/(\text{J} \cdot \text{mol}^{-1}) = 104.2$ and 101.8 for 22DMB and 23DMB, respectively.

For the DNPE (1) + 22DMB (2), and DNPE (1) + 23DMB (2) systems, the maximum values of excess enthalpy are $H_m^E/(\text{J} \cdot \text{mol}^{-1}) = 154.7$ and 157.6 , for 22DMB and 23DMB, respectively. The symbol(\boxplus), represent these two systems in Figures 4.1(a) and 4.1(b) note that these systems appear to be symmetric about $x_1 = 0.5000$. In general, it can be conclude that the excess enthalpy value for the system of branched alkanes (22DMB, or 23DMB) with ethers (THF, DNPE, and DNBE) decreases with the increase of carbon number in ether molecule.

The excess molar enthalpy of mixtures of THF with the two normal chain ethers (DNPE and DNBE) are presented in Figure 4.1(c). The DNPE (1) + THF (2) binary system is represented by the symbol(Δ), and has a maximum value of $248.6 \text{ J} \cdot \text{mol}^{-1}$ which occurs at the mole fraction, $x_1 \approx 0.5000$. In DNBE (1) + THF (2) system the maximum value of heats of mixing occurs at $x_1 \approx 0.4500$ with a magnitude of $H_m^E/(\text{J} \cdot \text{mol}^{-1}) = 341.5$.

In Figure 4.1(d) the excess molar enthalpies of the DNPE (1) + DNBE (2), and DNPE (1) + 1HX (2) mixtures are presented. For the DNPE (1) + DNBE (2) system, the magnitude of the excess molar enthalpy is moderately low. This phenomenon occurs due to the similar structures of DNPE and DNBE. For the DNPE (1) + 1HX (2) the maximum excess molar enthalpy occurs at $x_1 \approx 0.5000$ with a magnitude of $H_m^E/(\text{J} \cdot \text{mol}^{-1}) = 28.0$.

Representation of Binary Heats of Mixing by Means of the Solution Theories

For representing the experimental excess molar enthalpy data for binary and ternary systems, a solution theory is understandably superior to empirical correlation in terms of theoretical view point. It is a fact that solution theories describe the behavior of real liquid mixture in terms of molecular interaction where as empirical approaches are only mathematical.

In this section, the Flory theory (1965) and the Liebermann-Fried model (1975) are used to correlate the binary excess molar enthalpies of hydrocarbon and ether binary systems.

Flory Theory

The equation for the excess molar enthalpy from the Flory theory was simplified and presented by Benson and Pflug (1970). Wang et al. (1993) presented a generalized Flory equation for a multicomponent system. For a better understanding of the representation of excess molar enthalpy by means of the Flory theory, only the expressions for ternary excess molar enthalpy are presented here.

The expression of excess molar enthalpy for a multicomponent mixture using the Flory theory is

$$H_m^E = (\sum x_i V_i^*) \left[\sum \left\{ \Phi_i P_i^* \left(\frac{1}{\bar{v}_i} - \frac{1}{\bar{v}} \right) \right\} + \frac{1}{\bar{v}} \Psi \right] \quad (4.3)$$

where, P_i^* and V_i^* are the hardcore (characteristic) pressure and volume of pure component, respectively, and are obtained by the relation give by Flory (1965):

$$P_i^* = \left(\frac{\alpha_{P_i}}{\kappa_{T_i}} \right) T \tilde{V}_i^2 \quad (4.4)$$

and

$$\tilde{V}_i^{1/3} = \left(\frac{V_{m_i}}{V_i^*} \right)^{1/3} = 1 + \frac{\alpha_{P_i} T}{3(1 + \alpha_{P_i} T)} \quad (4.5)$$

In equations (4.4) and (4.5) T is the system temperature and, α_{P_i} , κ_{T_i} , \tilde{V}_i , and V_{m_i} represent, respectively, the isobaric thermal expansivity, isothermal compressibility, reduced volume, and molar volume of pure component i .

Table 4.4. Parameters used in Flory theory correlation

| Component | $\frac{V_{m_i}}{(\text{cm}^3 \text{mol}^{-1})}$ | $\frac{\alpha_{P_i}^a}{(\text{kK}^{-1})}$ | $\frac{\kappa_{T_i} \times 10^6^b}{(\text{atm}^{-1})}$ |
|-----------|---|---|--|
| DNPE | 137.71 | 1.261 | 145.46 |
| DNBE | 170.50 | 1.126 | 122.30 |
| THF | 81.75 | 1.138 | 901.29 |
| 1HX | 125.84 | 1.411 | 171.14 |
| 22DMB | 133.69 | 1.468 | 203.62 |
| 23DMB | 131.17 | 1.391 | 181.39 |

^aWang et al. (2005); ^bPeng et al. (1999)

This reduced volume of mixing in equation (4.3) is calculated from the relation

$$\tilde{V} = \sum \Phi_j \tilde{V}_j \quad (4.6)$$

where Φ_j is the segment fraction and is defined by

$$\Phi_j = \frac{x_j V_j^*}{\sum x_i V_i^*} \quad (4.7)$$

In equation (4.3) θ_j is defined as the site fraction and is obtained from the relation

$$\theta_j = \frac{\Phi_j}{\sum \Phi_i (s_i/s_j)} \quad (4.8)$$

Finally, Ψ in equation (4.3) is given by

$$\Psi = \Phi_1 \theta_2 \chi_{12} + \Phi_2 \theta_3 \chi_{23} + \Phi_3 \theta_1 \chi_{13} (s_3/s_1) \quad (4.9)$$

and the sums are taken over the three components i .

The parameter χ_{ij} ($i < j$) in equation (4.9) is the mixed-pair interchange interaction energies between sites on species i and j . Also in this equation the factor s_3/s_1 is introduced to allow the asymmetry in the definition of χ_{ij} in the Flory theory. The interchange energy

parameter χ_{ij} in eq (4.3) is determined by regressing the experimental excess molar enthalpy $H_{m,ij}^E$ data of the constituent binary mixtures. In representing the excess molar enthalpy from the Flory theory all molecules of interest are assumed to be spherical and the site ratio is calculated by the relation given by

$$s_i/s_j = (V_j^*/V_i^*)^{1/3} \quad (4.10)$$

Table 4.5. Interchange energy parameter, χ_{ij} , site fraction ratio, s_i/s_j , and standard deviations, σ , for the representations of the excess molar enthalpies $H_{m,ij}^E$ of the constituent binary mixtures at 298.15 K by equation (4.3)

| Components | | χ_{ij} | s_i/s_j | $\frac{\sigma}{(\text{J} \cdot \text{mol}^{-1})}$ |
|------------|-------|-------------|-----------|---|
| i | j | | | |
| THF | 22DMB | 34.6610 | 1.1599 | 20.77 |
| THF | 23DMB | 34.5493 | 1.1565 | 22.21 |
| DNBE | 22DMB | 3.8860 | 0.9073 | 3.46 |
| DNBE | 23DMB | 3.6515 | 0.9046 | 3.28 |
| DNBE | THF | 12.7194 | 0.7822 | 9.20 |
| DNPE | THF | 10.6922 | 0.8456 | 7.90 |
| DNPE | 1HX | 1.1899 | 0.9637 | 0.80 |
| DNPE | DNBE | 0.5216 | 1.0810 | 0.21 |
| DNPE | 22DMB | 5.8503 | 0.9809 | 5.03 |
| DNPE | 23DMB | 5.8475 | 0.9779 | 2.06 |

Another parameter, χ_{ji} can be obtained from the following relation

$$\chi_{ji} = \chi_{ij}(V_j^*/V_i^*)^{1/3} \quad (4.11)$$

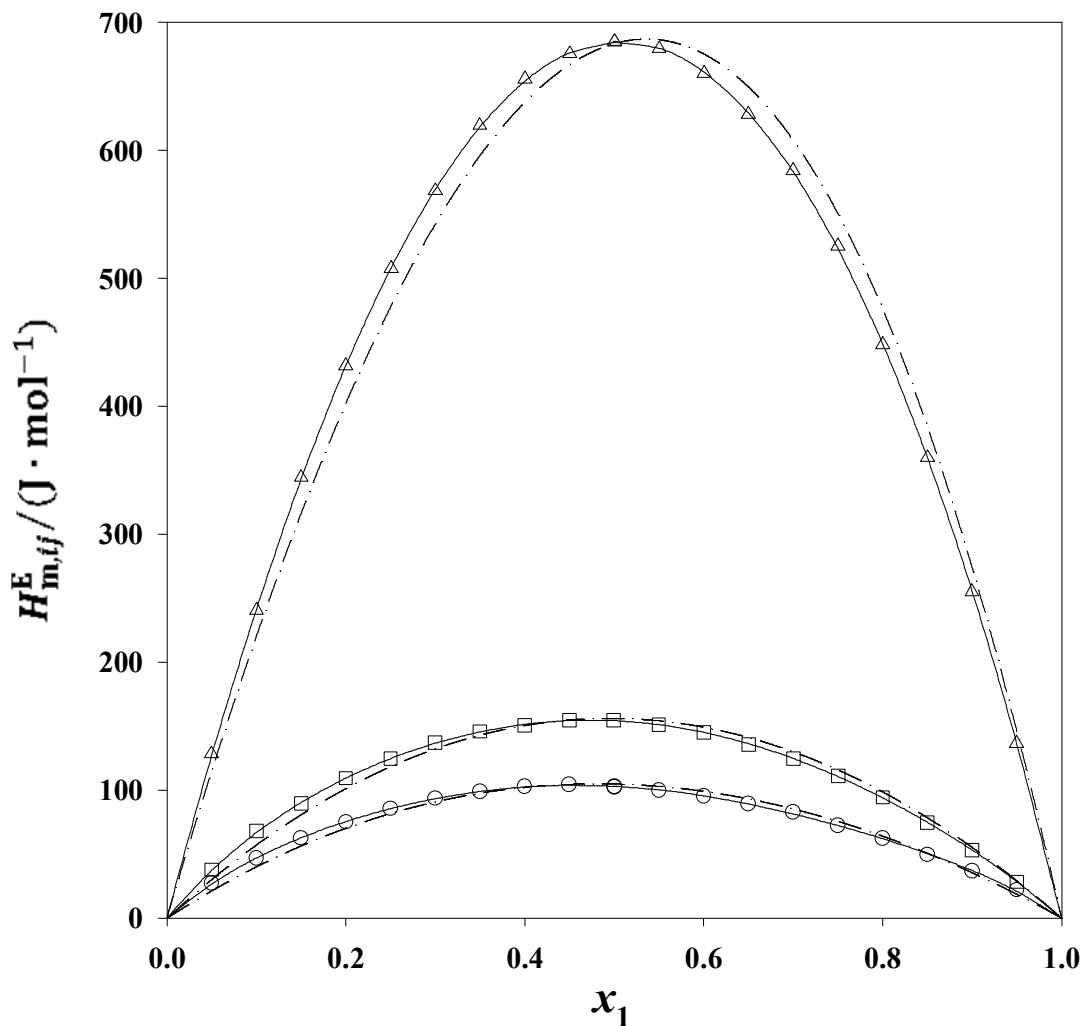


Figure 4.2. Excess molar enthalpies $H_{m,ij}^E$ for the binary systems presented in Tables 4.2a and 4.2b at the temperature 298.15 K. Experimental results: Δ , x_1 THF + $(1 - x_1)$ 22DMB; \boxplus , x_1 DNPE + $(1 - x_1)$ 22DMB; \oplus , x_1 DNBE + $(1 - x_1)$ 22DMB. Curves: —, calculated from the representations of the results by equation (4.1) with values of the coefficients given in Table 4.3; — · —, calculated by means of the Flory theory.

For a binary system, equation (4.3) reduces to the form

$$H_{m,12}^E = x_1 P_1^* V_1^* \left(\frac{1}{\bar{v}_1} - \frac{1}{\bar{v}} \right) + x_2 P_2^* V_2^* \left(\frac{1}{\bar{v}_2} - \frac{1}{\bar{v}} \right) + x_1 V_1^* \theta_2 \chi_{12} \frac{1}{\bar{v}} \quad (4.12)$$

The pure component properties used in the Flory equation and the values of the interchange energy parameter, χ_{12} , (obtained by fitting the Flory theory to the experimental data of the binary mixtures by the method of least square) are presented in Tables 4.4 and 4.5, respectively.

Figure 4.2 serves to present the correlation of the THF (1) + 22DMB (2), DNPE (1) + 22DMB (2), and the DNBE (1) + 22DMB (2) excess enthalpies using the Redlich-Kister polynomial and the Flory theory. The correlated excess molar enthalpies for the ten binary systems using the Flory theory are presented in Appendix C2.

Liebermann-Fried Model

Previously, Wang et al. (2001) found that the Liebermann-Fried model can be used for representing both binary and multicomponent mixtures. For representing multicomponent mixtures, only the properties of the pure components and interaction parameters derived from an analysis of the excess enthalpies of their constituent binaries are required. This approach was investigated for the present binary and ternary mixtures. Details of the thermodynamic relations in connection with the derivation of Liebermann-Fried model are described by Peng et al. (2001). To facilitate the understanding of the application of the Liebermann-Fried model, only the equations used in the excess molar enthalpy calculation process were presented here.

The expression for H_m^E of a N -component mixture has the following form

$$H_m^E = H_I^E + H_V^E \quad (4.13)$$

where H_I^E has the form

$$H_I^E = RT^2 \sum_{j=1}^N \sum_{k=1}^N x_j x_k \left[\frac{\left(\frac{\partial A_{jk}}{\partial T} \right) + \left(\frac{\partial A_{kj}}{\partial T} \right) - \ln(A_{jk} A_{kj}) \left\{ \frac{\sum_{p=1}^N x_p \left(\frac{\partial A_{jp}}{\partial T} \right) + \sum_{q=1}^N x_q \left(\frac{\partial A_{kq}}{\partial T} \right)}{\sum_{p=1}^N x_p A_{jp} + \sum_{q=1}^N x_q A_{kq}} \right\}}{2 \left(\sum_{p=1}^N x_p A_{jp} \right) \left(\sum_{q=1}^N x_q A_{kq} \right)} \right] \quad (4.14)$$

$$\text{where } \frac{1}{A_{jk}} \frac{\partial A_{jk}}{\partial T} = \left(\frac{2}{T} \right) \frac{\ln(A_{jk} A_{kj})}{\ln(A_{jk} A_{kj}) - 2} = \frac{1}{A_{kj}} \frac{\partial A_{kj}}{\partial T} \quad (4.15)$$

and

$$H_V^E = RT^2 \frac{\sum_{j=1}^N \sum_{k=1}^N x_j x_k V_{m,k} [(\alpha_P)_k - (\alpha_P)_j]}{\sum_{k=1}^N x_k V_{m,k}}, \quad (4.16)$$

H_I^E represents the non-ideal behavior that arises from interaction between molecules and H_V^E , accounts for the different sizes of molecules present in the mixture. V_m and α_P represent the molar volume and isobaric thermal expansivity of pure component, respectively.

Pure component properties used in the Liebermann-Fried model are presented in Table 4.6.

Table 4.6. Parameter used in the Liebermann-Fried model correlation

| Component | $\frac{V_{m,i}}{(\text{cm}^3 \text{mol}^{-1})}$ | $\frac{\alpha_{P,i}^a}{(\text{kK}^{-1})}$ |
|-----------|---|---|
| DNPE | 137.71 | 1.261 |
| DNBE | 170.50 | 1.126 |
| THF | 81.75 | 1.138 |
| 1HX | 125.84 | 1.411 |
| 22DMB | 133.69 | 1.468 |
| 23DMB | 131.17 | 1.391 |

^aWang et al. (2005)

For binary mixture equation (4.13) reduces to

$$H_m^E = \frac{2RTx_1x_2[\ln(A_{12}A_{21})]^2}{(x_1+x_2A_{12})(x_2+x_1A_{21})[2-\ln(A_{12}A_{21})]} \times \left[\frac{x_2A_{12}}{x_1+x_2A_{12}} + \frac{x_1A_{21}}{x_2+x_1A_{21}} - \frac{2}{\ln(A_{12}A_{21})} \right] - RT^2 \left[\frac{x_1x_2(V_{m1}-V_{m2})(\alpha_{P1}-\alpha_{P2})}{x_1V_{m1}+x_2V_{m2}} \right] \quad (4.17)$$

Table 4.7. Liebermann-Fried model parameters A_{ij} and A_{ji} , and standard deviations, σ , for the representations of the excess molar enthalpies $H_{m,ij}^E$ of the constituent binary mixtures at 298.15 K by means of the equation (4.17)

| Components | | A_{ij} | A_{ji} | $\frac{\sigma}{(\text{J} \cdot \text{mol}^{-1})}$ |
|------------|-------|----------|----------|---|
| i | j | | | |
| THF | 22DMB | 0.8220 | 0.7855 | 2.00 |
| THF | 23DMB | 0.8171 | 0.7896 | 1.56 |
| DNBE | 22DMB | 0.8065 | 1.1299 | 2.33 |
| DNBE | 23DMB | 0.8844 | 1.0332 | 3.44 |
| DNBE | THF | 0.7579 | 1.0287 | 2.41 |
| DNPE | THF | 0.8743 | 0.9575 | 2.38 |
| DNPE | 1HX | 0.9329 | 1.0455 | 0.86 |
| DNPE | DNBE | 1.1072 | 0.8908 | 0.15 |
| DNPE | 22DMB | 0.8276 | 1.0718 | 2.20 |
| DNPE | 23DMB | 0.9058 | 0.9775 | 2.08 |

Values of the Liebermann-Fried model interaction parameters A_{ij} and A_{ji} , for each binary mixture are given in Table 4.7. These parameters are obtained by fitting the Liebermann-Fried model (eq 4.17) to the experimental results of the binary systems listed in Tables 4.1(a) and 4.1(b). Also included in Table 4.7 are values of the standard deviation found in the fitting process.

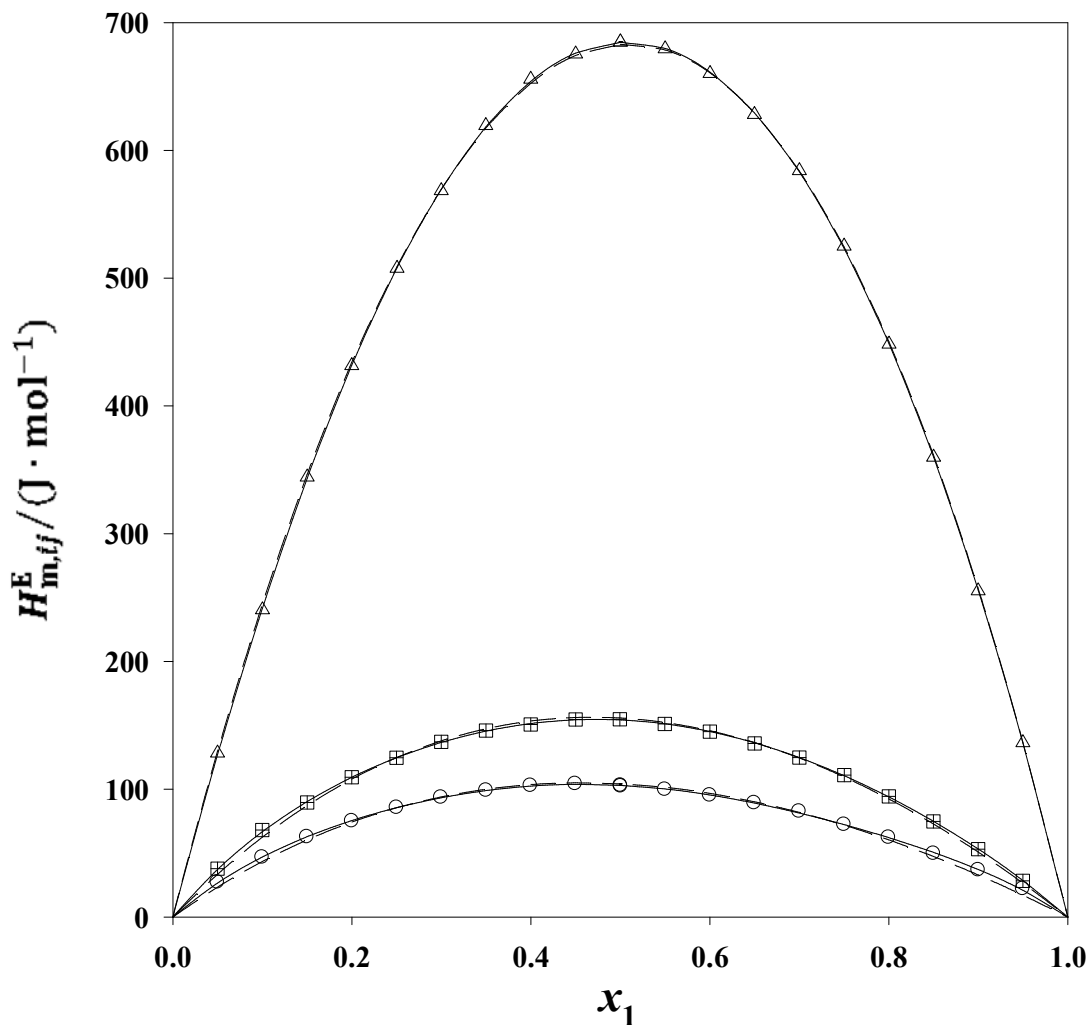


Figure 4.3. Excess molar enthalpies $H_{m,ij}^E$ for the binary systems presented in Tables 4.2a and 4.2b at the temperature 298.15 K. Experimental results: Δ , x_1 THF + $(1 - x_1)$ 22DMB; \boxplus , x_1 DNPE + $(1 - x_1)$ 22DMB; \oplus , x_1 DNBE + $(1 - x_1)$ 22DMB. Curves: —, calculated from the representations of the results by equation (4.1) with values of the coefficients given in Table 4.3; - - -, calculated from the Liebermann-Fried model.

Figure 4.3 shows the correlation of the THF (1) + 22DMB (2), DNPE (1) + 22DMB (2), and DNBE (1) + 22DMB (2) systems using the Redlich-Kister polynomial and the Liebermann-Fried model. The fits of the Liebermann-Fried model for all the binary systems analyzed are presented in Appendix C2.

4.2 Excess Molar Enthalpy of Ternary systems

The six (6) ternary systems studied are presented in Table 4.8. Experimental result for the ternary mixture DNPE (1) + DNBE (2) + 1HX (3) and the correlation using the Tsao and Smith (1953) equation are presented in this section. The experimental and correlated results of the five (5) remaining ternary mixtures are also presented here.

Table 4.8. Ternary mixtures studied

| System | Component 1 | Component 2 | Component 3 |
|--------|-------------|-------------|-------------|
| 1 | DNPE | DNBE | 1HX |
| 2 | DNPE | DNBE | THF |
| 3 | DNPE | 22DMB | 23DMB |
| 4 | DNBE | 22DMB | 23DMB |
| 5 | 1HX | THF | 22DMB |
| 6 | 1HX | THF | 23DMB |

Ternary System: DNPE (1) + DNBE (2) + 1HX (3)

Experimental results for the DNPE (1) + DNBE (2) + 1HX (3) mixture are reported in Table 4.9, where values of $H_{m,1+23}^E$ are listed against the mole fraction x_1 of component 1. Also included in the table are the corresponding values of $H_{m,123}^E$. In studying the ternary system x_1 DNPE + x_2 DNBE + $(1 - x_1 - x_2)$ 1HX, the excess molar enthalpies $H_{m,1+23}^E$ were

determined for several pseudo-binary mixtures. The ternary mixture was formed by adding component 1 (DNPE) to binary mixtures of fixed composition of component 2 (DNBE) and component 3(1HX). The excess molar enthalpy $H_{m,123}^E$ for the ternary mixture was then obtained by means of equation (3.6).

The excess enthalpy values of $H_{m,1+23}^E$ are plotted in Figure 4.4, along with curves for the constituent binary mixtures having $x_1 + x_2 = 1.0$ and $x_2 = 0.0$.

Calculation of the values of $H_{m,1+23}^E$ is based on the relation (Tsao and Smith, 1953)

$$H_{m,1+23}^E = \left(\frac{x_2}{1-x_1}\right)H_{m,12}^E + \left(\frac{x_3}{1-x_1}\right)H_{m,13}^E + H_{m,T}^E \quad (4.18)$$

which consists of the sum of the binary contributions and an added ternary term $H_{m,T}^E$. The ternary term is given by

$$H_{m,T}^E/(\text{J} \cdot \text{mol}^{-1}) = x_1x_2 \left(\frac{1-x_1-x_2}{1-x_1+x_2}\right) (c_0 + c_1x_1 + c_2x_2 + c_3x_1^2 + c_4x_1x_2 + c_5x_2^2 + \dots) \quad (4.19)$$

and is similar to that used by Morris et al. (1975) with an extra skewing factor $(1 - x_1 + x_2)^{-1}$ (Benson and coworker, 1993-2006).

Table 4.9. Experimental excess molar enthalpies $H_{m,1+23}^E$ and the calculated values of $H_{m,123}^E$ for the x_1 DNPE + x_2 DNBE + $(1 - x_1 - x_2)$ 1HX ternary system at 298.15 K

| x_1 | $\frac{H_{m,1+23}^E}{(\text{J} \cdot \text{mol}^{-1})}$ | $\frac{H_{m,123}^E}{(\text{J} \cdot \text{mol}^{-1})}$ | x_1 | $\frac{H_{m,1+23}^E}{(\text{J} \cdot \text{mol}^{-1})}$ | $\frac{H_{m,123}^E}{(\text{J} \cdot \text{mol}^{-1})}$ | x_1 | $\frac{H_{m,1+23}^E}{(\text{J} \cdot \text{mol}^{-1})}$ | $\frac{H_{m,123}^E}{(\text{J} \cdot \text{mol}^{-1})}$ |
|---|---|--|--------|---|--|--------|---|--|
| $x_2/x_3 = 0.3333, H_{m,23}^E/(\text{J} \cdot \text{mol}^{-1}) = -18.9$ | | | | | | | | |
| 0.0500 | 5.2 | -12.8 | 0.4001 | 25.6 | 14.2 | 0.7003 | 23.4 | 17.7 |
| 0.1000 | 9.6 | -7.4 | 0.4496 | 26.4 | 16.0 | 0.7500 | 21.4 | 16.7 |
| 0.1500 | 13.6 | -2.5 | 0.5002 | 26.7 | 17.3 | 0.7998 | 19.0 | 15.2 |
| 0.1998 | 17.0 | 1.9 | 0.5002 | 26.8 | 17.3 | 0.8500 | 15.8 | 13.0 |
| 0.2501 | 20.0 | 5.9 | 0.5503 | 26.6 | 18.1 | 0.9000 | 12.2 | 10.3 |
| 0.3001 | 22.3 | 9.1 | 0.5999 | 26.0 | 18.5 | 0.9500 | 7.1 | 6.2 |
| 0.3501 | 24.3 | 12.1 | 0.6501 | 24.9 | 18.3 | | | |
| $x_2/x_3 = 0.9996, H_{m,23}^E/(\text{J} \cdot \text{mol}^{-1}) = -24.1$ | | | | | | | | |
| 0.0500 | 4.3 | -18.6 | 0.4001 | 22.7 | 8.2 | 0.7001 | 21.3 | 14.1 |
| 0.1000 | 8.2 | -13.5 | 0.4502 | 23.4 | 10.2 | 0.7499 | 19.6 | 13.6 |
| 0.1499 | 11.7 | -8.8 | 0.5000 | 23.9 | 11.8 | 0.8001 | 17.3 | 12.5 |
| 0.2001 | 14.7 | -4.5 | 0.5000 | 23.9 | 11.9 | 0.8500 | 14.7 | 11.1 |
| 0.2499 | 17.3 | -0.8 | 0.5500 | 23.9 | 13.1 | 0.9000 | 11.7 | 9.2 |
| 0.2999 | 19.5 | 2.6 | 0.6003 | 23.5 | 13.9 | 0.9500 | 7.8 | 6.6 |
| 0.3502 | 21.2 | 5.5 | 0.6500 | 22.5 | 14.1 | | | |
| $x_2/x_3 = 3.0000, H_{m,23}^E/(\text{J} \cdot \text{mol}^{-1}) = -18.1$ | | | | | | | | |
| 0.0500 | 3.0 | -14.2 | 0.4000 | 16.9 | 6.0 | 0.6997 | 16.8 | 11.3 |
| 0.1000 | 5.8 | -10.5 | 0.4501 | 17.6 | 7.7 | 0.7497 | 15.4 | 10.9 |
| 0.1500 | 8.5 | -6.9 | 0.4996 | 18.1 | 9.1 | 0.7998 | 13.9 | 10.3 |
| 0.1999 | 10.7 | -3.8 | 0.4997 | 18.2 | 9.1 | 0.8497 | 12.1 | 9.3 |
| 0.2501 | 12.8 | -0.8 | 0.5497 | 18.3 | 10.1 | 0.9000 | 9.7 | 7.9 |
| 0.3001 | 14.4 | 1.8 | 0.6001 | 18.1 | 10.8 | 0.9500 | 6.4 | 5.5 |
| 0.3499 | 15.9 | 4.1 | 0.6497 | 17.5 | 11.2 | | | |

Table 4.10. Values of the coefficients in equation (4.19) and standard deviations, σ , of the fit for the ternary mixtures of current interest

| Coefficient | System 1 | System 2 | System 3 | System 4 | System 5 | System 6 |
|---|----------|----------|----------|----------|-----------|-----------|
| c_1 | -251.11 | -2979.96 | -929.15 | -196.20 | -4330.81 | -3780.64 |
| c_2 | 1270.01 | 2782.56 | 3541.70 | 989.91 | 6637.49 | -3943.23 |
| c_3 | 699.74 | 675.29 | 2218.97 | -352.02 | 3842.48 | 3038.73 |
| c_4 | -2238.89 | -1947.11 | -5901.97 | 3253.08 | -14765.93 | 14887.28 |
| c_5 | -428.01 | -2677.41 | -1690.83 | 2380.02 | -5726.64 | 2911.24 |
| c_6 | -789.02 | - | -3488.55 | -2.44 | - | -7566.06 |
| c_7 | 1557.48 | - | 3580.01 | 3415.04 | - | -11671.61 |
| c_8 | - | - | - | - | - | -22359.71 |
| $\frac{\sigma}{(\text{J}\cdot\text{mol}^{-1})}$ | 0.43 | 0.69 | 0.72 | 0.97 | 2.47 | 1.74 |

Values of the coefficients c_i were obtained from a least-square analysis in which equations (4.18) and (4.19) were fitted to the experimental values of the ternary systems. In doing this, the values of $H_{m,ij}^E$ for the binary contributions were calculated from equation (4.1) using appropriate coefficients (h_k). Table 4.2 provided the coefficients for the ten binary mixtures studied. Coefficients for the other five binary mixtures were found in literature and are also provided in Table 4.2. For the six ternary systems, the coefficients (c_i) in equation (4.19) are presented in Table 4.10 along with the standard deviations, σ , of the fit. The solid curves representing $H_{m,1+23}^E$ in Figure 4.4 were calculated from equation (4.18). Equations (4.1), (4.18), and (4.19) were also used to calculate the constant $H_{m,123}^E$ contours plotted on the Roozeboom diagram in Figure 4.5. For the DNPE (1) + DNBE (2) + 1HX (3) ternary system in Figure 4.5 an

internal saddle point exists. The maximum value of $H_{m,123}^E$ is located on the edge of the plot for the constituent binary comprising of DNPE and 1HX.

Ternary systems (2-6), as presented in Table 4.1, have been treated by an identical procedure. The experimental data along with their correlated plots are provided in the following section. For the DNPE (1) + DNBE (2) + THF (2) ternary system, Figure 4.7 shows that there is no internal extremum. That is, the point representing the maximum value of $H_{m,123}^E$ (341.5 J·mol⁻¹) is located on the DNBE-THF edge.

The ternary systems, DNPE (1) + 22DMB (2) + 23 DMB (3), and DNPE (1) + 22DMB (2) + 23 DMB (3) are very similar, both of which show an internal saddle point. However, the maximum value of $H_{m,123}^E$ for DNPE (1) + 22DMB (2) + 23 DMB (3) ternary system, occurs on the DNPE + 23DMB edge where as for DNPE (1) + 22DMB (2) + 23 DMB (3) ternary system, the maximum value occurs on the DNBE + 22DMB edge of the triangles (Figures 4.9 and 4.11).

For the ternary systems of 1HX (1) + THF (2) with either 22DMB or 23DMB (3), the form of the contours presented in Figures 4.13 and 4.15 are identical. There is no indication of internal maxima and all the contours extend to the edge of the triangle.

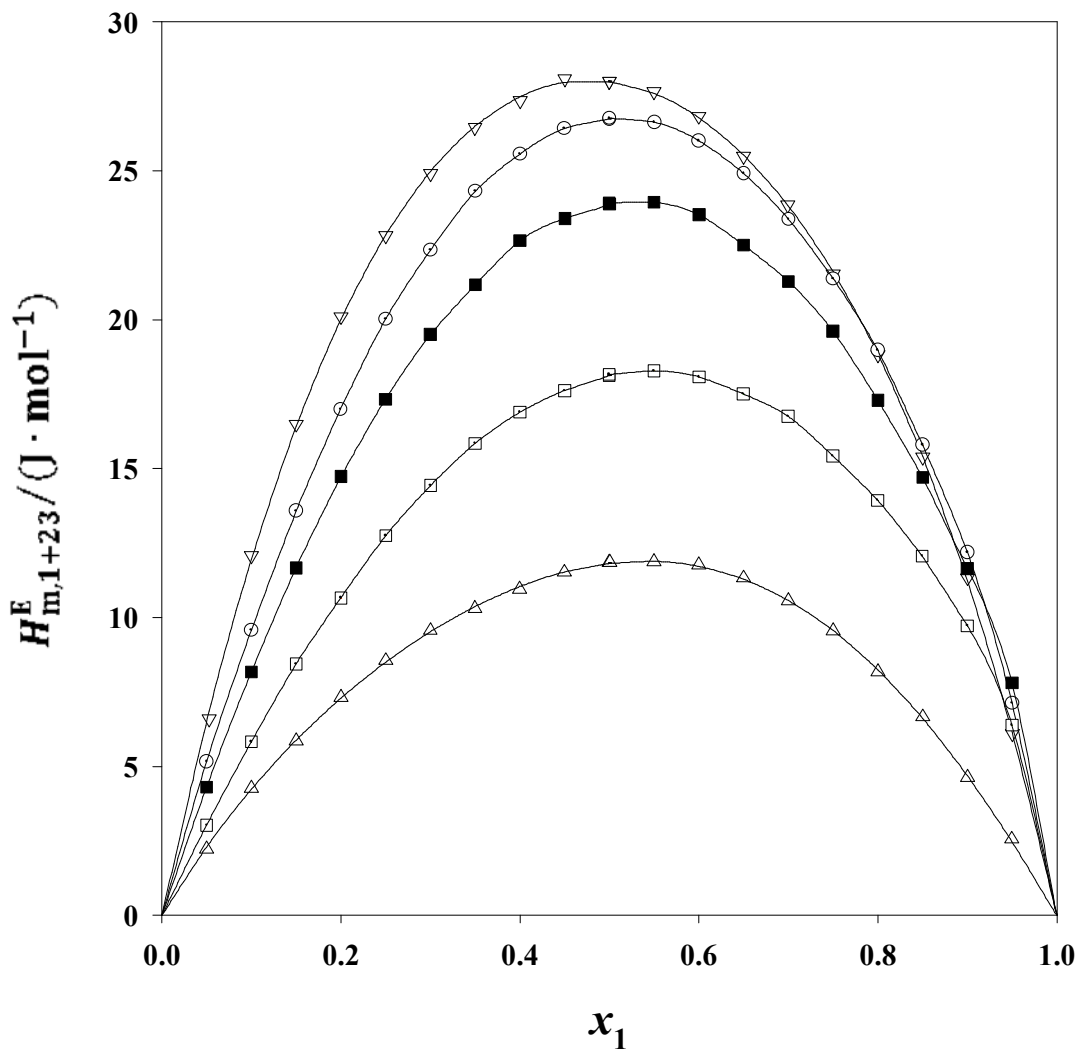


Figure 4.4. Excess molar enthalpies, $H_{m,1+23}^E$, for the x_1 DNPE + x_2 DNBE + $(1 - x_1 - x_2)$ HX mixture at the temperature 298.15 K. Plotted against mole fraction x_1 . Experimental results: Δ , $x_3 = 0.0$; \odot , $x_2/x_3 = 0.3333$; \blacksquare , $x_2/x_3 = 0.9996$; \square , $x_2/x_3 = 3.0000$; ∇ , $x_2 = 0.0$; Curves: —, calculated from the representation of the results by equations (4.18) and (4.19) using the ternary term $H_{m,T}^E$.

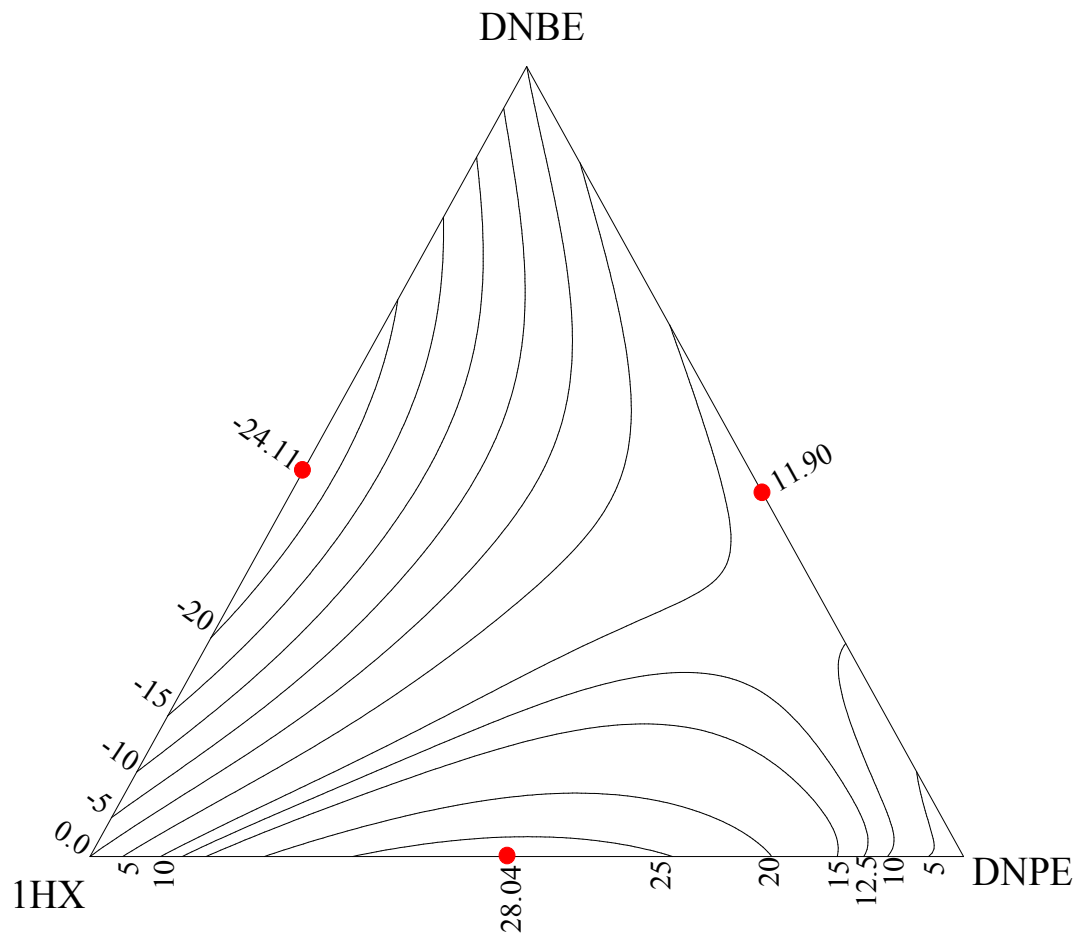


Figure 4.5. Contours for constant values of $H_{m,123}^E / (\text{J} \cdot \text{mol}^{-1})$ for the $x_1 \text{DNPE} + x_2 \text{DNBE} + (1 - x_1 - x_2) \text{1HX}$ system at 298.15 K. Calculated from the representation of the experimental results by equations (4.18) and (4.19).

Ternary System: DNPE (1) + DNBE (2) + THF (3)

Table 4.11. Experimental excess molar enthalpies $H_{m,1+23}^E$ and the calculated values of $H_{m,123}^E$ for the x_1 DNPE + x_2 DNBE + $(1 - x_1 - x_2)$ THF ternary system at 298.15 K

| x_1 | $\frac{H_{m,1+23}^E}{(\text{J} \cdot \text{mol}^{-1})}$ | $\frac{H_{m,123}^E}{(\text{J} \cdot \text{mol}^{-1})}$ | x_1 | $\frac{H_{m,1+23}^E}{(\text{J} \cdot \text{mol}^{-1})}$ | $\frac{H_{m,123}^E}{(\text{J} \cdot \text{mol}^{-1})}$ | x_1 | $\frac{H_{m,1+23}^E}{(\text{J} \cdot \text{mol}^{-1})}$ | $\frac{H_{m,123}^E}{(\text{J} \cdot \text{mol}^{-1})}$ |
|---|---|--|--------|---|--|--------|---|--|
| $x_2/x_3 = 0.3332, H_{m,23}^E/(\text{J} \cdot \text{mol}^{-1}) = 278.7$ | | | | | | | | |
| 0.0500 | 21.2 | 286.0 | 0.4002 | 104.2 | 271.3 | 0.7016 | 91.3 | 174.5 |
| 0.1000 | 38.8 | 289.6 | 0.4497 | 106.8 | 260.2 | 0.7501 | 82.8 | 152.4 |
| 0.1500 | 55.3 | 292.2 | 0.5001 | 108.1 | 247.4 | 0.8000 | 70.8 | 126.5 |
| 0.2002 | 69.2 | 292.1 | 0.5001 | 108.1 | 247.4 | 0.8500 | 58.2 | 100.0 |
| 0.2502 | 80.9 | 289.9 | 0.5501 | 107.2 | 232.6 | 0.9001 | 42.5 | 70.4 |
| 0.3000 | 90.8 | 285.9 | 0.5999 | 104.6 | 216.1 | 0.9500 | 24.1 | 38.1 |
| 0.3499 | 98.4 | 279.5 | 0.6503 | 98.9 | 196.4 | | | |
| $x_2/x_3 = 1.0004, H_{m,23}^E/(\text{J} \cdot \text{mol}^{-1}) = 339.7$ | | | | | | | | |
| 0.0500 | 6.5 | 329.2 | 0.4002 | 35.1 | 238.9 | 0.7000 | 33.2 | 135.1 |
| 0.1000 | 12.6 | 318.3 | 0.4502 | 36.5 | 223.2 | 0.7498 | 30.3 | 115.2 |
| 0.1500 | 17.9 | 306.6 | 0.5002 | 37.3 | 207.1 | 0.8001 | 26.7 | 94.6 |
| 0.2000 | 22.8 | 294.5 | 0.5001 | 37.3 | 207.1 | 0.8500 | 21.9 | 72.8 |
| 0.2503 | 27.0 | 281.7 | 0.5501 | 37.3 | 190.1 | 0.9000 | 15.9 | 49.9 |
| 0.3002 | 30.2 | 267.9 | 0.5998 | 36.6 | 172.6 | 0.9500 | 8.7 | 25.7 |
| 0.3499 | 32.9 | 253.7 | 0.6500 | 35.1 | 154.0 | | | |
| $x_2/x_3 = 3.0000, H_{m,23}^E/(\text{J} \cdot \text{mol}^{-1}) = 241.0$ | | | | | | | | |
| 0.0500 | 1.93 | 230.9 | 0.4002 | 8.50 | 153.1 | 0.7001 | 7.80 | 80.09 |
| 0.1000 | 3.52 | 220.4 | 0.4503 | 8.80 | 141.3 | 0.7498 | 7.11 | 67.40 |
| 0.1555 | 5.01 | 208.5 | 0.5001 | 8.91 | 129.4 | 0.8000 | 6.25 | 54.45 |
| 0.2000 | 5.95 | 198.8 | 0.5001 | 8.91 | 129.4 | 0.8500 | 5.13 | 41.29 |
| 0.2498 | 6.89 | 187.7 | 0.5501 | 8.89 | 117.3 | 0.9000 | 3.75 | 27.86 |
| 0.2999 | 7.55 | 176.3 | 0.6000 | 8.68 | 105.1 | 0.9500 | 2.03 | 14.07 |
| 0.3502 | 8.16 | 164.8 | 0.6501 | 8.35 | 92.68 | | | |

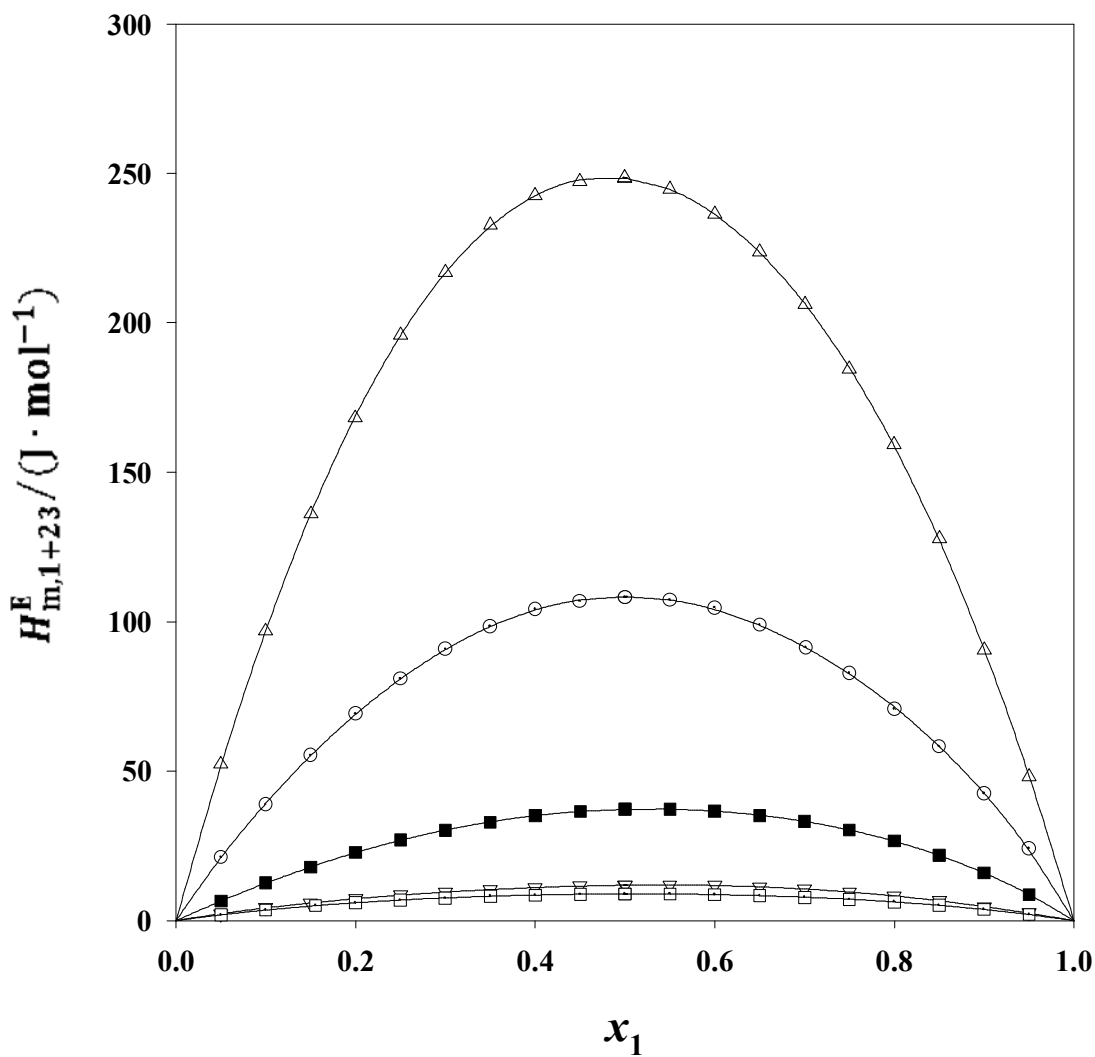


Figure 4.6. Excess molar enthalpies, $H_{m,1+23}^E$, for the x_1 DNPE + x_2 DNBE + $(1 - x_1 - x_2)$ THF mixture at the temperature 298.15 K. Plotted against mole fraction x_1 . Experimental results: Δ , $x_2/x_3 = 0.0$; \odot , $x_2/x_3 = 0.3332$; \blacksquare , $x_2/x_3 = 1.0004$; \square , $x_2/x_3 = 3.0000$; ∇ , $x_2 = 0.0$; Curves: —, calculated from the representation of the results by equations (4.18) and (4.19) using the ternary term $H_{m,T}^E$.

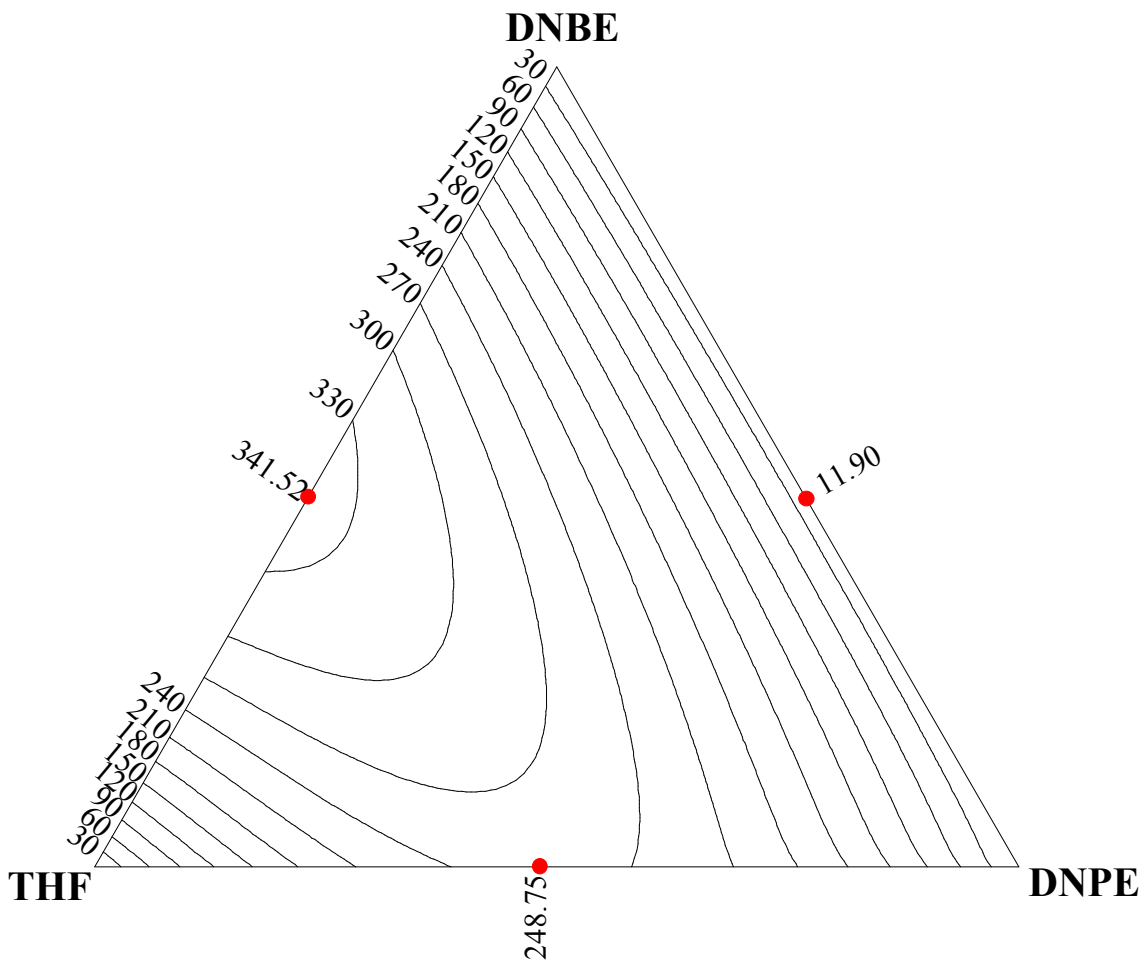


Figure 4.7. Contours for constant values of $H_{m,123}^E / (\text{J} \cdot \text{mol}^{-1})$ for the $x_1 \text{DNPE} + x_2 \text{DNBE} + (1 - x_1 - x_2) \text{THF}$ system at 298.15 K. Calculated from the representation of the experimental results by equations (4.18) and (4.19).

Ternary System: DNPE (1) + 22DMB (2) + 23DMB (3)

Table 4.12. Experimental excess molar enthalpies $H_{m,1+23}^E$ and the calculated values of $H_{m,123}^E$ for the x_1 DNPE + x_2 22DMB + $(1 - x_1 - x_2)$ 23DMB ternary system at 298.15 K

| x_1 | $\frac{H_{m,1+23}^E}{(\text{J} \cdot \text{mol}^{-1})}$ | $\frac{H_{m,123}^E}{(\text{J} \cdot \text{mol}^{-1})}$ | x_1 | $\frac{H_{m,1+23}^E}{(\text{J} \cdot \text{mol}^{-1})}$ | $\frac{H_{m,123}^E}{(\text{J} \cdot \text{mol}^{-1})}$ | x_1 | $\frac{H_{m,1+23}^E}{(\text{J} \cdot \text{mol}^{-1})}$ | $\frac{H_{m,123}^E}{(\text{J} \cdot \text{mol}^{-1})}$ |
|---|---|--|--------|---|--|--------|---|--|
| $x_2/x_3 = 0.3257, H_{m,23}^E/(\text{J} \cdot \text{mol}^{-1}) = 1.0$ | | | | | | | | |
| 0.0500 | 30.9 | 31.8 | 0.4000 | 148.7 | 149.3 | 0.7003 | 128.1 | 128.4 |
| 0.1000 | 59.0 | 59.9 | 0.4498 | 152.9 | 153.4 | 0.7505 | 115.4 | 115.7 |
| 0.1501 | 82.7 | 83.5 | 0.4998 | 154.1 | 154.6 | 0.8001 | 97.2 | 97.4 |
| 0.1998 | 100.6 | 101.3 | 0.4998 | 154.2 | 154.7 | 0.8500 | 79.3 | 79.4 |
| 0.2499 | 119.1 | 119.8 | 0.5500 | 151.9 | 152.3 | 0.9000 | 58.4 | 58.5 |
| 0.2999 | 132.6 | 133.2 | 0.6000 | 145.9 | 146.3 | 0.9500 | 30.1 | 30.2 |
| 0.3499 | 142.1 | 142.7 | 0.6501 | 138.5 | 138.8 | | | |
| $x_2/x_3 = 0.9747, H_{m,23}^E/(\text{J} \cdot \text{mol}^{-1}) = 1.3$ | | | | | | | | |
| 0.0500 | 32.1 | 33.3 | 0.4000 | 147.6 | 148.4 | 0.7002 | 127.3 | 127.7 |
| 0.1000 | 58.5 | 59.7 | 0.4499 | 152.2 | 152.9 | 0.7501 | 114.7 | 115.0 |
| 0.1500 | 81.5 | 82.6 | 0.4999 | 153.9 | 154.5 | 0.8003 | 98.5 | 98.7 |
| 0.2000 | 101.3 | 102.3 | 0.4999 | 153.8 | 154.4 | 0.8501 | 79.6 | 79.8 |
| 0.2501 | 118.1 | 119.1 | 0.5496 | 151.4 | 152.0 | 0.9000 | 58.1 | 58.2 |
| 0.2999 | 131.6 | 132.5 | 0.5999 | 146.0 | 146.5 | 0.9500 | 32.2 | 32.3 |
| 0.3498 | 140.4 | 141.3 | 0.6500 | 137.8 | 138.3 | | | |
| $x_2/x_3 = 2.9968, H_{m,23}^E/(\text{J} \cdot \text{mol}^{-1}) = 1.0$ | | | | | | | | |
| 0.0500 | 31.4 | 32.3 | 0.4001 | 144.6 | 145.2 | 0.7002 | 125.7 | 125.9 |
| 0.1000 | 58.1 | 58.9 | 0.4499 | 149.2 | 149.7 | 0.7500 | 111.3 | 111.6 |
| 0.1500 | 79.6 | 80.4 | 0.4999 | 150.6 | 151.0 | 0.7999 | 96.3 | 96.5 |
| 0.2002 | 99.3 | 100.1 | 0.5000 | 150.6 | 151.1 | 0.8500 | 76.1 | 76.3 |
| 0.2499 | 115.3 | 116.0 | 0.5501 | 148.5 | 149.0 | 0.9000 | 55.5 | 55.6 |
| 0.2999 | 128.4 | 129.1 | 0.6000 | 143.9 | 144.3 | 0.9500 | 31.2 | 31.2 |
| 0.3498 | 138.0 | 138.6 | 0.6502 | 135.9 | 136.2 | | | |

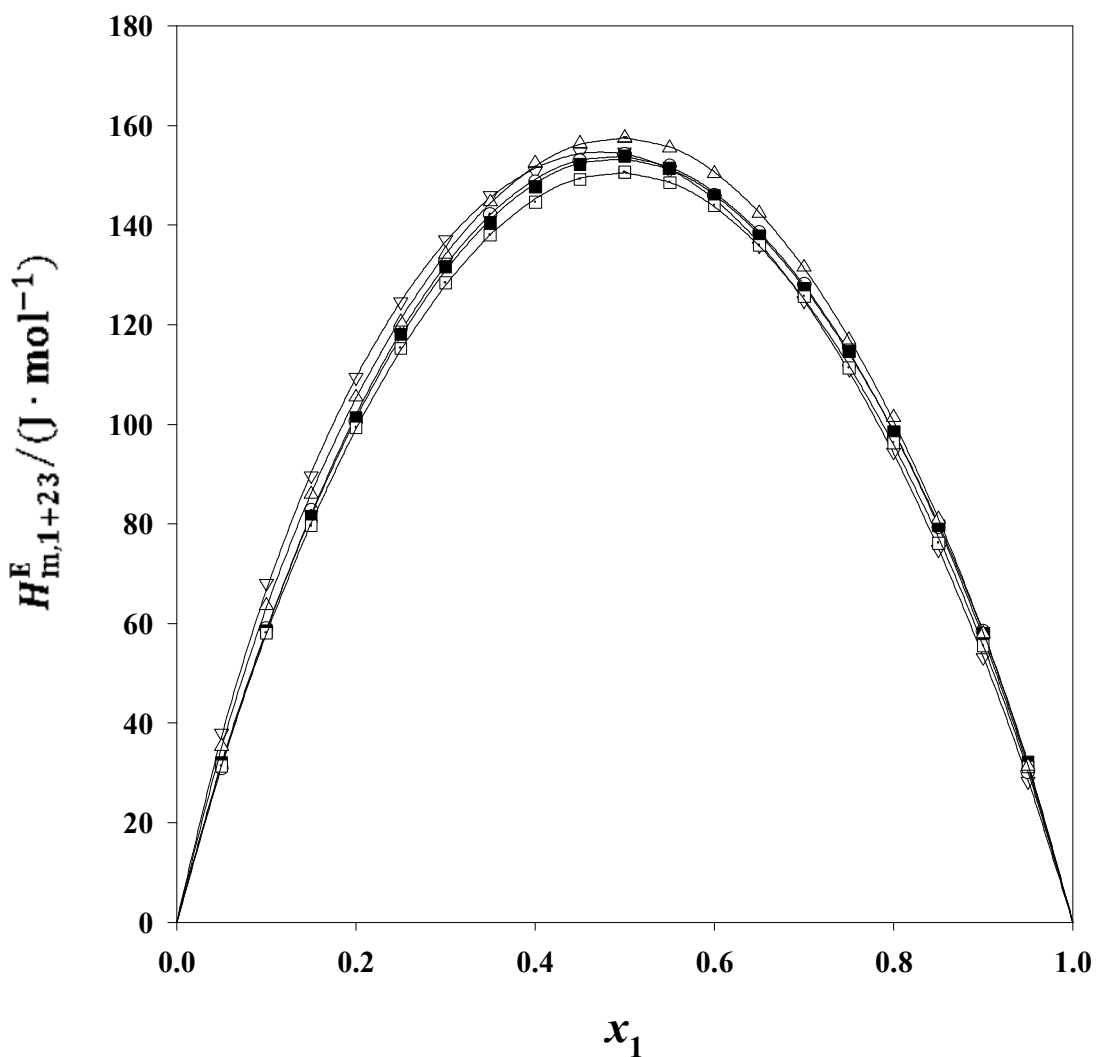


Figure 4.8. Excess molar enthalpies, $H_{m,1+23}^E$, for the x_1 DNPE + x_2 22DMB + $(1 - x_1 - x_2)$ 23DMB mixture at the temperature 298.15 K. Plotted against mole fraction x_1 . Experimental results: Δ , $x_3 = 0.0$; \odot , $x_2/x_3 = 0.3257$; \blacksquare , $x_2/x_3 = 0.9747$; \square , $x_2/x_3 = 2.9968$; ∇ , $x_2 = 0.0$; Curves: —, calculated from the representation of the results by equations (4.18) and (4.19) using the ternary term $H_{m,T}^E$.

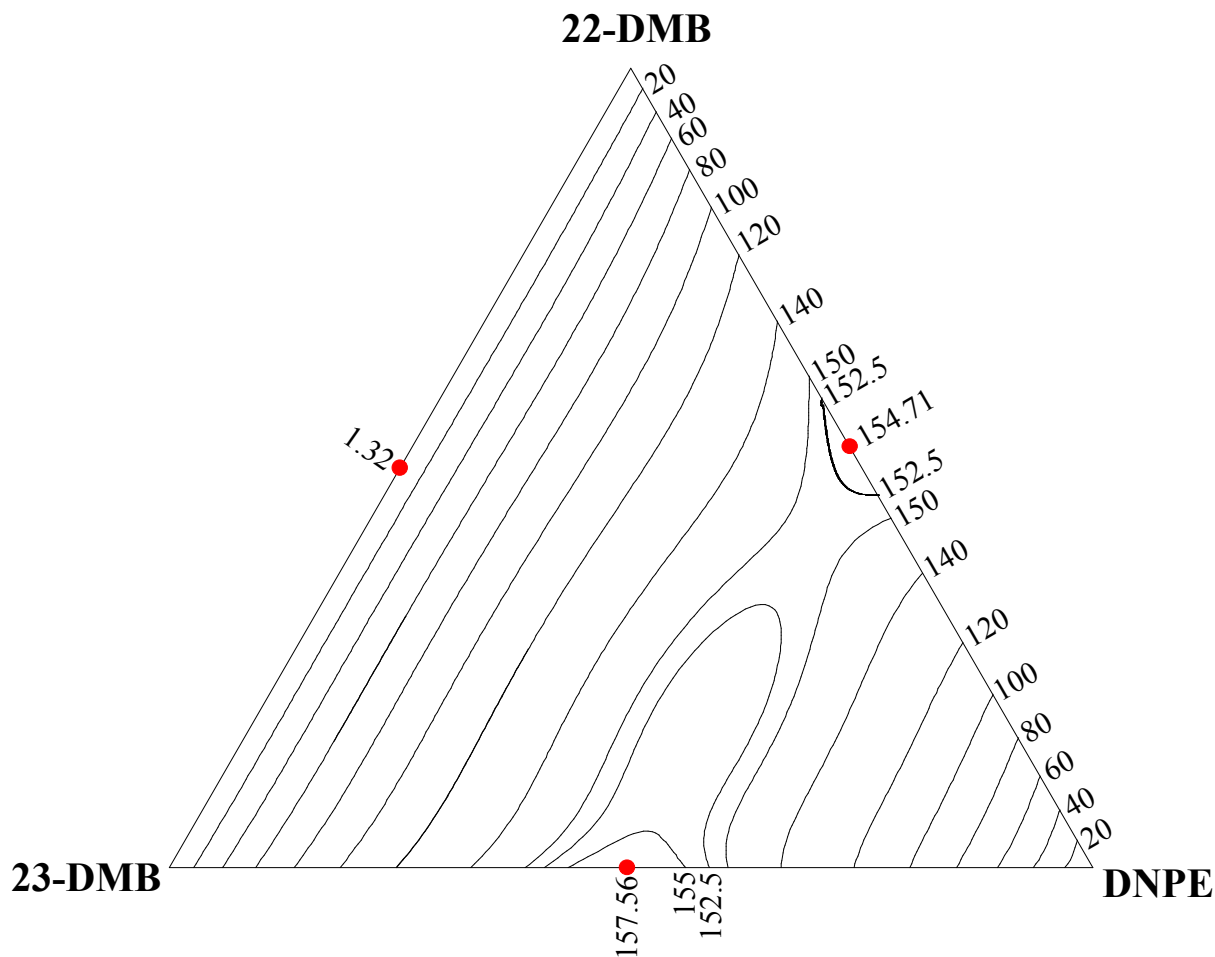


Figure 4.9. Contours for constant values of $H_{m,123}^E / (\text{J} \cdot \text{mol}^{-1})$ for the $x_1 \text{DNPE} + x_2 \text{22DMB} + (1 - x_1 - x_2) \text{23DMB}$ system at 298.15 K. Calculated from the representation of the experimental results by equations (4.18) and (4.19).

Ternary System: DNBE (1) + 22DMB (2) + 23DMB (3)

Table 4.13. Experimental excess molar enthalpies $H_{m,1+23}^E$ and the calculated values of $H_{m,123}^E$ for the x_1 DNBE+ x_2 22DMB + $(1 - x_1 - x_2)$ 23DMB ternary system at 298.15 K

| x_1 | $\frac{H_{m,1+23}^E}{(\text{J} \cdot \text{mol}^{-1})}$ | $\frac{H_{m,123}^E}{(\text{J} \cdot \text{mol}^{-1})}$ | x_1 | $\frac{H_{m,1+23}^E}{(\text{J} \cdot \text{mol}^{-1})}$ | $\frac{H_{m,123}^E}{(\text{J} \cdot \text{mol}^{-1})}$ | x_1 | $\frac{H_{m,1+23}^E}{(\text{J} \cdot \text{mol}^{-1})}$ | $\frac{H_{m,123}^E}{(\text{J} \cdot \text{mol}^{-1})}$ |
|---|---|--|--------|---|--|--------|---|--|
| $x_2/x_3 = 0.3261, H_{m,23}^E/(\text{J} \cdot \text{mol}^{-1}) = 1.0$ | | | | | | | | |
| 0.0500 | 23.1 | 24.0 | 0.4001 | 100.3 | 100.8 | 0.7000 | 88.6 | 88.9 |
| 0.1000 | 41.4 | 42.2 | 0.4497 | 102.7 | 103.3 | 0.7490 | 81.0 | 81.3 |
| 0.1500 | 57.0 | 57.9 | 0.4999 | 103.0 | 103.4 | 0.8000 | 73.3 | 73.5 |
| 0.2000 | 70.8 | 71.6 | 0.5000 | 102.9 | 103.3 | 0.8500 | 63.9 | 64.1 |
| 0.2499 | 80.9 | 81.7 | 0.5499 | 102.3 | 102.8 | 0.9000 | 49.8 | 49.9 |
| 0.3001 | 90.0 | 90.7 | 0.6002 | 99.1 | 99.47 | 0.9500 | 29.3 | 29.3 |
| 0.3497 | 95.6 | 96.3 | 0.6504 | 94.8 | 95.14 | | | |
| $x_2/x_3 = 0.9747, H_{m,23}^E/(\text{J} \cdot \text{mol}^{-1}) = 1.3$ | | | | | | | | |
| 0.0500 | 23.8 | 25.0 | 0.3998 | 103.4 | 104.2 | 0.7004 | 91.1 | 91.5 |
| 0.1000 | 43.3 | 44.4 | 0.4500 | 105.8 | 106.5 | 0.7502 | 83.6 | 83.9 |
| 0.1498 | 59.5 | 60.6 | 0.4996 | 106.6 | 107.3 | 0.8000 | 73.9 | 74.1 |
| 0.1999 | 73.2 | 74.2 | 0.4997 | 106.9 | 107.6 | 0.8501 | 62.5 | 62.7 |
| 0.2499 | 84.3 | 85.2 | 0.5500 | 104.7 | 105.3 | 0.9000 | 48.7 | 48.8 |
| 0.2998 | 93.2 | 94.1 | 0.6003 | 102.2 | 102.8 | 0.9500 | 28.3 | 28.4 |
| 0.3499 | 99.1 | 100.0 | 0.6504 | 97.1 | 97.6 | | | |
| $x_2/x_3 = 2.9968, H_{m,23}^E/(\text{J} \cdot \text{mol}^{-1}) = 1.0$ | | | | | | | | |
| 0.0500 | 24.1 | 25.1 | 0.4000 | 105.9 | 106.4 | 0.7002 | 92.2 | 92.5 |
| 0.1005 | 44.0 | 44.9 | 0.4501 | 107.7 | 108.2 | 0.7499 | 84.0 | 84.2 |
| 0.1505 | 60.3 | 61.2 | 0.4998 | 108.4 | 108.9 | 0.8000 | 73.4 | 73.6 |
| 0.1998 | 74.5 | 75.3 | 0.4998 | 108.5 | 109.0 | 0.8500 | 61.7 | 61.9 |
| 0.2497 | 85.7 | 86.4 | 0.5501 | 107.1 | 107.6 | 0.9000 | 46.9 | 47.0 |
| 0.2998 | 94.3 | 95.0 | 0.5999 | 104.3 | 104.7 | 0.9500 | 26.4 | 26.5 |
| 0.3500 | 101.0 | 101.6 | 0.6504 | 99.0 | 99.3 | | | |

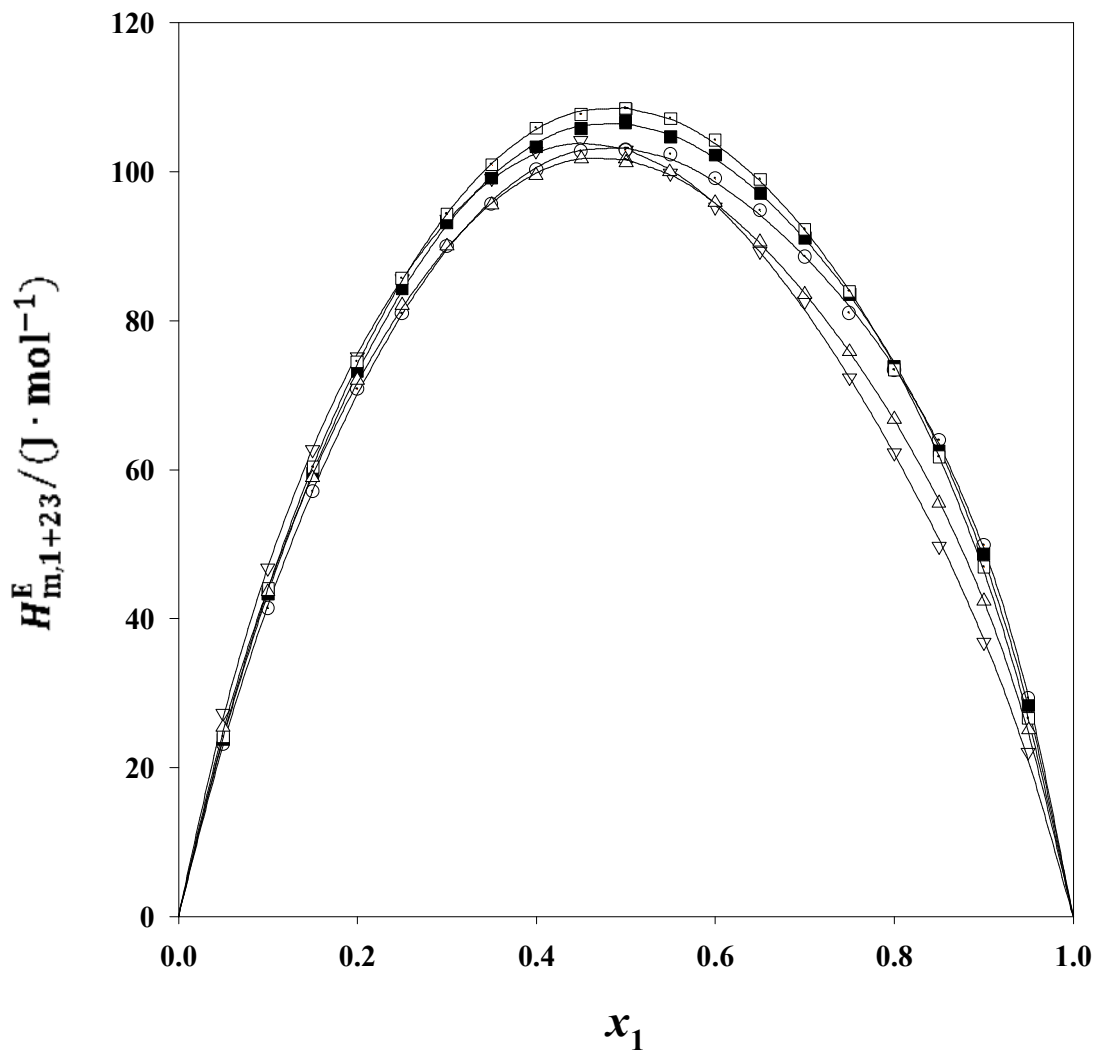


Figure 4.10. Excess molar enthalpies, $H_{m,1+23}^E$, for the x_1 DNBE + x_2 22DMB + $(1 - x_1 - x_2)$ 23DMB mixture at the temperature 298.15 K. Plotted against mole fraction x_1 . Experimental results: Δ , $x_3 = 0.0$; \odot , $x_2/x_3 = 0.3261$; \blacksquare , $x_2/x_3 = 0.9747$; \square , $x_2/x_3 = 2.9968$; ∇ , $x_2 = 0.0$; Curves: —, calculated from the representation of the results by equations (4.18) and (4.19) using the ternary term $H_{m,T}^E$.

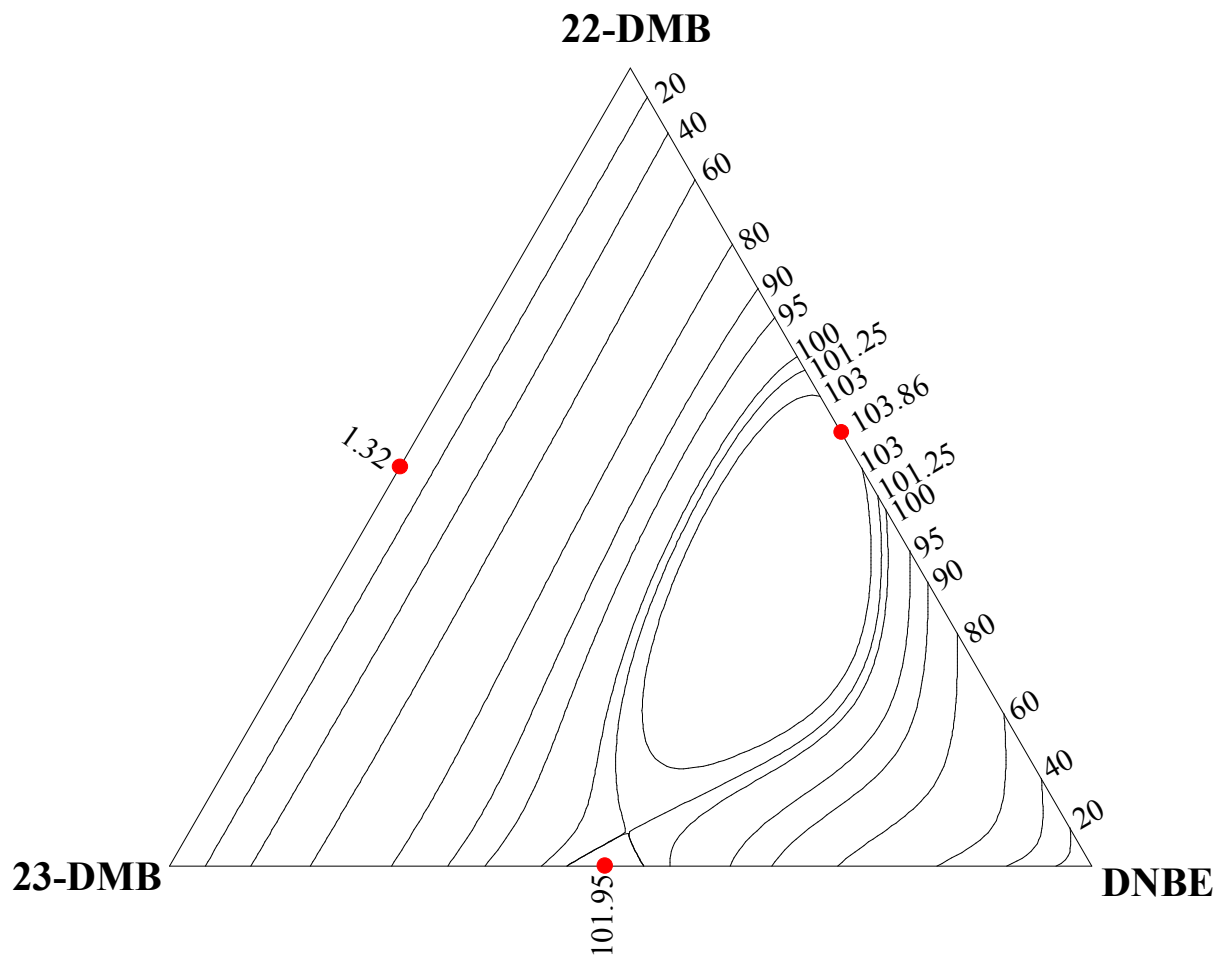


Figure 4.11. Contours for constant values of $H_{m,123}^E / (\text{J} \cdot \text{mol}^{-1})$ for the $x_1 \text{DNBE} + x_2 \text{22DMB} + (1 - x_1 - x_2) \text{23DMB}$ system at 298.15 K. Calculated from the representation of the experimental results by equations (4.18) and (4.19).

Ternary System: 1HX (1) + THF (2) + 22DMB (3)

Table 4.14. Experimental excess molar enthalpies $H_{m,1+23}^E$ and the calculated values of $H_{m,123}^E$ for the x_1 1HX + x_2 THF + $(1 - x_1 - x_2)$ 22DMB ternary system at 298.15 K

| x_1 | $\frac{H_{m,1+23}^E}{(\text{J} \cdot \text{mol}^{-1})}$ | $\frac{H_{m,123}^E}{(\text{J} \cdot \text{mol}^{-1})}$ | x_1 | $\frac{H_{m,1+23}^E}{(\text{J} \cdot \text{mol}^{-1})}$ | $\frac{H_{m,123}^E}{(\text{J} \cdot \text{mol}^{-1})}$ | x_1 | $\frac{H_{m,1+23}^E}{(\text{J} \cdot \text{mol}^{-1})}$ | $\frac{H_{m,123}^E}{(\text{J} \cdot \text{mol}^{-1})}$ |
|---|---|--|--------|---|--|--------|---|--|
| $x_2/x_3 = 0.3329, H_{m,23}^E/(\text{J} \cdot \text{mol}^{-1}) = 507.2$ | | | | | | | | |
| 0.0500 | 3.2 | 481.9 | 0.3999 | 18.0 | 304.4 | 0.6998 | 15.8 | 152.3 |
| 0.1000 | 6.1 | 456.5 | 0.4497 | 18.7 | 279.1 | 0.7504 | 14.1 | 126.6 |
| 0.1501 | 9.1 | 431.1 | 0.4997 | 18.7 | 253.8 | 0.8000 | 11.6 | 101.5 |
| 0.2002 | 11.4 | 405.7 | 0.4997 | 18.9 | 253.8 | 0.8500 | 9.3 | 76.1 |
| 0.2502 | 13.5 | 380.3 | 0.5500 | 18.6 | 228.3 | 0.9001 | 6.5 | 50.7 |
| 0.2999 | 15.6 | 355.1 | 0.5999 | 18.0 | 203.0 | 0.9500 | 3.5 | 25.4 |
| 0.3498 | 17.1 | 329.8 | 0.6500 | 17.2 | 177.5 | | | |
| $x_2/x_3 = 1.0004, H_{m,23}^E/(\text{J} \cdot \text{mol}^{-1}) = 684.7$ | | | | | | | | |
| 0.0500 | 9.8 | 650.5 | 0.4001 | 52.4 | 410.8 | 0.6998 | 47.7 | 205.5 |
| 0.1000 | 19.2 | 616.2 | 0.4504 | 54.6 | 376.3 | 0.7499 | 42.5 | 171.3 |
| 0.1501 | 27.2 | 581.9 | 0.4998 | 55.1 | 342.5 | 0.8002 | 36.8 | 137.0 |
| 0.2000 | 33.7 | 547.7 | 0.4999 | 55.3 | 342.4 | 0.8500 | 29.6 | 102.7 |
| 0.2501 | 40.0 | 513.4 | 0.5501 | 55.0 | 308.0 | 0.9000 | 21.8 | 68.5 |
| 0.3002 | 45.1 | 479.2 | 0.6000 | 53.5 | 273.9 | 0.9500 | 11.3 | 34.3 |
| 0.3500 | 49.1 | 445.0 | 0.6501 | 51.5 | 239.6 | | | |
| $x_2/x_3 = 3.0000, H_{m,23}^E/(\text{J} \cdot \text{mol}^{-1}) = 523.4$ | | | | | | | | |
| 0.0500 | 30.2 | 497.2 | 0.3999 | 156.3 | 314.1 | 0.7002 | 143.4 | 156.9 |
| 0.1000 | 56.8 | 471.1 | 0.4499 | 161.7 | 287.9 | 0.7499 | 130.5 | 130.9 |
| 0.1498 | 80.9 | 445.0 | 0.4998 | 164.5 | 261.8 | 0.8000 | 111.3 | 104.7 |
| 0.1999 | 100.4 | 418.8 | 0.4998 | 164.6 | 261.8 | 0.8500 | 89.2 | 78.5 |
| 0.2500 | 118.7 | 392.5 | 0.5499 | 164.3 | 235.6 | 0.9000 | 65.9 | 52.3 |
| 0.2998 | 132.9 | 366.5 | 0.5997 | 161.2 | 209.5 | 0.9500 | 34.3 | 26.2 |
| 0.3502 | 146.3 | 340.1 | 0.6501 | 154.0 | 183.1 | | | |

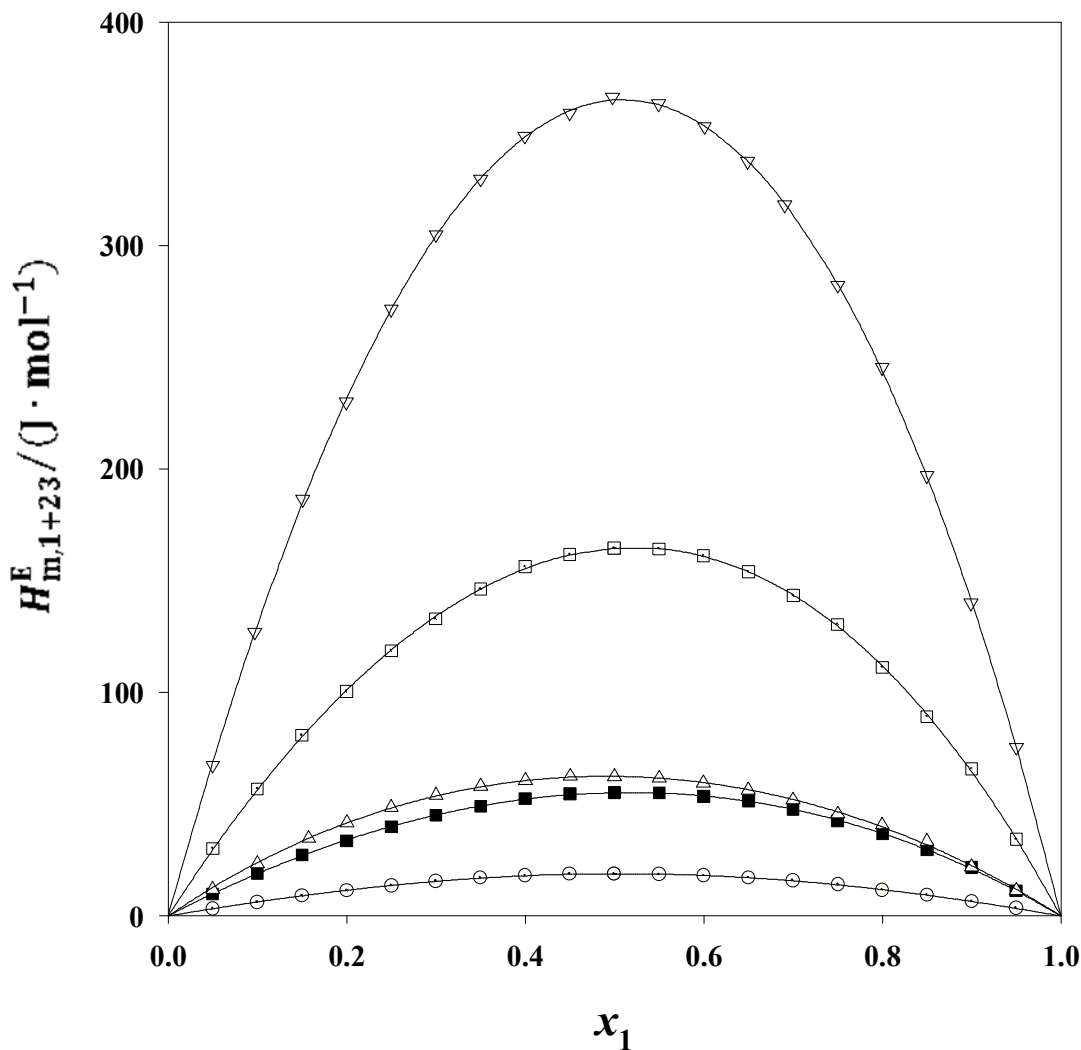


Figure 4.12. Excess molar enthalpies, $H_{m,1+23}^E$, for the x_1 1HX + x_2 THF + $(1 - x_1 - x_2)$ 22DMB mixture at the temperature 298.15 K. Plotted against mole fraction x_1 . Experimental results: Δ , $x_3 = 0.0$; \odot , $x_2/x_3 = 0.3329$; \blacksquare , $x_2/x_3 = 1.0004$; \square , $x_2/x_3 = 3.0000$; ∇ , $x_2 = 0.0$; Curves: —, calculated from the representation of the results by equations (4.18) and (4.19) using the ternary term $H_{m,T}^E$.

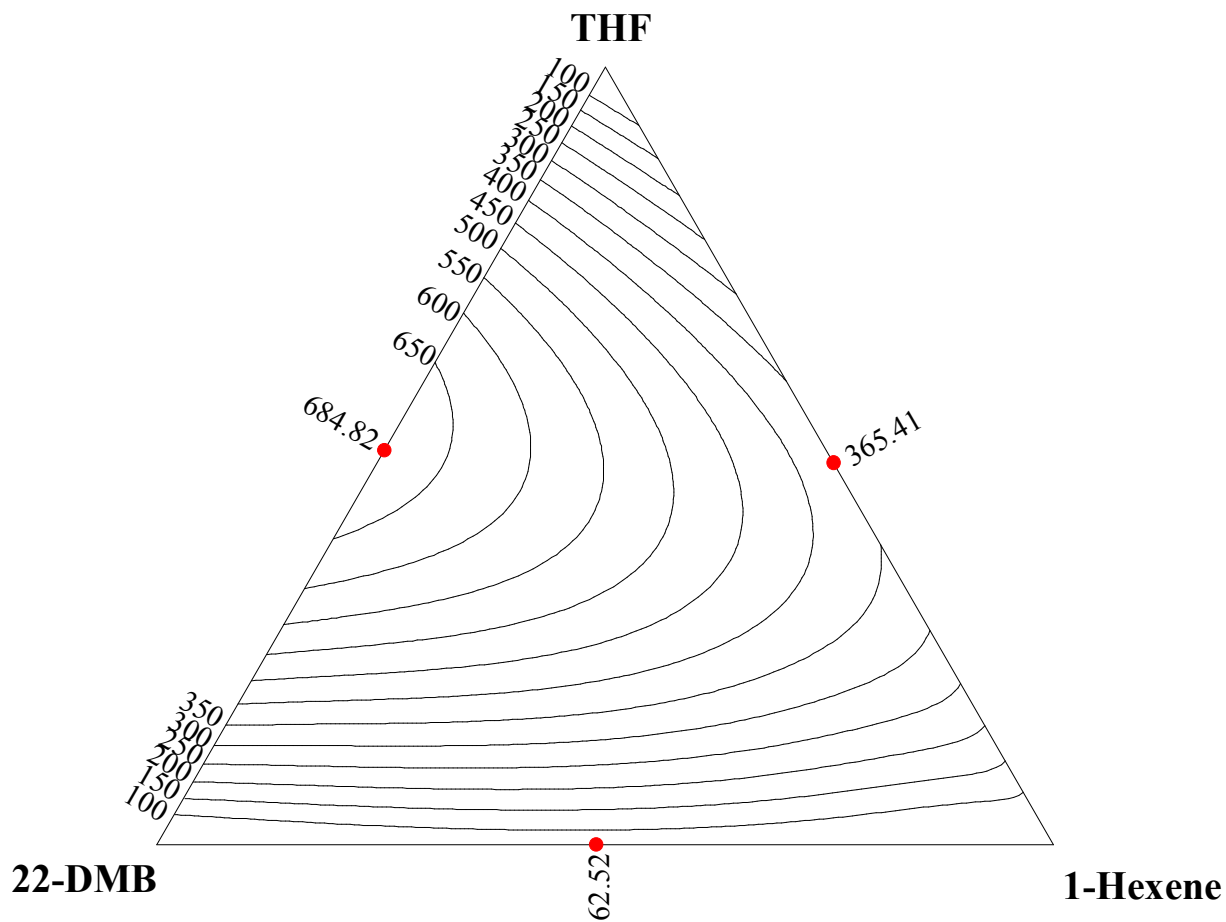


Figure 4.13. Contours for constant values of $H_{m,123}^E / (\text{J} \cdot \text{mol}^{-1})$ for the $x_1 1\text{HX} + x_2 \text{THF} + (1 - x_1 - x_2) 22\text{DMB}$ system at 298.15 K. Calculated from the representation of the experimental results by equations (4.18) and (4.19).

Ternary System: 1HX (1) + THF (2) + 23DMB (3)

Table 4.15. Experimental excess molar enthalpies $H_{m,1+23}^E$ and the calculated values of $H_{m,123}^E$ for the x_1 1HX + x_2 THF + $(1 - x_1 - x_2)$ 23DMB ternary system at 298.15 K

| x_1 | $\frac{H_{m,1+23}^E}{(\text{J} \cdot \text{mol}^{-1})}$ | $\frac{H_{m,123}^E}{(\text{J} \cdot \text{mol}^{-1})}$ | x_1 | $\frac{H_{m,1+23}^E}{(\text{J} \cdot \text{mol}^{-1})}$ | $\frac{H_{m,123}^E}{(\text{J} \cdot \text{mol}^{-1})}$ | x_1 | $\frac{H_{m,1+23}^E}{(\text{J} \cdot \text{mol}^{-1})}$ | $\frac{H_{m,123}^E}{(\text{J} \cdot \text{mol}^{-1})}$ |
|---|---|--|--------|---|--|--------|---|--|
| $x_2/x_3 = 0.3332, H_{m,23}^E/(\text{J} \cdot \text{mol}^{-1}) = 510.8$ | | | | | | | | |
| 0.0500 | 1.7 | 485.2 | 0.4001 | 9.0 | 306.4 | 0.6999 | 7.8 | 153.3 |
| 0.1000 | 3.4 | 459.7 | 0.4498 | 9.3 | 281.0 | 0.7502 | 7.0 | 127.6 |
| 0.1500 | 4.7 | 434.1 | 0.4998 | 9.3 | 255.5 | 0.8002 | 5.9 | 102.0 |
| 0.2002 | 6.0 | 408.5 | 0.4998 | 9.4 | 255.5 | 0.8501 | 4.6 | 76.6 |
| 0.2499 | 6.8 | 383.1 | 0.5500 | 9.3 | 229.8 | 0.9000 | 3.2 | 51.1 |
| 0.2998 | 7.7 | 357.6 | 0.6000 | 9.0 | 204.3 | 0.9500 | 1.6 | 25.6 |
| 0.3501 | 8.5 | 332.0 | 0.6498 | 8.6 | 178.9 | | | |
| $x_2/x_3 = 0.9996, H_{m,23}^E/(\text{J} \cdot \text{mol}^{-1}) = 676.9$ | | | | | | | | |
| 0.0500 | 8.4 | 643.1 | 0.4001 | 44.7 | 406.1 | 0.6999 | 40.0 | 203.2 |
| 0.1000 | 16.1 | 609.2 | 0.4504 | 46.3 | 372.0 | 0.7498 | 36.4 | 169.4 |
| 0.1503 | 23.0 | 575.2 | 0.4999 | 47.1 | 338.5 | 0.8000 | 31.2 | 135.4 |
| 0.2001 | 29.4 | 541.4 | 0.4999 | 47.1 | 338.5 | 0.8499 | 24.9 | 101.6 |
| 0.2502 | 34.5 | 507.6 | 0.5502 | 46.7 | 304.5 | 0.9000 | 18.2 | 67.9 |
| 0.3001 | 38.4 | 473.8 | 0.6002 | 45.4 | 270.6 | 0.9500 | 9.6 | 33.9 |
| 0.3501 | 41.9 | 439.9 | 0.6498 | 43.1 | 237.0 | | | |
| $x_2/x_3 = 3.0000, H_{m,23}^E/(\text{J} \cdot \text{mol}^{-1}) = 512.1$ | | | | | | | | |
| 0.0500 | 28.9 | 486.5 | 0.4002 | 151.6 | 307.2 | 0.7005 | 139.6 | 153.4 |
| 0.1000 | 55.0 | 460.9 | 0.4497 | 157.1 | 281.8 | 0.7501 | 125.9 | 128.0 |
| 0.1499 | 78.0 | 435.3 | 0.5002 | 161.8 | 256.0 | 0.8001 | 106.9 | 102.4 |
| 0.1999 | 99.5 | 409.7 | 0.5001 | 161.2 | 256.0 | 0.8500 | 86.6 | 76.8 |
| 0.2501 | 117.1 | 384.1 | 0.5498 | 160.8 | 230.8 | 0.9000 | 62.2 | 51.2 |
| 0.3000 | 130.9 | 358.5 | 0.5996 | 157.2 | 205.0 | 0.9500 | 32.9 | 25.6 |
| 0.3500 | 142.9 | 332.9 | 0.6501 | 149.7 | 179.2 | | | |

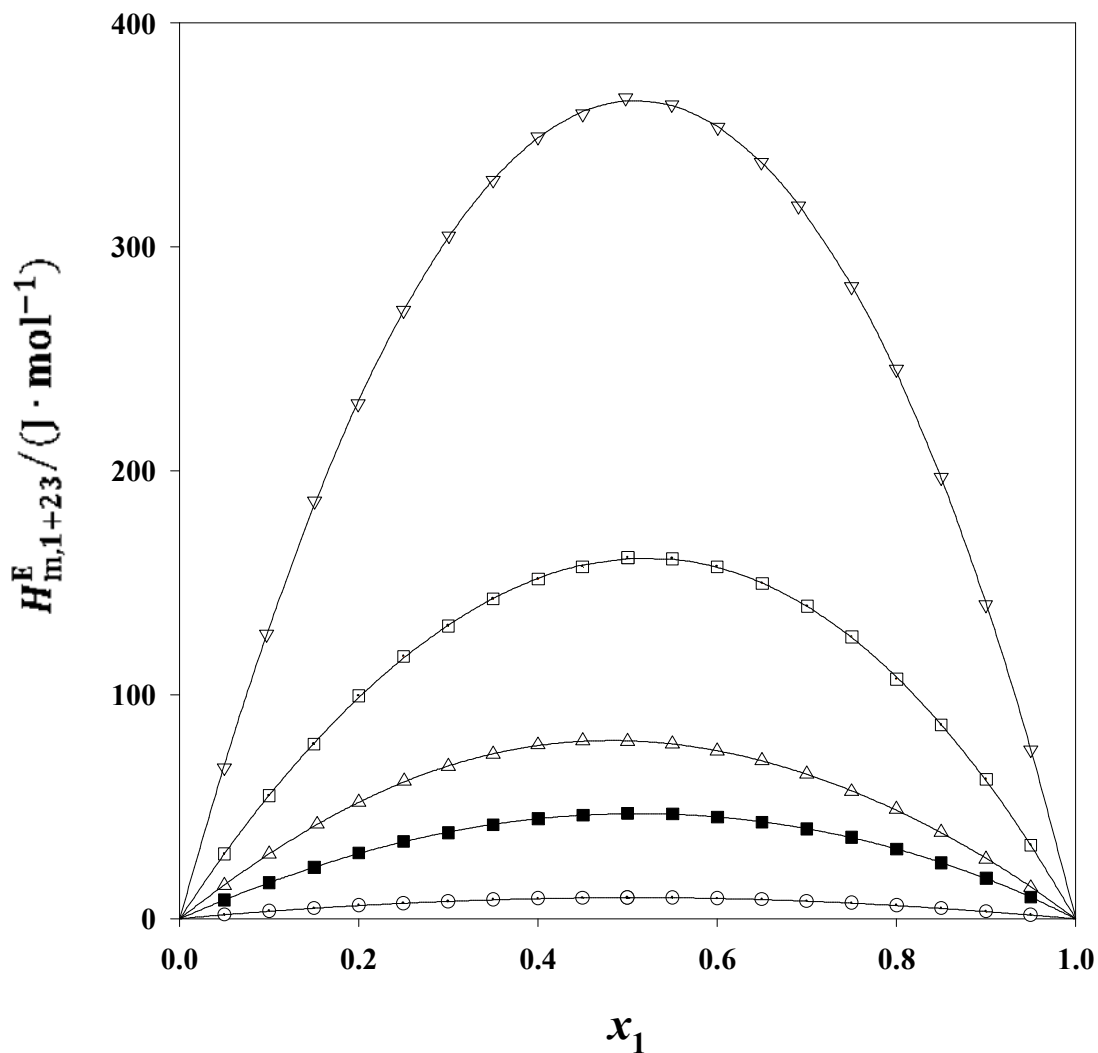


Figure 4.14. Excess molar enthalpies, $H_{m,1+23}^E$, for the x_1 1HX + x_2 THF + $(1 - x_1 - x_2)$ 23DMB mixture at the temperature 298.15 K. Plotted against mole fraction x_1 . Experimental results: Δ , $x_3 = 0.0$; \odot , $x_2/x_3 = 0.3329$; \blacksquare , $x_2/x_3 = 1.0004$; \square , $x_2/x_3 = 3.0000$; ∇ , $x_2 = 0.0$; Curves: —, calculated from the representation of the results by equations (4.18) and (4.19) using the ternary term $H_{m,T}^E$.

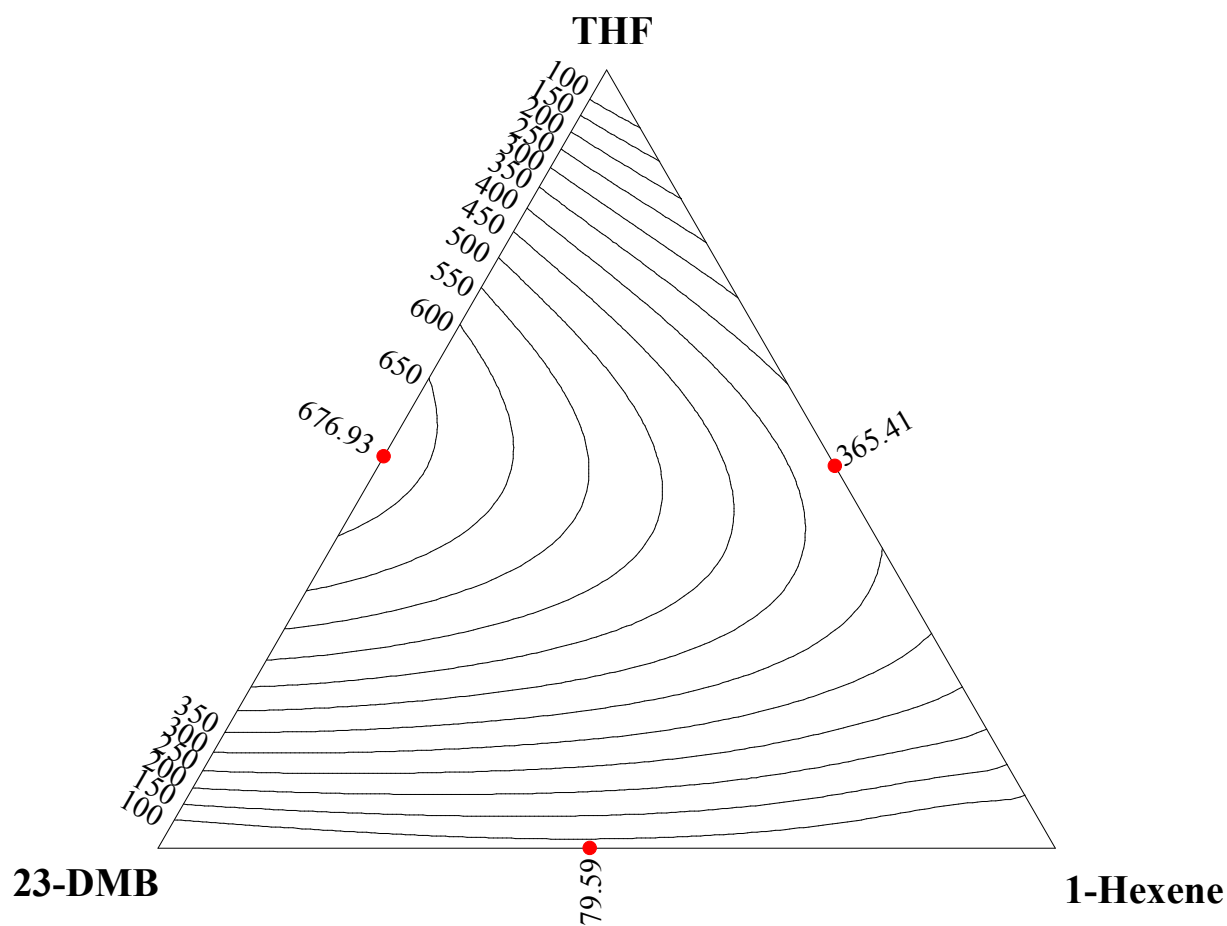


Figure 4.15. Contours for constant values of $H_{m,123}^E / (\text{J} \cdot \text{mol}^{-1})$ for the x_1 1HX + x_2 THF + $(1 - x_1 - x_2)$ 23DMB system at 298.15 K. Calculated from the representation of the experimental results by equations (4.18) and (4.19).

4.2.1 Predictions by means of the Flory Theory

Benson and coworkers (1993-2001) predicted the excess molar enthalpy values with the Flory theory, for a large number of ternary systems. In Table 4.16, the interchange energy parameters for the constituent binary systems along with the standard deviations, σ , of the estimates are presented for the six ternary systems involved in this study. As an example of the ternary excess enthalpy prediction by means of the Flory theory, the DNPE (1) + DNBE (2) + 1HX (3) system is presented.

Table 4.16. Interchange energy parameter χ_{ij} and the standard deviation σ of the prediction of ternary system excess enthalpies by means of the Flory theory

| System | Component | | | χ_{12} | χ_{13} | χ_{23} | $\frac{\sigma}{(\text{J} \cdot \text{mol}^{-1})}$ |
|--------|-----------|-------|-------|-------------------------|------------------------|-------------------------|---|
| | 1 | 2 | 3 | | | | |
| 1 | DNPE | DNBE | 1HX | 0.5216 | 1.1899 | -0.3457 ^{*(1)} | 1.77 |
| 2 | DNPE | DNBE | THF | 0.5216 | 10.6922 | 12.7194 | 6.00 |
| 3 | DNPE | 22DMB | 23DMB | 5.8503 | 5.8475 | 0.0766 ^{*(4)} | 3.37 |
| 4 | DNBE | 22DMB | 23DMB | 3.8860 | 3.6515 | 0.0776 | 6.26 |
| 5 | 1HX | THF | 22DMB | 16.6649 ^{*(2)} | 2.5444 ^{*(3)} | 34.6610 | 19.65 |
| 6 | 1HX | THF | 23DMB | 16.6649 | 3.0702 ^{*(3)} | 34.5493 | 13.27 |

*These binary interchange energy parameters are obtained by fitting the literature heats of mixing data to the Flory theory. ⁽¹⁾Wang et al. (2004b); ⁽²⁾Lan et al. (2006); ⁽³⁾Wang et al. (2004a); ⁽⁴⁾Hamam and Benson (1986)

The other parameters χ_{21} , χ_{31} , χ_{32} are calculated from equation (4.11).

Ternary System: DNPE (1) + DNBE (2) + 1HX (3)

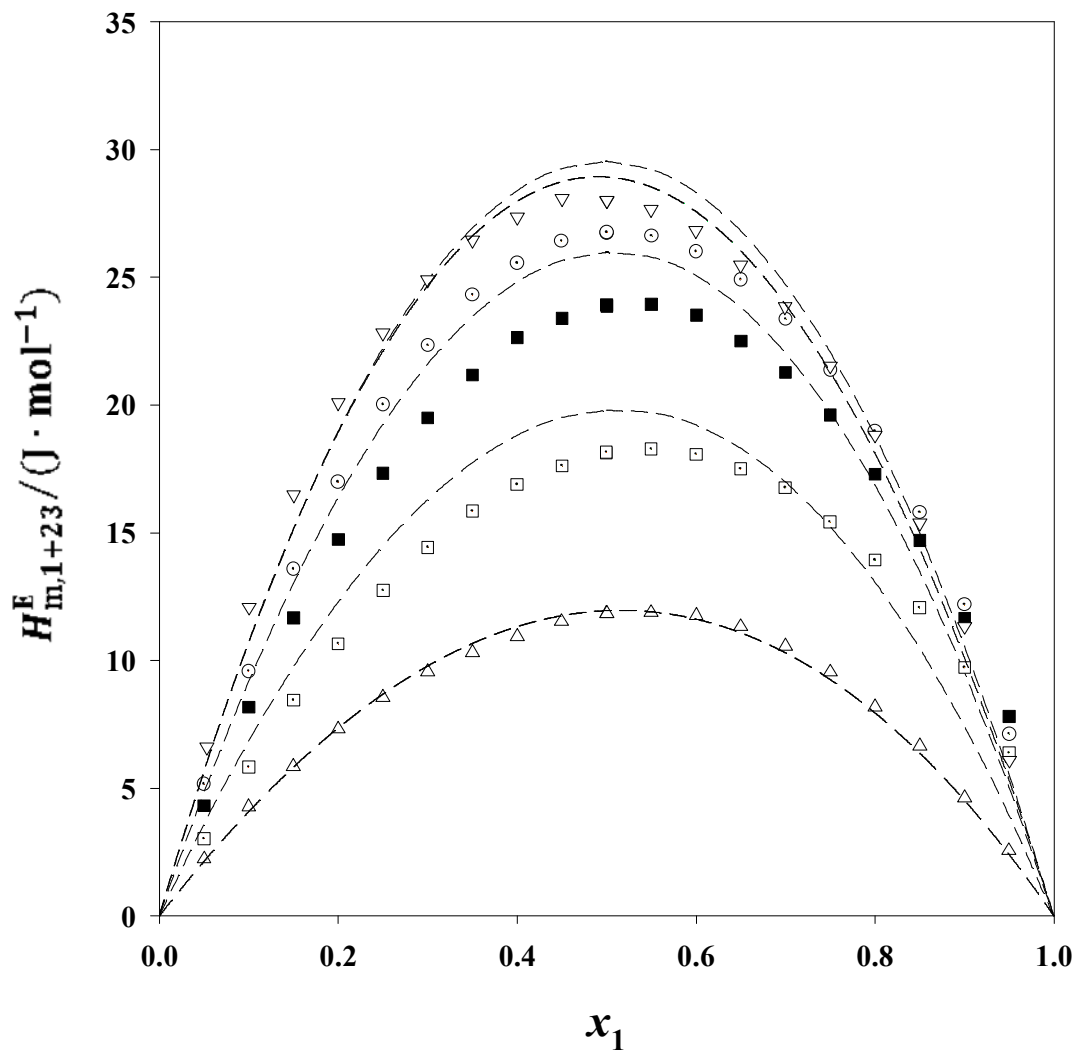


Figure 4.16. Excess molar enthalpies, $H_{m,1+23}^E$, for the x_1 DNPE + x_2 DNBE + $(1 - x_1 - x_2)$ 1HX mixture at the temperature 298.15 K. Plotted against mole fraction x_1 . Experimental results: Δ , $x_3 = 0.0$; \odot , $x_2/x_3 = 0.3333$; \blacksquare , $x_2/x_3 = 0.9996$; \square , $x_2/x_3 = 3.0000$; ∇ , $x_2 = 0.0$; Curves: $-\cdot-\cdot-$, estimated from the Flory theory.

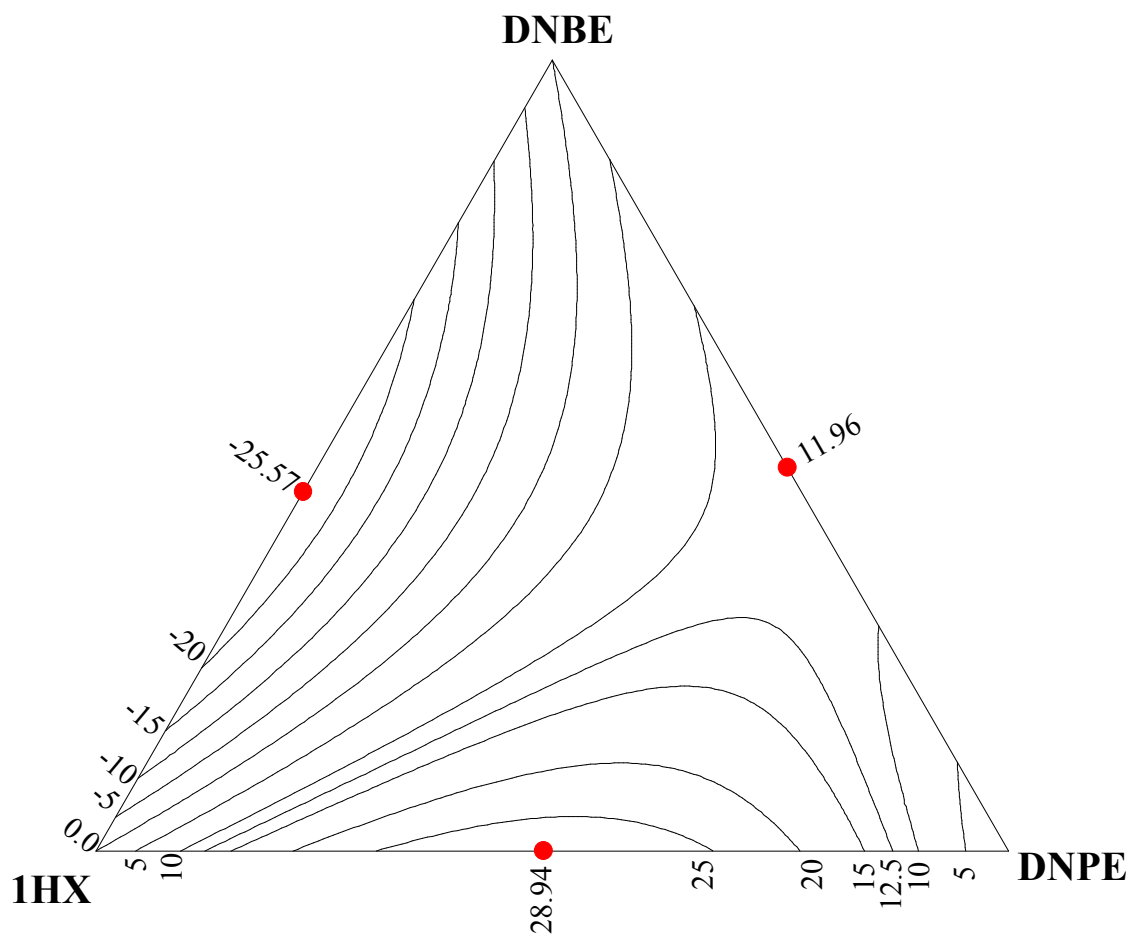


Figure 4.17. Contours for constant values of $H_{m,123}^E / (\text{J} \cdot \text{mol}^{-1})$ for the $x_1 \text{DNPE} + x_2 \text{DNBE} + (1 - x_1 - x_2) \text{1HX}$ system at 298.15 K. Estimated by means of the Flory theory.

Estimates of $H_{m,1+23}^E$, derived from the Flory theory, are shown in Figure 4.16. It can be seen that the theory predicts correctly the magnitude of the three experimental curves and their positions relative to the curves for the two constituent binaries. The root mean square deviation for the ternary mixtures in Table 4.9 for 60 data points is $1.8 \text{ J} \cdot \text{mol}^{-1}$.

Constant $H_{m,123}^E$ contours, estimated on the basis of the Flory theory, are shown on the Roozeboom diagram in Figure 4.17. The contours in the Figure 4.17 show that the Flory theory provides estimates of $H_{m,123}^E$ for the mixture that include predictions of the locations and magnitudes of the internal saddle point with reasonable accuracy.

The graphical representations of the five (5) ternary systems are presented in the Appendix C3.

For the ternary systems 1HX (1) + THF (2) + 22DMB (3), and 1HX (1) + THF (2) + 23DMB (3) the standard deviation is relatively higher than the other systems. For these two systems there is no indication of internal maxima. However, for the ternary systems DNPE (1) + 22DMB (2) + 23DMB (3), and DNBE (1) + 22DMB (2) + 23DMB (3) the standard deviation is low but the Flory theory cannot represent the internal saddle point. The Flory theory fairly estimates the enthalpy of the DNPE (1) + DNBE (2) + THF (3) ternary system.

4.2.2 Prediction by means of the Liebermann-Fried Model

Excess molar enthalpies of the ternary systems studied have also been estimated by means of the Liebermann-Fried model. In predicting the ternary heats of mixing by means of the Liebermann-Fried model, only the pure component properties and the interaction parameters of the constituent binaries are used. The interaction parameters of the binary system used in the prediction of ternary system excess enthalpy, by means of the Liebermann-Fried model, are presented in Table 4.17. The standard deviations of the excess enthalpy prediction for six ternary systems are presented in Table 4.18. As an example of the ternary excess enthalpy prediction by means of the Liebermann-Fried model, the DNPE (1) + DNBE (2) + 1HX (3) ternary system is presented.

Table 4.17. Liebermann-Fried model parameter (A_{ij} and A_{ji}) matrix for binary systems

| $i \backslash j$ | DNPE | DNBE | 1HX | THF | 22DMB | 23DMB |
|------------------|--------|-----------------------|-----------------------|-----------------------|------------------------|------------------------|
| DNPE | 1.0000 | 1.1072 | 0.9329 | 0.8743 | 0.8276 | 0.9058 |
| DNBE | 0.8908 | 1.0000 | 1.0759 ⁽¹⁾ | 0.7579 | 0.8069 | 0.8845 |
| 1HX | 1.0455 | 0.9354 ⁽¹⁾ | 1.0000 | 0.9371 ⁽²⁾ | 0.9401 ⁽³⁾ | 0.9133 ⁽³⁾ |
| THF | 0.9575 | 1.0287 | 0.8319 ⁽¹⁾ | 1.0000 | 0.8220 | 0.8171 |
| 22DMB | 1.0718 | 1.1299 | 1.0128 ⁽³⁾ | 0.7855 | 1.0000 | 1.0212 ^{§(4)} |
| 23DMB | 0.9775 | 1.0331 | 1.0291 ⁽³⁾ | 0.7896 | 0.9785 ^{§(4)} | 1.0000 |

⁽¹⁾Wang et al. (2004b); ⁽²⁾Lan et al. (2006); ⁽³⁾Wang et al. (2004a); ⁽⁴⁾Hamam and Benson (1986). [§]These binary interaction parameters were obtained by fitting the literature heats of mixing data to the Liebermann-Fried model.

Table 4.18. Standard deviation, σ , of the prediction of excess enthalpies for ternary systems by means of the Liebermann-Fried model

| System | Component | | | σ (J · mol ⁻¹) |
|--------|-----------|-------|-------|--------------------------------------|
| | 1 | 2 | 3 | |
| 1 | DNPE | DNBE | 1HX | 1.59 |
| 2 | DNPE | DNBE | THF | 3.18 |
| 3 | DNPE | 22DMB | 23DMB | 4.18 |
| 4 | DNBE | 22DMB | 23DMB | 6.97 |
| 5 | 1HX | THF | 22DMB | 1.78 |
| 6 | 1HX | THF | 23DMB | 14.21 |

Figure 4.18 shows the estimate of $H_{m,1+23}^E$ by means of the Liebermann-Fried model along with the DNPE (1) + DNBE (2) and DNPE (1) + 1HX (2) binary systems. This figure shows that the Liebermann-Fried model can be used to predict the excess molar enthalpy of the three pseudo binary mixtures fairly well. The standard deviation for the 60 data points in Table 4.9 is 1.6 J · mol⁻¹.

The Roozeboom diagram in Figure 4.19 shows the constant $H_{m,123}^E$ contours predicted by means of the Liebermann-Fried model. In comparison with Figure 4.5, it is clear that the model can be used to predict constant H_m^E contours with correct location and magnitude of the internal saddle point for the ternary system.

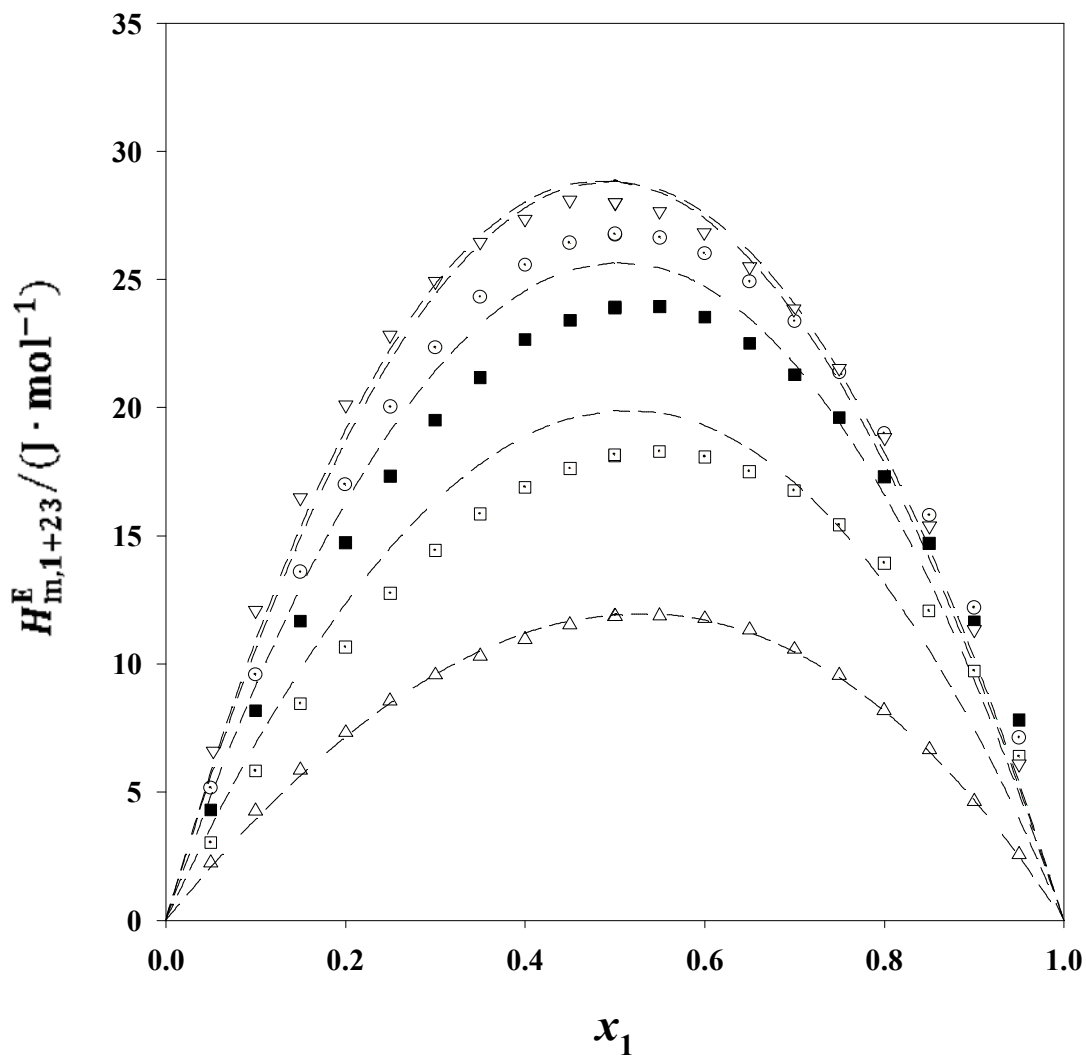


Figure 4.18. Excess molar enthalpies, $H_{m,1+23}^E$, for the x_1 DNPE + x_2 DNBE + $(1 - x_1 - x_2)$ 1HX mixture at the temperature 298.15 K. Plotted against mole fraction x_1 . Experimental results: Δ , $x_3 = 0.0$; \odot , $x_2/x_3 = 0.3333$; \blacksquare , $x_2/x_3 = 0.9996$; \square , $x_2/x_3 = 3.0000$; ∇ , $x_2 = 0.0$; Curves:-----, estimated from the Liebermann-Fried model.

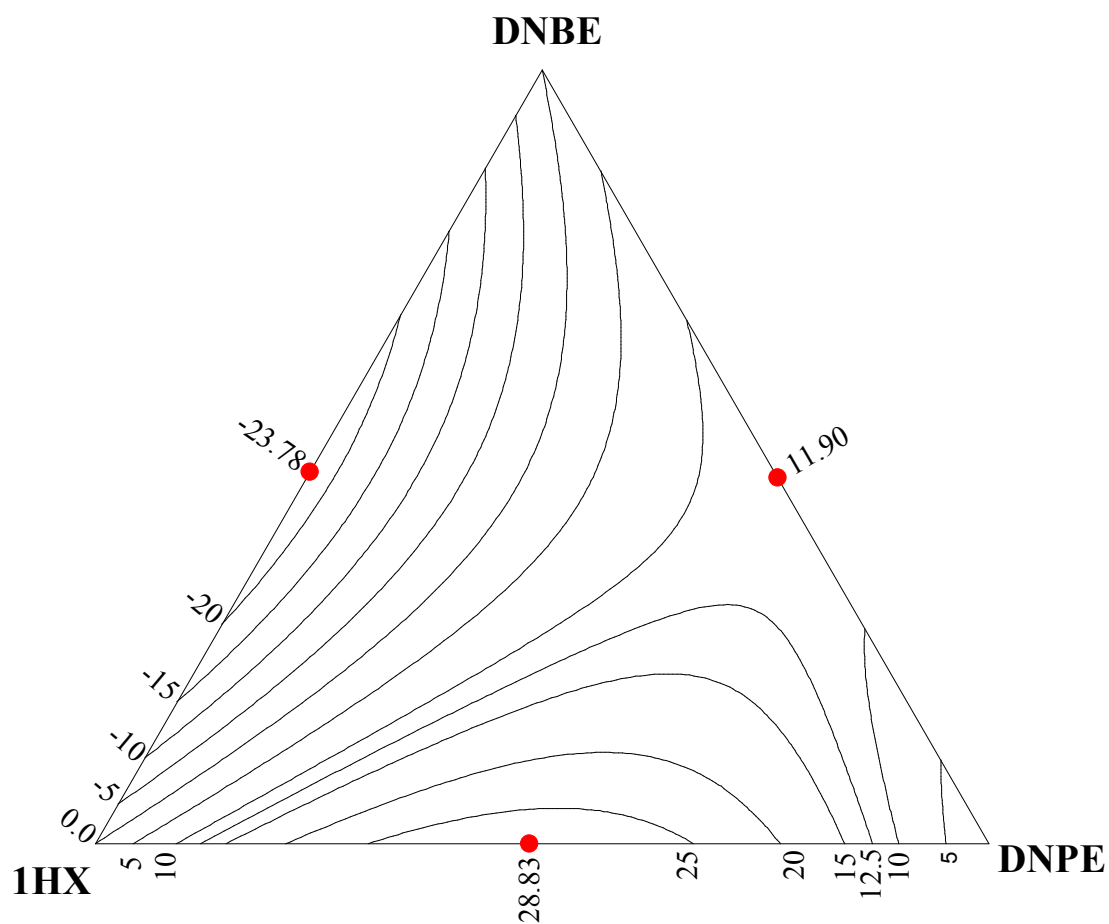


Figure 4.19. Contours for constant values of $H_{m,123}^E / (\text{J} \cdot \text{mol}^{-1})$ for the $x_1 \text{DNPE} + x_2 \text{DNBE} + (1 - x_1 - x_2) \text{1HX}$ system at 298.15 K. Estimated by means of the Liebermann-Fried model.

Excess molar enthalpies for the other five ternary systems predicted by means of the Liebermann-Fried model are presented in Appendix C3.

For the ternary system DNPE (1) + DNBE (2) + THF (3) the model predicts the constant enthalpy contour within reliable accuracy. But for the DNPE (1) + 22DMB (2) + 23DMB (3), and DNBE (1) + 22DMB (2) + 23DMB (3) ternary systems, the model fails to estimate the internal saddle point. For the 1HX (1) + THF (2) + 22DMB (3) ternary system, the standard deviation is quite low, but for the 1HX (1) + THF (2) + 23DMB (3) ternary system, the standard deviation is relatively higher than those for the other systems. For these two systems there is no indication of internal maxima.

5 CONCLUSIONS AND RECOMMENDATIONS

5.1 Conclusions

The experimental determination of excess molar enthalpy values for 10 binary and six ternary systems has been successfully performed by means of a modified flow microcalorimeter.

On the basis of the results obtained in this study, the following conclusion can be drawn:

- The heats of mixing values for binary systems studied are endothermic in nature.
- Over the most of the composition range, the errors of the excess molar enthalpies and those of the mole fractions of the binary and ternary systems are less than $0.005 \cdot |H_m^E|$ and $5 \cdot 10^{-4}$, respectively.
- The Flory theory and the Liebermann-Fried model can be used to correlate the excess molar enthalpy of binary mixtures successfully.
- Both the Flory theory and the Liebermann-Fried model predict the ternary excess enthalpy values with reasonable accuracy.
- It appears that the Liebermann-Fried model correlates and predicts the present binary and ternary excess enthalpy data better than the Flory theory, respectively.

5.2 Recommendation

The following recommendations are made for future studies:

- The excess enthalpy of the systems containing ethers (DNPE and THF) and other branched alkanes should be investigated to understand their general characteristics.
- The excess enthalpy of hydrocarbons and ethers binary systems can be performed at different temperature to verify the temperature dependency of the Liebermann-Fried model parameters.
- The Liebermann-Fried model parameters obtained in this study can be used to represent the vapor-liquid equilibria by means of this model.

6 REFERENCES

- Abe, A.; Flory, P. J. The Thermodynamic Properties of Mixtures of Small, Nonpolar Molecules. *J. Am. Chem. Soc.*, **1965**, 87, 1838-1846.
- Abrams, D. S.; Prausnitz, J. M. Statistical Thermodynamics of Liquid Mixtures: A New Expression for Excess Gibbs Energy of Partly or Completely Miscible System. *AIChE J.* **1975**, 21, 116-128.
- Ashcroft, S. J.; Isa, M. B. Effect of Dissolved Gas on the Densities of Hydrocarbons. *J. Chem. Eng. Data*, **1997**, 42, 1244-1248.
- Bauer, N. *Determination of Density; Physical Methods of Organic Chemistry, Part I*; Weissberger, A. editor, Interscience: New York, 1959, Chapter IV.
- Benson, G. C.; Pflug, H. D. Molar Excess Volumes of Binary Systems of Normal Alcohols at 25 °C. *J. Chem. Eng. Data*, **1970**, 15, 382-386.
- Bevington, P. R.; Robinson, D. K. *Data Reduction and Error Analysis for the Physical Sciences*; McGraw-Hill: New York, 2003.
- Brostow, W.; Sochanski, J. S. Prediction of Thermodynamic Properties of Ternary Liquid Solutions Including Metal Alloys. *J. Mater. Sci.*, **1975**, 10, 2134-2145.
- Castro, I.; Pintos, A.; Amig, A.; Bravo, R.; Paz Andrade, M. I. Excess Enthalpies of (Tetrahydrofuran or Tetrahydropyran + *n*-Alkane) at the Temperature 298.15 K. *J. Chem. Thermodynamics*, **1994**, 26, 29-33.
- Christensen, J. J.; Johnston, H. D.; Izatt, R. M. An Isothermal Titration Calorimeter. *Rev. Sci. Instr.*, **1968**, 39, 1356-1359.
- Flory, P. J. Statistical Thermodynamics of Liquid Mixtures. *J. Am. Chem. Soc.*, **1965**, 87, 1833-1838.
- Hamam, S. E. M.; Benson, G. C. Excess Enthalpies of Some Binary Mixtures of Hexane Isomers. *J. Chem. Thermodynamics*, **1986**, 18, 591-594.
- Holt, D. L.; Smith, B. D. Measurement of Excess Enthalpies with Tronac Titration Calorimeter. Data for Some C, Aromatic Binaries. *J. Chem. Eng. Data*, **1974**, 19, 129-133.
- Jablonski, P.; Muller-Blecking, A.; Borchard, W. A Method to Determine Mixing Enthalpies by DSC. *J. Therm. Anal. Cal.*, **2003**, 74, 779-787.
- Kimura, F.; Benson, G. C.; Halpin, C. J. Excess Enthalpies of Binary Mixture of *n*-Heptane with Hexane Isomers. *Fluid Phase Equilib.*, **1983**, 11, 245-250.

- Kohler, F. Estimation of Thermodynamic Data for a Ternary System from the Corresponding Binary Systems. *Monatsh. Chem.*, **1960**, 91, 738-740.
- Lan, Q. C.; Kodama, D.; Wang, Z.; Lu, B. C.-Y. Excess Molar Enthalpies of Mixtures (1-Hexene + Tetrahydrofuran or 2-Methyltetrahydrofuran + Methyl *tert*-butyl ether) at the Temperature 298.15 K. *J. Chem. Thermodynamics*, **2006**, 38, 1606-1611.
- Leskiv, M.; Bernardes, C. E.; Minas da Piedade, M. E. A Calorimetric System Based on the LKB 10700-1 Flow Microcalorimeter. *Meas. Sci. Technol.*, **2009**, 20, 1-9.
- Liao, W.-C.; Lin, H.-M.; Lee, M.-J. Excess Molar Enthalpies of Binary Systems of 2-Octanone or 3-Octanone with Dodecane, Tetradecane, or Hexadecane at 298.15 K. *J. Chem. Eng. Data*, **2010**, 55, 217-222.
- Liebermann, E.; Fried, V. Estimation of the Excess Gibbs Free Energy and Enthalpy of Mixing of Binary Nonassociated Mixtures. *Ind. Eng. Chem. Fundam.*, **1972a**, 11, 350-354.
- Liebermann, E.; Fried, V. The Temperature Dependence of Excess Gibbs Free Energy of Binary Nonassociated Mixtures. *Ind. Eng. Chem. Fundam.*, **1972b**, 11, 354-355.
- Liao, D. K.; Tong, Z. F.; Benson, G. C.; Lu, B. C.-Y. Excess Enthalpies of (*n*-C7 or *n*-C10) + MTBE + DNPE Ternary Mixtures at 298.15 K, *Fluid Phase Equilib.* **1997**, 131, 133-143.
- Mackenzie, R. C. Nomenclature for Thermal Analysis-IV, *Pure & Appl. Chem.*, **1985**, 57, 1737-1740.
- Marquardt, D. W. An Algorithm for Least-Squares Estimation of Nonlinear Parameters. *J. Soc. Indust. Appl. Math.*, **1963**, 11, 431-441.
- Marsh, K. N.; O'Hare, P. A. G. *Solution Calorimetry*; Blackwell Scientific Publications: Oxford, 1994.
- Marsh, K. N.; Niamskul, P.; Gmehling, J.; Bölts, R. Review of Thermophysical Property Measurement on Mixtures Containing MTBE, TAME, and Other Ethers with Non-polar Solvents. *Fluid Phase Equilib.*, **1999**, 156, 207-227.
- Mato, M. M.; Illobre, M.; Verdes, P.V.; Paz Andrade, M. I. Excess Molar Enthalpies of the Ternary System MTBE + Ethanol + Hexane. *J. Therm. Anal. Cal.*, **2006**, 84, 291-295.
- Monk, P.; Wadso, I. A Flow Micro Reaction Calorimeter. *Acta Chemica Scandinavica*, **1968**, 22, 1842-1852.

- Morris, J. W.; Mulvey, P. J.; Abbott, M. M.; Van Ness, H. C. Excess Thermodynamic Functions for Ternary Systems. I. Acetone – Chloroform-Methanol at 50 °C. *J. Chem. Eng. Data*, **1975**, 20, 403-405.
- Navidi, W. *Statistics for Engineers and Scientists*; McGraw-Hill: New York, 2006.
- O'shea, S. J.; Stokes, R. H. Activity Coefficients and Excess Partial Molar Enthalpies for (Ethanol + Hexane) from 283 to 318 K. *J. Chem. Thermodynamics*, **1986**, 18, 691-696.
- Peng, D.-Y.; Benson, G. C.; Lu, B. C.-Y. Excess Enthalpies of Heptane + Ethanol + 1,2-Dimethoxyethane at 298.15 K. *J. Chem. Eng. Data*, **1998**, 45, 880-883.
- Peng, D.-Y.; Benson, G. C.; Lu, B. C.-Y. Predicting Excess Enthalpies of Ether and/or Hydrocarbon Binary Mixtures. *J. Sol. Chem.*, **1999**, 28, 505-519.
- Peng, D.-Y.; Wang, Z.; Benson, G. C.; Lu, B. C.-Y. Predicting the Excess Enthalpies and Vapor-Liquid Equilibria of Multicomponent Systems Containing Ether and Hydrocarbons. *Fluid Phase Equilib.*, **2001a**, 182, 217-227.
- Peng, D.-Y.; Wang, Z.; Benson, G. C.; Lu, B. C.-Y. Excess Enthalpies and (Vapor + Liquid) Equilibrium for (Oxygenated Additive + *n*-Alkane). *J. Chem. Thermodynamics*, **2001b**, 33, 83-93.
- Peng, D.-Y.; Benson, G. C.; Lu, B. C.-Y. Excess Enthalpies of (Di-*n*-butyl ether + 2,2,4-Trimethylpentane + Heptane, or Octane) at the Temperature 298.15 K. *J. Chem. Thermodynamics*, **2002**, 34, 413-422.
- Redlich, O.; Kister, A. T. Algebraic Representation of Thermodynamic Properties and the Classification of Solutions. *Ind. Eng. Chem.*, **1948**, 40, 345-348.
- Renon, H.; Prausnitz, J. M. Local Composition Thermodynamic Excess Function for Liquid Mixtures. *AIChE J.*, **1968**, 14, 135-144.
- Riddick, J. A.; Bunger, W. B.; Sakano, T. K. *Organic Solvents: Physical Properties and Methods of Purification*; Wiley: New York, 1986.
- Rodriguez de Rivera, M.; Socorro, F.; Matos, J. S. Heats of Mixing Using an Isothermal Titration Calorimeter: Associated Thermal Effects. *Int. J. Mol. Sci.* **2009**, 10, 2911-2920
- Sandler, S. I. *Chemical and Engineering Thermodynamics*; Wiley: New York, 1999.
- Scatchard, G; Ticknor, L. B.; Goates, J. R.; McCartney, E. R. Heats of Mixing in Some Nonelectrolyte Solutions. *J. Am. Chem. Soc.*, **1952**, 73, 3721-3724.
- Smith, J. M.; Van Ness, H. C.; Abbott, M. M. *Introduction to Chemical Engineering Thermodynamics*; McGraw-Hill's: New York, 2007.

- Tanaka, R.; D'Arcy, P. J.; Benson, G. C. Application of a Flow Microcalorimeter to Determine the Excess Enthalpies of Binary Mixtures of Non-electrolytes. *Thermochim. Acta*, **1975**, 11, 163-175.
- Tsao, C. C.; Smith, J. M. Heats of Mixing of Liquids. *Chem. Eng. Prog. Symp. Ser.*, **1953**, No. 7, 49, 107-117.
- Wadso, I. Design and Testing of Micro Reaction Calorimeter. *Acta chemica Scandinavica*, **1968**, 22, 927-937.
- Wang, L.; Benson, G. C.; Lu, B. C.-Y. Excess Enthalpies of (Ethanol + Hexane + Decane or Dodecane) at the Temperature 298.15 K. *J. Chem. Thermodynamics*, **1992**, 24, 1135-1143.
- Wang, L.; Benson, G. C.; Lu, B. C.-Y. Excess Enthalpies of Methyl *tert*-butyl ether + *n*-Hexane + (*n*-Decane or *n*-Docecane) Ternary Mixture at 298.15 K. *Thermochim. Acta*, **1993**, 213, 83-93.
- Wang, Z.; Lu, B. C.-Y. Prediction of Isobaric Vapour-Liquid Equilibrium from Excess Enthalpies for (Methyl *tert*-butylether + Alkane(s)) Mixtures. *J. Chem. Thermodynamics*, **2000**, 32, 175-186.
- Wang, Z.; Peng, D.-Y.; Benson, G. C.; Lu, B. C.-Y. Excess Enthalpies of (Ethyl *tert*-butylether + Hexane + Heptanes, or Octane) at the Temperature 298.15 K. *J. Chem. Thermodynamics*, **2001**, 33, 1181-1191.
- Wang, Z.; Benson, G. C.; Lu, B. C.-Y. Excess Enthalpies of Binary Mixtures of 1-Hexene with Some Branched Alkanes at the Temperature 298.15 K. *J. Chem. Thermodynamics*, **2004a**, 36, 45-47.
- Wang, Z.; Benson, G. C.; Lu, B. C.-Y. Excess Enthalpies of Binary Mixtures of 1-Hexene with Some Ethers at 25 °C. *J. Sol. Chem.*, **2004b**, 33, 143-147.
- Wang, Z.; Lu, B. C.-Y.; Peng, D.-Y.; Lan, C. Q. Liebermann-Fried Model Parameters for Calculating Vapour-Liquid Equilibria of Oxygenate and Hydrocarbon Mixture. *J. Chinese Inst. Eng.*, **2005**, 28, 1089-1105.
- Watson, E. S.; O'Neill, M. J.; Justin, J.; Brenner, N. A Differential Scanning Calorimeter for Quantitative Differential Thermal Analysis. *J. Anal. Chem.*, **1964**, 36, 1233-1238.
- Wilson, G. M. A New Expression for the Excess Free Energy of Mixing. *J. Am. Chem. So.*, **1964**, 86, 127-130.
- DECHEMA, Gesellschaft für Chemische Technik und Biotechnologie e. V. **2009**, Theodor-Heuss-Allee 25, D-60486 Frankfurt am Main, Germany (www.dechema.de/)

[impressum.html](#))

Dortmund Data Bank **2009**, DDBST, Marie-Curie-Str. 10, D-26129 Oldenburg, Germany
(www.ddbst.com/en/ddbst).

APPENDIX A

A1. Modification of Syringe Pump Motor Controller

A2. Determination of Pump Constant

A1. Modification of Syringe Pump Motor Controller

The flow measuring system of the calorimeter was modified to get more precise flow rates (i.e., mole fractions). Previously, the displacement pump was driven by a variable-speed direct current (DC) motor (Bodine Electric, Type NSH-12). A disk with 120 equally photo masked sector was mounted on the motor shaft. The photo masked disk passes through a photo sensor, which gives the motor speed in number of counts per second through a feedback

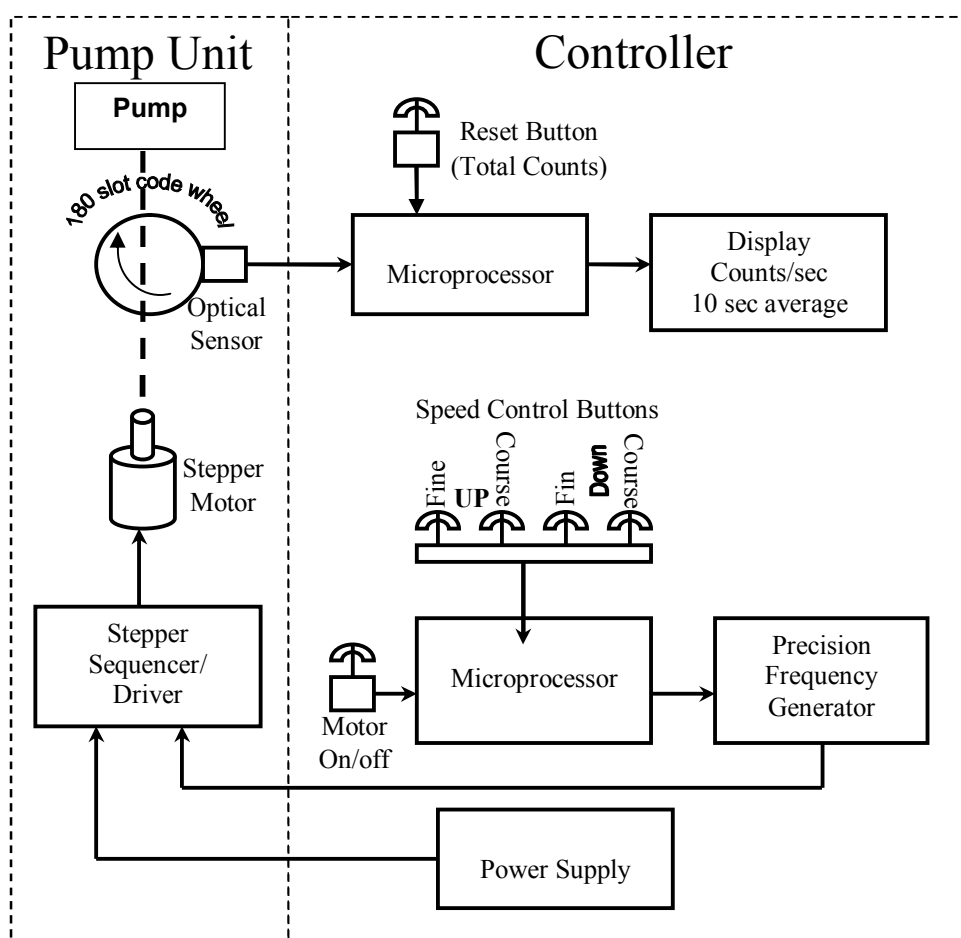


Figure A1.1. Schematic diagram of syringe pump controller (Courtesy: Rlee Prokopishyn)

controller (Tanaka et al. 1975). In the present study, the variable-speed DC motors along with the photo masked disks and the controllers were replaced by stepper motors (Lin Engineering, Model-WO-4118S-01) and similar disks with 180 photo masked sector. Each of the stepper motors is driven by microprocessor-equipped controller. The controllers were built in the Chemical Engineering department electronic shop. Previously, a feedback control circuit was used to control the motor speed (Tanaka et al. 1975). In the present study, the microprocessor equipped controller uses a precision frequency generator (PFG) to control the stepper motor speed. The PFG generates 4400 Hz. for $800 \text{ steps} \cdot \text{rev}^{-1}$ of the stepper motor. This PFG provides a precise speed control for the stepper motor. There are two different buttons to control speed, one is coarse that increases or decreases the motor speed by 20 to 40 counts per second and the second one is for fine tuning, which allows varying the motor speed by one counts/sec. This new pump driver and control system give more precise motor speed control which in turn gives a more precise mole fraction. Previously, the motor speed control has an uncertainty of $\pm 3 \text{ counts} \cdot \text{s}^{-1}$ (Tanaka et al. 1975), now it is reduced to $\pm 1 \text{ counts} \cdot \text{s}^{-1}$.

A2. Determination of Pump Constant

The purpose of the calibration was to determine the coefficient K_p (pump constant) which was used to calculate the volumetric flow rate Q , delivered by pump n ($n = A, B$) (Tanaka et al. 1975):

$$Q = K_p \mathbb{G} \mathcal{R} \quad (\text{A2.1})$$

where, K_p is the characteristic constant of the pump, \mathbb{G} adjustable gear ratio (1.0; 0.1; 0.01; 0.001), and \mathcal{R} is the motor speed in counts $\cdot \text{s}^{-1}$ displayed by the microcontroller.

The calibration (characteristic constant determination) procedure of the pump is described as follows:

The calibrations were made by running the pumps filled with the reverse osmosis (RO) water at 25 °C and weighing the water collected from the pump output during a known time period. A plastic bottle (50 cm³ capacity) was dried and weight with stopper. While running the pump, water was collected for 30-90 minutes, depending on the flow setting, after which the bottle was weight again. The volumetric flow rate was then calculated from the known mass, time interval, and the density of water ($\rho_{H_2O} = 0.99705 \text{ g} \cdot \text{cm}^{-3}$) at 25 °C . During the course of calibration both the pumps were run at gear ratio 0.1, which is the normal operation setting of the syringe pumps. The results are summarized in Table A2.1 and A2.2 for pump A and Pump B respectively.

Table A2.1. Calibration Results for Pump A

| Motor Speed (\mathcal{R}) | Time | Mass of Water | Volumetric Flow Rate (Q) \times 10^3 |
|----------------------------------|---------|------------------|--|
| (counts \cdot s $^{-1}$) | (s) | (g) | (cm 3 \cdot s $^{-1}$) |
| 1800.5 | 1800.0 | 9.002 | 5.0159 |
| 1800.4 | 1800.0 | 9.003 | 5.0165 |
| 1300.3 | 2500.0 | 9.020 | 3.6187 |
| 1300.2 | 2500.0 | 9.026 | 3.6211 |
| 800.0 | 4050.0 | 8.992 | 2.2268 |
| 800.0 | 4050.0 | 8.990 | 2.2263 |
| 300.8 | 10800.0 | 8.990 | 8.3487 |
| 300.8 | 10800.0 | 8.991 | 8.3496 |

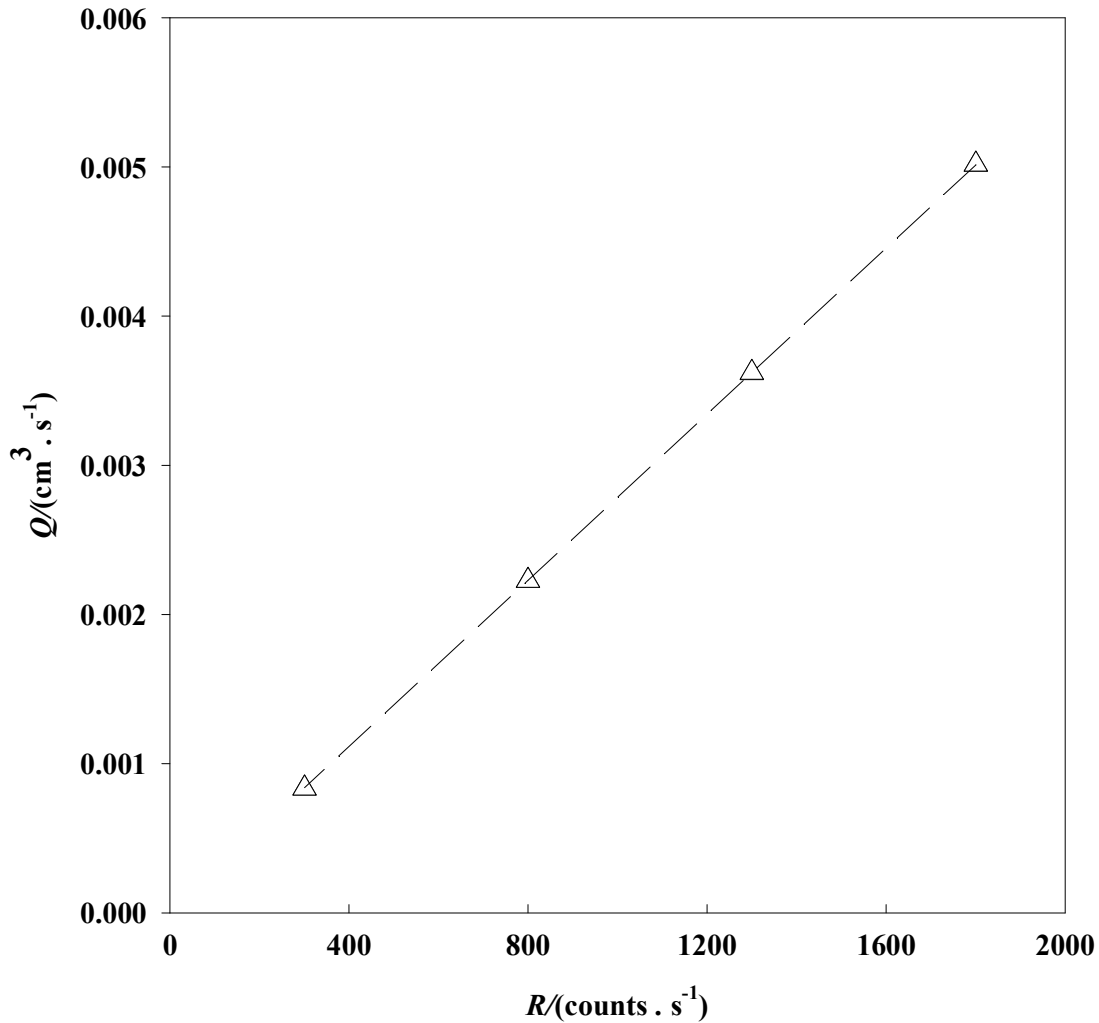


Figure A2.1. Calibration Curve for Pump A. Volumetric flow rate (Q) plotted against the counter reading (\mathcal{R}). Δ , experimental data; — —, calculated from equation (A2.1).

A calibration curve showing volumetric flow rate (Q) vs. counter reading (\mathcal{R}) was then plotted for each pump. The calibration results for both pumps were correlated with equation (A2.1) using the least squares method. The pump constants (K_p) obtained from this analysis are $2.7847 \times 10^{-6} \text{ cm}^3 \cdot \text{count}^{-1}$ and $2.7867 \times 10^{-6} \text{ cm}^3 \cdot \text{count}^{-1}$ for pump A and pump B, respectively.

Table A2. 2. Calibration Results for Pump B

| Motor Speed (\mathcal{R}) (counts \cdot s $^{-1}$) | Time (s) | Mass of Water (g) | Volumetric Flow Rate (Q) \times 10^3 (cm 3 \cdot s $^{-1}$) |
|---|-------------|-------------------------|--|
| 1800.5 | 1800 | 9.021 | 5.0265 |
| 1800.5 | 1800 | 9.023 | 5.0276 |
| 1300.2 | 2500 | 9.047 | 3.6295 |
| 1300.3 | 2500 | 9.038 | 3.6259 |
| 800.0 | 4050 | 9.007 | 2.2305 |
| 800.0 | 4050 | 8.991 | 2.2266 |
| 300.8 | 10800 | 9.027 | 8.3831 |
| 300.7 | 10800 | 9.026 | 8.3822 |

Previously, the characteristic constants of the positive displacement pumps were 4.1882×10^{-6} cm 3 \cdot count $^{-1}$ and 4.1889×10^{-6} cm 3 \cdot count $^{-1}$ for the pumps designated as pump A and pump B (Tanaka et al. 1975), respectively.

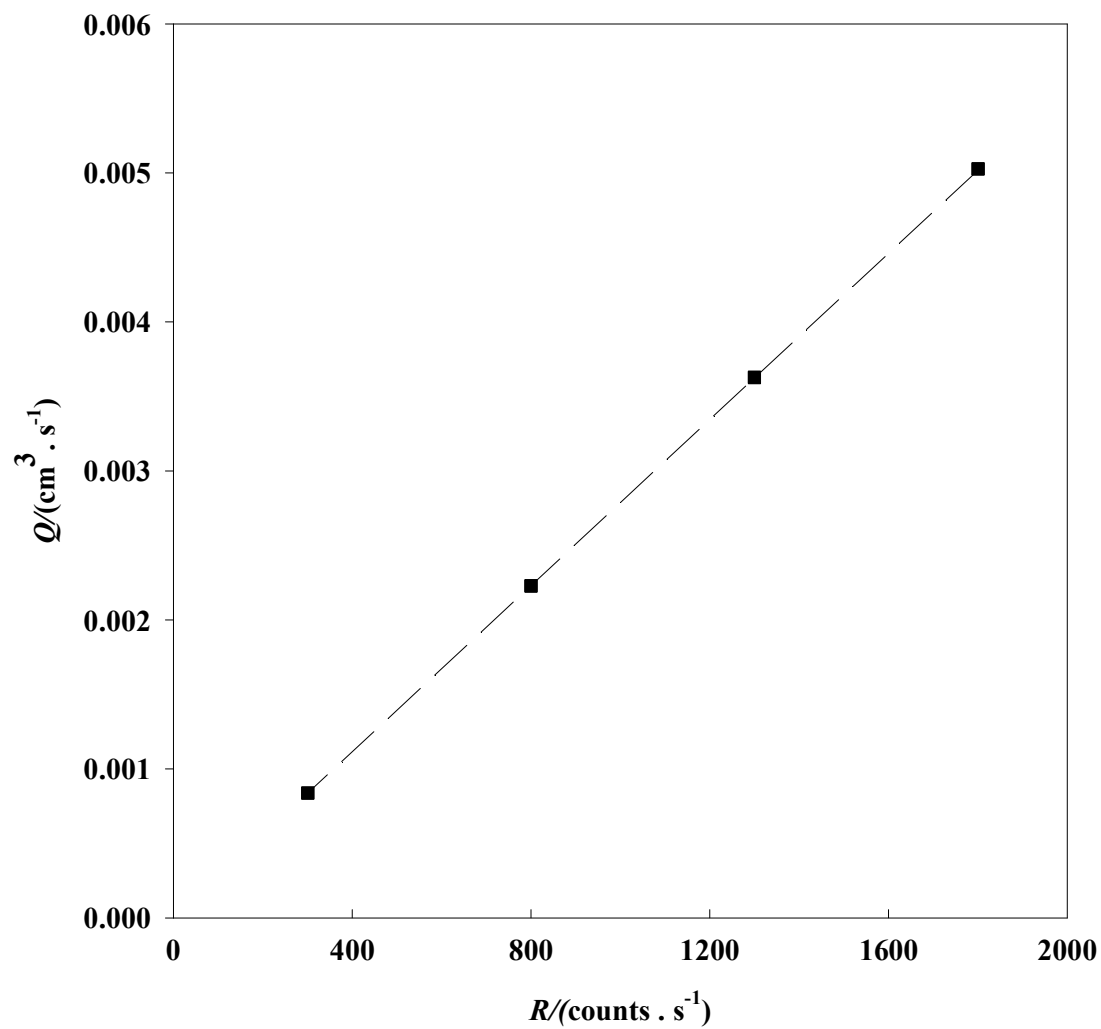


Figure A2.2. Calibration Curve for Pump B. Volumetric flow rate (Q) plotted against the counter reading (\mathcal{R}). ■, experimental data; — —, calculated from equation (A2.1).

APPENDIX B

B1. Heats of Mixing of Binary Mixture

B2. Correcting of Weights for the Buoyancy of Air

B3. Heats of Mixing of Pseudo-Binary Mixture

B1. Heats of Mixing of Binary Mixture

Binary heats of mixing were determined using the procedure described in section 3.3.1. Pure component properties and calibration results, primary and processed experimental data, along with a sample calculation are presented. The density of the pure component and mixture were measured at ($T = 298.15$ K) and the uncertainty in density measurement is provided in section 3.1.

Table B-1.1. Pure component properties

| Component | Molecular Weight | Density/(g · cm ⁻³) |
|-----------|------------------|---------------------------------|
| THF | 72.10572 | 0.88208 |
| 22DMB | 86.17536 | 0.64459 |

B1.1. Calibration results for pure components

Table B1.2. Calibration results of THF with pump A

| Motor Speed (\mathcal{R}) | Gear ratio (\mathbb{G}) | E_Q^0 | E_Q | ΔE | I | \mathcal{E} |
|-------------------------------|-----------------------------|---------|---------|------------|--------|--|
| (counts · s ⁻¹) | | (mv) | (mv) | (mv) | (amp) | (J · v ⁻¹ · s ⁻¹) |
| 1310.4 | 0.1 | -0.0421 | -0.4497 | -0.4076 | 0.0113 | 15.5958 |
| 1650.8 | 0.1 | -0.0409 | -0.4488 | -0.4079 | 0.0113 | 15.6118 |
| 1070.8 | 0.1 | -0.0425 | -0.4506 | -0.4081 | 0.0113 | 15.5766 |
| 830.3 | 0.1 | -0.0411 | -0.4480 | -0.4069 | 0.0113 | 15.5675 |
| 690.8 | 0.1 | -0.0427 | -0.4498 | -0.4071 | 0.0113 | 15.5598 |
| 450.3 | 0.1 | -0.0410 | -0.4486 | -0.4076 | 0.0113 | 15.5407 |

The expression for calibration constant (\mathcal{E}) obtained by fitting equation (3.2) to the experimental data has the form

$$\mathcal{E} = 15.5105 + 5.94994 \times 10^{-5} \cdot \mathcal{R}$$

where \mathcal{R} is the pump flow rates in $\text{counts} \cdot \text{s}^{-1}$. The standard deviation, σ , is $0.003 \text{ J} \cdot \text{v}^{-1} \cdot \text{s}^{-1}$ having an uncertainty in parameters k_0 and k_1 are $\pm 0.0031 \text{ J} \cdot \text{v}^{-1} \cdot \text{s}^{-1}$ and $\pm 0.000003 \text{ J} \cdot \text{v}^{-1} \cdot \text{counts}^{-1}$

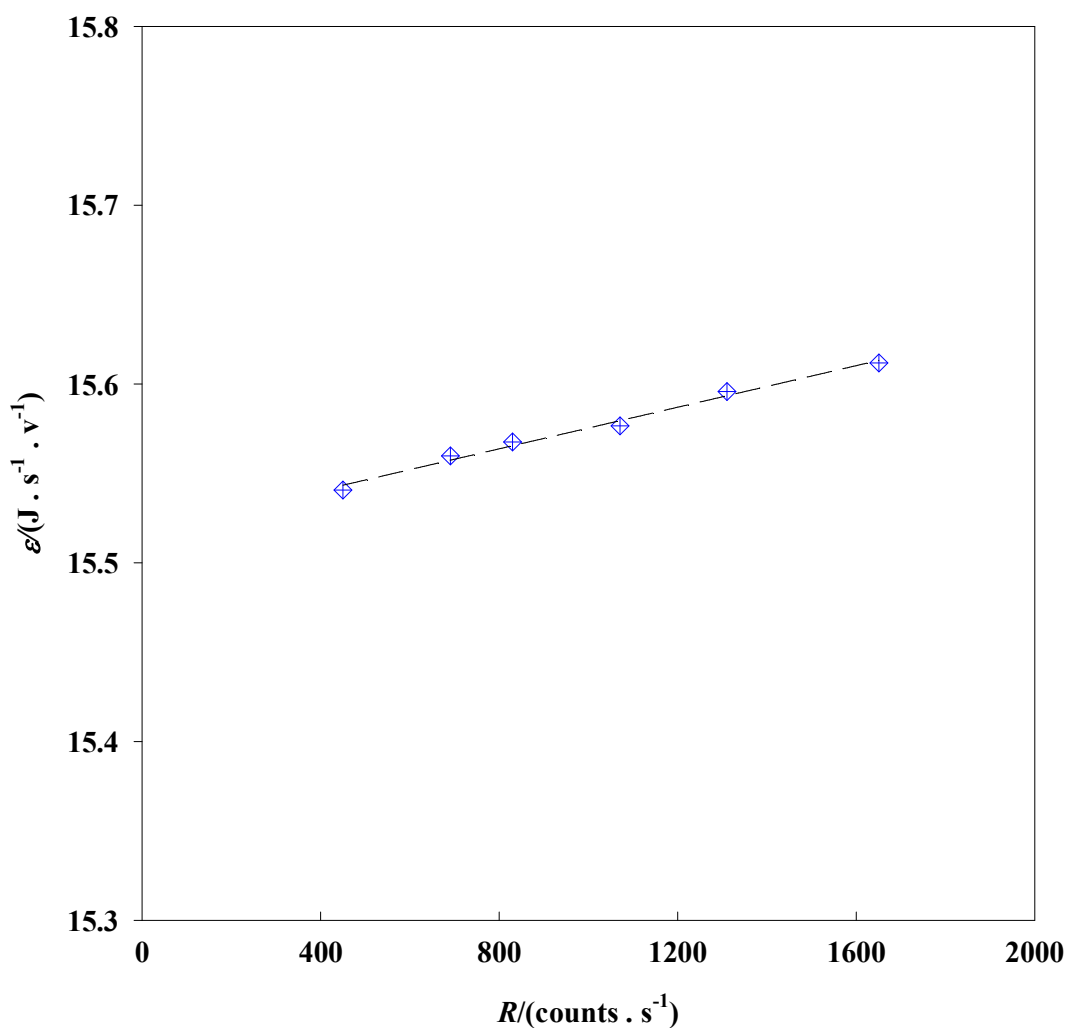


Figure B1.1. Calibration curve for THF in Pump A

Table B1.3. Calibration results of 22DMB with pump B

| Motor Speed (\mathcal{R}) | Gear ratio (\mathbb{G}) | E_Q^0 | E_Q | ΔE | I | \mathcal{E} |
|-------------------------------|-----------------------------|---------|---------|------------|--------|--|
| (counts \cdot s $^{-1}$) | | (mv) | (mv) | (mv) | (amp) | (J \cdot v $^{-1}$ \cdot s $^{-1}$) |
| 1052.2 | 0.1 | -0.0606 | -0.4831 | -0.4225 | 0.0116 | 15.6628 |
| 1352.3 | 0.1 | -0.0612 | -0.4815 | -0.4203 | 0.0115 | 15.6904 |
| 1653.6 | 0.1 | -0.0652 | -0.4834 | -0.4182 | 0.0115 | 15.7418 |
| 751.5 | 0.1 | -0.0592 | -0.4794 | -0.4202 | 0.0115 | 15.6397 |
| 451.8 | 0.1 | -0.0551 | -0.4773 | -0.4222 | 0.0115 | 15.5657 |
| 1052.2 | 0.1 | -0.0602 | -0.4791 | -0.4189 | 0.0115 | 15.6883 |

The expression for calibration constant (\mathcal{E}) obtained by fitting equation (3.2) to the experimental data has the form

$$\mathcal{E} = 15.5129 + 1.397851 \times 10^{-4} \cdot \mathcal{R}$$

where \mathcal{R} is the pump flow rates in counts \cdot s $^{-1}$. The standard deviation, σ , is 0.016 J \cdot v $^{-1}$ \cdot s $^{-1}$

having an uncertainty in parameters k_0 and k_1 are ± 0.0183 J \cdot v $^{-1}$ \cdot s $^{-1}$ and ± 0.000016 J \cdot v $^{-1}$ \cdot

counts $^{-1}$

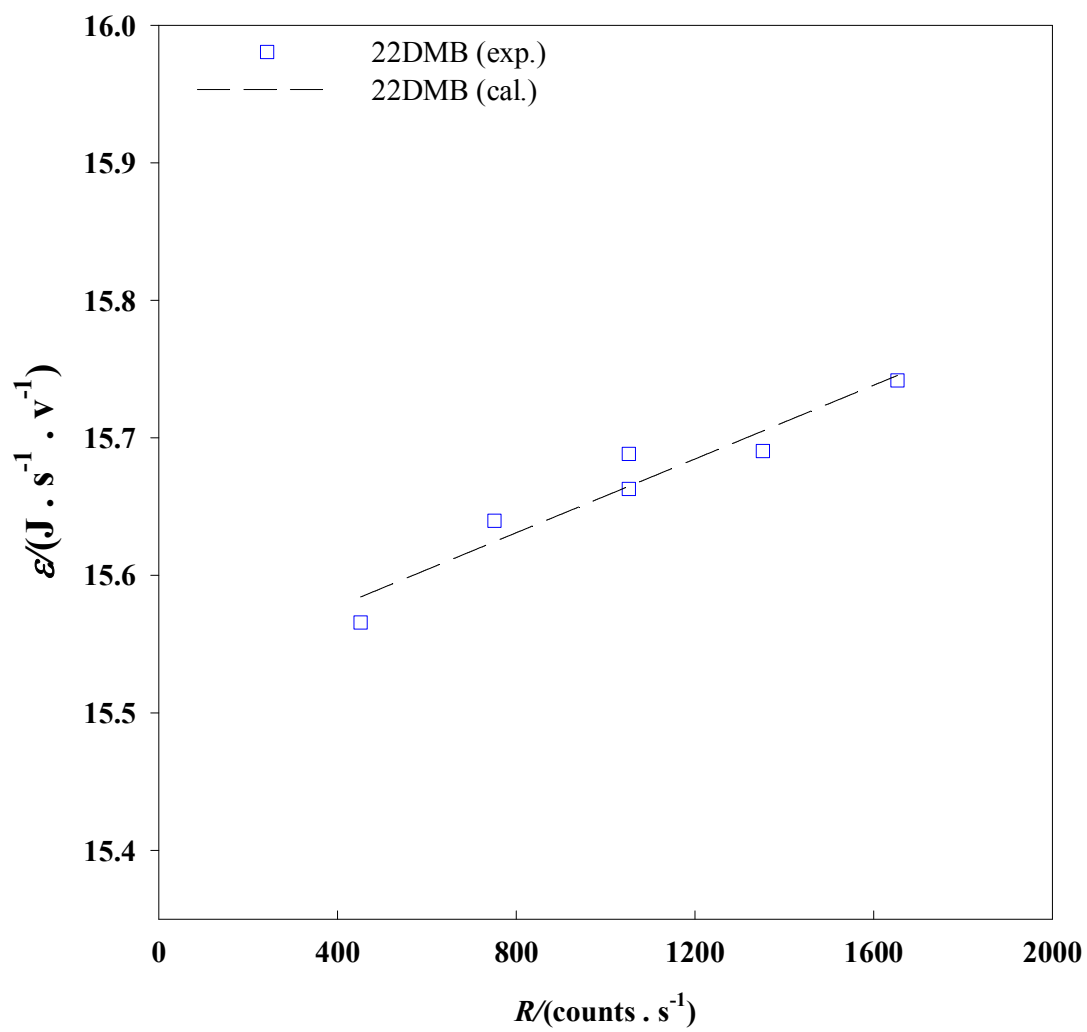


Figure B1.2. Calibration curve for 22DMB in Pump B

B1.2 Experimental data and calculated results of heats of mixing for THF (1) + 22DMB (2) binary system

Table B1.4. Primary experimental data for THF (1) + 22DMB (2) binary mixture

| Pump | # | Component | M | $\rho/(\text{g} \cdot \text{cm}^{-3})$ | k_1 | $k_0 \times 10^{-4}$ |
|--------|---|---|---|--|---------|----------------------|
| A | 1 | THF | 72.10572 | 0.88208 | 15.5105 | 0.594994 |
| B | 2 | 22-DMB | 86.17536 | 0.64459 | 15.5129 | 1.397851 |
| Points | | $\mathcal{R}_A/(\text{counts} \cdot \text{s}^{-1})$ | $\mathcal{R}_B/(\text{counts} \cdot \text{s}^{-1})$ | $E(\text{mv})$ | | |
| 1 | | 0.0 | 1794.2 | -0.0652 | | |
| 2 | | 56.0 | 1738.3 | 0.2463 | | |
| 3 | | 114.3 | 1680.1 | 0.5303 | | |
| 4 | | 174.9 | 1619.5 | 0.8057 | | |
| 5 | | 238.1 | 1556.5 | 1.0498 | | |
| 6 | | 304.8 | 1490.2 | 1.2762 | | |
| 7 | | 372.6 | 1421.5 | 1.4692 | | |
| 8 | | 444.3 | 1349.8 | 1.6453 | | |
| 9 | | 520.0 | 1274.8 | 1.7894 | | |
| 10 | | 598.9 | 1196.1 | 1.8915 | | |
| 11 | | 681.7 | 1113.3 | 1.9682 | | |
| 12 | | 681.6 | 1113.3 | 1.9688 | | |
| 13 | | 767.6 | 1026.3 | 2.0030 | | |
| 14 | | 859.6 | 935.4 | 1.9987 | | |
| 15 | | 954.6 | 840.4 | 1.9515 | | |
| 16 | | 1055.6 | 739.3 | 1.8634 | | |
| 17 | | 1162.6 | 633.3 | 1.7200 | | |
| 18 | | 1274.9 | 520.1 | 1.5062 | | |
| 19 | | 1394.1 | 401.8 | 1.2384 | | |
| 20 | | 1519.5 | 275.9 | 0.8944 | | |
| 21 | | 1653.5 | 142.2 | 0.4751 | | |
| 22 | | 1795.4 | 0.0 | -0.0404 | | |

Sample calculation for heat of mixing for the point no. 12 in table B1.4

Pumps gear ratio (G) = 0.1

Pump Constants:

$$K_{P_A} = 2.7847 \times 10^{-6} \text{cm}^3 \cdot \text{count}^{-1}$$

$$K_{P_B} = 2.7867 \times 10^{-6} \text{cm}^3 \cdot \text{count}^{-1}$$

Controllers reading for pump A and B,

$$\mathcal{R}_A = 681.6 \text{ counts} \cdot \text{s}^{-1}$$

$$\mathcal{R}_B = 1113.3 \text{ counts} \cdot \text{s}^{-1}$$

Volumetric flow rates for component 1 and 2

$$Q_1 = K_{P_A} \times \mathcal{R}_A = 1.898 \times 10^{-3} \text{cm}^3 \cdot \text{s}^{-1}$$

$$Q_2 = K_{P_B} \times \mathcal{R}_B = 3.102 \times 10^{-3} \text{cm}^3 \cdot \text{s}^{-1}$$

Total volumetric flow rate

$$Q = 5.001 \times 10^{-3} \text{cm}^3 \cdot \text{s}^{-1}$$

Molar flow rates of for component 1 and 2

$$f_1 = \frac{Q_1}{V_{m_1}} = 2.322 \times 10^{-5} \text{mol} \cdot \text{s}^{-1}$$

$$f_2 = \frac{Q_2}{V_{m_2}} = 2.321 \times 10^{-5} \text{mol} \cdot \text{s}^{-1}$$

where, V_{m_1} and V_{m_2} are the molar volume of component 1 and 2. Molar volumes are calculated

from molecular weight and density of pure component using the following relation; $V_{m_i} = \frac{M_i}{\rho_i}$.

Total molar flow rate, $f = 4.643 \times 10^{-5} \text{mol} \cdot \text{s}^{-1}$

Mole fraction of component 1, $x_1 = \frac{f_1}{f} = 0.5001$

Controller reading (\mathcal{R}) for both the pure components calculated using the relation, $\mathcal{R}_i = \frac{Q_i}{K_P}$

$$\mathcal{R}_{A_{Pure}} = 1795.6 \text{ counts} \cdot \text{s}^{-1}$$

$$\mathcal{R}_{B_{Pure}} = 1794.0 \text{ counts} \cdot \text{s}^{-1}$$

Calibration constant for mixture is calculated using the relation,

$$\varepsilon_M = Q_1 \varepsilon_1 + Q_2 \varepsilon_2 = Q_1 (k_1 + k_0 \mathcal{R}_{A_{Pure}}) + Q_2 (k_1 + k_0 \mathcal{R}_{B_{Pure}})$$

$$\varepsilon_M = 7.855 \times 10^{-2} \text{ J} \cdot \text{V}^{-1} \cdot \text{cm}^3$$

Baseline voltage for component 1 and 2,

$$E_1^0 = -40.4 \text{ } \mu\text{V}$$

$$E_2^0 = -65.2 \text{ } \mu\text{V}$$

Mixture baseline voltage,

$$E_M^0 = \phi_1 E_1^0 + \phi_2 E_2^0, \text{ where } \phi_i = Q_i / \sum Q_j$$

$$E_M^0 = -55.8 \text{ } \mu\text{V}$$

Corrected voltage,

$$E_{corr} = E - E_M^0 = (1968.8 + 55.8) \text{ } \mu\text{V} = 2024.6 \text{ } \mu\text{V}$$

Heat of mixing at $x_1 = 0.5001$

$$H_m^E = \frac{\varepsilon_M E_{corr}}{f \times Q} \times 10^{-6} = 685.0 \text{ J} \cdot \text{mol}^{-1}$$

Estimation of Error (or Uncertainty)

In order to determine the accuracy of the data, it is necessary to consider the propagation of the errors which appear as a result of the experimental method. Many methods are available for determining a composite error. Among the error estimation methods, the error propagation

method is widely used for determining the error in dependent variable that is a function of one or more different measured variables.

The general method can be describe by considering a dependent variable, U , to be a function of the several measured variables, u_1, u_2, \dots , etc.

$$U = f(u_1, u_2, \dots) \quad (\text{B1.1})$$

The error in the variable U (Bevington and Robinson, 2003)

$$s_U = \sqrt{\left(\frac{\partial U}{\partial u_1}\right)^2 s_{u_1}^2 + \left(\frac{\partial U}{\partial u_2}\right)^2 s_{u_2}^2 + \dots} \quad (\text{B1.2})$$

where,

s_{u_1} = the standard deviation of the u_1 variable

s_{u_2} =the standard deviation of the u_2 variable

s_U =the standard deviation of U dependent variable

$\frac{\partial U}{\partial u_i}$ =the partial derivative of the variable U with respect to u_i

In the present study simpler approximation of the error propagation method is used. Different forms of the approximation formulas for obtaining the error are presented.

Suppose the variables u_1 and u_2 have uncertainties Δu_1 and Δu_2 , respectively, then the uncertainties ΔU in the dependent variable U will be as follows:

- a. For addition and subtraction: $U = u_1 + u_2$ or $U = u_1 - u_2$

$$\Delta U = \sqrt{\Delta u_1^2 + \Delta u_2^2} \quad (\text{B1.3})$$

- b. For multiplication and division: $U = u_1 \times u_2$ or $U = u_1/u_2$

$$\Delta U = |U| \cdot \sqrt{\left(\frac{\Delta u_1}{u_1}\right)^2 + \left(\frac{\Delta u_2}{u_2}\right)^2} \quad (\text{B1.4})$$

Applying the equations (B1.3) and (B1.4) for mole fraction (x_1) and excess enthalpy (H_m^E) the uncertainties of these two variables were determined. A sample calculation of the error for the section B1.2 is presented.

Mole fraction, $x_1 = 0.5001$

Error in volumetric flow rate, Q_i

$$Q_i = \frac{m_i}{\rho_{H_2O}} \cdot \frac{1}{time}$$

$$\Delta Q_i = |Q_i| \cdot \sqrt{\left(\frac{\Delta m_i}{m_i}\right)^2 + \left(\frac{\Delta \rho_{H_2O}}{\rho_{H_2O}}\right)^2 + \left(\frac{\Delta time_i}{time_i}\right)^2}$$

where, $m = 9.002\text{g}$, $\Delta m = \pm 0.001\text{g}$; $\rho_{H_2O} = 0.99705\text{ g} \cdot \text{cm}^{-3}$, $\Delta \rho = \pm 0.00001\text{g} \cdot \text{cm}^{-3}$; $time = 1800\text{ s}$, $\Delta time = \pm 0.1\text{ s}$. So, the error in the flow rate measurement with a value of $Q_1 = 0.0050159\text{ cm}^3 \cdot \text{s}^{-1}$ the error, $\Delta Q_1 = \pm 0.0000006\text{ cm}^3 \cdot \text{s}^{-1}$.

Similarly for $Q_2 = 0.0050265\text{ cm}^3 \cdot \text{s}^{-1}$ the error, $\Delta Q_1 = \pm 0.0000006\text{ cm}^3 \cdot \text{s}^{-1}$.

Error in counter reading, R_A and R_B

$$\Delta R_A = \pm 1.0\text{ counts} \cdot \text{s}^{-1}\text{ and } \Delta R_B = \pm 1.0\text{ counts} \cdot \text{s}^{-1}$$

Error in molar volume, V_{m_i}

$$V_{m_i} = \frac{M_i}{\rho_i}$$

$$\Delta V_{m_i} = |V_{m_i}| \cdot \sqrt{\left(\frac{\Delta M_i}{M_i}\right)^2 + \left(\frac{\Delta \rho_i}{\rho_i}\right)^2}$$

where, $M_1 = 72.10572$, $\Delta M_1 = 0.0$ (Assuming); $\rho_1 = 0.88208\text{ g} \cdot \text{cm}^{-3}$, $\Delta \rho = \pm 0.00001\text{g} \cdot \text{cm}^{-3}$. So, the error in the molar volume with a value of $V_{m_1} = 81.1745\text{ cm}^3 \cdot \text{mol}^{-1}$ the error, $\Delta V_{m_1} = \pm 0.0009\text{ cm}^3 \cdot \text{mol}^{-1}$.

Similarly for $V_{m_2} = 133.6902\text{ cm}^3 \cdot \text{mol}^{-1}$ the error, $\Delta V_{m_2} = \pm 0.0021\text{ cm}^3 \cdot \text{mol}^{-1}$.

Error in molar flow rate, f_i

$$f_i = \frac{Q_i}{v_{m_i}}$$

$$\Delta f_i = |f_i| \cdot \sqrt{\left(\frac{\Delta Q_i}{Q_i}\right)^2 + \left(\frac{\Delta v_{m_i}}{v_{m_i}}\right)^2}$$

where, $Q_1 = 0.00188981 \text{ cm}^3 \cdot \text{s}^{-1}$, ;. So, the error in the molar flow rate with a value of $f_1 = 0.00002321 \text{ mol} \cdot \text{s}^{-1}$ the error, $\Delta f_1 = \pm 0.00000001 \text{ mol} \cdot \text{s}^{-1}$.

Similarly for $f_2 = 0.00002321 \text{ mol} \cdot \text{s}^{-1}$ the error, $\Delta f_2 = \pm 0.00000001 \text{ mol} \cdot \text{s}^{-1}$.

And the error in total molar flow rate f , is $\Delta f = \sqrt{(\Delta f_1)^2 + (\Delta f_2)^2} = \pm 0.00000001 \text{ mol} \cdot \text{s}^{-1}$

Finally the error in mole fraction measurement for $Q_2 = 0.0018981 \text{ cm}^3 \cdot \text{s}^{-1}$ and $Q_2 = 0.0031024 \text{ cm}^3 \cdot \text{s}^{-1}$ is given by

$$x_1 = \frac{f_1}{f} \text{ and}$$

the error is

$$\Delta x_1 = |x_1| \cdot \sqrt{\left(\frac{\Delta f_1}{f}\right)^2 + \left(\frac{\Delta f}{f}\right)^2} = \pm 0.0002$$

Excess enthalpy, $H_m^E = 685.0 \text{ J} \cdot \text{mol}^{-1}$

The excess enthalpy is obtained by the relation:

$$H_m^E = \frac{\varepsilon_M E_{corr}}{f \times Q}$$

where, $\varepsilon_M = \varepsilon_1 Q_1 + \varepsilon_2 Q_2 = X + Y$ where, $X = \varepsilon_1 Q_1$ and $Y = \varepsilon_2 Q_2$ and the error in X and Y can be estimated by the relation

$$\Delta X = |X| \cdot \sqrt{\left(\frac{\Delta \varepsilon_1}{\varepsilon_1}\right)^2 + \left(\frac{\Delta Q_1}{Q_1}\right)^2} \text{ and } \Delta Y = |Y| \cdot \sqrt{\left(\frac{\Delta \varepsilon_2}{\varepsilon_2}\right)^2 + \left(\frac{\Delta Q_2}{Q_2}\right)^2}$$

Finally the error in ε_M can be calculated by the relation

$$\Delta \mathcal{E}_M = \sqrt{(\Delta X)^2 + (\Delta Y)^2}$$

The uncertainty in the pure components calibration constants are estimated to be, $\Delta \mathcal{E}_1 = \pm 0.0003 \text{ J} \cdot \text{v}^{-1} \cdot \text{s}^{-1}$ and $\Delta \mathcal{E}_2 = \pm 0.0016 \text{ J} \cdot \text{v}^{-1} \cdot \text{s}^{-1}$.

Using these values the uncertainty in the calibration constant due to mixing is estimated for

$$\mathcal{E}_M = 0.07855 \text{ J} \cdot \text{v}^{-1} \cdot \text{cm}^3 \text{ the error } \Delta \mathcal{E}_M = \pm 0.00005 \text{ J} \cdot \text{v}^{-1} \cdot \text{cm}^3.$$

The uncertainty in the voltage measurement found to be $\Delta E_{corr} = \pm 0.01 \text{ } \mu\text{v}$.

The final uncertainty in the excess molar enthalpy $H_m^E = 685.0 \text{ J} \cdot \text{mol}^{-1}$ is

$$\Delta H_m^E = |H_m^E| \cdot \sqrt{\left(\frac{\Delta \mathcal{E}_M}{\mathcal{E}_M}\right)^2 + \left(\frac{\Delta E_{corr}}{E_{corr}}\right)^2 + \left(\frac{\Delta Q}{Q}\right)^2 + \left(\frac{\Delta f}{f}\right)^2} = \pm 1.0 \text{ J} \cdot \text{mol}^{-1}$$

Table B1.5. Calculated excess molar enthalpy for THF (1) + 22DMB (2) binary system over the whole mole fraction range

| Points | \mathcal{R}_A (counts $\cdot s^{-1}$) | \mathcal{R}_B (counts $\cdot s^{-1}$) | E (mv) | E_M^0 (mv) | E_{corr} (mv) | Q ($cm^3 \cdot s^{-1}$) | x_1 | H_m^E ($J \cdot mol^{-1}$) |
|--------|--|--|-------------|-----------------|--------------------|--------------------------------|--------|-----------------------------------|
| 1 | 0.0 | 1794.2 | -65.2 | -65.2 | 0.00 | 0.005 | 0.0000 | 0.0 |
| 2 | 56.0 | 1738.3 | 246.3 | -64.4 | 310.7 | 0.005 | 0.0500 | 128.4 |
| 3 | 114.3 | 1680.1 | 530.3 | -63.6 | 593.9 | 0.005 | 0.1000 | 240.4 |
| 4 | 174.9 | 1619.5 | 805.7 | -62.8 | 868.5 | 0.005 | 0.1500 | 344.3 |
| 5 | 238.1 | 1556.5 | 1049.8 | -61.9 | 1111.7 | 0.005 | 0.2000 | 431.5 |
| 6 | 304.8 | 1490.2 | 1276.2 | -61.0 | 1337.2 | 0.005 | 0.2505 | 507.7 |
| 7 | 372.6 | 1421.5 | 1469.2 | -60.1 | 1529.3 | 0.005 | 0.2999 | 568.4 |
| 8 | 444.3 | 1349.8 | 1645.3 | -59.1 | 1704.4 | 0.005 | 0.3498 | 619.4 |
| 9 | 520.0 | 1274.8 | 1789.4 | -58.0 | 1847.4 | 0.005 | 0.4000 | 655.7 |
| 10 | 598.9 | 1196.1 | 1891.5 | -56.9 | 1948.4 | 0.005 | 0.4500 | 675.4 |
| 11 | 681.7 | 1113.3 | 1968.2 | -55.8 | 2024.0 | 0.005 | 0.5002 | 684.7 |
| 12 | 681.6 | 1113.3 | 1968.8 | -55.8 | 2024.6 | 0.005 | 0.5001 | 685.0 |
| 13 | 767.6 | 1026.3 | 2003.0 | -54.6 | 2057.6 | 0.005 | 0.5500 | 679.5 |
| 14 | 859.6 | 935.4 | 1998.7 | -53.3 | 2052.0 | 0.005 | 0.6003 | 660.2 |
| 15 | 954.6 | 840.4 | 1951.5 | -52.0 | 2003.5 | 0.005 | 0.6499 | 628.1 |
| 16 | 1055.6 | 739.3 | 1863.4 | -50.6 | 1914.0 | 0.005 | 0.7000 | 584.2 |
| 17 | 1162.6 | 633.3 | 1720.0 | -49.2 | 1769.6 | 0.005 | 0.7500 | 525.0 |
| 18 | 1274.9 | 520.1 | 1506.2 | -47.6 | 1553.8 | 0.005 | 0.8002 | 448.4 |
| 19 | 1394.1 | 401.8 | 1238.4 | -46.0 | 1284.4 | 0.005 | 0.8501 | 359.8 |
| 20 | 1519.5 | 275.9 | 894.4 | -44.2 | 938.6 | 0.005 | 0.9000 | 255.3 |
| 21 | 1653.5 | 142.2 | 475.1 | -42.4 | 517.5 | 0.005 | 0.9500 | 136.4 |
| 22 | 1795.4 | 0.00 | -40.4 | -40.4 | 0.0 | 0.005 | 1.0000 | 0.0 |

B2. Correcting of Weights for the Buoyancy of Air

Buoyancy correction of weight is accomplished by means of the formula given by Bauer (1959). The formula has the following form:

$$m_c = m_o \frac{\left(1 - \frac{\rho_a}{\rho_B}\right)}{\left(1 - \frac{\rho_a}{\rho_s}\right)} \quad (\text{B2.1})$$

where m_c is the corrected mass of sample, m_o the observed mass, ρ_a the density of air, ρ_B density of brass, which is the built-in weights in the balance and has value of $8.4 \text{ g} \cdot \text{cm}^{-3}$, and ρ_s the density of sample whose weight has to be corrected.

As in most of the weighings, the environment surrounding the weighing apparatus is air. And the density of air acts as a buoyancy force on the weighed sample. The air density is calculated by the following equation (Bauer, 1959)

$$\rho_a / (\text{g} \cdot \text{cm}^{-3}) = \frac{0.000001701 \times (P \times R_H \times P_{H_2O}^v)}{(1 + 0.00367 \times t)} \quad (\text{B2.2})$$

where, P is the atmospheric pressure in mmHg, R_H the relative humidity in %, t the room temperature in °C, and $P_{H_2O}^v$ the vapor pressure of water at room temperature and is calculated by the Antoine equation

$$\log_{10}(P_{H_2O}^v / (\text{mmHg})) = A - \frac{B}{C+t} \quad (\text{B2.3})$$

where $A = 8.184254$, $B = 1791.3$, $C = 238.1$, and they were obtained from Riddik et al. (1986).

Table B2.1. Sample calculation: Binary mixture of {THF (1) + 22DMB (2)} of $x_1 \approx 0.2500$.

| | | | |
|-------------------|-------------|-------------------|-------------------------------------|
| Ambient Condition | Temperature | Relative Humidity | Pressure |
| | 22.76 °C | 45% | 710.76 mmHg |
| Pure | Component | Molecular Weight | Density/ (g · cm ⁻³) |
| | THF | 72.10572 | 0.88208 |
| | 22DMB | 86.17536 | 0.64459 |

Table B2.2. Summary of weighing

| | |
|-----------|-------------|
| Component | Weight/ (g) |
| THF | 25.3861 |
| 22DMB | 91.0591 |

Weight correction for THF

$$P_{H_2O}^v / (\text{mmHg}) = 10^{\left(8.184254 - \left(\frac{1791.3}{238.1 + 22.759}\right)\right)}$$

$$P_{H_2O}^v = 20.7647 \text{ mmHg}$$

$$\rho_a / (\text{g} \cdot \text{cm}^{-3}) = \frac{0.000001701 \times (710.758 \times 45 \times 20.7647)}{(1 + 0.00367 \times 22.759)}$$

$$\rho_a = 0.00111 \text{ g} \cdot \text{cm}^{-3}$$

$$\rho_B = 8.4 \text{ g} \cdot \text{cm}^{-3}$$

$$m_c = 25.3861 \frac{\left(1 - \frac{0.00111}{8.4}\right)}{\left(1 - \frac{0.00111}{0.88208}\right)}$$

$$m_c = 25.4147 \text{ g}$$

Similarly, for 22DMB the corrected weight is 91.2042 g.

So, the calculated mole fraction is

$$x_1 = \frac{\frac{m_1}{M_1}}{\frac{m_1}{M_1} + \frac{m_2}{M_2}} = \frac{\frac{25.4147}{72.10572}}{\frac{25.4147}{72.10572} + \frac{91.2042}{86.17536}} = 0.2498$$

and the mixture molecular weight is

$$M_{mix} = x_1 M_1 + (1 - x_1) M_2 = 82.6604 \text{ g} \cdot \text{mol}^{-1}$$

B3. Heats of Mixing of Pseudo-Binary Mixture

Excess molar enthalpy measurement of a pseudo-binary mixture involves several steps. These are the determination of pure component densities, pre-estimation of weights of pure components required for preparing the pseudo-pure mixture of a selected composition. After the pseudo binary mixture preparation, the measured weights are corrected for the buoyancy of air and then the mole fraction and the molecular weight are calculated. The density of the prepared pseudo pure mixture were measured in a densitometer (Anton Paar DMA 5000M). Details of the mixture preparation and buoyancy correction are presented in Appendix B2.

Table B3.1. Pseudo pure mixture of {THF (1) + 22DMB (2)}

| | | | |
|-------------------|------------------|-------------------------------------|-------------------------------------|
| Ambient Condition | Temperature | Relative Humidity | Pressure |
| | 22.39 °C | 40 % | 710.91 mmHg |
| Pure | Component | Molecular Weight | Density/ (g · cm ⁻³) |
| | THF | 72.10572 | 0.88208 |
| | 22DMB | 86.17536 | 0.64459 |
| Mixture | Component | Weight/(g) | Mole Fraction |
| | THF | 50.3156 | 0.5001 |
| | 22DMB | 60.1004 | 0.4999 |
| | Molecular Weight | Density/ (g · cm ⁻³) | |
| | 79.13861 | 0.73717 | |

Table B3.2. Calibration results of 1-hexene with pump A

| Motor Speed (\mathcal{R}) | Gear ratio (\mathbb{G}) | E_Q^0 | E_Q | ΔE | I | \mathcal{E} |
|-------------------------------|-----------------------------|---------|---------|------------|--------|--|
| (counts \cdot s $^{-1}$) | | (mv) | (mv) | (mv) | (amp) | (J \cdot v $^{-1}$ \cdot s $^{-1}$) |
| 830.3 | 0.1 | -0.0429 | -0.4544 | -0.4115 | 0.0114 | 15.5299 |
| 1070.8 | 0.1 | -0.0411 | -0.4498 | -0.4087 | 0.0113 | 15.5538 |
| 1310.3 | 0.1 | -0.0421 | -0.4508 | -0.4087 | 0.0113 | 15.5812 |
| 1650.8 | 0.1 | -0.0409 | -0.4496 | -0.4087 | 0.0114 | 15.6087 |
| 690.9 | 0.1 | -0.0419 | -0.4538 | -0.4119 | 0.0114 | 15.5148 |
| 450.3 | 0.1 | -0.0410 | -0.4530 | -0.4120 | 0.0114 | 15.4837 |

The expression for calibration constant (\mathcal{E}) obtained by fitting equation (3.2) to the experimental data has the form

$$\mathcal{E} = 15.4371 + 1.028193 \times 10^{-4} \cdot \mathcal{R}$$

where \mathcal{R} is the pump flow rates in counts \cdot s $^{-1}$. The standard deviation, σ , is 0.006 J \cdot v $^{-1}$ \cdot s $^{-1}$

having an uncertainty in parameters k_0 and k_1 are ± 0.0066 J \cdot v $^{-1}$ \cdot s $^{-1}$ and ± 0.000006 J \cdot v $^{-1}$ \cdot

counts $^{-1}$

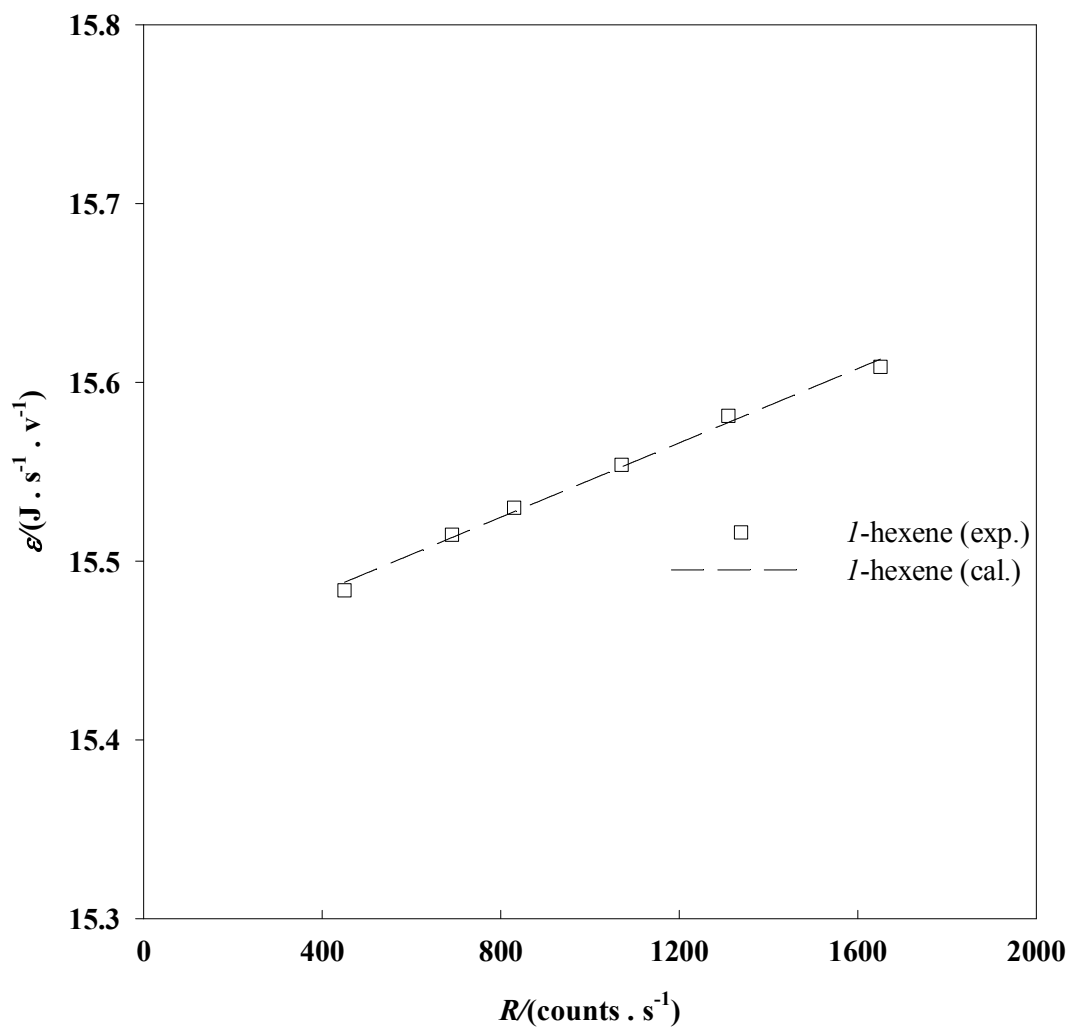


Figure B3.1. Calibration curve for 1-hexene in Pump A

Table B3.3. Calibration results of mixture # 2 {THF (1) + 22DMB (2)} with pump B

| Motor Speed (\mathcal{R}) | Gear ratio (\mathbb{G}) | E_Q^0 | E_Q | ΔE | I | \mathcal{E} |
|-------------------------------|-----------------------------|---------|---------|------------|--------|--|
| (counts \cdot s $^{-1}$) | | (mv) | (mv) | (mv) | (amp) | (J \cdot v $^{-1}$ \cdot s $^{-1}$) |
| 830.3 | 0.1 | -0.0414 | -0.4526 | -0.4112 | 0.0114 | 15.5686 |
| 1310.3 | 0.1 | -0.0422 | -0.4555 | -0.4133 | 0.0114 | 15.5986 |
| 1650.8 | 0.1 | -0.0411 | -0.4583 | -0.4172 | 0.0115 | 15.6158 |
| 1070.7 | 0.1 | -0.0428 | -0.4615 | -0.4187 | 0.0115 | 15.5870 |
| 690.9 | 0.1 | -0.0431 | -0.4545 | -0.4114 | 0.0114 | 15.5610 |
| 450.3 | 0.1 | -0.0411 | -0.4506 | -0.4095 | 0.0113 | 15.5508 |

The expression for calibration constant (\mathcal{E}) obtained by fitting equation (3.2) to the experimental data has the form

$$\mathcal{E} = 15.5238 + 5.12023 \times 10^{-5} \cdot \mathcal{R}$$

where \mathcal{R} is the pump flow rates in counts \cdot s $^{-1}$. The standard deviation, σ , is 0.004 J \cdot v $^{-1}$ \cdot s $^{-1}$

having an uncertainty in parameters k_0 and k_1 are ± 0.00041 J \cdot v $^{-1}$ \cdot s $^{-1}$ and ± 0.000004

J \cdot v $^{-1}$ \cdot counts $^{-1}$

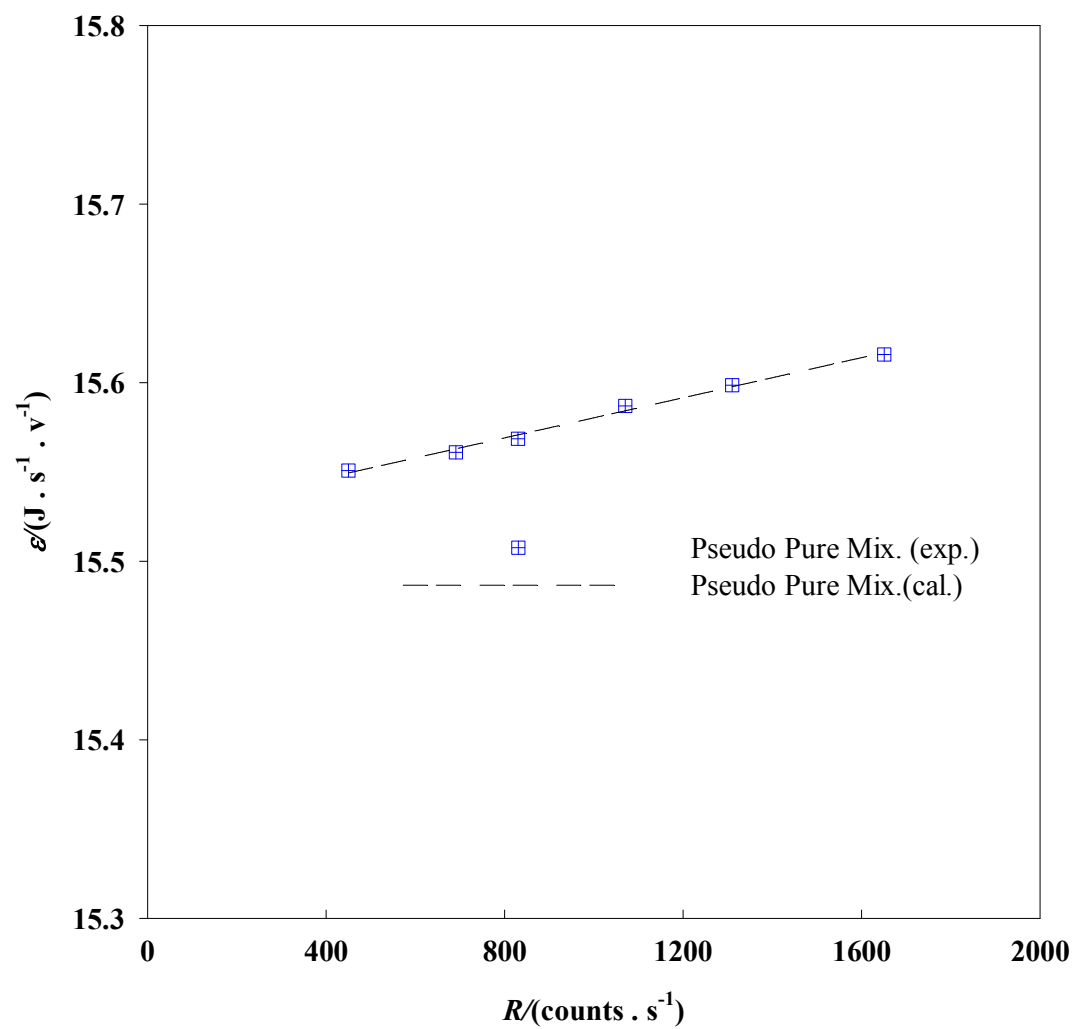


Figure B3.2. Mixture Calibration curve: THF (1) + 22DMB (2) pseudo-pure mixture in Pump B

Table B3.4. Primary experimental data for 1-hexene (1) + {THF (1) + 22DMB (2)} (2) binary mixture

| Pump | # | Component | M | $\rho/(\text{g} \cdot \text{cm}^{-3})$ | k_1 | $k_0 \times 10^{-4}$ |
|--------|---|-----------|---|--|----------------|----------------------|
| A | 1 | 1-hexene | 84.15948 | 0.66876 | 15.4371 | 1.028193 |
| B | 2 | Mixture | 79.13861 | 0.73717 | 15.5238 | 0.512023 |
| Points | $\mathcal{R}_A/(\text{counts} \cdot \text{s}^{-1})$ | | $\mathcal{R}_B/(\text{counts} \cdot \text{s}^{-1})$ | | $E(\text{mv})$ | |
| 1 | 0.0 | | 1794.4 | | -0.0402 | |
| 2 | 104.4 | | 1690.3 | | -0.0112 | |
| 3 | 206.9 | | 1587.1 | | 0.0159 | |
| 4 | 307.9 | | 1486.1 | | 0.0388 | |
| 5 | 406.9 | | 1387.1 | | 0.0566 | |
| 6 | 504.8 | | 1290.1 | | 0.0738 | |
| 7 | 600.9 | | 1194.1 | | 0.0874 | |
| 8 | 694.9 | | 1100.0 | | 0.0975 | |
| 9 | 787.9 | | 1007.1 | | 0.1057 | |
| 10 | 879.8 | | 915.2 | | 0.1106 | |
| 11 | 968.7 | | 826.3 | | 0.1108 | |
| 12 | 968.8 | | 826.2 | | 0.1112 | |
| 13 | 1057.7 | | 737.3 | | 0.1093 | |
| 14 | 1144.6 | | 650.4 | | 0.1039 | |
| 15 | 1230.5 | | 564.6 | | 0.0975 | |
| 16 | 1314.3 | | 480.6 | | 0.0861 | |
| 17 | 1398.2 | | 397.6 | | 0.0715 | |
| 18 | 1480.0 | | 315.0 | | 0.0556 | |
| 19 | 1560.7 | | 234.7 | | 0.0361 | |
| 20 | 1640.8 | | 155.4 | | 0.0154 | |
| 21 | 1718.4 | | 77.2 | | -0.0118 | |
| 24 | 1795.4 | | 0.0 | | -0.0408 | |

Excess molar enthalpy calculation procedure for the pseudo-binary mixture is similar to that of binary mixture described in Appendix B1. Only the final results are presented.

Table B3.5. Calculated excess molar enthalpy for the 1-hexene (1) + {THF (1) + 22DMB (2)} (2) pseudo binary mixture over the whole mole fraction range

| Points | \mathcal{R}_A (counts $\cdot s^{-1}$) | \mathcal{R}_B (counts $\cdot s^{-1}$) | E (mv) | E_M^0 (mv) | E_{corr} (mv) | Q ($cm^3 \cdot s^{-1}$) | x_1 | H_m^E ($J \cdot mol^{-1}$) |
|--------|--|--|-------------|-----------------|--------------------|--------------------------------|--------|-----------------------------------|
| 1 | 0.0 | 1794.4 | -40.2 | -40.2 | 0.0 | 0.005 | 0.0000 | 0.00 |
| 2 | 104.4 | 1690.3 | -11.2 | -40.2 | 29.0 | 0.005 | 0.0500 | 9.8 |
| 3 | 206.9 | 1587.1 | 15.9 | -40.3 | 56.2 | 0.005 | 0.1000 | 19.2 |
| 4 | 307.9 | 1486.1 | 38.8 | -40.3 | 79.1 | 0.005 | 0.1501 | 27.2 |
| 5 | 406.9 | 1387.1 | 56.6 | -40.3 | 96.9 | 0.005 | 0.2000 | 33.7 |
| 6 | 504.8 | 1290.1 | 73.8 | -40.4 | 114.2 | 0.005 | 0.2501 | 40.0 |
| 7 | 600.9 | 1194.1 | 87.4 | -40.4 | 127.8 | 0.005 | 0.3002 | 45.1 |
| 8 | 694.9 | 1100.0 | 97.5 | -40.4 | 137.9 | 0.005 | 0.3500 | 49.1 |
| 9 | 787.9 | 1007.1 | 105.7 | -40.5 | 146.2 | 0.005 | 0.4001 | 52.4 |
| 10 | 879.8 | 915.2 | 110.6 | -40.5 | 151.1 | 0.005 | 0.4504 | 54.6 |
| 11 | 968.7 | 826.3 | 110.8 | -40.5 | 151.3 | 0.005 | 0.4998 | 55.1 |
| 12 | 968.8 | 826.2 | 111.2 | -40.5 | 151.7 | 0.005 | 0.4999 | 55.3 |
| 13 | 1057.7 | 737.3 | 109.3 | -40.6 | 149.9 | 0.005 | 0.5501 | 55.0 |
| 14 | 1144.6 | 650.4 | 103.9 | -40.6 | 144.5 | 0.005 | 0.6000 | 53.5 |
| 15 | 1230.5 | 564.6 | 97.5 | -40.6 | 138.1 | 0.005 | 0.6501 | 51.5 |
| 16 | 1314.3 | 480.6 | 86.1 | -40.6 | 126.7 | 0.005 | 0.6998 | 47.7 |
| 17 | 1398.2 | 397.6 | 71.5 | -40.7 | 112.2 | 0.005 | 0.7499 | 42.5 |
| 18 | 1480.0 | 315.0 | 55.6 | -40.7 | 96.3 | 0.005 | 0.8002 | 36.8 |
| 19 | 1560.7 | 234.7 | 36.1 | -40.7 | 76.8 | 0.005 | 0.8500 | 29.6 |
| 20 | 1640.8 | 155.4 | 15.4 | -40.8 | 56.2 | 0.005 | 0.9000 | 21.8 |
| 21 | 1718.4 | 77.2 | -11.8 | -40.8 | 29.0 | 0.005 | 0.9500 | 11.3 |
| 22 | 1795.4 | 0.0 | -40.8 | -40.8 | 0.0 | 0.005 | 1.0000 | 0.0 |

APPENDIX C

1. Statistics of Data Correlation

2. Solution Theory Representation of Binary Systems

3. Solution Theory Representation of Ternary Systems

C1.1 Statistics of Data Correlation

Experimental data were fitted to the empirical and solution theory models by means of an unweighted least square method. The programs used to fit the experimental data are the same as those used by Benson and coworkers (1993-2006). The Marquardt method (Levenberg-Marquardt algorithm; (Marquardt, 1963)) was used in all the programs to get the best parameters of the models. The standard error was used as the objective function and was defined as

$$\sigma = \sqrt{\frac{\sum_{i=1}^n (\text{Experimental values} - \text{Calculated values})^2}{n-p}} \quad (\text{C1.1})$$

where n , is the number of experimental data points, and p , the number of adjustable parameters of the model. The chosen parameters were based on the minimization of this objective function.

In fitting the experimental excess molar enthalpy data to the solution theory models, there are no further statistical test were used as the parameters of these models are fixed. Empirical models used in the current study for representing the experimental data, have an arbitrary number of parameters. The numbers of parameters of the empirical models were selected by means of the *F-statistical test*. This statistical test is described in the following section.

C1.2 *F-statistical test*

In the fitting of the empirical models (Redlich-Kister polynomials) to the experimental data, the numbers of parameters selected is based on the *F-statistical test*. If it is found that model # 2 with p_2 parameters has a smaller standard error than model # 1 with p_1 parameters (where $p_2 > p_1$), then the model # 2 provides a somewhat better representation of the

experimental data. However, it is known that a model with more parameters will always provide a better fit of the experimental data. But, a model with more parameters does not always provide a statistically better fit than a model with less number of parameters. To resolve this dilemma engineers often use the *F-statistical test* to determine if the simpler model is statistically as “good” as the more complicated one. The formula for performing the *F-statistical test* is

$$F(\nu, \iota) = \frac{\frac{(SSE_1 - SSE_2)}{(p_2 - p_1)}}{\frac{SSE_2}{(n - p_2)}} \quad (C1.2)$$

where

SSE_1 = sum of square error of model # 1 with p_1 parameters

SSE_2 = sum of square error of model # 2 with p_2 parameters

n = number of data points

ν = degree of freedom of model # 1 ($\nu = n - p_1$)

ι = degree of freedom of model # 2 ($\iota = n - p_2$)

The value of $F_{(\nu, \iota)}$ will have an *F* distribution, assuming errors due to lack of fit are normally distributed. At a significance level $q (= 0.05)$, the value can be compared with the tabulated values of $F_{(1-q)}(\nu, \iota)$. If $F(\nu, \iota)$ is greater than $F_{(1-q)}(\nu, \iota)$, one concludes that model # 2 is better than model # 1 (Bevington and Robinson, 2003; Navidi, 2006).

As an example, the parameter selection of the Redlich-Kister polynomials for the THF (1) + 22DMB (2) system is illustrated in Table C1.1.

Table C1.1. *F*-statistical test summary

| Test no. | Parameters | $\frac{\sigma}{(\text{J} \cdot \text{md}^{-1})}$ | $\frac{\text{SSE}}{(\text{J} \cdot \text{md}^{-1})}$ | <i>DoF</i> | <i>F</i> | $F_{(1-q)}$ | Result |
|----------|------------|--|--|------------|----------|-------------|-----------------|
| 1 | 3 | 1.2 | 23.62 | 17 | 5.455 | 2.317 | $F > F_{(1-q)}$ |
| | 4 | 1.1 | 17.60 | 16 | | | |
| 2 | 4 | 1.1 | 17.60 | 16 | 0.015 | 2.385 | $F < F_{(1-q)}$ |
| | 5 | 1.1 | 17.58 | 15 | | | |
| 3 | 5 | 1.1 | 17.58 | 15 | 2.400 | 2.465 | $F < F_{(1-q)}$ |
| | 6 | 1.0 | 2.17 | 14 | | | |

**DoF* = degree of freedom; $q = 0.05$

This table serves to indicate that the polynomial with four parameters provides a statistically better fit than the polynomial with five or six parameters. The tabulated values for the *F*-distribution with a 95% confidence level indicate that any difference in standard deviation is due to random error.

C2. Solution Theory Representation of Binary Systems

C2.1 Flory theory Representation of Binary systems

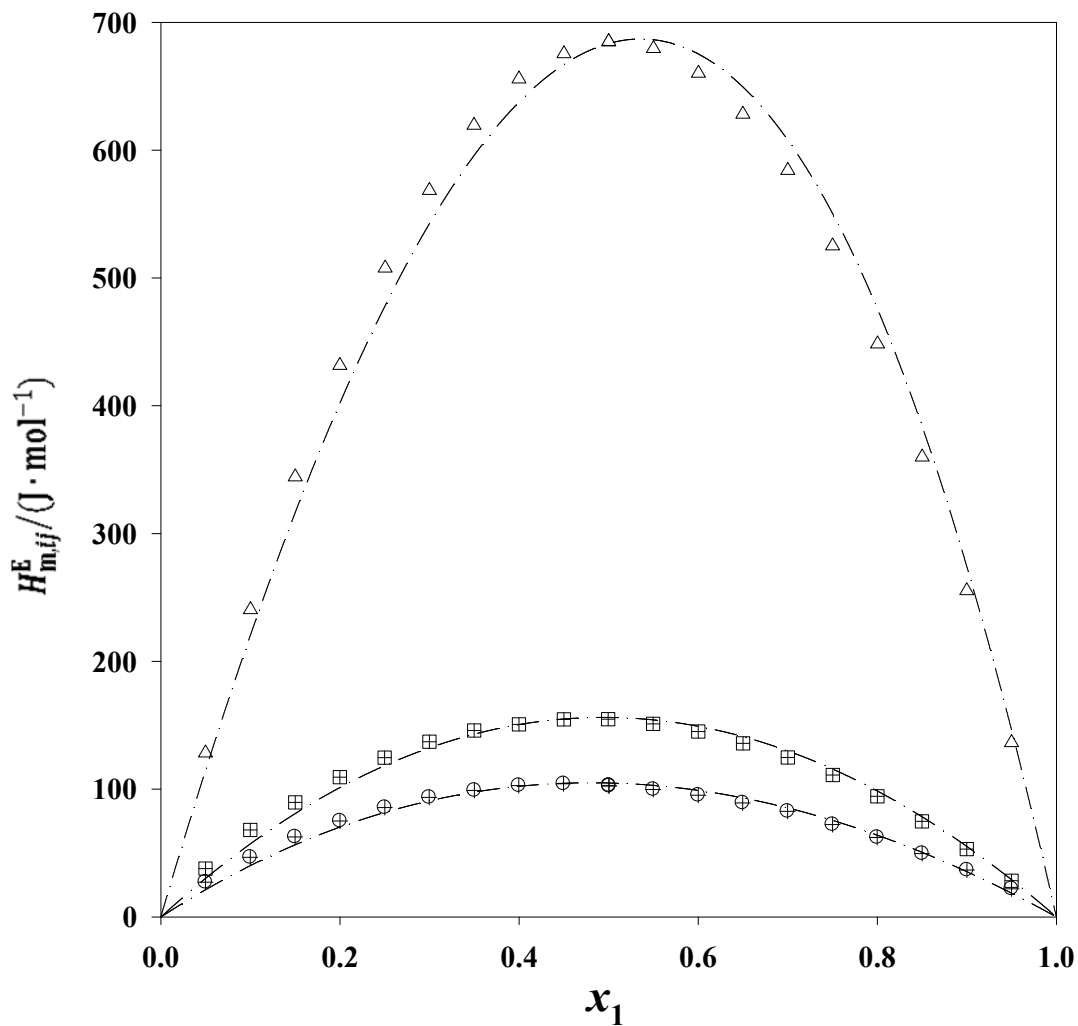


Figure C2.1(a). Excess molar enthalpies $H_{m,ij}^E$ for the binary systems presented in Table 4.2a and 4.2b at the temperature 298.15 K. Experimental results: Δ , x_1 THF + $(1 - x_1)$ 22DMB; \boxplus , x_1 DNPE + $(1 - x_1)$ 22DMB; \oplus , x_1 DNBE + $(1 - x_1)$ 22DMB. Curves: $- \cdot -$, calculated by means of the Flory theory.

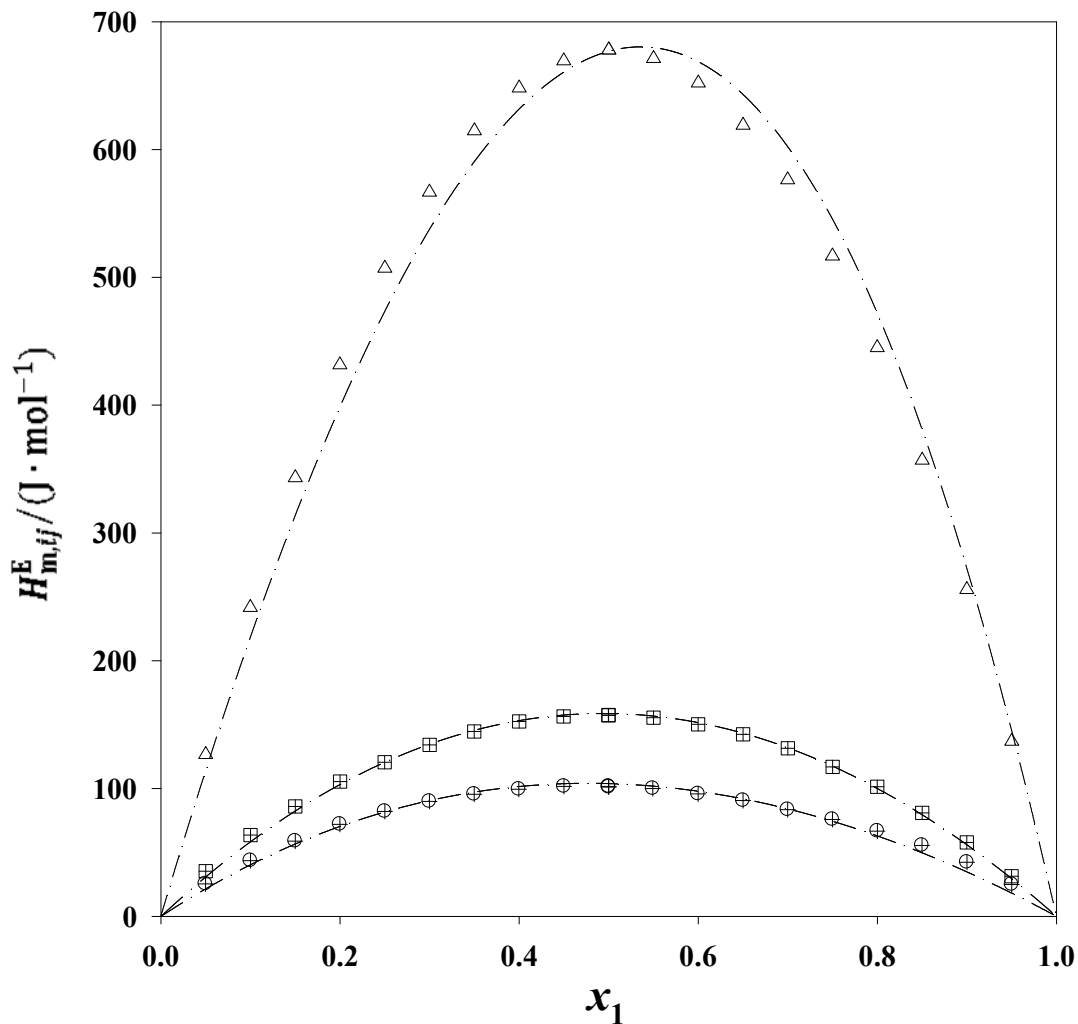


Figure C2.1(b). Excess molar enthalpies $H_{m,ij}^E$ for the binary systems presented in Table 4.2a and 4.2b at the temperature 298.15 K. Experimental results: Δ , x_1 THF + $(1 - x_1)$ 23DMB; \boxplus , x_1 DNPE + $(1 - x_1)$ 23DMB; \oplus , x_1 DNBE + $(1 - x_1)$ 23DMB Curves: $- \cdot -$, calculated by means of the Flory theory.

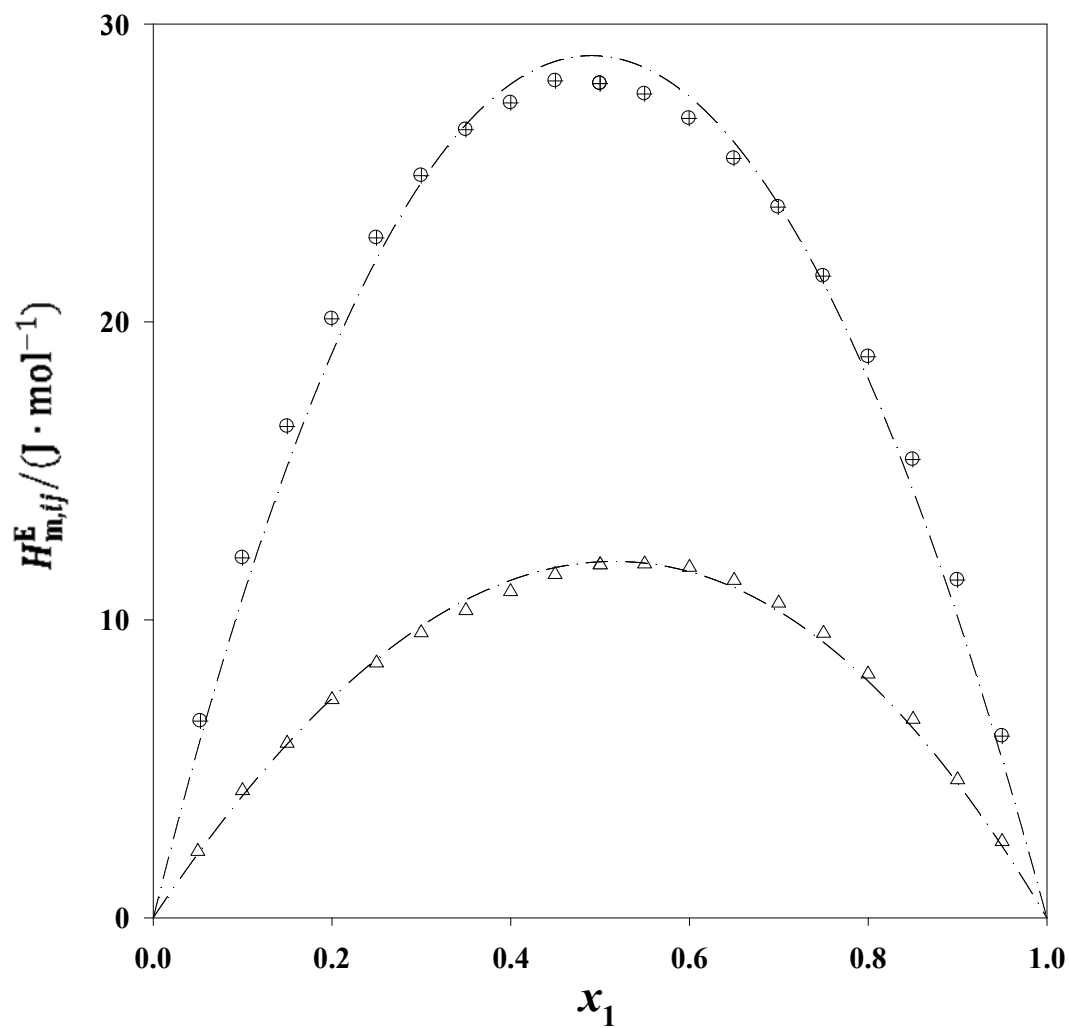


Figure C2.1(c). Excess molar enthalpies $H_{m,ij}^E$ for the binary systems presented in Table 4.2a and 4.2b at the temperature 298.15 K. Experimental results: Δ , $x_1 \text{DNPE} + (1 - x_1) \text{THF}$; \oplus , $x_1 \text{DNBE} + (1 - x_1) \text{THF}$. Curves: $- \cdot -$, calculated by means of the Flory theory.

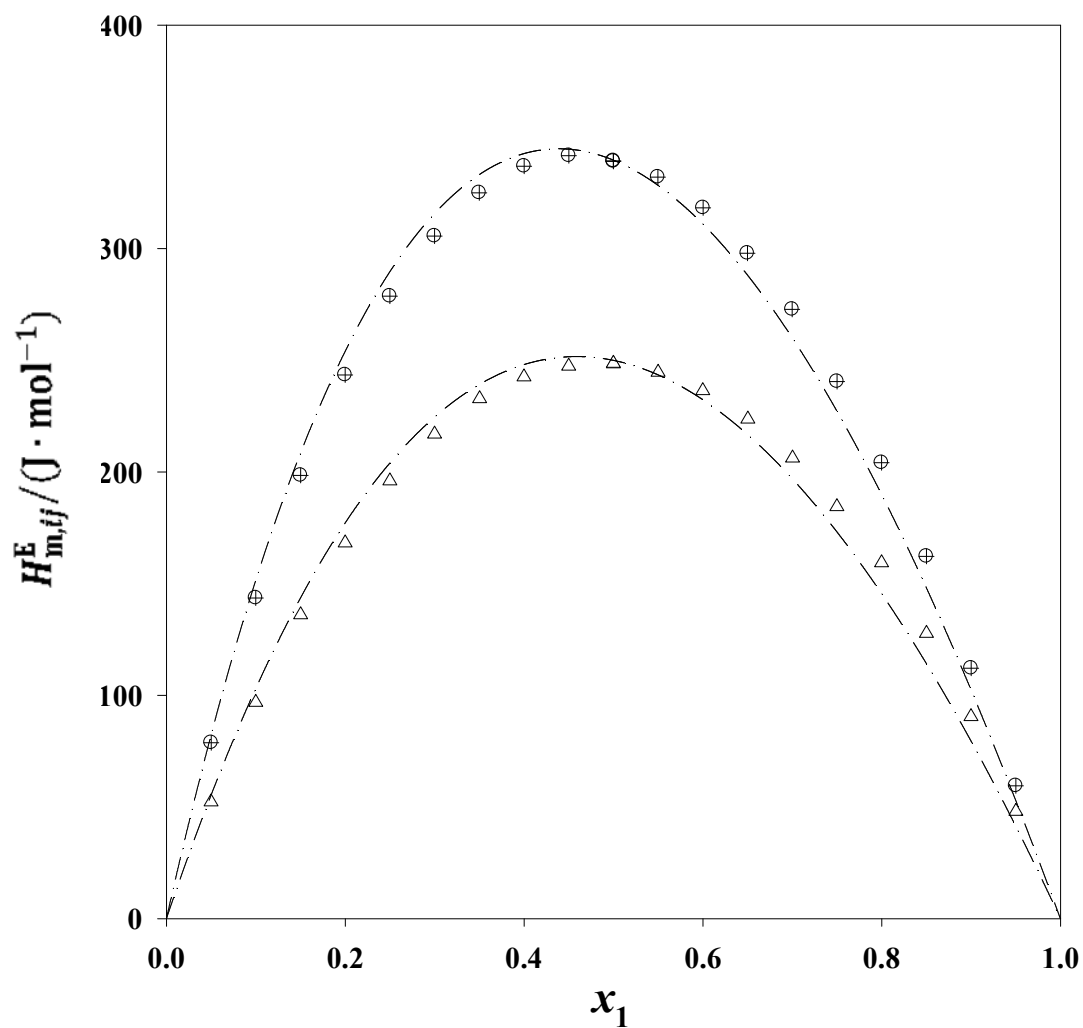


Figure C2.1(d). Excess molar enthalpies $H_{m,ij}^E$ for the binary systems presented in Table 4.2b at the temperature 298.15 K. Experimental results: Δ , x_1 DNPE + $(1 - x_1)$ DNBE; \oplus , x_1 DNPE + $(1 - x_1)$ 1HX Curves: $- \cdot -$, calculated by means of the Flory theory.

C2.2 Liebermann-Fried model Representation of Binary systems

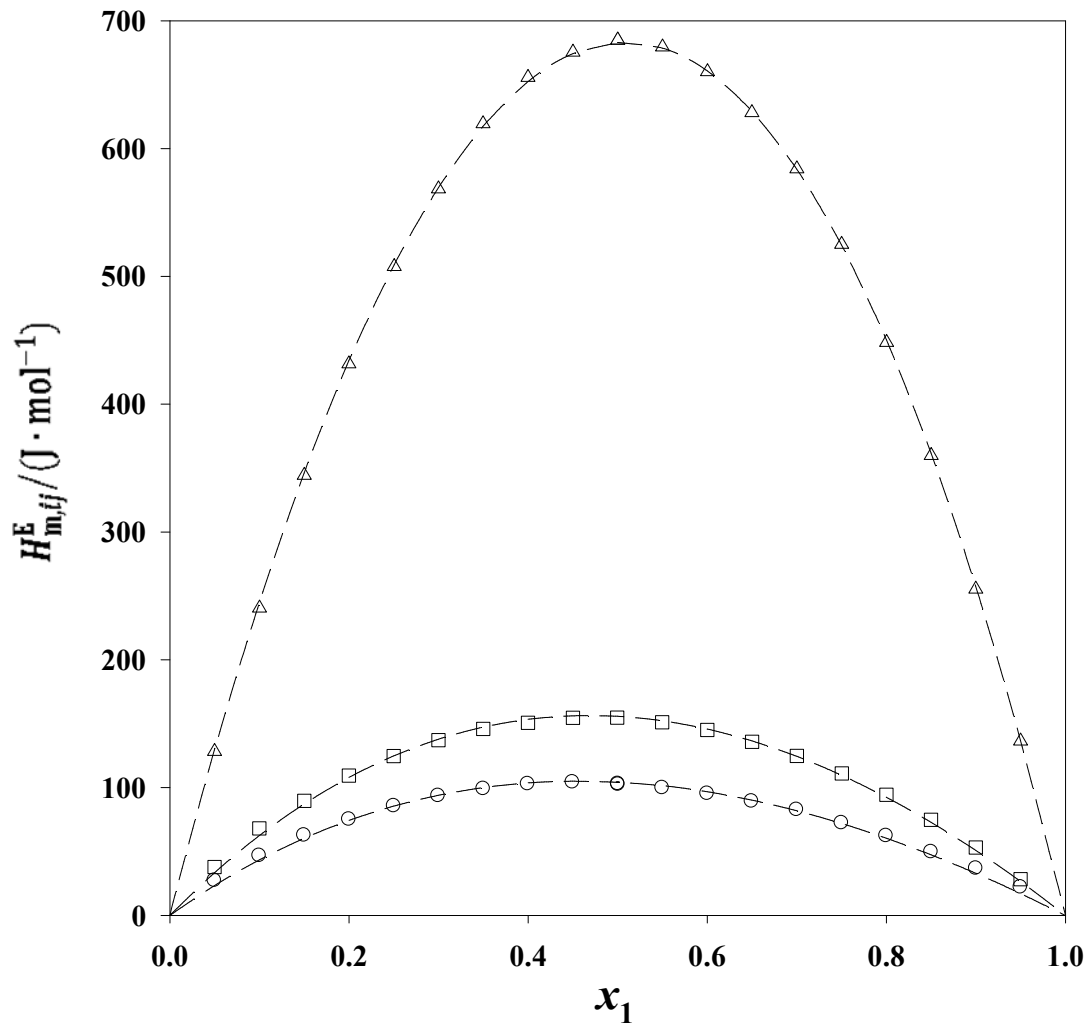


Figure C2.2(a). Excess molar enthalpies $H_{m,ij}^E$ for the binary systems presented in Table 4.2a and 4.2b at the temperature 298.15 K. Experimental results: Δ , x_1 THF + (1 - x_1) 22DMB; \boxplus , x_1 DNPE + (1 - x_1) 22DMB; \oplus , x_1 DNBE + (1 - x_1) 22DMB. Curves: - - - , calculated by means of the Liebermann-Fried model.

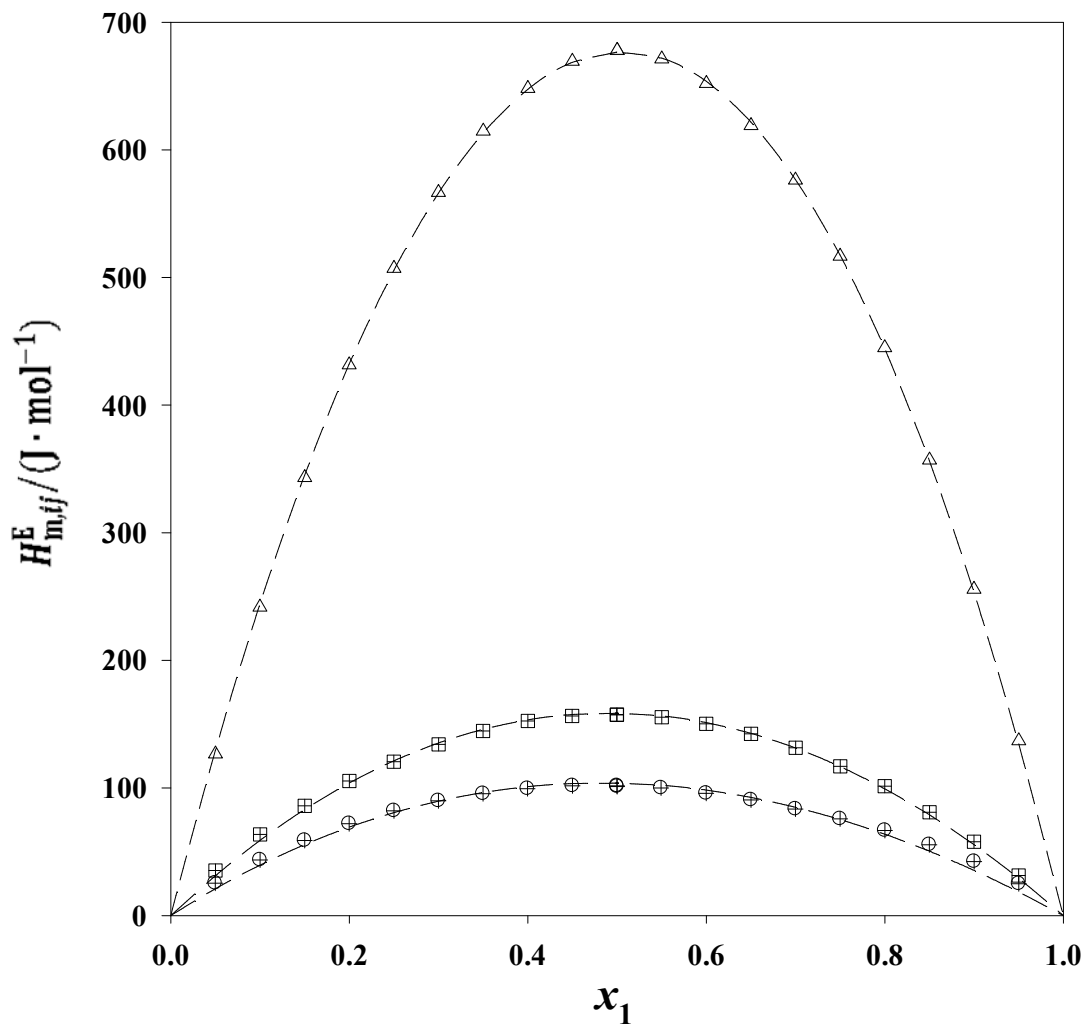


Figure C2.2(b). Excess molar enthalpies, $H_{m,ij}^E$ for the binary systems presented in Table 4.2a and 4.2b at the temperature 298.15 K. Experimental results: Δ , x_1 THF + $(1 - x_1)$ 23DMB; \boxplus , x_1 DNPE + $(1 - x_1)$ 23DMB; \oplus , x_1 DNBE + $(1 - x_1)$ 23DMB Curves: - - -, calculated by means of the Liebermann-Fried model.

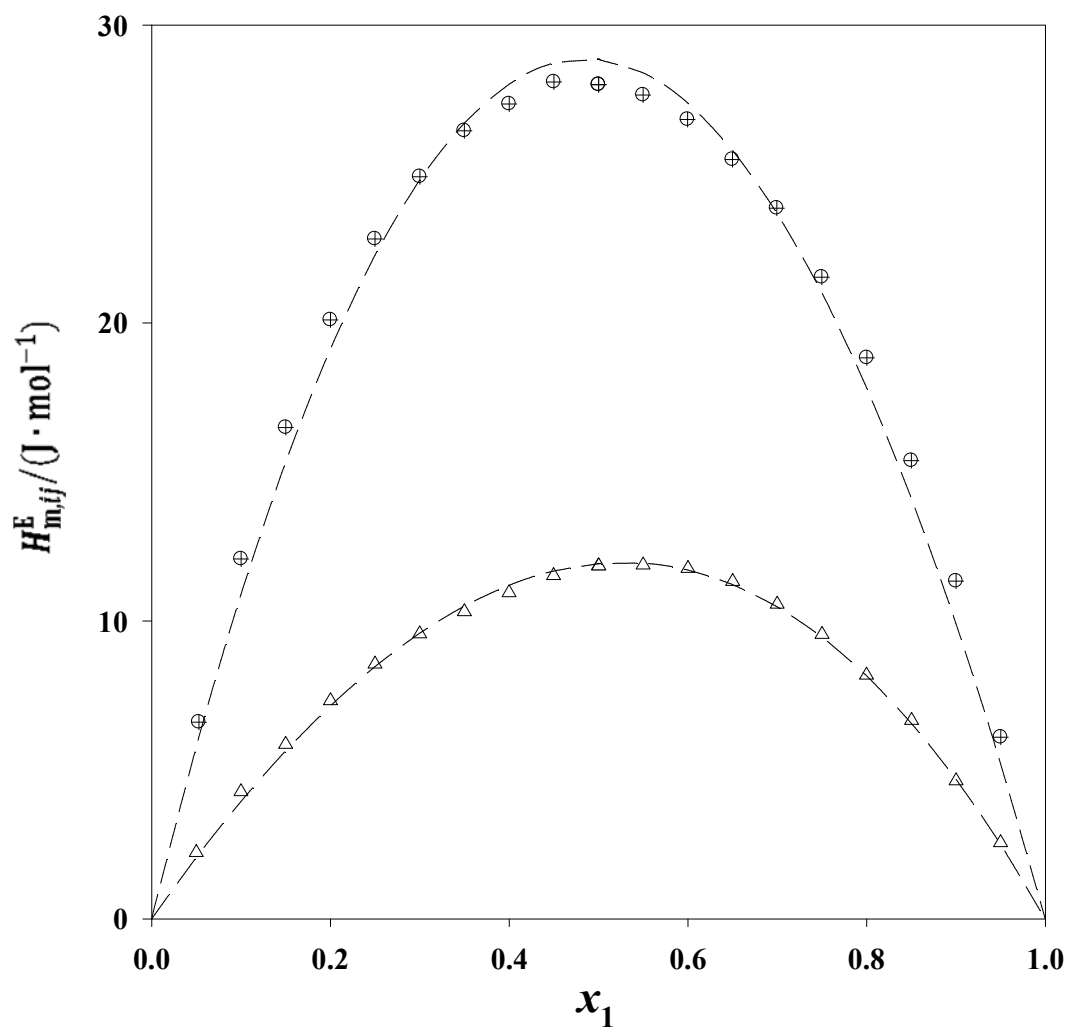


Figure C.2(c). Excess molar enthalpies, $H_{m,ij}^E$ for the binary systems presented in Table 4.2a and 4.2b at the temperature 298.15 K. Experimental results: Δ , x_1 DNPE + $(1 - x_1)$ THF ; \oplus , x_1 DNBE+ $(1 - x_1)$ THF Curves: - - -, calculated by means of the Liebermann-Fried model.

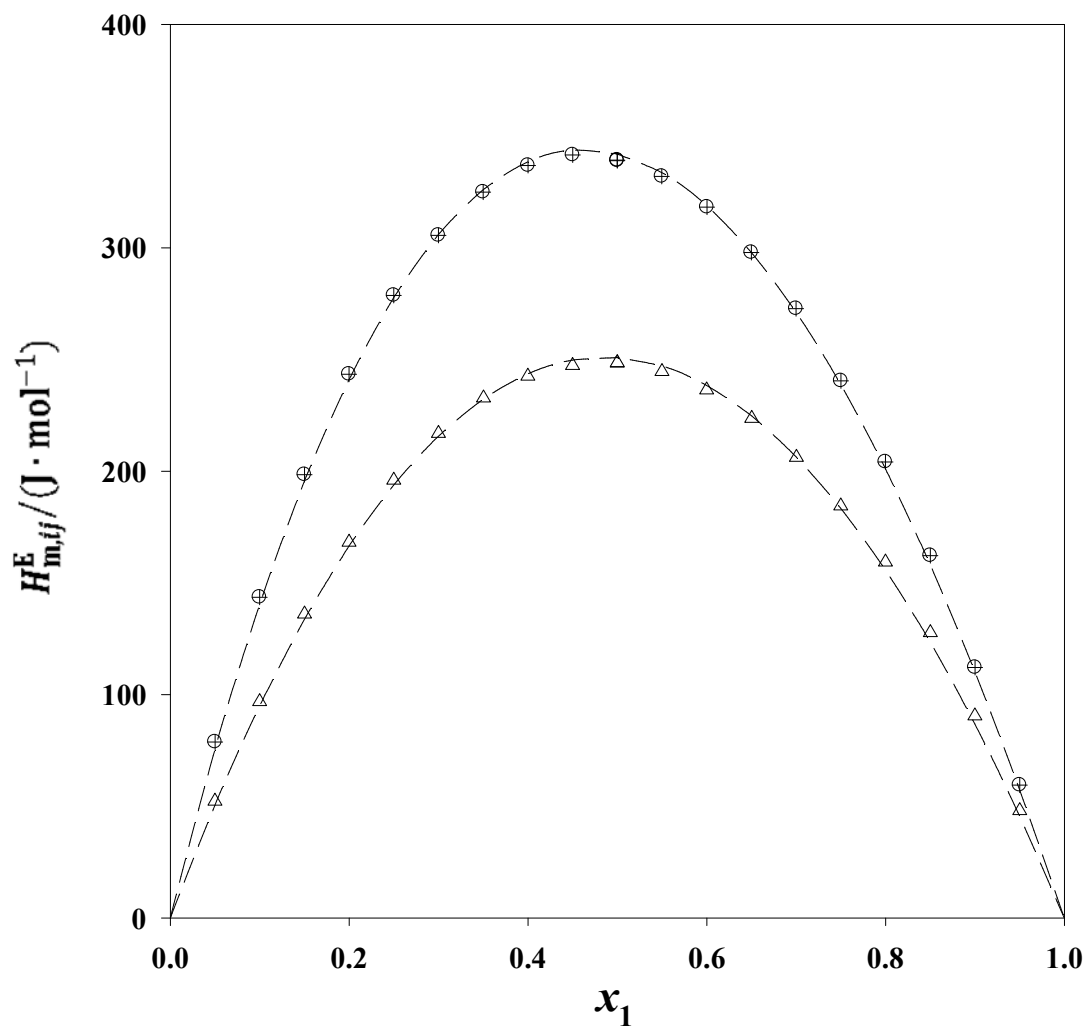


Figure C2.2(d). Excess molar enthalpies, $H_{m,ij}^E$ for the binary systems presented in Table 4.2b at the temperature 298.15 K. Experimental results: Δ , x_1 DNPE + $(1 - x_1)$ DNBE; \oplus , x_1 DNPE + $(1 - x_1)$ 1HX Curves: - - -, calculated by means of the Liebermann-Fried model.

C3. Solution Theory Representation of Ternary Systems

C3.1 Flory theory Representation of Ternary System

Ternary System: DNPE (1) + DNBE (2) + THF (3)

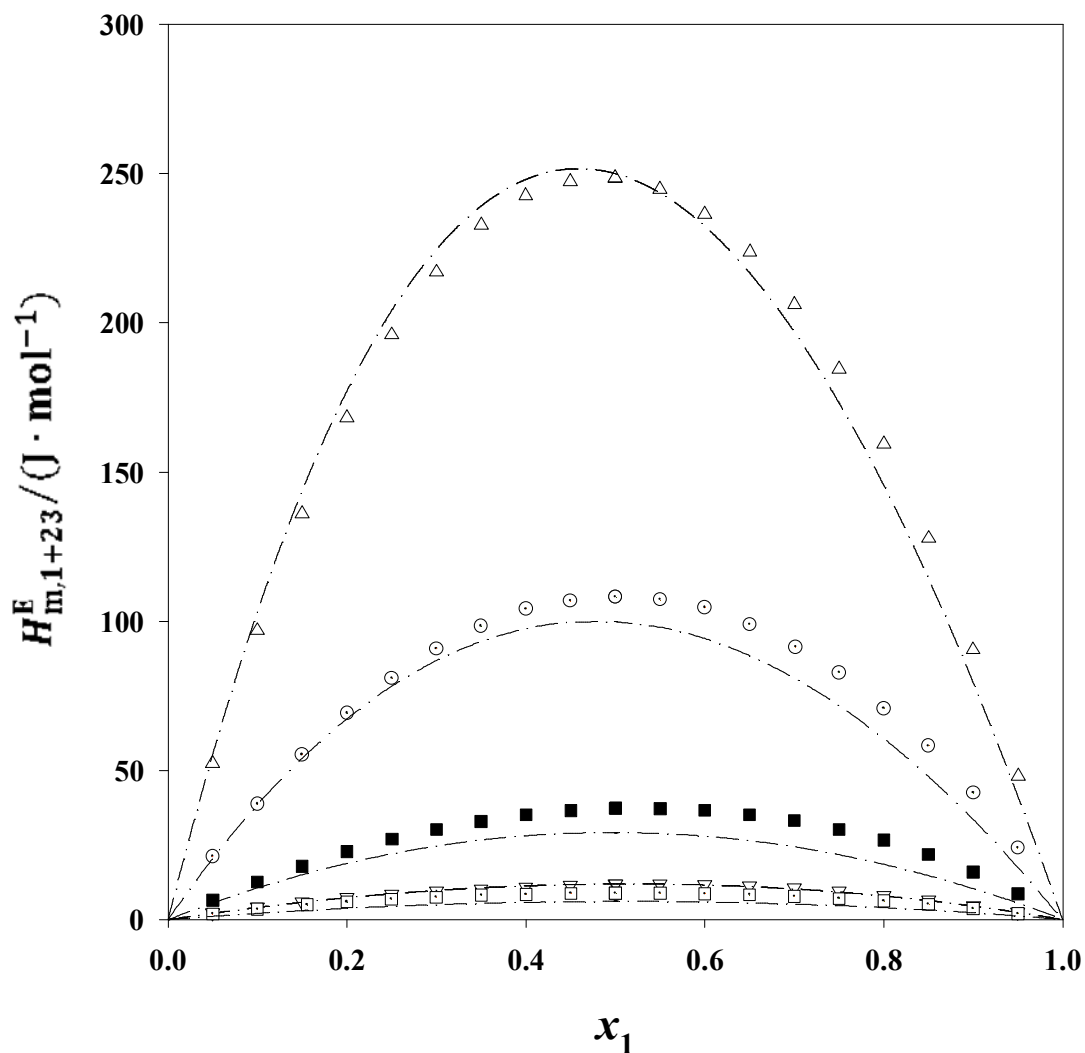


Figure C3.1. Excess molar enthalpies, $H_{m,1+23}^E$, for the x_1 DNPE + x_2 DNBE + $(1 - x_1 - x_2)$ THF mixture at the temperature 298.15 K. Plotted against mole fraction x_1 . Experimental results: Δ , $x_3 = 0.0$; \odot , $x_2/x_3 = 0.3332$; \blacksquare , $x_2/x_3 = 1.0004$; \square , $x_2/x_3 = 3.0000$; ∇ , $x_2 = 0.0$; Curves: - - -, predicted by means of the Flory theory.

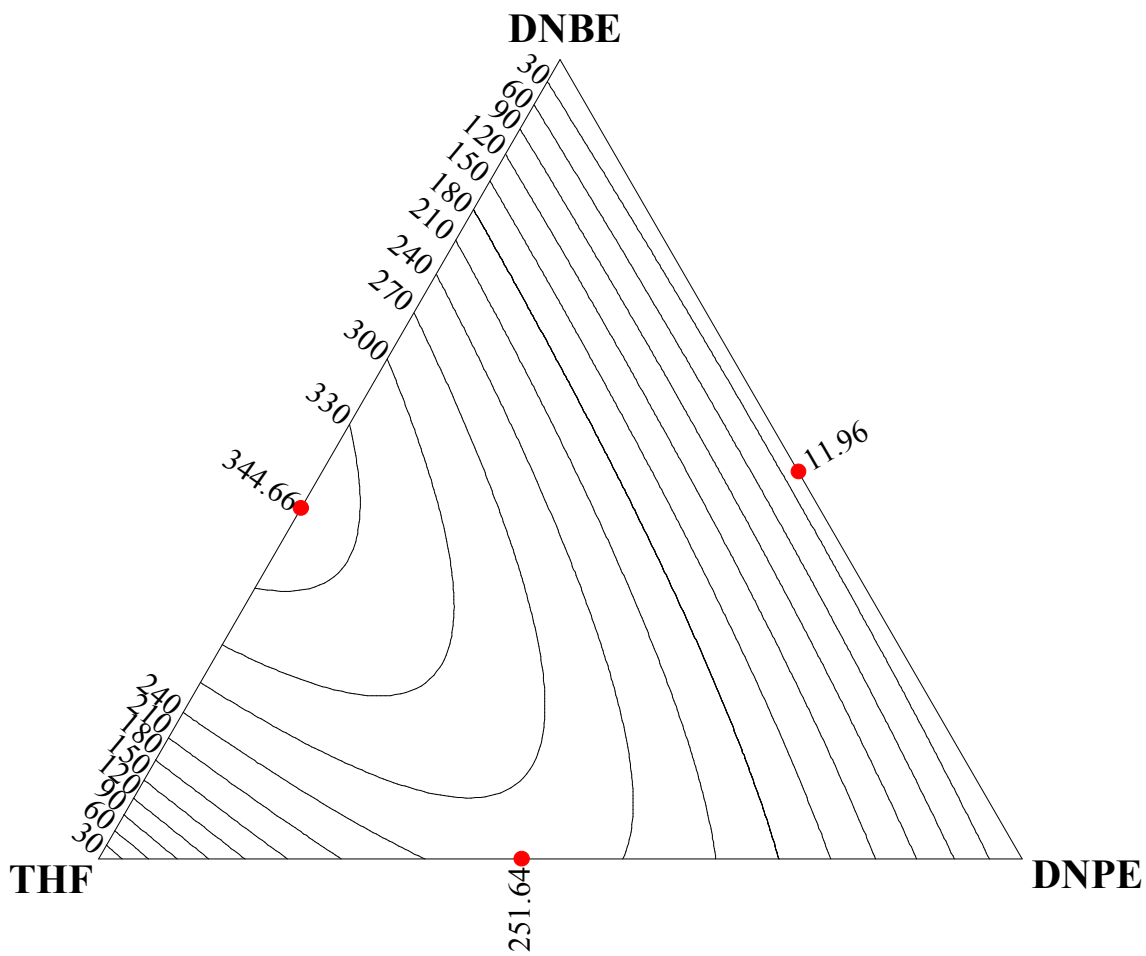


Figure C3.2. Contours for constant values of $H_{m,123}^E / (\text{J} \cdot \text{mol}^{-1})$ for the $x_1 \text{DNPE} + x_2 \text{DNBE} + (1 - x_1 - x_2) \text{THF}$ system at 298.15 K. Predicted by means of the Flory theory.

Ternary System: DNPE (1) + 22DMB (2) + 23DMB (3)

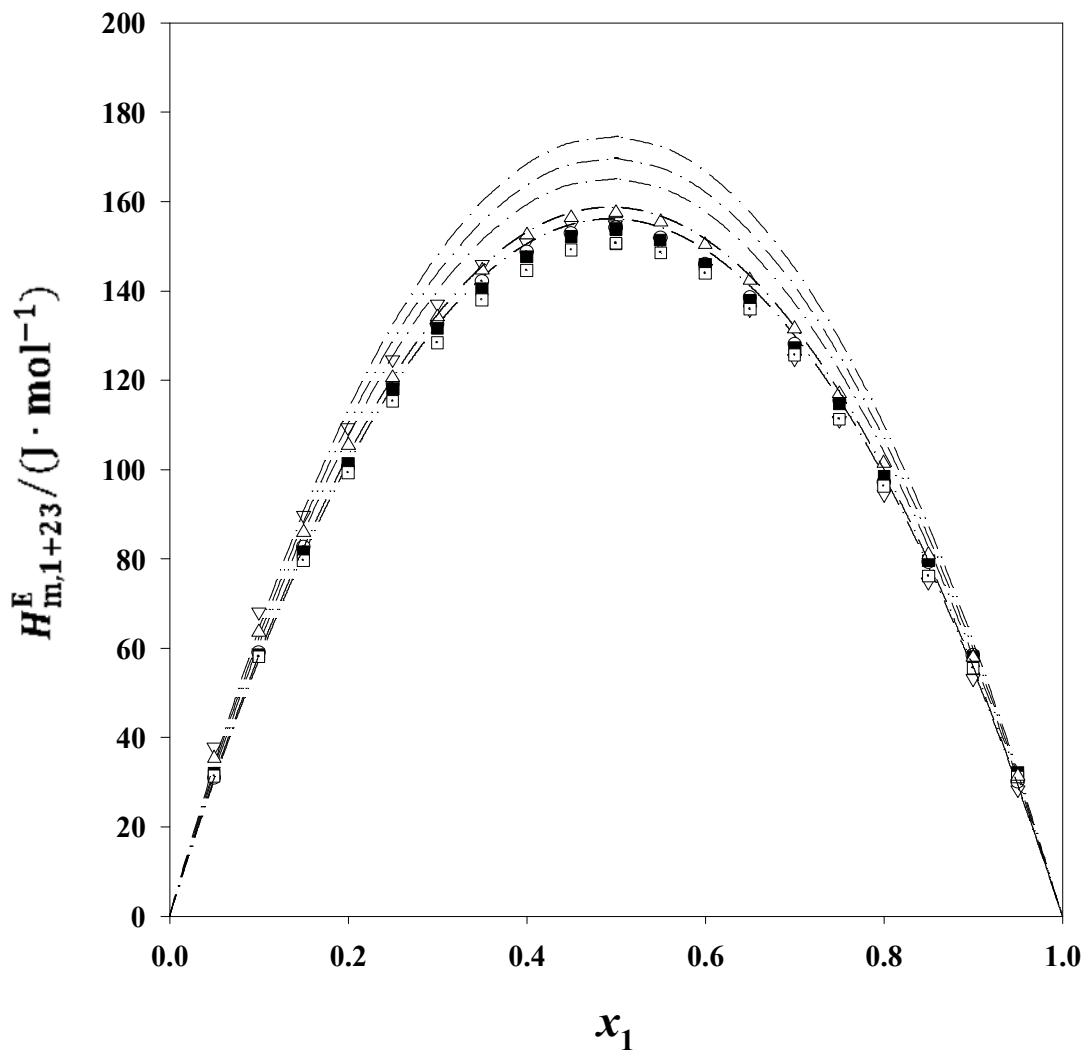


Figure C3.3. Excess molar enthalpies, $H_{m,1+23}^E$, for the x_1 DNPE + x_2 22DMB + $(1 - x_1 - x_2)$ 23DMB mixture at the temperature 298.15 K. Plotted against mole fraction x_1 . Experimental results: Δ , $x_3 = 0.0$; \odot , $x_2/x_3 = 0.3257$; \blacksquare , $x_2/x_3 = 0.9747$; \square , $x_2/x_3 = 2.9968$; ∇ , $x_2 = 0.0$; Curves: - - - -, predicted by means of the Flory theory.

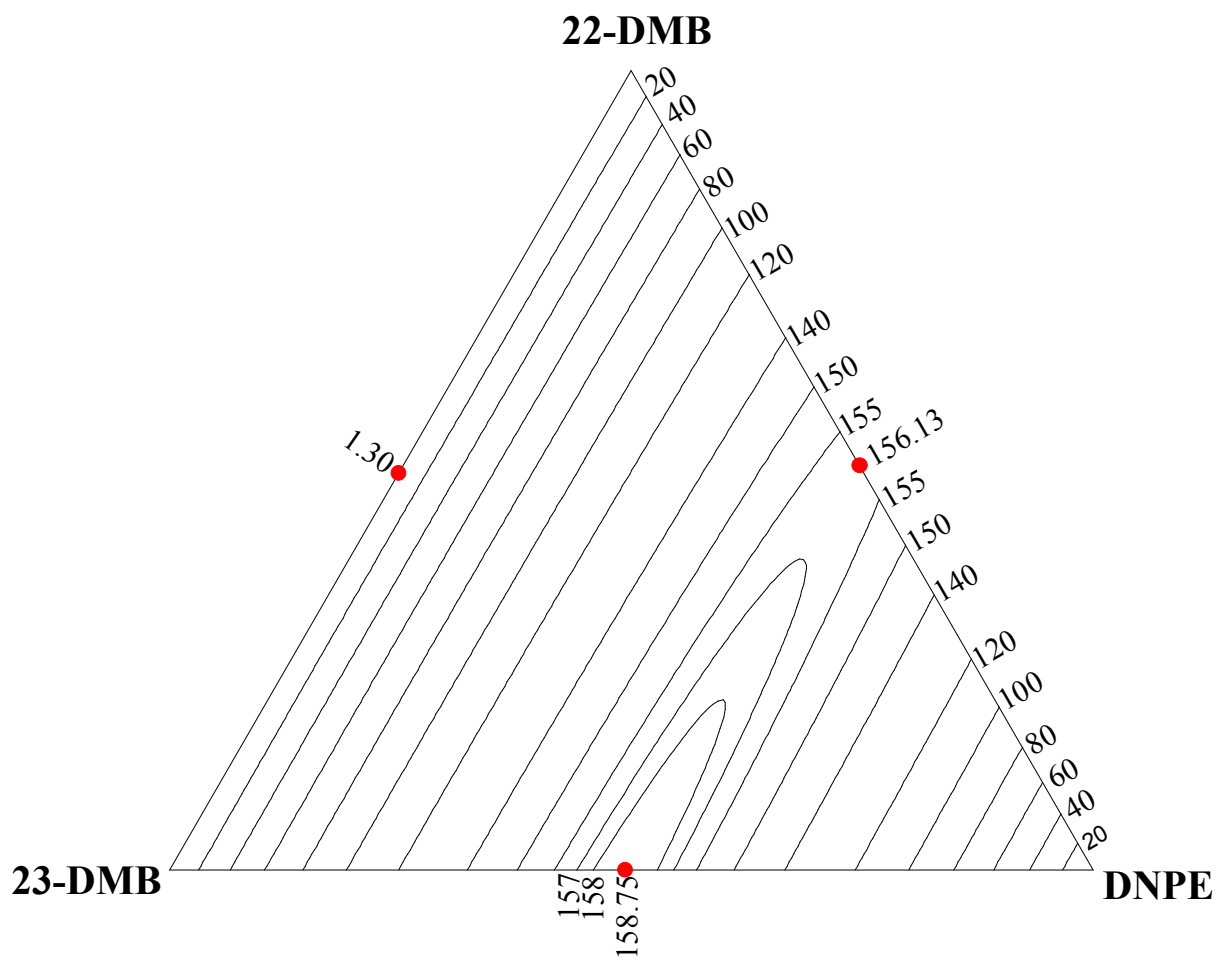


Figure C3.4. Contours for constant values of $H_{m,123}^E / (\text{J} \cdot \text{mol}^{-1})$ for the $x_1 \text{DNPE} + x_2 \text{22DMB} + (1 - x_1 - x_2) \text{23DMB}$ system at 298.15 K. Predicted by means of the Flory theory.

Ternary System: DNBE (1) + 22DMB (2) + 23DMB (3)

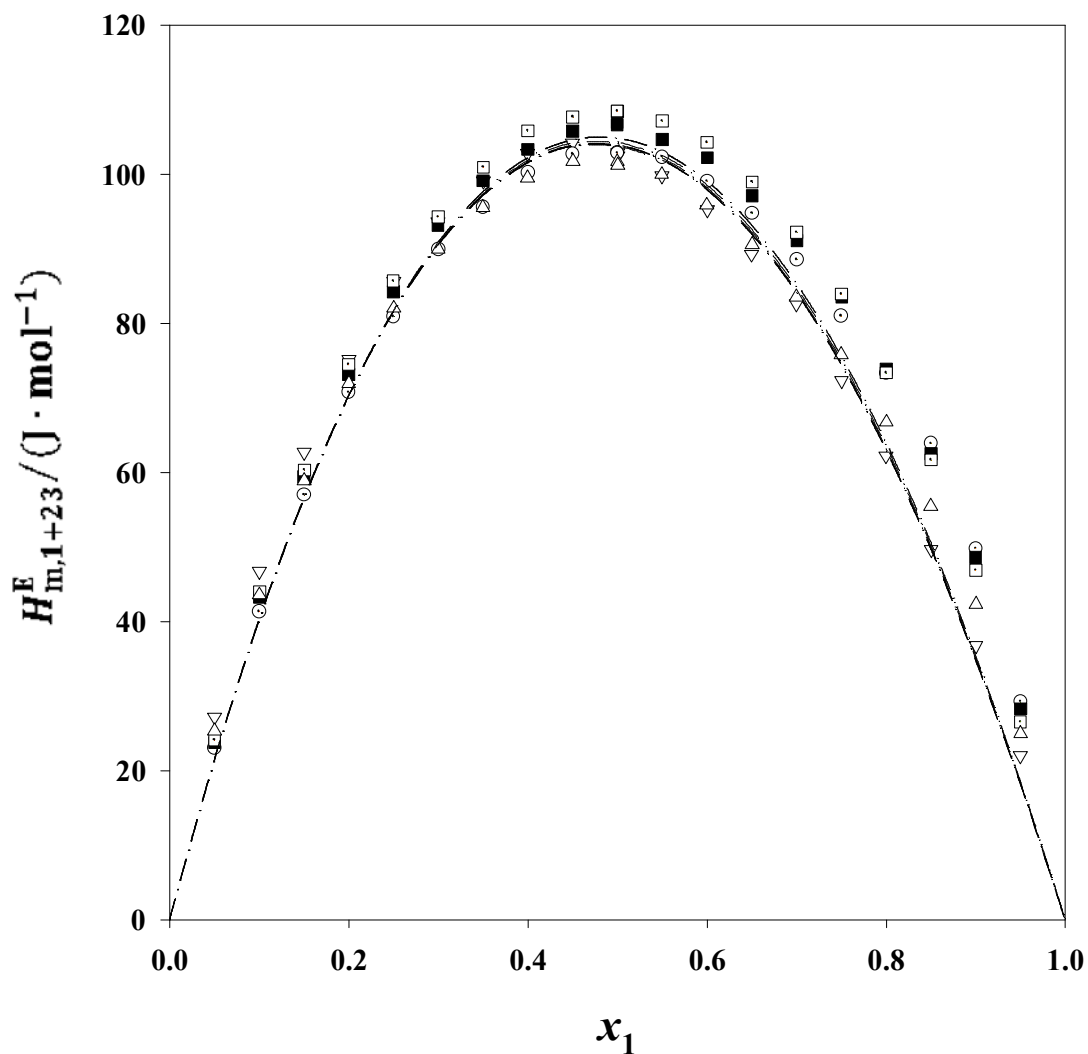


Figure C3.5. Excess molar enthalpies, $H_{m,1+23}^E$, for the x_1 DNBE + x_2 22DMB + $(1 - x_1 - x_2)$ 23DMB mixture at the temperature 298.15 K. Plotted against mole fraction x_1 . Experimental results: Δ , $x_3 = 0.0$; \ominus , $x_2/x_3 = 0.3261$; \blacksquare , $x_2/x_3 = 0.9747$; \square , $x_2/x_3 = 2.9968$; ∇ , $x_2 = 0.0$; Curves: ---, predicted by means of the Flory theory.

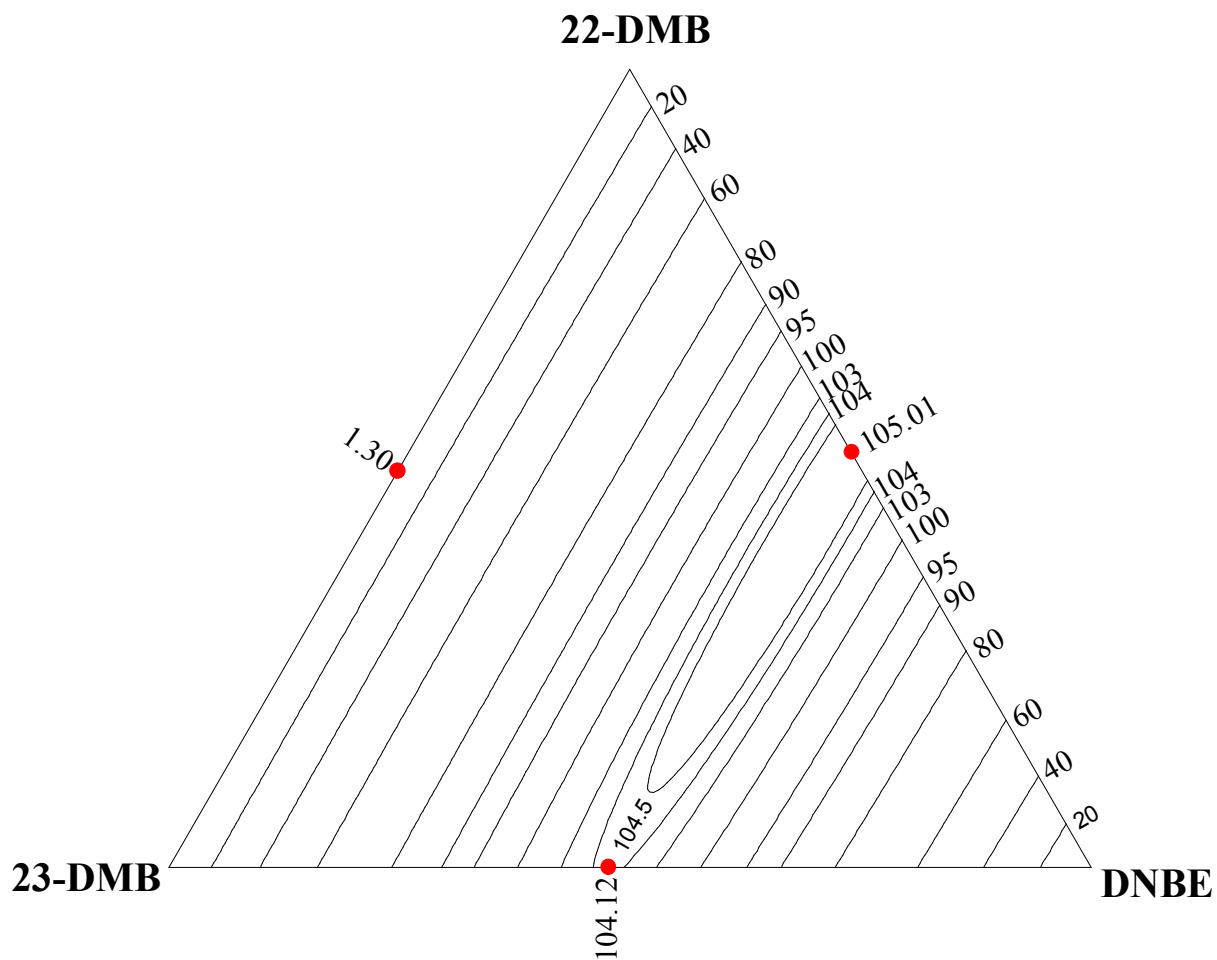


Figure C3.6. Contours for constant values of $H_{m,123}^E / (\text{J} \cdot \text{mol}^{-1})$ for the $x_1 \text{DNBE} + x_2 \text{22DMB} + (1 - x_1 - x_2) \text{23DMB}$ system at 298.15 K. Predicted by means of the Flory theory.

Ternary System: 1HX (1) + THF (2) + 22DMB (3)

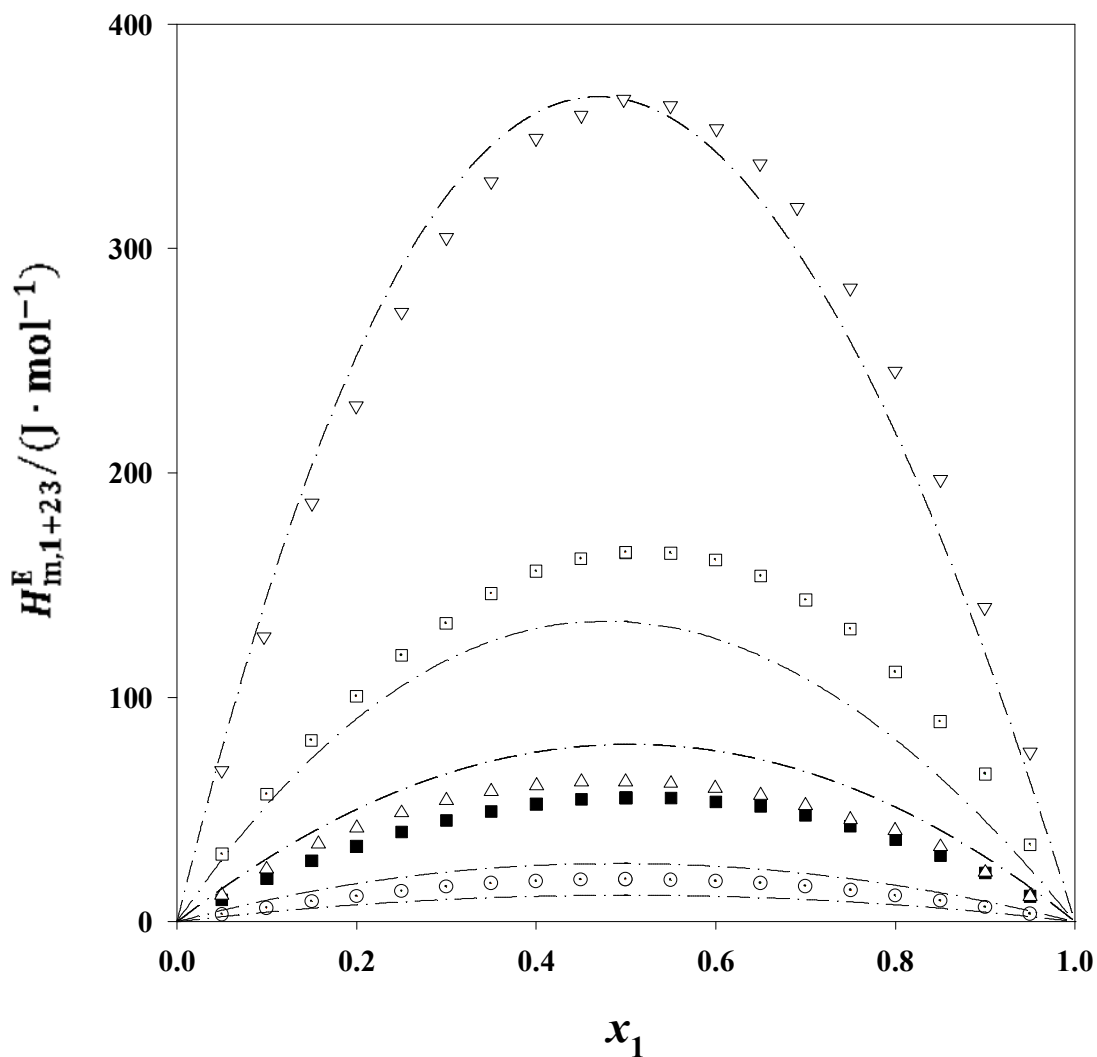


Figure C3.7. Excess molar enthalpies, $H_{m,1+23}^E$, for the x_1 1HX + x_2 THF + $(1 - x_1 - x_2)$ 22DMB mixture at the temperature 298.15 K. Plotted against mole fraction x_1 . Experimental results: Δ , $x_3 = 0.0$; \odot , $x_2/x_3 = 0.3329$; \blacksquare , $x_2/x_3 = 1.0004$; \square , $x_2/x_3 = 3.0000$; ∇ , $x_2 = 0.0$; Curves: $-\cdot-\cdot-$, predicted by means of the Flory theory.

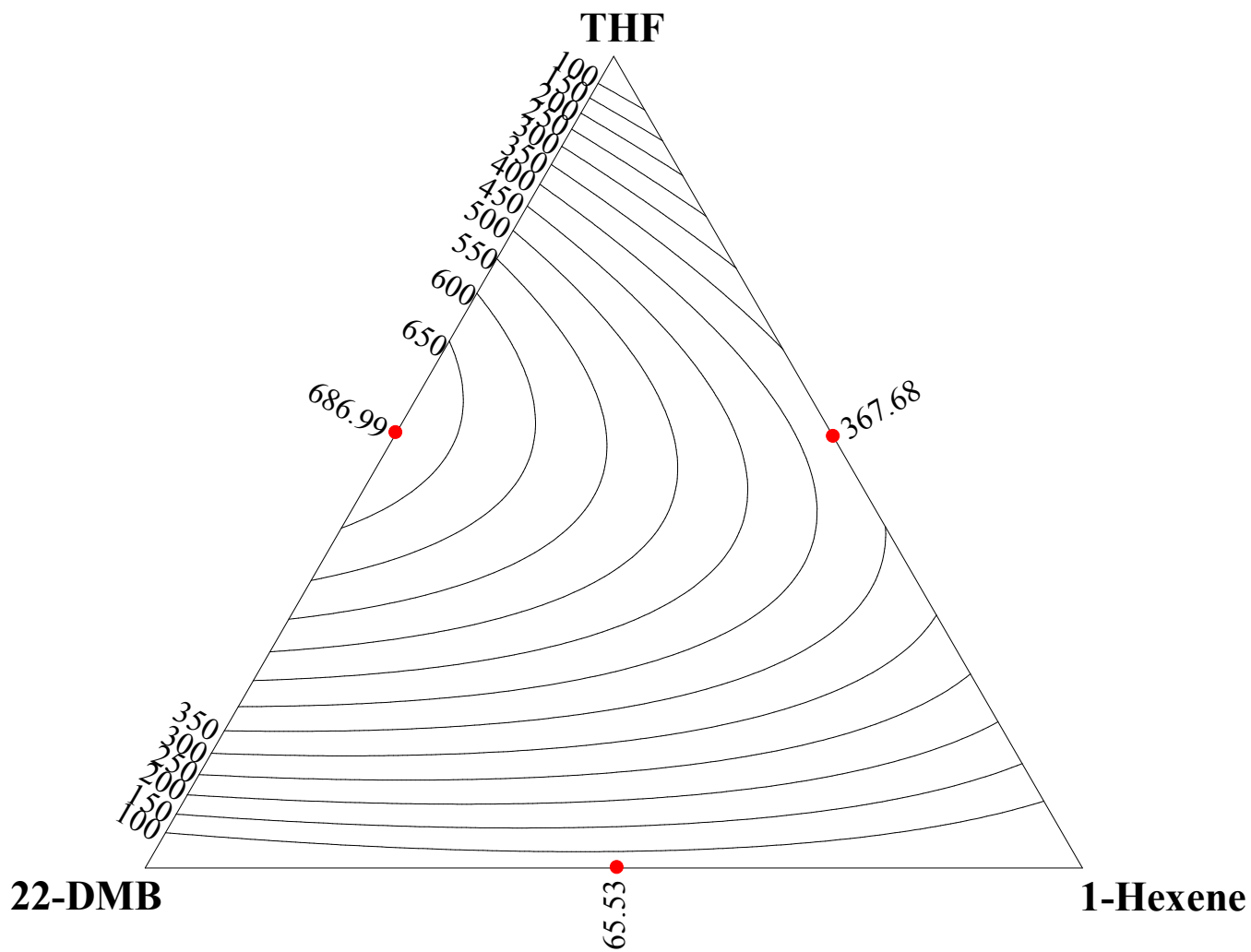


Figure C3.8. Contours for constant values of $H_{m,123}^E / (\text{J} \cdot \text{mol}^{-1})$ for the x_1 1HX + x_2 THF + $(1 - x_1 - x_2)$ 22DMB system at 298.15 K. Predicted by means of the Flory theory.

Ternary System: 1HX (1) + THF (2) + 23DMB (3)

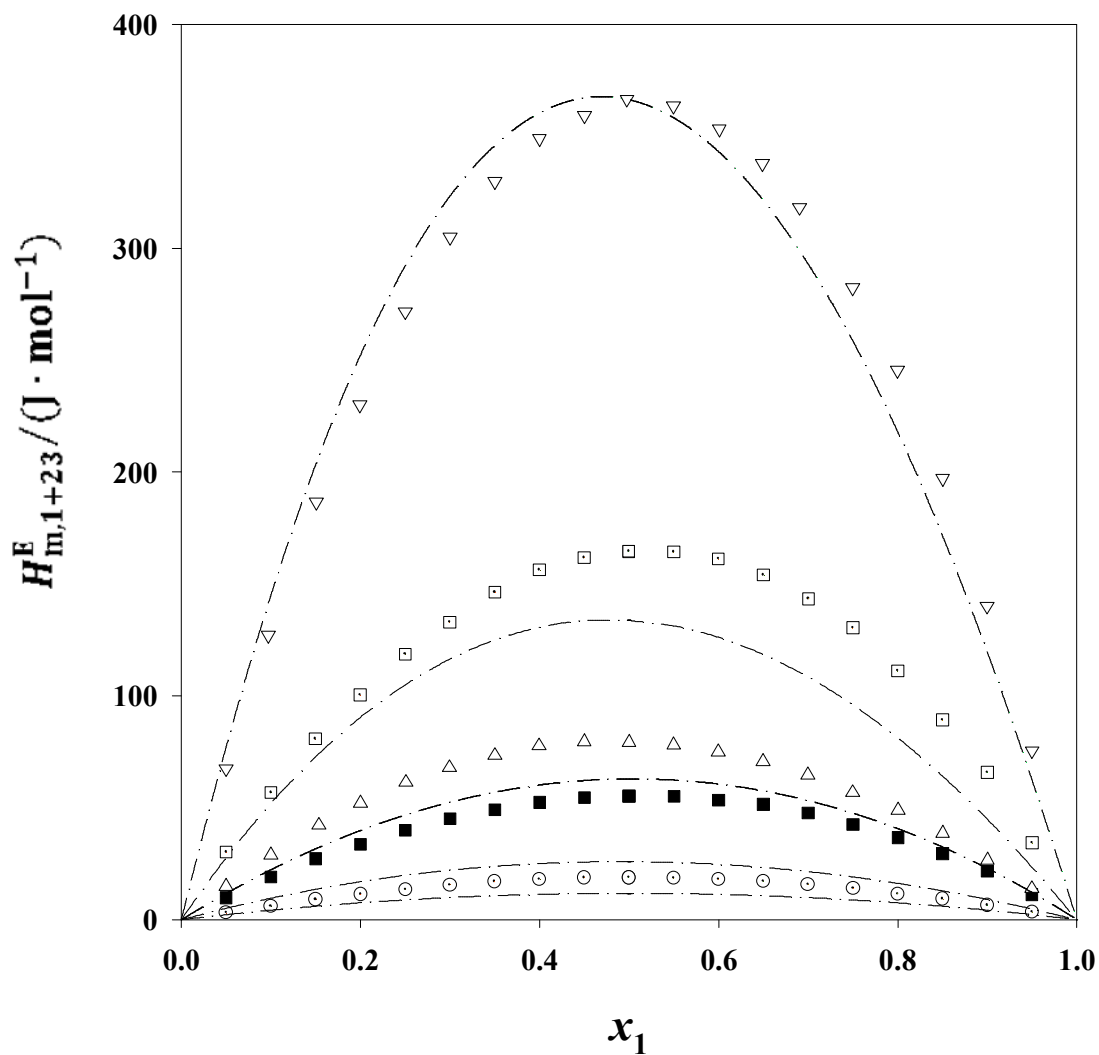


Figure C3.9. Excess molar enthalpies, $H_{m,1+23}^E$, for the x_1 1HX + x_2 THF + $(1 - x_1 - x_2)$ 23DMB mixture at the temperature 298.15 K. Plotted against mole fraction x_1 . Experimental results: Δ , $x_3 = 0.0$; \odot , $x_2/x_3 = 0.3332$; \blacksquare , $x_2/x_3 = 0.9996$; \square , $x_2/x_3 = 3.0000$; ∇ , $x_2 = 0.0$; Curves: $-\cdot-\cdot-$, predicted by means of the Flory theory.

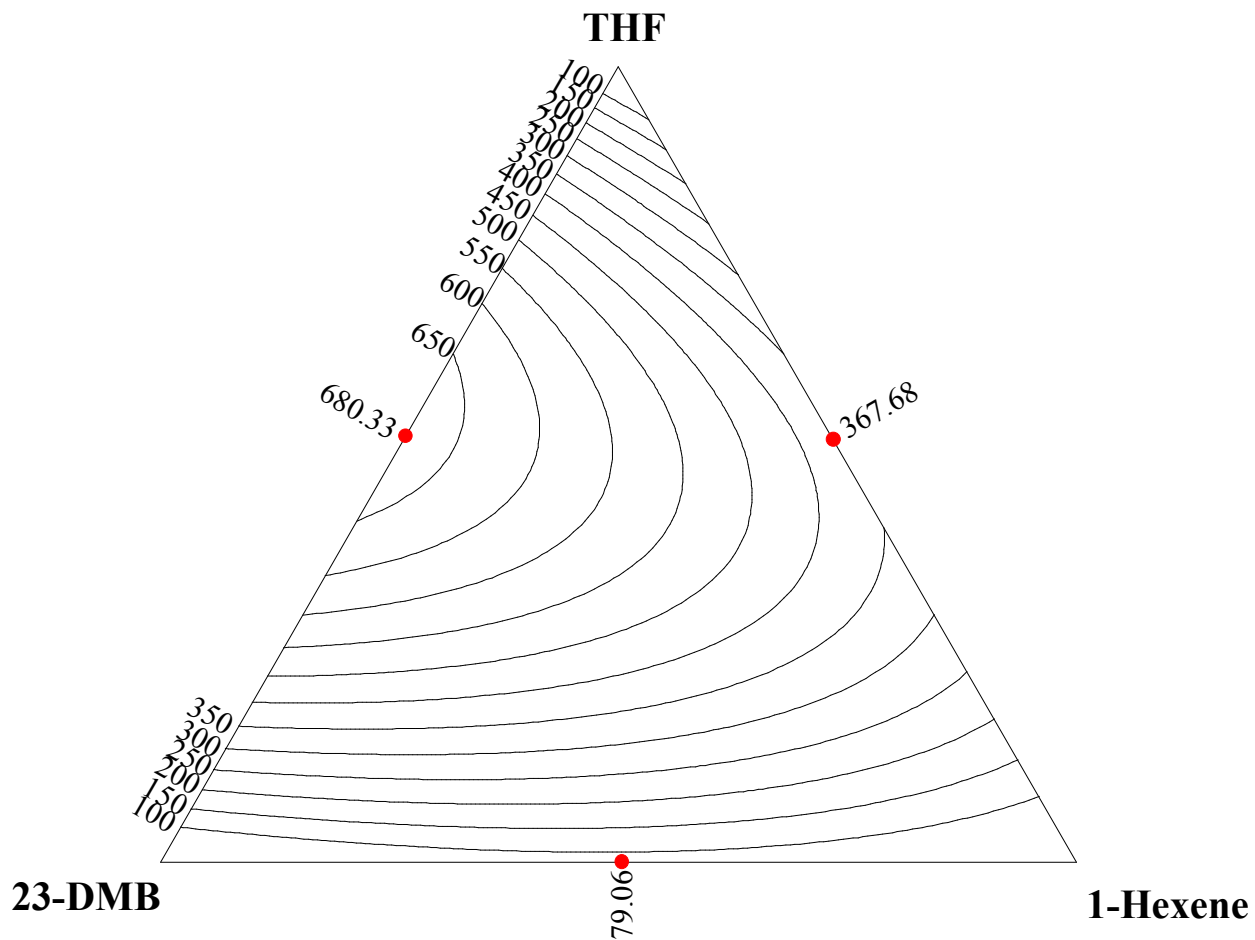


Figure C3.10. Contours for constant values of $H_{m,123}^E / (\text{J} \cdot \text{mol}^{-1})$ for the $x_1 1\text{HX} + x_2 \text{THF} + (1 - x_1 - x_2) 23\text{DMB}$ system at 298.15 K. Predicted by means of the Flory theory.

C3.2 Liebermann-Fried model Representation of Ternary Systems

Ternary System: DNPE (1) + DNBE (2) + THF (3)

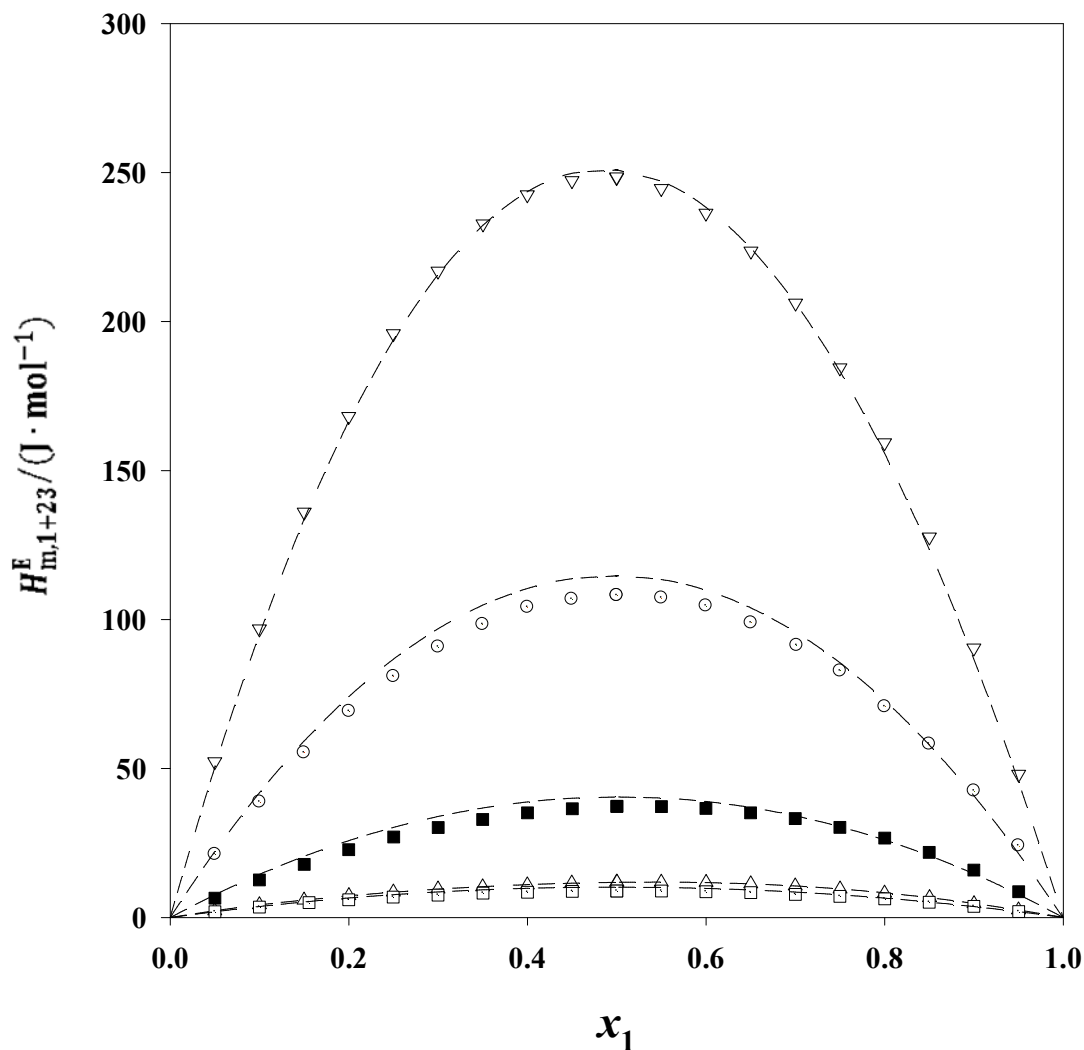


Figure C3.11. Excess molar enthalpies, $H_{m,1+23}^E$, for the x_1 DNPE + x_2 DNBE + $(1 - x_1 - x_2)$ THF mixture at the temperature 298.15 K. Plotted against mole fraction x_1 . Experimental results: Δ , $x_3 = 0.0$; \circ , $x_2/x_3 = 0.3332$; \blacksquare , $x_2/x_3 = 1.0004$; \square , $x_2/x_3 = 3.0000$; ∇ , $x_2 = 0.0$; Curves: -----, predicted by means of the Liebermann-Fried model.

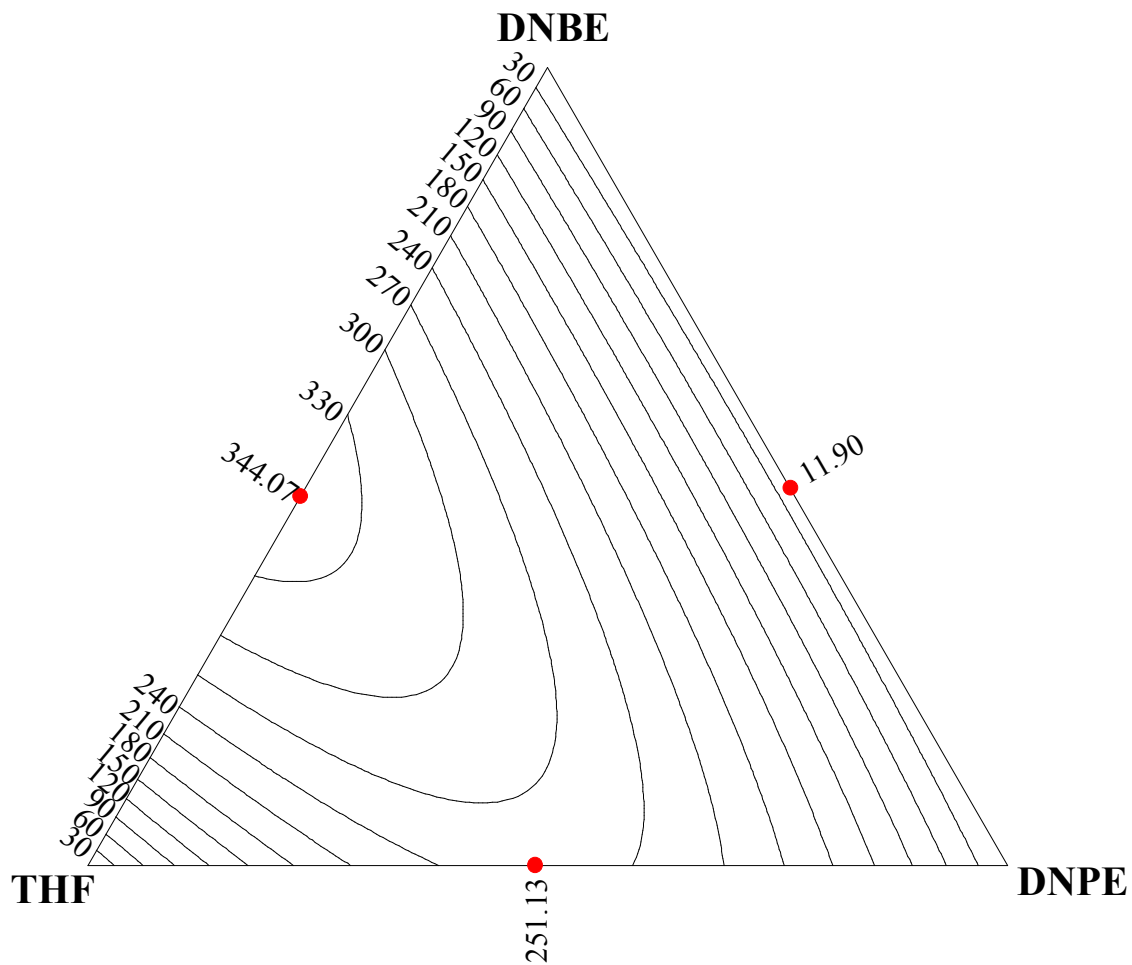


Figure C3.12. Contours for constant values of $H_{m,123}^E / (\text{J} \cdot \text{mol}^{-1})$ for the $x_1 \text{DNPE} + x_2 \text{DNBE} + (1 - x_1 - x_2) \text{THF}$ system at 298.15 K. Predicted by means of the Liebermann-Fried model.

Ternary System: DNPE (1) + 22DMB (2) + 23DMB (3)

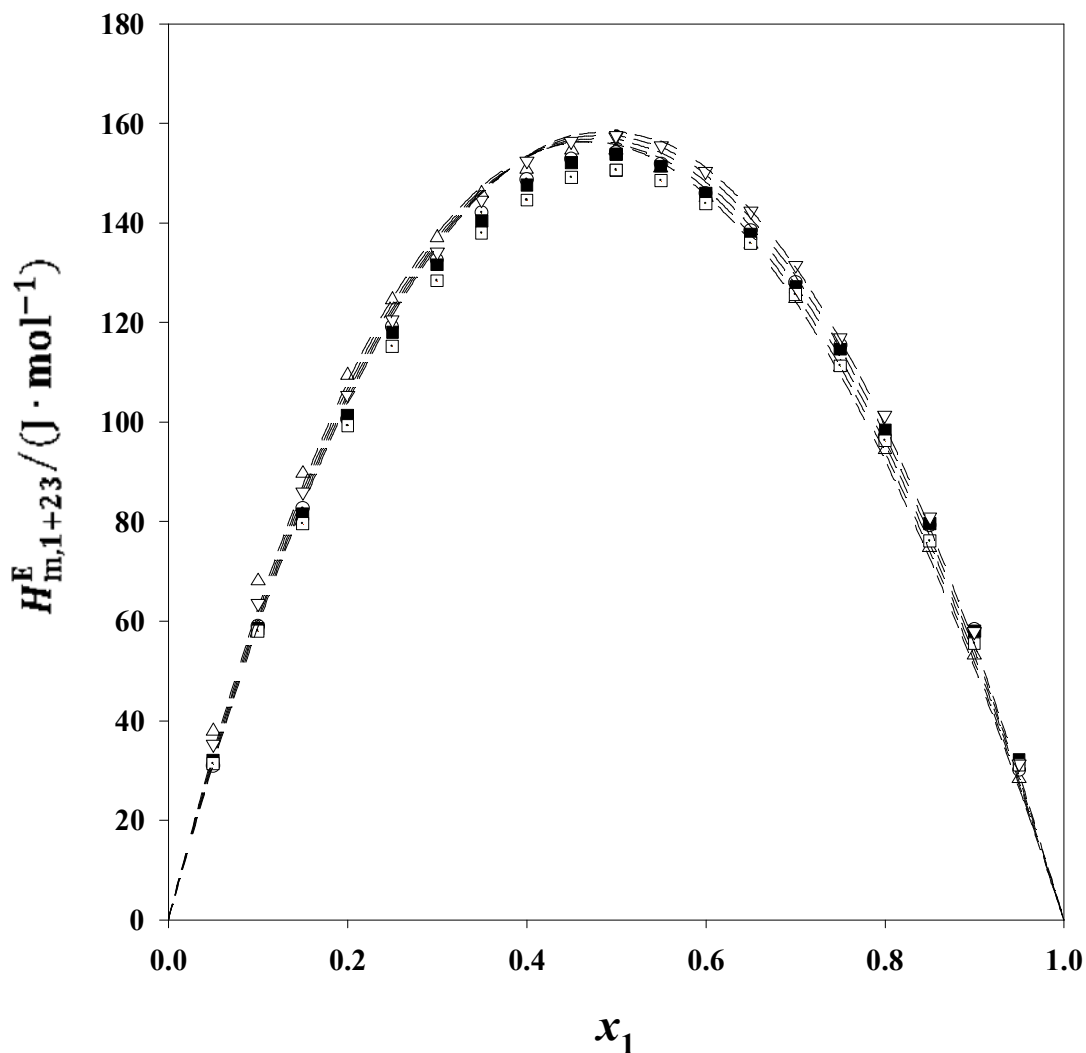


Figure C3.13. Excess molar enthalpies, $H_{m,1+23}^E$, for the x_1 DNPE + x_2 22DMB + $(1 - x_1 - x_2)$ 23DMB mixture at the temperature 298.15 K. Plotted against mole fraction x_1 . Experimental results: Δ , $x_3 = 0.0$; \odot , $x_2/x_3 = 0.3257$; \blacksquare , $x_2/x_3 = 0.9747$; \square , $x_2/x_3 = 2.9968$; ∇ , $x_2 = 0.0$; Curves: -----, predicted by means of the Liebermann-Fried model.

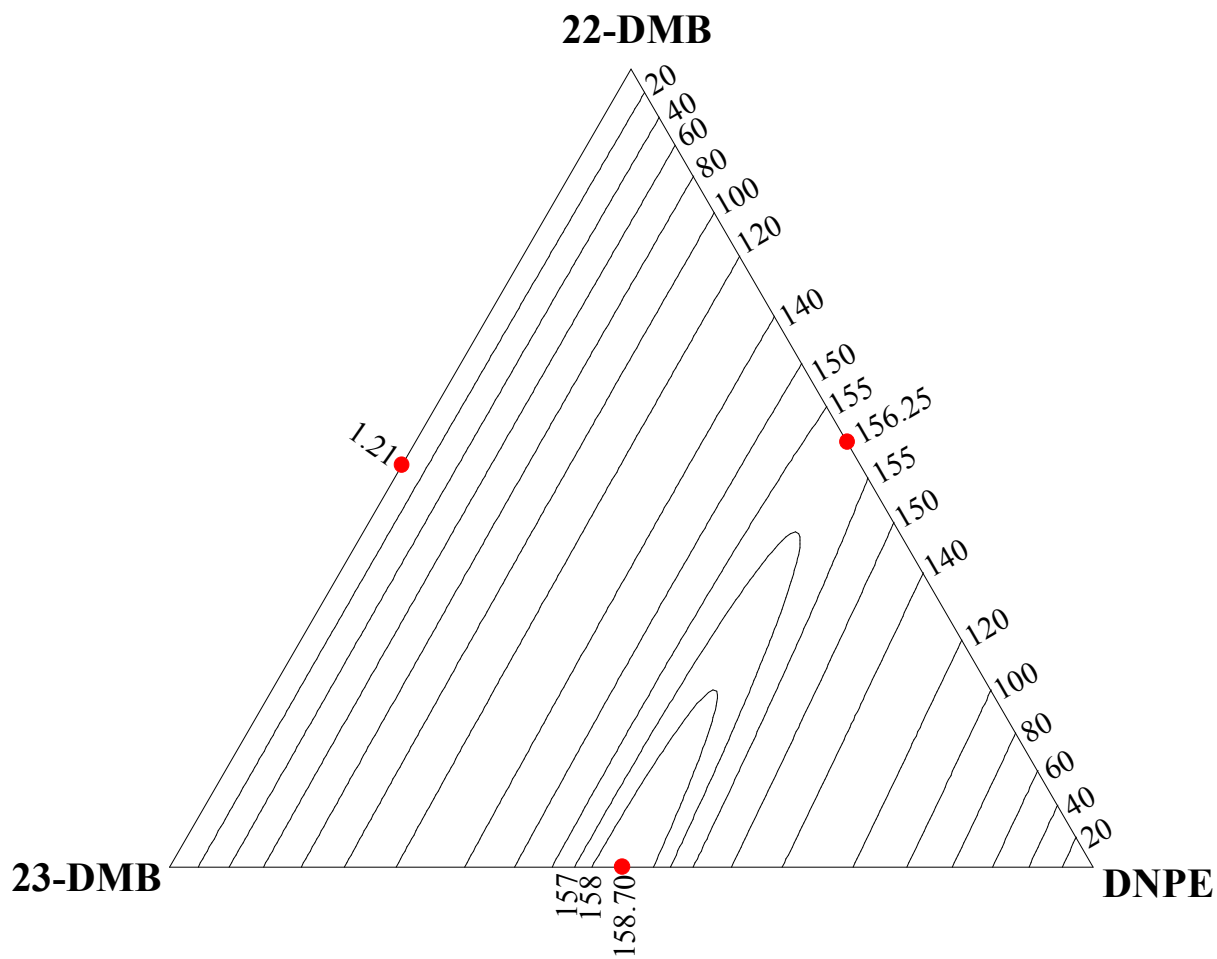


Figure C3.14. Contours for constant values of $H_{m,123}^E / (\text{J} \cdot \text{mol}^{-1})$ for the $x_1 \text{DNPE} + x_2 \text{22DMB} + (1 - x_1 - x_2) \text{23DMB}$ system at 298.15 K. Predicted by means of the Liebermann-Fried model.

Ternary System: DNBE (1) + 22DMB (2) + 23DMB (3)

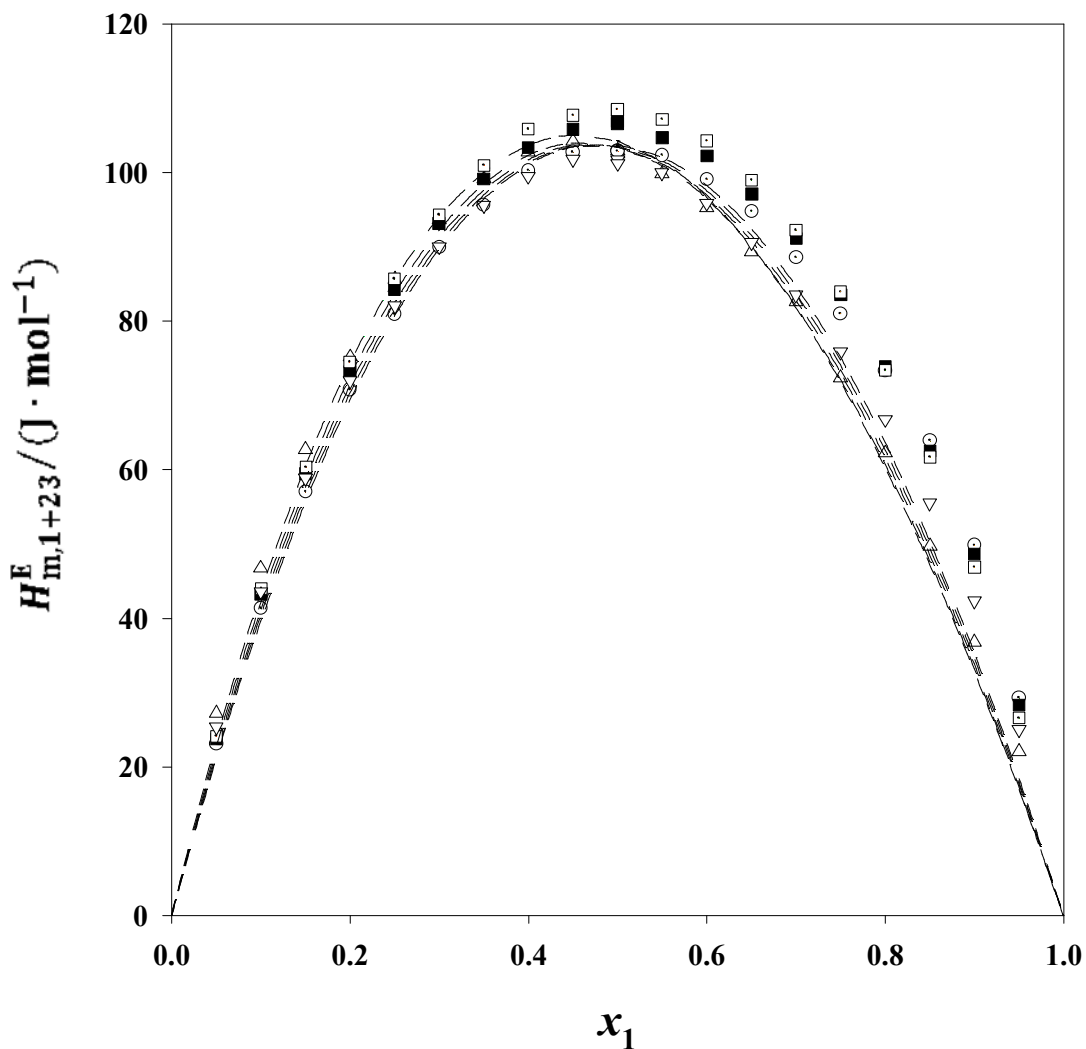


Figure C3.15. Excess molar enthalpies, $H_{m,1+23}^E$, for the x_1 DNBE + x_2 22DMB + $(1 - x_1 - x_2)$ 23DMB mixture at the temperature 298.15 K. Plotted against mole fraction x_1 . Experimental results: Δ , $x_3 = 0.0$; \odot , $x_2/x_3 = 0.3261$; \blacksquare , $x_2/x_3 = 0.9747$; \square , $x_2/x_3 = 2.9968$; ∇ , $x_2 = 0.0$; Curves: -----, predicted by means of the Liebermann-Fried model.

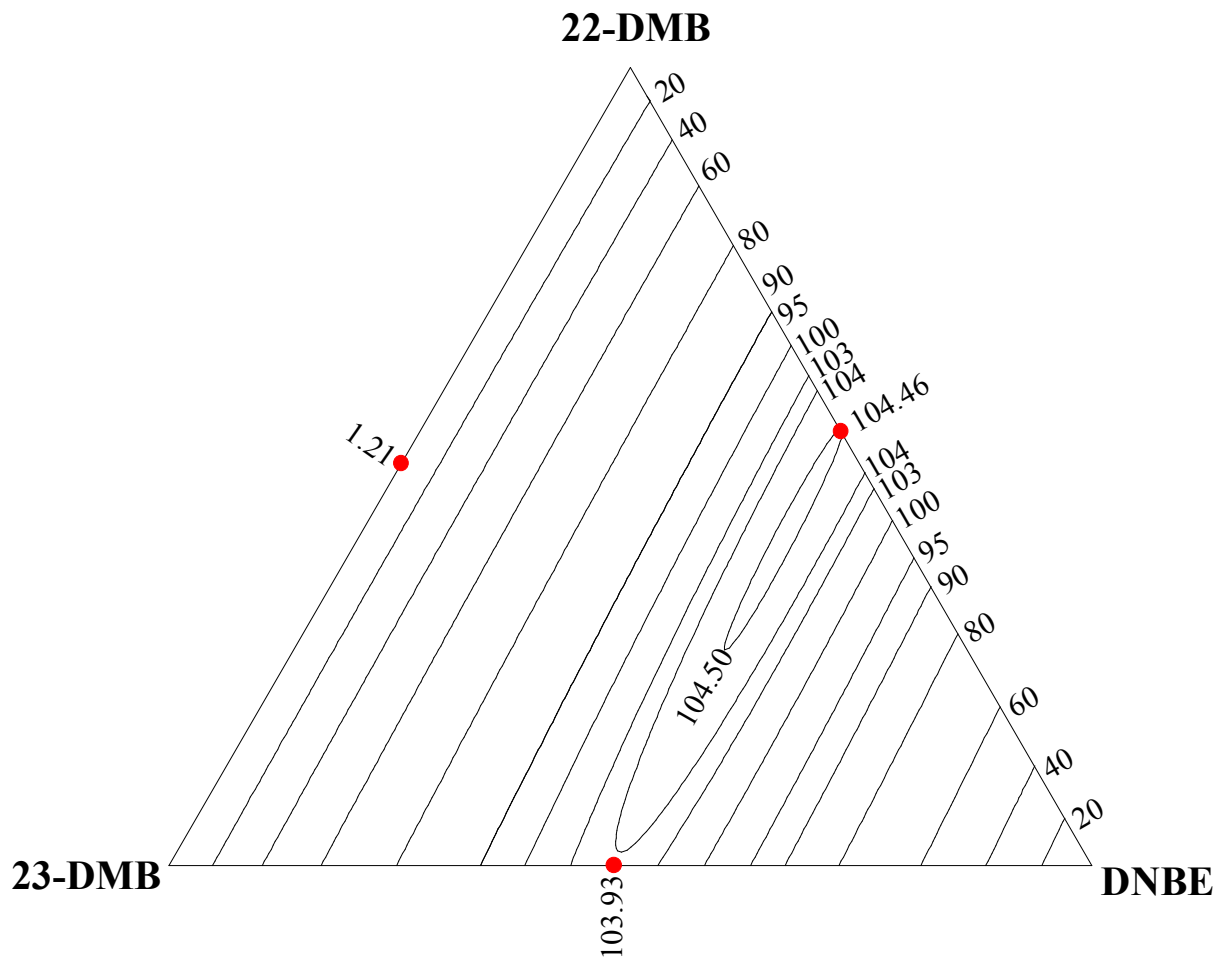


Figure C3.16. Contours for constant values of $H_{m,123}^E / (\text{J} \cdot \text{mol}^{-1})$ for the $x_1 \text{DNBE} + x_2 \text{22DMB} + (1 - x_1 - x_2) \text{23DMB}$ system at 298.15 K. Predicted by means of the Liebermann-Fried model.

Ternary System: 1HX (1) + THF (2) + 22DMB (3)

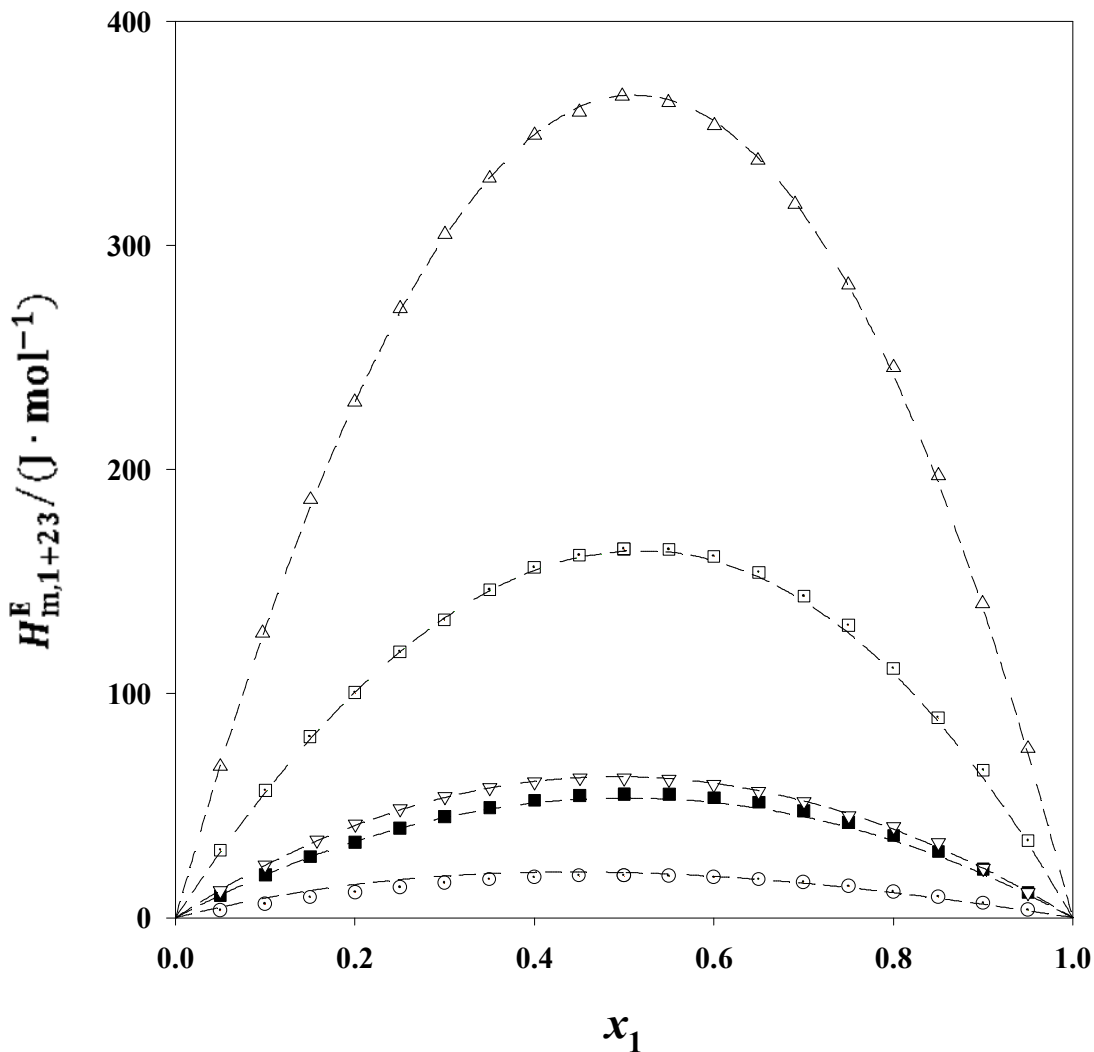


Figure C3.17. Excess molar enthalpies, $H_{m,1+23}^E$, for the x_1 1HX + x_2 THF + $(1 - x_1 - x_2)$ 22DMB mixture at the temperature 298.15 K. Plotted against mole fraction x_1 . Experimental results: Δ , $x_3 = 0.0$; \odot , $x_2/x_3 = 0.3329$; \blacksquare , $x_2/x_3 = 1.0004$; \square , $x_2/x_3 = 3.0000$; ∇ , $x_2 = 0.0$; Curves: - - - - , predicted by means of the Liebermann-Fried model.

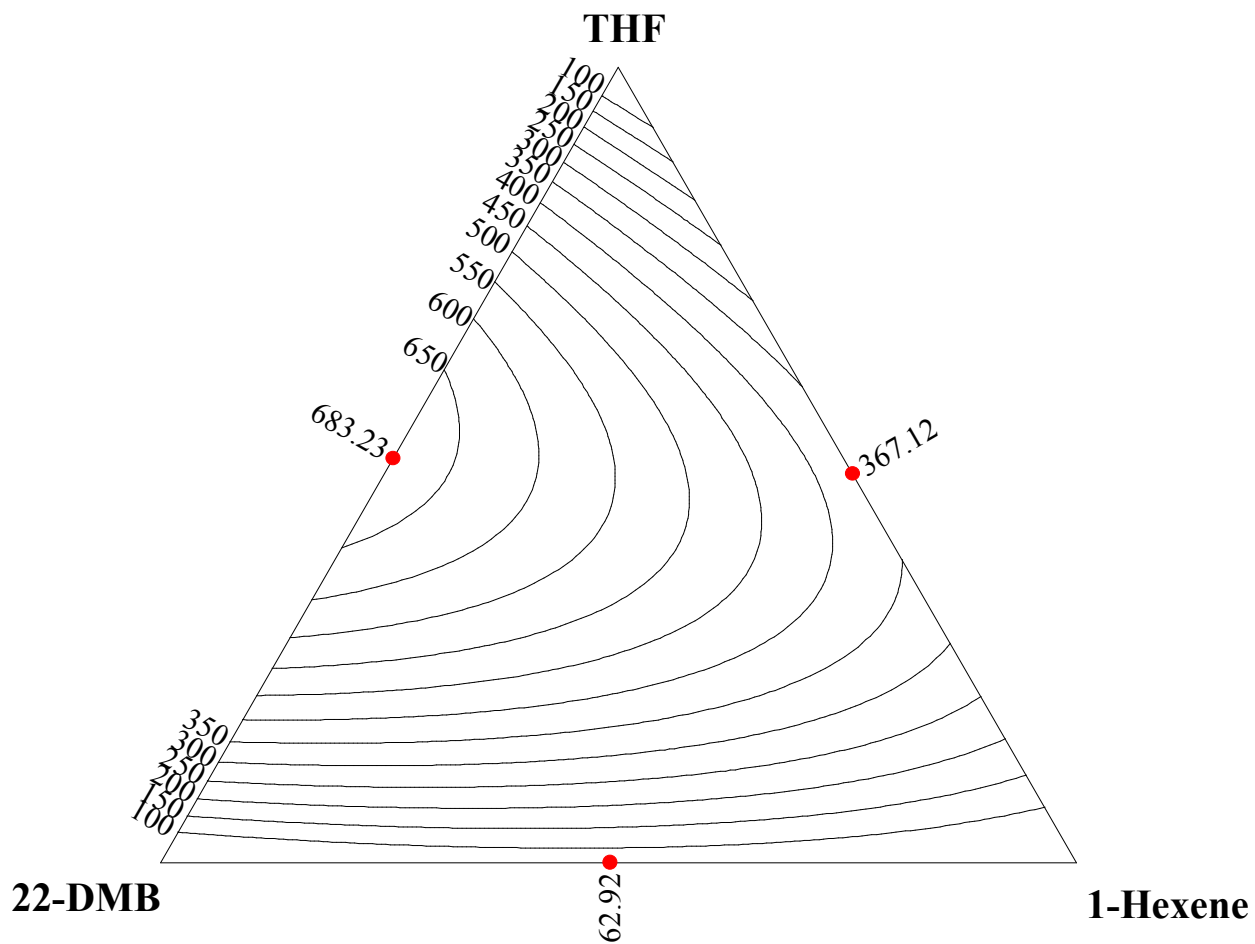


Figure C3.18. Contours for constant values of $H_{m,123}^E / (\text{J} \cdot \text{mol}^{-1})$ for the x_1 1HX + x_2 THF + $(1 - x_1 - x_2)$ 22DMB system at 298.15 K. Predicted by means of the Liebermann-Fried model.

Ternary System: 1HX (1) + THF (2) + 23DMB (3)

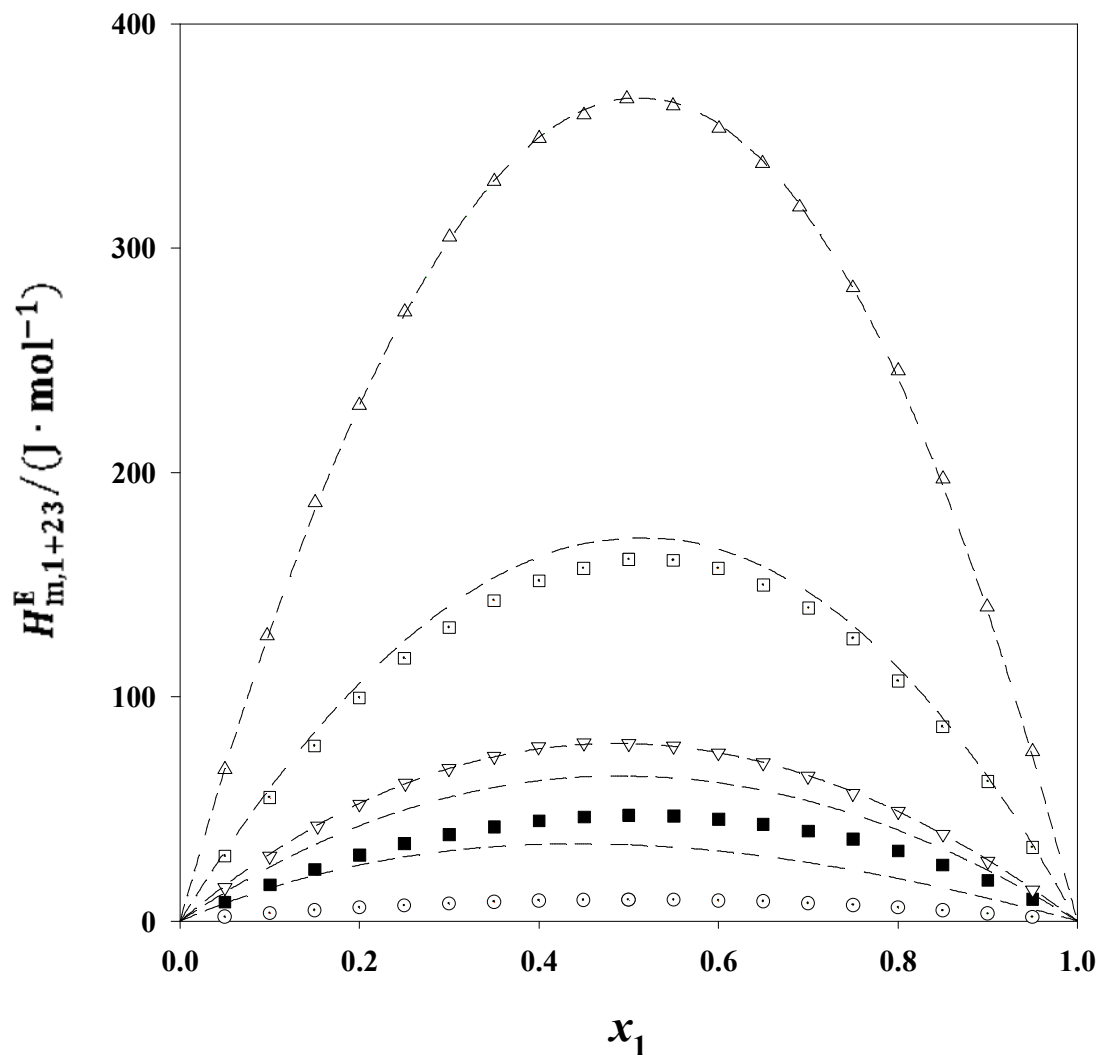


Figure C3.19. Excess molar enthalpies, $H_{m,1+23}^E$, for the x_1 1HX + x_2 THF + $(1 - x_1 - x_2)$ 23DMB mixture at the temperature 298.15 K. Plotted against mole fraction x_1 . Experimental results: Δ , $x_3 = 0.0$; \odot , $x_2/x_3 = 0.3332$; \blacksquare , $x_2/x_3 = 0.9996$; \square , $x_2/x_3 = 3.0000$; ∇ , $x_2 = 0.0$; Curves: -----, predicted by means of the Liebermann-Fried model.

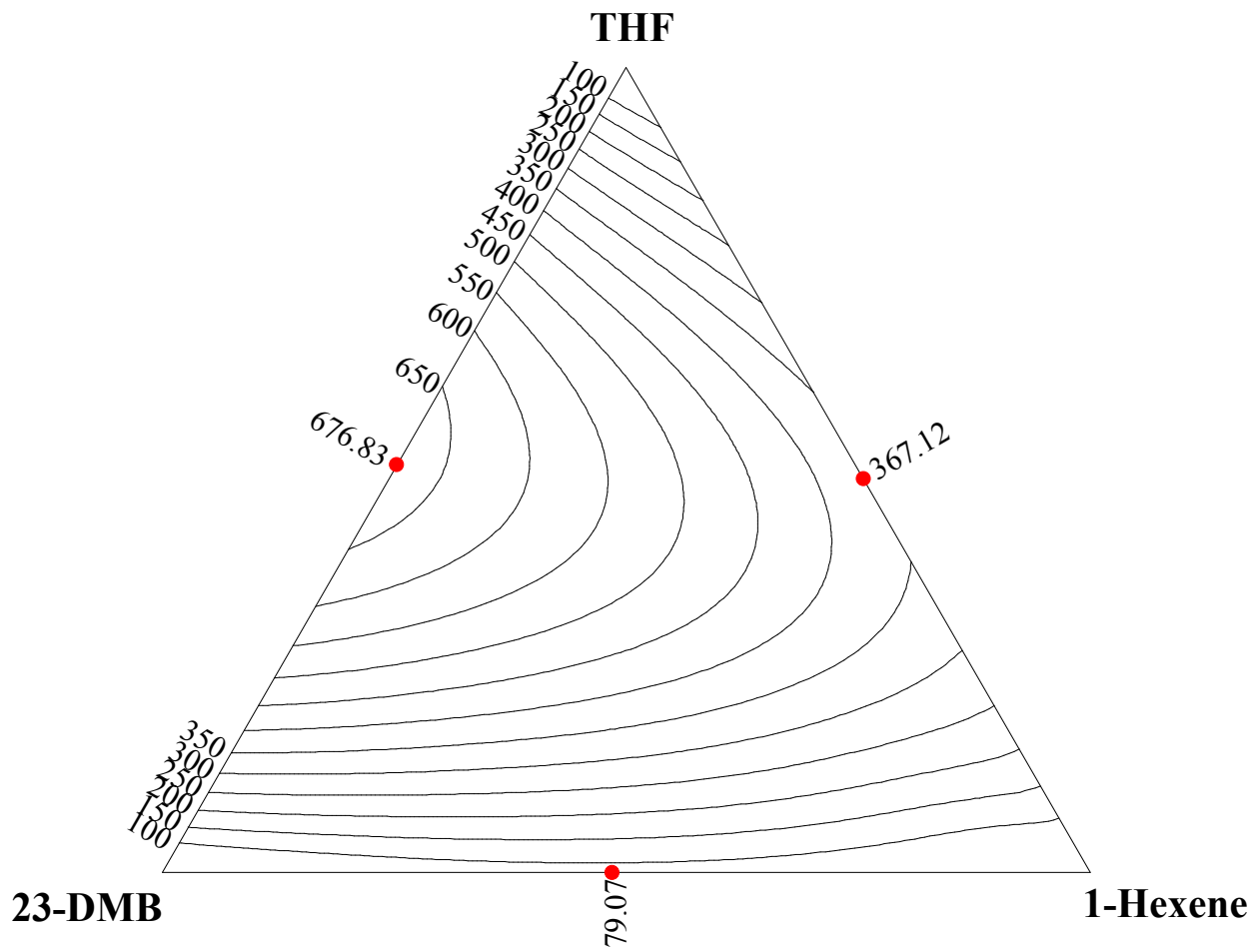


Figure C3.20. Contours for constant values of $H_{m,123}^E / (\text{J} \cdot \text{mol}^{-1})$ for the x_1 1HX + x_2 THF + $(1 - x_1 - x_2)$ 23DMB system at 298.15 K. Predicted by means of the Liebermann-Fried model.